Expression of the Blood-Brain Barrier Markers GLUT1 and EBA in the Spinal Cord and Male Reproductive Tract in Normal and Spinal Cord-Injured Rats

By

Jianjun Lu, MBBS, MSc

Thesis submitted for the degree of Doctor of Philosophy

to the University of Adelaide

Department of Anatomical Sciences

Medical School

Faculty of Health Sciences

The University of Adelaide

12 December 2005

Table of Contents

ABSTRACT

Microvessels in the central nervous system (CNS), most extensively studied in the brain, form a unique barrier system known as the blood-brain barrier (BBB). The spinal cord, an integral part of the CNS, has a similar blood-tissue barrier referred to as the blood-spinal cord barrier (BSB). The barrier regulates the exchange of solutes between the blood and neural tissues. The anatomical basis of this system are the endothelial cells (ECs) lining these microvessels. These cells are characterized by selective barrier properties and intercellular tight junctions (TJs) with high electrical resistance. The function of the BBB and BSB is critical for maintaining homeostasis of the mammalian CNS.

A group of proteins specifically present in ECs of the BBB and BSB have been identified as molecular markers for CNS microvessels, as they are specifically expressed by ECs with barrier properties, but not expressed or only weakly expressed by those without barrier properties. These include the endothelial barrier antigen (EBA) and the glucose transporter protein 1 (GLUT1). Although the morphological properties of the BBB in normal and experimental conditions have been extensively studied, molecular changes at the BBB after injury are incompletely understood. In particular, the expression, pattern and function of the BBB markers after injury have not been fully elucidated.

In the present study, two rat models were employed. Firstly, a model of sustained compression injury to the rat spinal cord was induced by application of 35g or 50g weights, for 5min or 15min to induce moderate or severe compression respectively. Secondly, an immunological targeting model was induced by intravenous injection of a monoclonal antibody to EBA. In both models, experimental animals were allowed to survive for different time periods. In the spinal cord injury model, quantitative and qualitative EBA and GLUT1 expression and morphological change in the spinal cord were investigated at LM and EM levels. In the immunological targeting model, the function of the BBB and BSB after immunological targeting was assessed by detecting the leakage of exogenous HRP at different time intervals. The hypothesis that other blood-tissue barriers also express the EBA was tested in the male rat reproductive tract, as it has been suggested that blood vessels of the testis contribute to the blood-testis barrier (BTB), traditionally considered to be formed by Sertoli cells.

The results showed that EBA and GLUT1 were expressed in the normal spinal cord. However, the expression of EBA was reduced in the spinal cord grey matter vessels at the trauma site and segments remote from the trauma site after injury. This reduction correlated with the function of the BSB and the pathological evolution of changes in the injured cord. Quantitative study showed that a remarkable reduction of EBA labelling started as early as 1 day at the trauma site after severe injury with a maximum reduction at 3 day post injury. The labelling started to recover at 2 weeks post injury. In moderate injury, the reduction of EBA also started at 1 day after injury

with a maximum reduction at 7 days post injury. The labelling intensity started to recover progressively at 1 and 2 weeks post injury. There was also remarkable reduction of GLUT1 expression at the trauma site as well as segments remote from trauma site at almost all time intervals post injury. EM of microvessels showed EBA and GLUT1 immunoreactivity was mainly localized to the luminal membrane of ECs. After injury, the reduced labelling was in two forms. (a) A reduction in labelling intensity in luminal membranes and the cytoplasm. (b) A reduction in the percentage of labelled luminal membranes in relation to total circumference of the vessel.

After immunological targeting of the EBA, there was widespread leakage of HRP in the brain and spinal cord which occurred as early as 17 min and was maximum at 30 min. HRP leakage was progressively reduced at 1h and 2h after injection, and was not detected at 3h post injection.

GLUT1 and EBA were detected in normal rat testicular microvessels whereas EBA was also found in epithelial cells of lateral prostate gland. However, after spinal cord injury, the GLUT1 expression in testicular vessels was reduced as early as 1 day after injury with a maxium reduction at 3 days after injury. The GLUT1 expression started to recover at 2 weeks after injury and became almost normal at 4 weeks. One and three days after cord injury, testicular microvessels showed a reduction in EBA immunoreactivity, with maximal reduction at one week. At 2 and 4 weeks most vessels were still non-reactive to anti-EBA. The lateral prostate showed a reduction

in EBA immunoreactivity in epithelial cells with maximal reduction at 2 weeks and incomplete restoration at 4 weeks. Injured animals at all time intervals showed distended prostatic acini, and the luminal secretion in the lateral lobe of the prostate was immunoreactive, in contrast to other lobes. This study demonstrated variable responses in the expression of EBA in endothelial and epithelial cells in the male rat reproductive tract after spinal cord injury.

The results of this study provided an insight into the functional properties of these molecular markers at the BSB in the injured spinal cord. The reduction of EBA and GLUT1 expression in spinal cord grey matter vessels remote from the site of direct trauma suggests that altered input to the grey matter from ascending and decending axons undergoing degeneration leads to altered BBB function and molecular markers expression. The result suggests that EBA plays an important putative role in upholding the normal function of the BBB and BSB. The finding that EBA was expressed by the testis and prostate gland suggests that the EBA has a wider tissue distribution and more diverse function than previously appreciated. The role of neural and endocrine factors in regulating EBA and GLUT1 expression in the male reproductive tract merits further investigations. The information generated from this study provides basis for further investigation into the molecular mechanisms involved in spinal cord injury.

DECLARATION

This work contains no material which has been accepted for the award of any other degree or diploma in any university or tertiary institution and, to the best of my knowledge and belief, contains no material previously published or written by another person, except where due reference has been made in the text.

I give my consent to this copy of my thesis, when deposited in the University of Adelaide Library, being available for loan and photocopying.

Date..27/10/2006

ACKNOWLEDGEMENTS

I would like to thank my supervisor Dr Mounir Ghabriel for his great help and patient and friendly guidance throughout my PhD studies. Thanks are also given for his critical reading, invaluable comments and suggestions during my thesis writing process. I appreciate his support including project planning, experimental design, and commitment to the practical experimental work and providing me with this opportunity to undertake my PhD study in this department.

Thanks go to all the staff in the Department of Anatomical Sciences, in particular, Chris Leigh for his excellent technical assistance in all aspects of the laboratory work, Gail Hermanis for excellent technical assistance and proof reading, and Nadia Gagliardi and Tavik Morgenstern for their great patience, friendliness and technical support in histology, computing and digital imaging.

The staff of Adelaide Microscopy provided me with excellent and friendly technical support in electron microscopy and image analysis, for which I am grateful.

I would like to thank Professor Peter Blumbergs, head of the Neuropathology section, the Institute of Medical and Veterinary Science and all members of neuropathology research group for their friendly help during the project and Jim Manavis for providing me with generous advice in immunocytochemistry.

Thanks to the International Postgraduate Research Scholarships and the University of Adelaide Scholarship programs for supporting me during my study in Australia. I appreciate this opportunity to study at the University of Adelaide.

I would like to dedicate this thesis to my parents, my parents-in-law, my wife and son and my sister's family for their love and great support during my study. Especially I appreciate very much my wife and my son's tolerance of the busiest time of my life. I hope I can give them more love in the future.

PUBLICATIONS AND PRESENTATIONS

Publications:

1. Ghabriel MN, **Lu JJ,** Hermanis G, Zhu C and Setchell BP (2002). Expression of a blood-brain barrier-specific antigen in the reproductive tract of the male rat. Reproduction, 123:389-397.

2. Ghabriel MN, **Lu JJ**, Tadros R and Hermanis G (2004). A narrow time-window for access to the brain by exogenous protein after immunological targeting of a blood-brain barrier antigen. Journal of Comparative Pathology, 131: 52-60.

3. **Lu JJ**, Ghrbriel MN, Lim WH and Setchell BP. Effect of moderate injury on the expression of endothelial barrier antigen in endothelial cells of the testis and in the prostate of rat (completed and in the process of being submitted to " Reproduction").

4. **Lu JJ**, Gabriel MN, Magar H, Jones N, Cai Z, and Blumbergs PC. Expression of GLUT1 and EBA in endothelial cells of spinal cord grey matter vessels at the site of trauma and remote from the trauma site (In preparation for submission).

5. **Lu JJ**, Ghabriel MN, Jones N, Cai Z, Blumberg PC. Pathological changes in a rat model of sustained spinal cord compression injury: changes at the trauma site and remote from the trauma site (In preparation for submission).

Conference Abstract :

1. **Lu JJ**, Ghabriel MN, Jones N, Blumbergs P (2000). Expression of endothelial barrier antigen immunoreactivity in blood vessels following compression trauma in the rat spinal cord. Proceedings of the 5th Scientific Paralympic Conference, Sydney 2000, pp.40.

2. **Lu JJ**, Ghabriel MN, Jones N, Blumbergs P (2001). The blood-spinal cord barrier: alteration of an endothelial cell protein rostral and caudal to cord compression. Proceedings of the Australian Neuroscience Society, 12:168.

3. **Lu JJ**, Ghabriel MN, Hermanis G. and Setchell BP (2001). Testicular blood vessels express a blood-brain barrier-specific protein. Proceedings of the Satellite Meeting of the International Congress of Physiological Sciences, on Blood-Brain Barrier Mechanisms. From Molecule to Patient, Tasmania, August 2001, p. 40.

4. **Lu JJ**, Setchell BP, Ghabriel MN, Hermanis G and Zhu C (2002). Testicular endothelial cells express endothelial barrier antigen, previously thought to be specific to vessels in the central nervous system. Proceedings of the 12th European Workshop on Molecular and Cellular Endocrinology of Testis, The Netherlands, 6th –10th April 2002, 4b-10.

5. **Lu JJ,** Ghabriel MN, Tadros R, Hermanis G and Magar P (2002). Time course of opening and closure of the blood-brain barrier following immunological targeting of

the endothelial barrier antigen. Proceedings of Third Asia Pacific Symposium on Neural Regeneration, Perth, 2002, p72.

6. **Lu JJ,** Ghabriel MN, Tadros R and Hermanis G (2003). A narrow time window for opening of the blood-brain barrier in an immunological model. Proceedings of the Australian Neuroscience Society, 14 Poster 390.

7. Ghabriel MN, **Lu JJ**, Lim WH, Setchel BP (2005). Effect of moderate spinal cord injury on the expression of a barrier marker in endothelial cells of the testis and in the prostate of rats. Reproduction, Fertility and Development, 17 (supplement), P.130.

ABBREVIATIONS

ABC	avidin-biotin complex
ADC	apparent diffusion coefficient
AIDS	acquired immunodeficiency syndrome
ATP	adenosine triphosphate
cAMP	cyclic adenosine monophosphate
Anti-RECA-1	anti-rat endothelial cell antigen-1
BBB	blood-brain barrier
BSA	bovine serum albumin
BSB	blood-spinal cord barrier
BTB	blood-testis barrier
CAM	chorioallantoic membrane
CBF	cerebral blood flow
CNS	central nervous system
DAB	3.3'-diaminobenzidine tetrahydrochloride
DPBS	Dulbecco's phosphate-buffered saline
EAE	experimental allergic encephalomyelitis
EBA	endothelial barrier antigen
EC(s)	endothelial cell(s)
EM	electron microscope, electron microcopy
Gd-DTPA	gadolinium-diethylenetriamine penta-acetic acid
GM-CSF	granulocyte-macrophage colony stimulating factor

GFAP	glial fibrillary acidic protein
γGTP	γ-glutamyl transpeptidase
GLUT1	glucose transporter protein 1
HIV	human immunodeficiency virus
HIVE	human immunodeficiency virus encephalitis
HRP	horseradish peroxidase
HUVEC	Human umbilical vein endothelial cells
ICP	intracranial pressure
Ig	immunoglobulin
kDa	KiloDalton
IL-	interleukin-
LM	light microscopy
LET	*Lycopersicon esculentum tomato*
IR	Immunoreactive
mAb	monoclonal antibody
MAGUK	membrane-associated guanylate kinase
MDR	multidrug resistant
Mg	Magnesium
min	minutes
MRI	magnetic resonance imaging
MS	multiple sclerosis
MW	molecular weight
NHS	normal horse serum

Na^+-K^+-ATPase	Sodium and Potasium-ATPase
PBS	phosphate-buffered saline
P-gp	P-glycoprotein
Rpm	rounds per minute
TBI	traumatic brain injury
TER	transendothelial electrical resistance
TJ	tight junction
TNF-α	tumour necrosis factor-alpha
TNF-β	tumour necrosis factor-beta

CHAPTER 1

INTRODUCTION

Chapter 1 Introduction

1.1 What are the blood-brain and blood-spinal cord barriers ?

Microvessels in the central nervous system (CNS), which is formed mainly by the brain and spinal cord, have barrier functions which prevent the free exchange of some molecules from neural tissues to the blood stream or vice versa. These microvessels of the brain and spinal cord form the blood-brain barrier (BBB) and blood-spinal cord barrier (BSB) respectively (Moody, 2006). There is no published evidence that the BBB is different from the BSB, therefore in this account the term BBB will be used to refer to barrier vessels in the brain and spinal cord unless stated otherwise. The barrier function of these vessels is vital to the CNS because it maintains homeostasis that is essential for the normal function of the CNS. Numerous previous studies have shown that endothelial cells (ECs) of these CNS microvessels possess some special structural features, which facilitate their barrier function. In the meantime, these ECs have some specific transport systems to facilitate the transport of essential nutrients such as glucose and certain amino acids to the CNS.

1.2 Historical review of the blood-brain barrier

Historical perspectives of the BBB have been addressed in a number of reviews (Bradbury, 1993; Pardridge, 1999, 2003; Rapoport, 2000). The development of the concept of the BBB can be traced back to the turn of the twentieth century, when barrier properties of microvessels in the brain were first demonstrated experimentally by intravenous injection of a dye into animals. When Evans Blue was injected into the blood stream, tissues of the animal's body were stained with the dye, except the CNS.

This experiment suggested the presence of a barrier system, which prevented the dye from leaving the microvessels to enter the perivascular tissues (See Dermietzel and Krause, 1991). This initial finding led to the development of the barrier concept between the blood and the CNS and prompted researchers to further investigate brain microvessels.

Initially, there were conflicting views with regard to the exact anatomical location of the BBB. The lack of high-resolution electron microscopy (EM) led early researchers to first assume that the restriction ascribed to the BBB was in fact due to the lack of the extracellular space (Maynard *et al.*, 1957). After standard fixation, the extracellular space in the brain could not be observed. They assumed that the plasma membranes of neurons and glia would have been exposed to the dye that leaked from capillaries, but the absence of the dye from the brain was ascribed to the lack of penetration between these plasma membranes. However, this assumption could not explain the earlier observation of rapid transport of the dye solute into the brain when injected into the CSF (Krogh, 1946). This view also encountered a strong opposition from Davson and his colleagues on the basis of their observation in which central nervous tissue was exposed to polar solutes, labelled with radiotracers, either from the blood side or from the CSF side (Davson and Kleenman, 1961). Only in the late 1960s did researchers finally reach the agreement that the ECs of microvessels form the anatomical basis of the BBB.

The idea of the initial experiment using a tracer to study the morphology and barrier properties of the BBB has become a basic methodology for numerous subsequent

studies on the BBB under physiological and pathological conditions. However, along with the development of molecular and cellular biology, research into the BBB is advancing to a new era, the focus of which is the molecular and cellular mechanisms of the BBB. Studies at the molecular and cellular levels will provide further insight into the physiology and pathology of the BBB.

1.3 Structure of the blood-brain barrier

In contrast to microvessels in other organs, the ECs of brain capillaries with barrier properties possess unique structural features (Dermietzel and Krause, 1991; Joo, 1996), which contribute to their barrier function. Firstly, the number of cytoplasmic vesicles in ECs of the CNS is much lower compared with other organs (Reese and Karnovsky, 1967). Secondly, the interendothelial space of barrier vessels is sealed by continuous tight junctions (TJs) displaying high electrical resistance (Brightman and Reese, 1969; Dermietzel, 1975; Crone and Olesen, 1982). Thirdly, the capillary walls of the BBB are thinner than those of other microvessels.

1.3.1 Non-fenestrated ECs with low density of cytoplasmic vesicles.

The number of cytoplasmic vesicles in the ECs was quantitatively studied. The difference in the number of vesicles in the leaky and barrier vessels was obvious. It has been well accepted that the density of cytoplasmic vesicles is very low in vessels with barrier properties compared to that in non-barrier vessels. The relative low density of cytoplasmic vesicles in non-fenestrated ECs of barrier vessels suggests a low rate of transendothelial transport. This is generally considered to be a morphological constituent of the physiological BBB. The low density of vesicles in cerebral ECs was

first noted in classic HRP studies (Reese and Karnovsky, 1967; Brightman and Reese, 1969). Quantitative studies of vesicles containing HRP confirmed their low density. The density of brain EC vesicles recorded by a number of studies varied from 3 to 14 per μm^2, which is much lower than that of other tissues. The number of cytoplasmic vesicles in ECs of barrier vessels in the brain is one third lower than that in vessels of the area postrema and seven times lower than that of smooth muscle vessels (Frank et al., 1987). Using ultrathin serial sectioning and three-dimensional vesicle reconstruction, it was revealed that the densities of vesicular clusters and surface-connected vesicles were much higher in the area postrema, choroid plexus and skeletal muscle vessels than in BBB vessels (Coomber and Stewart, 1986). However, a more recent quantitative study comparing EC vesicular densities in nine tissues showed that the vesicular density of brain capillaries was significantly lower than that of all tissues examined except the testis and ovary (Stewart, 2000). Since both testicular and ovarian capillaries are highly permeable to proteins, this study demonstrated a weak correlation between low vesicle density and protein permeability.

The role of the vesicles in the permeablity of the BBB remains controversial. First, EM studies revealed that most vesicles in ECs other than those of the BBB are not self-limited, but are connected together by channels, which communicate with the extracellular fluid either on the blood or interstitial side. These vesicles are therefore thought to be invaginations of the plasma membrane, which are still in contact with the cell surface (Bundgaard *et al.*, 1979). Quantitative studies of the vesicles in the brain capillaries of the frog with two different fixation methods showed different vesicle densities in the same tissue. Vesicles in the frog brain were 3-4 times fewer

after acetone fixation followed by glutaraldehyde fixation than those present after straight glutaraldehyde fixation. This result suggested that the vesicles might be created by glutaraldehyde fixation. Experimental results also suggested little role for the intracellular vesicular system in transendothelial movement of hydrophilic solutes. Furthermore, there is also evidence that opening of the barrier in osmotic shock is due to the separation of the TJ (Brightman et al., 1973). Another evidence for the lack of correlation between vesicular density and permeability is the confirmation that the vesicles in barrier ECs are in fact membrane bound invaginations (Gordon and Essner, 1985). Moreover, although the endothelium of brain capillaries in the hagfish contains very numerous apparent vesicles and tubules, it halts HRP movement (Bundgaard *et al.*, 1979) and has very low permeability to polyethelene glycols (Bundgaard and Cserr, 1981).

Broadwell has critically studied the possible role of transcytosis at the BBB. When the luminal surface of the endothelium was exposed to HRP some endocytosis of HRP occurred. However, there was no endocytosis of HRP from the abluminal surface when the tracer was presented in the interstitial fluid by ventriculo-cisternal perfusion. The fate of intraendothelial HRP was not exocytosis at the abluminal membrane but rather, histolysis by enzymes present in the endosomes and lyzosomes (Broadwell, 1989).

Results from another study suggest that the transcytoplasmatic vesicles may be related to the permeability of the BBB (Coomber and Stewart, 1986). In that study, the vesicles from leaky and non-leaky vessels were reconstructed using three dimensional

approach and ultrathin sectioning methods. The vesicles were classified as to whether they were attached to other vesicles (fused), connected to Golgi apparatus or endoplasmic reticulum (tubule-connected), open to vessel lumen or ablumen (surface-connected) or isolated in the cytoplasm (free). The densities of tubule-connected vesicles and free vesicles were the same in leaky and BBB vessels suggesting that these vesicles are unlikely to be related to vascular permeability. Vesicular clusters and surface-connected vesicles were found in much higher densities in the area postrema, choroid plexus, and skeletal muscle vessels than in BBB vessels. Single-vesicle transendothelial channels were found in attenuated endothelia of the area postrema and choroid plexus. The results from that study support the hypothesis that endothelial vesicles play a role in vascular permeability, possibly by transient fusion of vesicle clusters to the plasmalemma, to form transendothelial channels (Coomber and Stewart, 1986).

1.3.2 Tight junctions

Tight junctions (TJs) between two adjacent ECs form the fundamental basis of the BBB. The TJ is formed by the fusion of the two adjacent plasma membranes. There is fusion at the TJ, rather than loose contact, between two plasma membranes as evidenced by the fact that the distance between the cytoplasmic face of the membranes of the adjoined cells is less than the summed widths of two cell membranes (Reese and Karnovsky, 1967; Brightman and Reese, 1969). The characteristic fusion between two membranes contributes significantly to the tightness of the junction. In the biochemical sense, the TJ is formed of a belt of anatomosing strands of proteins and lipids. In conventional ultrathin sections, the TJ appears to form a pentalaminar arrangement

that results from the fusion of the external leaflets of the membranes of the partner cells.

Tight junctions have been morphologically studied using freeze-fracture and ultrathin sectioning techniques (Tani *et al.*, 1977; Nagy *et al.*, 1984; Sedlakova *et al.*, 1999). In freeze-fracture replicas, the BBB TJs are characterized by the highest complexity found in the vasculature (Nagy *et al.*, 1984). In addition, the P-face association with protein particles is high in the BBB (55%) compared to that observed in the P-face of ECs of the fenestrated vessels (10%).

The TJs not only appear morphologically tight, but also they are functionally tight, preventing the passive paracellular movement of ions and other molecules. The restriction to the ion movement is visible with ionic lanthanum (Bouldin and Krigman, 1975) and can be measured by the low conductance and high electrical resistance across epithelium or endothelium monolayers in situ and in vitro. Crone and Olesen (1982) first measured the electrical resistance of pial capillaries in the frog by measuring the decrement in transmural potential difference with the distance from a site at which current was microinjected (Crone and Olesen, 1982). The resistance was estimated as 1900Ω cm^2. Based on a different experiment, the average of the true resistance however was estimated to be about 3000Ω cm^2 and the arterial microvessels are rather tighter than the venous microvessels (Butt and Jones, 1992). The high transendothelial electrical resistance (TER) reflects low ion transport across the BBB. The BBB permeability to the major monovalent ions, Na^+, Cl^- and K^+ and the divalent calcium is about 1.4, 0.9, 13.5×10^{-7} and 5×10^{-8}cm s^{-1} respectively, which is up to

500-fold less than those at the choroid plexus epithelium (Smith and Rapoport, 1986; Tai *et al.*, 1986).

The hydrophobic cell membrane organization of the TJ restricts the lateral movement of hydrophilic molecules such as proteins between luminal and abluminal membranes of ECs across the junction. Electron microscopy reveals that in normal conditions, the passage of proteins such as HRP (MW 40,000) (Reese and Karnovsky, 1967) and microperoxidase (MW 2000) (Reese *et al.*, 1971; Bundgaard *et al.*, 1981) from the blood to the brain is prevented by TJs. Numerous investigations also showed that brain capillaries are also typically impermeable to albumin (MW 60,000) and myofer (MW 7800) (Dermietzel and Krause, 1991).

The polarity of ECs of the BBB is a very important functional and physiological feature of the TJ. The polarity has been demonstrated both by localization of enzymes and other special molecules to either the luminal or abluminal plasma membrane and by eliciting asymmetric transport activity. For example, alkaline phosphatase occurs particularly in the luminal plasma membrane (Kreutzberg and Toth, 1983; Vorbrodt *et al.*, 1983). The enzyme is especially active in developing cerebral capillaries. It is present in the basal membrane of the choroidal epithelium but not in the fenestrated capillaries of the choroids plexus. In contrast, Na^+-K^+-ATPase is particularly dense in the abluminal plasma membrane of the cerebral endothelium (Firth, 1977; Betz *et al.*, 1980). This enzyme actively transports potassium ions out of the cerebral interstitial fluid (Bradbury and Stulcova, 1970; Goldstein, 1979) and may, via Na^+ ion transport in the opposite direction, lead to a slow production of cerebral interstitial fluid. Lipids

also show a polar distribution pattern in the BBB. The possible function of this lipid polarity for BBB mechanism is the generation of a suitable lipid environment for polar distributed membrane proteins and the generation of two plasma membrane domains with different biophysical properties and permeabilities (Tewes and Galla, 2001).

Polarity provides the necessary vectoriality for substances to be transported across epithelia or endothelia towards or away from the lumen. Therefore, the polarity of the endothelium of the BBB implies that the cerebral endothelium has the potential for active transcellular transport. In other words, TJs and polarity are not static features of cells, rather they represent highly dynamic arrangements of molecules in the plasma membrane that are sensitive to the composition of the extracellular matrix, contacts with neighboring cells, growth and differentiation factors, hormones, pharmacological agents and cell cycle stages (Cereijido *et al.*, 2000).

1.4 Other components of the blood-brain barrier

1.4.1 Pericytes

Pericytes are polymorphic, elongated, multibranched periendothelial cells that vary in their degree of envelopment of ECs in the microvasculature. Pericytes are abundant in the microvasculature of the CNS and are an important cellular constituent of the BBB. They share a common basement membrane with capillary ECs (Carlson *et al.*, 1978). In isolated brain capillary preparations, there is approximately one pericyte for every three ECs, and pericytes cover 22-30% of the cerebral microvascular circumference (Frank *et al.*, 1987). However, for different organs the coverage by the pericytes of the circumference of microvessels varies. In the retina, pericytes cover the vessel

circumference more extensively than in cerebral microvessels (Frank *et al.*, 1987). The substantial quantitative difference in pericyte coverage of the microvessel circumference between the retinal and cerebral microvessels may have important implications for normal and pathological microcirculatory dynamics in these two organs (Frank *et al.*, 1987). The in situ ratio of pericytes to ECs and the degree of the endothelial area covered by pericytes appears to be related to the tightness of the blood vessels and the level of microvascular blood pressure (Frank *et al.*, 1987; Shepro and Morel, 1993). Theoretically, the greater the pericyte number and coverage, the better the microvascular barrier: retina> lung >skeletal muscle >cardiac muscle> adrenal gland, and the higher the capillary and venular blood pressure (Shepro and Morel, 1993).

The pericyte may have a spherical cell body with a prominent nucleus (Lafarga and Palacios, 1975). Pericytes have abundant electron dense lysosomal particles in their cytoplasm (Farrell *et al.*, 1987). They display considerable heterogeneity between the CNS and other tissues. Cultured bovine retinal and brain pericytes are different in their growth patterns, glucose dependency and morphology (Wong *et al.*, 1992). The enzyme, γ-glutamyl transpeptidase (γ-GTP), a BBB marker, is also expressed by the pericytes (Risau *et al.*, 1992).

The function of pericytes at the BBB is not fully understood. Pericytes are thought to be contractile cells and a smooth muscle analogue. Studies in vitro generally support the view that the pericytes have a contractile function as contraction of bovine retinal pericytes in culture was observed (Kelley *et al.*, 1987). In vitro studies also showed

that the contraction of pericytes responds to the Mg^{++} ATP and receptor-based histamine or angiotensin II but not to the GTP, pyrophosphate or beta, gamma-methylene ATP (Das *et al.*, 1988).

Contractile cells such as smooth muscle cells express α-actin isoform. In vitro studies showed that retinal pericytes in culture produce abundant α-smooth muscle specific-actin (DeNofrio *et al.*, 1989). However, in brain pericytes culture, only a small portion of pericytes (0-10%) was found to express α-smooth muscle actin (Verbeek *et al.*, 1994). The α-actin gene is found to be expressed in brain capillary pericytes grown in cell culture (Herman and D'Amore, 1985). However, some in vivo studies failed to detect the expression of α-actin mRNA or α-actin isoform in capillary pericytes in the retina and brain (Nehls and Drenckhahn, 1991; Boado and Pardridge, 1994) while using electron microscopy and monoclonal antibody labelled with colloidal gold, Skalli and his coworkers confirmed the existence of vascular smooth muscle actin within the microfilamentous bundles (stress fibers) of pericytes in vivo (Skalli *et al.*, 1989). Smooth muscle specific microfilaments are only detected in a minority of pericytes in the brain, although they are distributed widely in intestinal pericytes. Pericytes also express receptors for endothelin (Dehouck *et al.*, 1997) and a variety of vasoactive amines, such as vasoactive intestinal peptide (Ferrari Dileo *et al.*, 1996), vasopressin (van Zwieten *et al.*, 1988) and angiotensin II (Ferrari-Dileo *et al.*, 1991) indicating that pericytes may be involved in regulating the blood flow in the microcirculation of the CNS.

CNS pericytes have also been regarded as phagocytic cells and form the second line of defence of the BBB. One of the well-known features of the macrophages is their

uptake ability for soluble and small molecules in addition to their phagocytic activity. It has been shown that cerebral capillary pericytes actively took up HRP after cold injury to the brain (Cancilla *et al.*, 1972). An electron microscopic study on human brain oedema associated with brain tumors, brain trauma and congenital malformation showed that brain pericytes exhibited phagocytic activity as well as remarkable oedematous changes (Castejon, 1984). Phagocytic pericytes contained ingested erythrocytes, suggesting that pericytes might play some role in oedema resolution (Castejon, 1984). One of the remarkable structural features of macrophages is the presence of lysosomes. Pericytes have been shown to contain notable lysosomes and inclusion bodies, which increase in number upon tissue injury and with age. Moreover, pericytes have also been reported to express numerous marker components of macrophages. Nearly every macrophage marker component investigated has been found to be expressed in pericytes under some conditions, these include complement receptor-3 (CR3) (Sasaki *et al.*, 1996).

1.4.2 Astrocytes

Astrocytes are intimately associated with brain capillaries. Astrocytes surround with their endfeet 80-95% of the brain capillary circumference (Wolff, 1970) and their endfeet are only separated from the plasma membrane of ECs by the basal lamina. Thus, astrocytes are suggested to be the cell member that regulates BBB properties. It is now generally accepted that astrocytes in the developing brain are responsible for the induction and maintenance of TJs in cerebral ECs as well as other features of brain barrier mechanisms, although this evidence has been challenged (Abbott *et al.*, 2006) . This evidence includes either transplantation of avascular tissues into the developing

brain (Stewart and Wiley, 1981) or in vitro culture of isolated cerebral ECs in the presence or absence of astrocytes or astrocyte conditioned medium (Tao-Cheng and Brightman, 1988; Rubin *et al.*, 1991).

The first well-known in vivo evidence came from the study by Stewart and her colleagues in 1981. When quail embryonic brain fragments were transplanted to the chick embryonic coelomic cavity, and quail embryonic mesoderm fragments to the chick embryonic brain, the host blood vessels derived from the coelomic cavity were found to vascularise the transplanted brain tissues and these blood vessels gained barrier function. In contrast, blood vessels derived from the brain, vascularised the transplanted mesodermal fragments and these blood vessels lost BBB features (Stewart and Wiley, 1981).

The study by Janzer and Raff (Janzer and Raff, 1987) provided further evidence that astrocytes can induce barrier features in non-neural ECs. When injected into the rat eye anterior chamber or the chick chorioallantoic membrane (CAM), purified type I astrocytes formed aggregates on the surface of the iris, or grew on chick CAM. The astrocyte aggregates were able to exclude the BBB tracer Evans blue, indicating that capillaries and venules in the aggregates had a barrier function. Thus, they concluded that astrocytes were responsible for inducing non-neural ECs to form barrier vessels (Janzer and Raff, 1987). However, the interpretation of the results of this study encountered a challenge in a later study by Holash *et al.* (Holash *et al.*, 1993b). They argued that the lack of tracer in the graft is not really because of the low permeability of vessels but due to the poor vascularization of the grafts. This argument is based on

their finding that astrocytes implanted into the anterior chamber form poorly vascularized grafts and grafting of cells to the CAM induces an extensive inflammatory response which could virtually affect the permeability of blood vessels. They claimed that the CAM grafting experiments performed by Janzer and Raff was not reproducible and astrocytes did not induce barrier features in CAM vessels (Holash *et al.*, 1993b).

There is some in vivo evidence that astrocytes do not influence the induction of BBB properties. In transplanted superior cervical ganglia, the host astrocytes migration occurred much later than the host endothelial proliferation and re-perfusion, which indicated that astrocytes were not responsible for inducing barrier functions in ECs (Rosenstein and Brightman, 1986). More recently, when superior cervical ganglia autografts were transplanted to the brain fouth ventricle or parenchyma of the cortex, the host astroglia migrate to the autografts but no typical end-feet of the astrocytes could be found in the autografts, and the host astrocytic responses to the graft tissues occurred later than the host ECs response suggesting that the astrocytes are not responsible for the induction of the barrier (Rosenstein *et al.*, 1989).

In vitro studies however appear to provide more consistent results than the in vivo studies. Numerous studies in vitro reported that TJs could form in ECs in the presence but not in the absence of astrocytes (Arthur *et al.*, 1987). The co-culture of cerebral endothelial cells with astrocytes has been shown to stimulate the ECs to express some specific markers of barrier endothelial cells, such as α-glutamyl transpeptidase (DeBault and Cancilla, 1980; Meyer *et al.*, 1991; Tontsch and Bauer, 1991), alkaline

phosphatase (Meyer *et al.*, 1991) and Na^+-K^+-ATPase (Tontsch and Bauer, 1991). The presence of astrocytes also leads to the TJs between the ECs being of greater length, width and complexity whereas gap junctions were suppressed (Tao-Cheng *et al.*, 1987). The enhancement of TJs could also be induced by adding astrocytes-conditioned medium to EC culture, indicating that astrocytes secrete factor(s) that influence the differentiation of brain ECs in culture (Arthur *et al.*, 1987). Treating brain ECs with astrocytes-conditioned medium, increased the TER by twofold, although the TER did not reach the level observed in vivo (Rubin *et al.*, 1991). Interestingly, increasing cAMP levels in endothelial cell culture already treated with astrocytes-conditioned medium, resulted in a significant change in cell morphology and a rapid increase in TER (Rubin *et al.*, 1991). C6 glioma cells, a commonly used substitute for astrocytes, could also increase the TER of brain ECs in culture by 200-440% (Rauh *et al.*, 1992).

There is accumulating evidence to suggest that the astrocytes can influence the phenotype of ECs at least in vitro. There are many BBB specific proteins and enzymes in the endothelial cells. In vitro studies showed that the expression of many BBB specific markers can be induced or triggered by astrocytes. γGTP is regarded as a BBB marker as it is abundant in ECs of the brain. It is not expressed by other ECs at a detectable amount. Astrocytes could increase the expression of γGTP by 34% when cultured with ECs (Tontsch and Bauer, 1991). HT7 is a BBB marker in the chick. Astrocytes-conditioned medium was shown to be able to induce the expression of HT7 in ECs of chorioallantoic vessels (Janzer *et al.*, 1993). Both in vivo and in vitro studies showed that human umbilical vein ECs (HUVECs) can acquire BBB properties under

certain conditions, when transplanted into the rat brain or cultured in astrocytes conditioned medium (Akiyama *et al.*, 2000). When co-cultured with astrocytes or treated with astrocyte-conditioned culture medium, HUVECs expressed some BBB features such as the formation of tight junctions, increased TER, high activity of γGTP and expression of GLUT1 (Akiyama *et al.*, 2000).

On the other hand, some authors argued that the ECs used for these experiments are always from adult brain which already possesses characteristics of adult cerebral ECs. So far no experiments have been done using ECs from foetal brain because of technical difficulties. Therefore, these studies only demonstrated the maintenance effects of astrocytes (Holash *et al.*, 1993b). Several studies also showed that there is very limited contact between astrocytes and ECs in immature brain (Caley and Maxwell, 1970; Rakic, 1971). Therefore it is not feasible to propose that astrocytes are able to induce the BBB properties. The mechanism by which the astrocytes act on the ECs is still not known. It is not clear how astrocytes influence brain capillary ECs. As mentioned above, astrocytes-conditioned medium is able to enhance BBB characteristics in cultured cerebral capillary ECs, which suggests that astrocytes may produce factors to influence ECs. However, so far nothing is known about any factor(s) secreted by astrocytes which is (are) responsible for the induction and maintenance of the BBB. A systematic study is needed to elucidate the relationship between astrocytes and blood vessels in the immature brain in parallel with permeability experiments to test the different types of the barrier mechanisms.

1.5 Molecular anatomy of the blood-brain barrier

In addition to the unique structure of brain and spinal cord vessels described above, many molecules have been identified and found to be specifically present in ECs of the BBB and the BSB. Interestingly, most of these molecules are present only at ECs with barrier properties but not expressed or only weakly expressed by those without barrier properties. It is now generally agreed that the specific molecular and structural properties of CNS ECs and their morphological adjuncts facilitate the unique barrier function of central neural vessels (Cervos Navarro *et al.*, 1988; Dermietzel and Krause, 1991). Thus, these specific molecules and structures are used as markers for the BBB and BSB. Molecular markers found so far include the endothelial barrier antigen (EBA), glucose transporter protein GLUT1, activated lymphocyte antigen recognized by MRC OX-47 antibody and γGTP (Dermietzel and Krause, 1991). Some molecules are transporters while others are receptors. The precise function of these molecules, with the exception of the brain glucose transporter, remains unknown.

1.5.1 Endothelial barrier antigen (EBA)

The endothelial barrier antigen (EBA), a relatively new marker, was first recognized by a monoclonal antibody, which was raised against a rat brain microvessel preparation in 1987 (Sternberger and Sternberger, 1987). It was identified as a protein triplet with 30, 25 and 23.5 kDa located at the membrane surface of the ECs. It is generally agreed that EBA is a protein selectively expressed by ECs of microvessels with barrier properties such as the BBB, BSB, blood-retinal barrier, and blood-optic nerve barrier (Sternberger and Sternberger, 1987). Blood vessels without barrier functions in the brain and in other peripheral body organs, including the heart,

muscles, intestines and liver are not immunoreactive for EBA (Sternberger, and Sternberger 1987). Thus, EBA has been considered as a 'barrier protein' of the BBB. Surprisingly however, several non-barrier vessels in the eye, in the ciliary processes and inner part of the choroids, also express the antigen. Non-barrier vessels of the sclera, conjunctiva, dura mater, the outer vessels in the choroid and ciliary body are negative for EBA (Lawrenson *et al.*, 1995a). Although non-barrier vessels in other body organs generally do not express this protein (Sternberger and Sternberger, 1987; Lawrenson *et al.*, 1995a). Some unidentified cells in the spleen and Langerhan's cells of the epidermis are immunoreactive for EBA. ECs of the sciatic nerve are either negative or only weakly immunoreactive for EBA (Lawrenson *et al.*, 1995b). These findings seem to be not in full agreement with the concept that the EBA is a barrier protein. EBA may have wider tissue distribution and more diverse physiological role than currently being appreciated.

The ontogenesis of EBA expression has not been studied in detail. Since the molecular composition and structure of EBA have not been characterized, so far there is still no report available regarding the gene expression of EBA during development and in the adult. However, it has been revealed that no EBA immunoreactivity (IR) was found in rat brain vessels at embryonic day 18, when the BBB was already impermeable to injected macromolecular tracer. Its expression started at postnatal day 7 and was sustained in the adult rat. (Kimelberg, 1995; Cassella *et al.*, 1996).

The regulation of EBA expression has not been well addressed in previous studies. As mentioned above, it is generally agreed that astrocytes may play an important role in

the induction of the BBB during development although there are conflicting views. The time course of EBA immunoreactivity in rat brain ECs correlates well with the developing investment of astrocytic end-feet in cerebral capillaries. In the foetal brain, few capillaries are covered by astrocyte end-feet but by postnatal day 10 over 90% of the capillary surface is covered by astrocytes. Thus it has been hypothesized that astrocytes may be able to induce the expression of some BBB markers including EBA. This hypothesis was tested by the in vivo injection of the anti-metabolite 6-aminonicotinamide which induces severe degeneration of the astrocytes but leaves microvessels intact. Interestingly, after injection, astrocytes were damaged but the ECs continued to express EBA, suggesting that the astrocytes may not function as a regulator for EBA expression (Krum et al., 1997). Accordingly, at 28 days after ischaemic brain injury, some newly formed brain vessels showed EBA expression but were not surrounded by cells reactive for the glial fibrillary acidic protein (GFAP), indicating that the presence of astrocytes is not critical for EBA expression (Nishigaya *et al.*, 2000). Furthermore, both pial and iris vessels, which have physiological properties nearly identical to CNS vessels, also have strong EBA expression although they are not normally contacted by astrocytic end-feet. In experimental conditions, direct injury to neurons and astrocytes resulted in a rapid reduction of EBA expression during the first 3 weeks. However, the immunoreactivity of EBA began to recover by 4 weeks post-injury in areas that had minimal numbers of neurons and astrocytes (Krum *et al.*, 1997). Taken together, the results of previous studies suggested that the influence of astrocytes may be important for the induction of EBA expression during development but not for its maintenance at the BBB in the adult.

Although the significance of EBA in the normal function of the BBB is unknown, EBA immunoreactivity appears to correlate with an intact BBB. In pathological conditions of the BBB such as cerebral oedema, EBA expression is lost, but this loss is restored along with the reconstitution of the BBB. For example, the temporal loss of EBA expression has been reported in stab wound brain injury, compression spinal cord injury and other pathological conditions associated with brain oedema and inflammation (Sternberger *et al.*, 1989; Perdiki *et al.*, 1998 ; Nishigaya *et al.*, 2000). But its expression recovers along with reconstitution of the BBB and the disapperance of oedema in injured tissue. In experimental allergic encephalomyelitis (EAE), disruption of the BBB has been documented by numerous studies (Juhler *et al.*, 1984, 1986; Claudio *et al.*, 1990; Hawkins *et al.*, 1991). EBA expression is abolished in blood vessels surrounded by inflammatory cells during experimental allergic encephalomyelitis. EBA expression recovers along with the reconstitution of the BBB but not in residual inflammatory areas (Sternberger *et al.*, 1989). In brain angiogenesis induced by stab wound, regenerating vessels do not stain or only show weak staining for EBA even after 10 days of postoperative healing (Rosenstein *et al.*, 1992). In moderate or severe compression injury to the spinal cord, EBA expression in the ECs is remarkably reduced at 4 days after the injury but is restored at 9 days after injury (Perdiki *et al.*, 1998). In rat cerebral ischemia, both qualitative and quantitative studies demonstrated a decrease of EBA expression in brain endothelium (Bart *et al.*, 2000; Nishigaya *et al.*, 2000), but immunoreactivity started to recover at day 14 after the injury (Nishigaya *et al.*, 2000). The possible mechanism of the down-regulation of EBA after pathological insults is still not clear. The decrease and/or disappearance of

EBA are most likely due to its degradation in vivo, alteration of EBA structure or reduced production of the protein as a result of the injury.

Although a remarkable reduction of EBA expression in different pathological conditions associated with brain oedema has been reported, it is not clear whether the reduction of EBA is a primary or a secondary event to pathological insults. A recent study in our laboratory elegantly demonstrated that EBA reduction might be the primary event which can lead to wide opening of BBB following pathological insults (Ghabriel *et al.*, 2000). In this study, anti-EBA monoclonal antibody was intravenously injected into the rat to induce immunological targeting of EBA. The injected antibody was subsequently found to be bound to ECs. A tracer study using HRP and endogenous albumin showed that the antibody injection caused a wide and immediate opening of BBB. This finding provided direct evidence that EBA plays a putative role in the maintenance of the normal barrier function of the BBB (Ghabriel *et al.*, 2000).

1.5.2 Glucose transporter 1 (GLUT1)

The glucose transporter protein is another specific marker of the BBB that has been well characterized by previous studies. Under normal conditions, glucose is the primary metabolic fuel for the brain. Since the brain cannot store or synthesize glucose, a constant glucose supply is essential to maintain normal cerebral development and function. The glucose transporter protein present at the ECs facilitates the transport of glucose from the blood to the brain parenchyma. To date, seven genes encoding homologous but distinct proteins, and one pseudogene that does not encode protein, have been identified and designated GLUT1-7, based on the order

in which they were cloned (Dermietzel and Krause., 1991; Maher *et al.*, 1993; Bell *et al.*, 1993). Three of these proteins, GLUT 1, 3 and 5, have now been identified as cell-specific transporters in the mammalian brain, and GLUT1 is most abundant in the endothelium of brain vessels. The biochemical properties, distribution and functional role of these proteins have been intensively studied previously. This review will mainly focus on the GLUT1 transporter protein.

GLUT1 is the predominant, if not exclusive, facilitative glucose transporter in brain microvascular ECs. It is a 492 amino acid protein and is detected in whole brain homogenate as two molecular mass forms of 55 kDa and 45 kDa, which are encoded by a single gene but differ in their extent of glycosylation. In humans the gene is assigned to a chromosomal location at chromosome 1p33. The GLUT1 mRNA sequence is highly conserved in the different species studied, and shows a range of 93% to 78% similarity to the human sequence (Drews, 1998). The density of GLUT1 in the brain is congruent with local cerebral glucose utilisation and capillary density (Zeller *et al.*, 1997). GLUT1 is detected in cerebral microvessel ECs, choroidal epithelium and ependymal cells but is absent from the endothelia of the circumventricular organs and choroid plexus which do not exert barrier properties (Dick *et al.*, 1984; Kalaria *et al.*, 1988; Gerhart *et al.*, 1989; Boado and Pardridge, 1990; Harik *et al.*, 1990; Farrell and Pardridge, 1991; Rahner-Welsch *et al.*, 1995; Dobrogowska and Vorbrodt, 1999). GLUT1 is also expressed by some astrocytes and oligodendrocytes but not by microglial cells (Devaskar and deMello, 1996; McCall *et al.*, 1996). The cellular distribution of the two GLUT1 isoforms is different. The 55 kDa form of GLUT1 is expressed at the BBB whereas the lower molecular weight

form of GLUT1 is detected in the choroid plexus epithelium, astrocytes and oligodendrocytes (Kumagai *et al.*, 1994; Yu and Ding, 1998).

GLUT1 immunoreactivity has distinct cellular distributions in different tissues. On the epithelium of the choroid plexus, it is restricted to the basolateral surfaces whereas on the ependymal epithelium lining the third ventricle, it is distributed on the apical surface (Farrell *et al.*, 1992). Moreover, there are varied reports about the subcellular distribution in brain capillaries. Farrell *et al.*,(1991) reported an asymmetrical distribution of GLUT1 on rat brain capillary endothelial luminal and abluminal membrane, with distribution of immunoreactivity on luminal membrane, abluminal membrane and cytoplasm averaging 12%, 48%, and 40%, respectively. The observations that about 40% of the endothelial glucose transporter is contained within the cytoplasmic compartment, and the distribution of transporter being asymmetric on luminal and abluminal membranes, are consistent with transporter recruitment; a mechanism postulated for acute modulation of glucose transport. The relocation of transporter molecules from a cytoplasmic compartment to the luminal plasma membrane (the transporter recruitment hypothesis) could produce a rapid up-regulation of BBB glucose transport. Similarly, in another report on rat brain capillaries, 50% of the transporter was abluminal, 36% luminal, and 14% cytoplasmic (Dermietzel and Krause, 1991). Cornford reported that in rabbit brain capillary endothelia, there was a three to four-fold greater abundance of transporter molecules on the abluminal than on the luminal membranes of brain ECs (Cornford *et al.*, 1993b). A more recent quantitative immunogold study of GLUT1 distribution in mouse brain also showed an approximately three-fold higher immunolabelling density of the abluminal than the

luminal plasma membrane of ECs (Dobrogowska and Vorbrodt, 1999). In human brain, asymmetric distribution of GLUT1 has also been documented, with the ratio of luminal to abluminal being 1:3 (Cornford *et al.*, 1994a).

In contrast to reports of asymmetrical distribution of GLUT1 some studies demonstrated symmetrical distribution of GLUT1 in luminal and abluminal membranes. For example, in canine brain, Gerhart *et al.* (1989) reported a symmetrical distribution of GLUT1 epitopes between the luminal and abluminal membranes. A lower proportion of cytoplasmic epitopes (9%) was seen in the canine brain endothelia. In isolated bovine microvessel plasma membranes, the distribution of GLUT1 between the luminal and abluminal membranes is also symmetrical (Lee *et al.*, 1997). Another EM study of the subcellular distribution of GLUT1 in rat brain also showed that the distribution of GLUT1 is symmetrical on both the luminal and albuminal membranes of the vessels (Bolz *et al.*, 1996). The reason for the discrepancy between these studies is still not clear.

Both in vivo and in vitro studies demonstrated up-regulation of GLUT1 immunoreactivity in brain vessels during brain development in the rat and rabbit (Cornford *et al.*, 1994a; Bolz et al., 1996; Devaskar and deMello, 1996). The upregulation in vivo has been suggested to occur in two phases. Initially, during early intrauterine development, there is four-fold increase in the density of the GLUT1 transporter in brain vessel profiles, and later, from E 19 to adult life, there is further two-fold increase. This increase in density was suggested to be due to an increase in absolute amount of GLUT1 protein (Bolz *et al.*, 1996). A postnatal study on the

distribution of GLUT1 in rats showed a complete congruence between the regional relative capillary density and the density of GLUT1 staining in all BBB structures during postnatal development (Zeller *et al.*, 1996). Relative capillary density mainly increases between postnatal days (P) 10 and P20 in the grey matter. In contrast, investigation of the circumventricular organs and subfornical organ showed some GLUT1 staining at birth but the immunoreactivity decreased at P10 and P15, and had disappeared in the adult animals (Zeller *et al.*, 1996). 55-kDa GLUT1 levels remains low during the early postnatal period but increase during the next two weeks, coincident with the increases in BBB glucose transport. Immunogold electron microscopic analysis revealed a similar pattern of BBB glucose transporter expression in developing rabbit brain (Cornford *et al.*, 1993a).

Ontogenesis and distribution of the GLUT1 expression in the rat neural tube has been well studied. As early as E11, before blood vessels invade the neuroectodermal tube, GLUT1 immunoreactivity (IR) is already detectable in the perineural plexus of vessels and in most of the vascular endothelium of the embryo. GLUT1 IR is also evident in the neuroectoderm (Harik *et al.*, 1993) although the neuroectodermal epithelium gradually loses GLUT1 expression. At about E16, GLUT1 is no longer detectable in most of the neuroectodermal epithelium while CNS microvessels increase their GLUT1 IR. By birth, GLUT1 IR in the CNS is restricted to the endothelium, the epithelium (but not the endothelium) of the choroid plexus, and tanocytes. This cellular distribution of GLUT1 does not change much between birth and senescence despite considerable postnatal brain development and the increased brain capillary density (Harik *et al.*, 1990). Cassella *et al.* (1996) further confirmed that GLUT1 IR in

cortical microvessels started from E 16 and this expression continues until the adult age is reached (Cassella *et al.*, 1996). The relatively late expression of GLUT1 during early neurogenesis suggests that while CNS factors may not have a role in the induction of the high expression of GLUT1 in CNS endothelium, such factors are probably important in maintaining the high level of GLUT1 in these endothelia.

GLUT1 expression can be regulated by some physiological and pathological conditions, in particular, the increase or decrease in cerebral glucose metabolism. Following chronic changes in blood glucose levels, altered glucose transport at the BBB and changes in the glucose transporter protein density can be observed. In chronic hyperglycaemia cerebral glucose utilization in rat brain is increased but glucose transporter GLUT1 is decreased (Duelli *et al.*, 2000). A remarkable decrease in the expression of GLUT1 was shown by Pardridge et al. after 1 week of hyperglycaemia using quantitative immunoblotting technique of cerebral microvessel preparation (Pardridge *et al.*, 1990b). Down regulation of BBB glucose transporter protein was also documented in the hyperglycaemic non-obese diabetic mouse (Harik *et al.*, 1990).

Conflicting findings however were reported in the genetically diabetic *db/db* mouse (Vannucci *et al.*, 1997). Genetically diabetic *db/db* mice with hyperglycaemia and obesity show a significant reduction of cerebral glucose utilisation. Up-regulation of BBB GLUT1 expression and mRNA were reported by some investigators (Maher *et al.*, 1993) but these results were not confirmed by other studies. No changes of GLUT1 expression were observed in these mice although mRNA level of GLUT1 was

regionally increased (Vannucci *et al.*, 1997). In contrast, decreased GLUT1 expression in chronic hyperglycaemia, accompanied by an increase in glucose utilisation was reported recently (Duelli *et al.*, 2000).

In chronic hypoglycaemia an up-regulation of GLUT1 mRNA was found (Cornford *et al.*, 1995). Consistent with enhanced glucose uptake, the expression of GLUT1 and GLUT1 mRNA at the BBB is increased in hypoglycaemia (Kumagai *et al.*, 1994). A more recent study on hypoglycaemia induced by insulin, demonstrated a 25-45% increase in regional BBB glucose uptake (Simpson *et al.*, 1999), in addition to a 23% increase in the 55 kDa GLUT1 isoform expression, with a greater increase in luminal GLUT1, which indicated a redistribution of GLUT1 to luminal membrane of ECs. GLUT1 mRNA also increased two-fold. However, no change was observed in the expression of the 45 kDa GLUT1 isoform.

Studies of glucose transporters in human neurodegenerative diseases have shown a down-regulation of GLUT1 level in the brain. Patients with Alzheimer's disease have shown a marked decrease in the glucose transporter protein in the brain (Harik, 1992; Simpson *et al.*, 1999). The reduction of reactivity was selective in the cerebral neocortex and hippocampus, regions that are severely affected in Alzheimer's disease, but not in the putamen or cerebellum, which are not affected to a major extent in this disease (Harik, 1992). Studies of cerebral glucose transporter expression in human immunodeficiency virus (HIV) infection, demonstrated that GLUT1 level in grey and white matter regions increased with human HIV infection without neuropathology when compared to normal controls, and decreased to baseline with HIV encephalitis

(HIV) (Kovitz and Morgello, 1997). These findings may parallel glucose hypermetabolism found in patients with early acquired immunodeficiency syndrome (AIDS) dementia complex and glucose hypometabolism in patients with late clinical stage dementia (Rottenberg *et al.*, 1987). However, studies of the GLUT1 expression after traumatic brain and spinal cord injury are sparse. The molecular mechanism of the regulation of GLUT1 expression is still not completely understood.

1.5.3 P-glycoprotein (P-gp)

P-glycoprotein (P-gp) is a large, glycosylated membrane protein, which localizes predominantly to the plasma membrane of the cell. P-gp is an *N*-glycosylated membrane protein of about 1280 amino acids (170 kDa). Two isoforms have been identified, 155 kDa and 190 kDa forms (Beaulieu *et al.*, 1995). It belongs to the superfamily of ATP-binding cassette (ABC) transporters. It is present in the BBB of all mammals investigated, including humans (Cordon-Cardo *et al.*, 1989, 1990; Jette *et al.*, 1993). P-gp appears to be a BBB endothelial-specific marker, which could regulate brain penetration of xenobiotics and thus participate in the neuroprotection of the brain (Lechardeur *et al.*, 1996).

P-gp was first identified in Chinese hamster ovary cells selected for colchicine resistance and was demonstrated to mediate resistance to a wide range of anticancer agents (Juliano and Ling, 1976). Later studies showed that P-gp was also detectable in brain capillaries of humans, rats, mice, pigs and cattle (Hegmann *et al.*, 1992; Tsuji *et al.*, 1993; Barrand *et al.*, 1995; Toth *et al.*, 1996). In the human, there are two P-gp gene families, MDR1 and MDR3 whereas in the rodent (mice and rats) there are three

gene families, MDR1a and MDR1b and MDR2. Human MDR3 is also called MDR2 while mouse MDR1b is called MDR1 (Sparreboom *et al.*, 1997). The human MDR1, and the mouse MDR1a and MDR1b P-gps can confer multidrug resistance. In contrast, the closely related human MDR3 and mouse MDR2 P-gps (> 75% amino acid identity with the MDR1-isoform) do not confer multidrug resistance (Gros *et al.*, 1988; Schinkel *et al.*, 1991; Buschman and Gros, 1994).

The tissue distribution of the P-gp has been widely studied. In the periphery, P-gp has been detected on the apical surface of intestinal and renal epithelia, pancreas, the secretory glands in the endometrium of pregnant mice, biliary canalicular membranes of hapatocytes and on the luminal side of the blood-testis barrier (Fojo *et al.*, 1987). In the brain, P-gp has primarily been investigated at the barrier site. Although P-gp has been shown to be expressed on the apical side of the choroid plexus epithelia (Rao *et al.*, 1999), the exact location of P-gp along the brain endothelial microvessels remains debatable. Studies using immunohistochemistry and luminal membrane isolation have shown that P-gp is localized to the luminal surface of brain ECs (Jette *et al.*, 1993; Beaulieu *et al.*, 1997; Drion *et al.*, 1997). However, P-gp has also been identified at the abluminal surface of ECs neighbouring astrocyte foot processes (Golden and Pardridge, 1999). The localization of P-gp to the luminal membrane of ECs would enable P-gp to immediately extrude substrates that had diffused into the ECs, to return back to the blood stream.

Pardridge and co-workers reported a conflicting P-gp subcellular localisation (Agus *et al.*, 1997; Golden and Pardridge, 1999). Using the anti-P-gp antibody MRK16 and

double-labelling confocal fluorescence microscopy, they demonstrated that the cellular origin of P-gp in isolated human brain microvessels is the astrocyte foot process, not the endothelium. In their studies, anti-GFAP antibody was used as a marker for astrocyte foot processes and anti-GLUT1 antibody was used as a marker for ECs. The localization of anti-GFAP, anti-GLUT1 and MRK16 was detected by confocal fluorescence microscopy. The labelling patterns of anti-GFAP and MRK16 at isolated human brain capillaries were identically discontinuous. Double labelling by these two antibodies showed complete overlap. However, anti-GLUT1 antibody continuously labelled the capillaries. Double labelling with anti-GLUT1 and MRK16 showed that they were not colocalized at the capillaries suggesting that the P-gp is not localized at the endothelial cells. However, using only one antibody may have its technical limitations and may not generate conclusive results. It has been reported that the epitope of human MDR1 P-gp for the MRK16 antibody can be completely shielded in some cell types by heavy N-glycosylation of P-gp (Cumber *et al.*, 1990). Therefore, it has been proposed that at least two, and preferably three or more different antibodies should be used to study the immunolocalisation of P-gp (van der Valk *et al.*, 1990). An in situ hybridization study showed a similar discontinuous pattern of P-gp transcripts in the brain microvasculature (Qin and Sato, 1995). More work is needed to clarify the subcellular localization of P-gp as it is of great significance in the determination of the function of P-gp at the BBB.

The P-gp plays an important role in drug resistance. This has been demonstrated by several experimental methods including the use of knockout mice lacking the *mdr1a*, the *mdr1b* or both the *mdr1a* and *mdr1b* genes. Although these *mdr1a* (-/-) or *mdr1 b*

(-/-) mice appear physically normal and fertile, they are very sensitive to neurotoxic substances such as ivermectin, an acaricide antihelmintic drug of natural origin. A routine safety spray of ivermectin to treat mite infestation accidentally resulted in the death of almost all *mdr1a* (-/-) mice. A further study showed that the accumulation of ivermectin was 50 -100 fold greater in knockout mice than in normal wild-type mice (Schinkel *et al.*, 1994). Many other drugs have been also shown to accumulate to higher extents in the brains of P-gp gene knockout mice (Schinkel *et al.*, 1994, 1996; van Asperen *et al.*, 1997; Kim *et al.*, 1998). The results indicated that P-gp can exclude certain substances from the brain compartment and is directly involved in the protection of the brain. A number of P-gp blockers or reversal agents have been discovered (Tsuruo *et al.*, 1981; Hyafil *et al.*, 1993; Dantzig *et al.*, 1996). The P-gp blockers can inhibit the drug transport effect mediated by P-gp without apparent cytotoxicity. Most of the reversal agents are actually substrates for P-gp. They may inhibit P-gp activity by competitive transportation.

Most recently, evidence of direct implication of P-gp in the barrier functions of the BBB has been provided by generation of mice homozygous for a disruption of the class I isoform (mdr3) (Schinkel *et al.*, 1994). Injection of Vlastine to these mice lacking cellular expression of P-gp resulted in elevated drug levels in many tissues, especially in the brain. Thus, P-gp contributes to the barrier functions of the BBB by extruding compounds that are potentially toxic to the brain from the capillary endothelial cells. The function of the P-gp was also demonstrated by a quantitative study in which Rhodamine 123 was observed to be accumulated obviously, after the

treatment of bovine microvessel endothelial cell (BMEC) monolayer with the P-gp modifying agents.

The cellular mechanism underlying P-pg transport function remains controversial. The localization of P-pg at the luminal membrane of brain capillary ECs suggests that P-gp regulates blood-to-brain transport, whereas the localization of P-gp at the astrocyte foot process indicates that P-gp mediates drug efflux across the astrocyte foot process membrane from the brain interstitial fluid into astrocytes. In the latter location, knocking out P-gp genes would result in increased drug distribution into brain cells such as astrocytes without significantly increasing BBB permeability (Golden *et al.*, 1997; Pardridge, 1997).

1.5.4 OX-47 antigen

An integral membrane glycoprotein of unknown function has been identified at the rat BBB using a monoclonal antibody (MRC OX-47) and is referred to here as OX-47 antigen (OX-47A). It is a member of the immunoglobulin superfamily with an unusual transmembrane sequence (Fossum *et al.*, 1991). Previous studies demonstrated that OX-47A is homologous to the HT7 or neurothelin of the chick, basigin or gp42 of the mouse, and M6 or EMMPRIN of the human (Kasinrerk *et al.*, 1992; Seulberger *et al.*, 1992). There is 94% identity in the amino acid sequence between OX-47A and HT7 (Seulberger *et al.*, 1992). Further studies at the molecular level revealed that HT7, neurothelin, gp42, basigin and OX-47A share a similar molecular structure. The results of these studies suggest that HT7, neurothelin, gp42, basigin and OX-47A may be different names for the same glycoprotein in different

species (Seulberger *et al.*, 1992).

The OX-47A, like HT7, is located on ECs of the BBB but it has a more extensive distribution. It is also found on most epithelial cells including the kidney, small intestine and liver (Nehme *et al.*, 1995). It is present at low levels on most thymocytes and bone marrow cells but increases markedly upon activation of both B and T cells. The cell types expressing the OX-47A can be divided into four main groups: (a) immature, activated and dividing cells, e.g. bone marrow cells, cortical thymocytes, lymphoblasts, spermatogonia B, basal layers of epidermis and hair follicles, (b) epithelial cells involved in transepithelial transport, e.g. nephronic tubular cells, salivary duct cells, hepatocytes, intestinal absorptive cells, brain endothelium, choroid plexus, perineurial cells, (c) cells with excitable membranes, e.g. nerve and muscle cells and (d) other cells including endocrine cells such as Leydig cells and ovarian follicular cells (Fossum *et al.*, 1991). It is likely that the OX-47A is part of a complex of surface proteins and it is possible that the other components vary between the different cell types. Although the function of OX-47A remains unclear, Nehme *et al.* (1995) reported remarkably increased levels of the integral plasma membrane glycoprotein mRNA and protein in brown adipose tissue, liver and the lymphoid organ after metabolic activation. They suggested that the level, and possibly also the localization, of OX-47A might be correlated in a positive fashion with metabolic activity in a diverse array. The localization of OX-47A on ECs and activated lymphocytes also indicated a function as a cell transporter in cell-cell signaling.

The chick protein HT7, which is much more extensively studied than the rat OX-47A, is a specific marker for chick brain ECs. The HT-7 antigen is also detected in other

cell types, which form a tissue barrier, such as the pigment epithelium of the retina, choriod plexus epithelium and the epithelial cells of kidney tubules. During embryonic development, HT7 antigen is induced in the brain capillaries at day 10 of chick embryo, which correlates with the induction of the BBB. In the posthatch chick, HT7 expression is found on ECs within the brain but not on those of the systemic blood vessels (Seulberger *et al.*, 1992) and it is also absent from ECs of the choroid plexus, subfornical organ, and pineal and pituitary glands, all of which lack BBB (Albrecht *et al.*, 1990). An ontogenic study showed that HT7 is a very early BBB marker even when compared with the early embryonic brain endothelial cell markers, alkaline phosphatase and transferrin receptor, which appear slightly later. HT7 is first detectable at embryonic day (E) 9-10 in chick development, and becomes more extensive from E11 onwards (Risau *et al.*, 1986).

The neurothelin antigen is also a chick-specific cell-surface glycoprotein expressed by the brain ECs and widely utilized in experimental studies as a marker of barrier vessels (Moller and Kummer, 2003). An immunocytochemical study has shown that HT7 has cross immmunoreactivity with neurothelin (Seulberger *et al.*, 1992). The epithelium of the pigment layer which forms a barrier between the outer layer of the eyeball and the retina, and the epithelium of the choroid plexus, which forms the blood-cerebrospinal fluid barrier, also express neurothelin, indicating a role in the transport process (Unger *et al.*, 1993) of various cell types. In vitro studies of choroid epithelial cells showed that the expression of neurothelin was at the cell-cell site, indicating that the distribution of neurothelin was regulated by cell-cell interaction. The neurothelin antibody 1W5 does recognize the isolated HT7 (Seulberger *et al.*, 1992). The

appearance of neurothelin coincides with the maturation of CNS ECs. Neurothelin is an inducible protein in ECs. The induction may be mediated by cell-cell interactions or by factors produced by astrocytes. Although the localization of neurothelin strongly indicated its involvement in the barrier function, its expression by transplanted brain tumour cells has been reported (Papoutsi *et al.*, 2000). Four tumour cell lines were inoculated on the chorioallantoic membrane (CAM) of chick embryos. Neurothelin was expressed by ECs in all four tumours. As it is well known that BBB function is compromised in brain tumour blood vessels, this finding suggests that the expression of neurothelin does not correlate with a functional BBB.

Like OX-47A, HT7 and neurothelin, basigin (Bsg) is another transmembrane glycoprotein belonging to the immunoglobulin superfamily. Chicken Bsg is expressed in neuroblasts, but disappears from neurons after a specific stage of cytodifferentiation, and becomes restricted to the capillary endothelium in the adult brain. Studies by in situ hybridization showed that basigin mRNA was expressed in neuroblasts in 13.5 day old mouse embryos. In the adult mouse, Bsg was differentially expressed in subregions of the brain. Strong Bsg expression was detected in the limbic system, including the olfactory system, hippocampal formation, septal area, amygdala, thalamic anterior nuclei, hypothalamus, mesencephalic tegmentum, entorhinal cortex, and cingulate gyrus. Basigin was also intensely expressed in the retinal neuronal layers, the fifth layer of the cerebral neocortex, Purkinje cells of the cerebellum, several nuclei of the brainstem, and the grey matter of the spinal cord. Although in situ hybridization showed a weak signal in the brain capillary endothelium, protein expression of basigin was strong enough to be detected by immunohistochemistry.

Basigin knockout mice exhibit abnormalities in behaviour, but a normal blood-brain barrier function. A study using knockout mice lacking the basigin gene showed that the BBB of the knockout basigin (-/-) mice was impermeable to Evans blue, indicating a normal barrier function of the mutant mice (Igakura *et al.*, 1996).

1.5.5 Gamma-Glutamyl transpeptidase

Gamma-glutamyl transpeptidase (γGTP) is probably the most widely used marker for the BBB. Orlowski *et al.*, (1974) were the first to report the presence of γGTP in the BBB. γGTP is also found in the epithelium of secretory tissues (Chiba and Jimbow, 1986; Hanigan and Frierson, 1996) and in many organ barriers, e.g. the BBB and the blood-cerebrospinal fluid barrier (Ogawa *et al.*, 1998; Lawrenson *et al.*, 1999).

In the rat CNS, the activity of γGTP is mainly present in areas where the BBB is expressed, such as the cerebral cortex, cerebellum, striatum, and spinal cord. In areas where the BBB is absent, γGTP activity is not detectable or only a few blood vessels show γGTP activity (Wolff *et al.*, 1992). The percentage of γGTP positive vessels varies considerably in different areas of the rat brain, from 100% in the anterior commissure to only 8% in the optic nerve (Wolff *et al.*, 1992). γGTP is absent from all rat pial microvessels. It was proposed that the regional difference of γGTP activity might be related to the influence of astrocytes. This view is supported by another study which showed that blood vessels in the pia mater lack γGTP activity but capillaries with barrier function show γGTP at higher concentration in pericytes (Frey *et al.*, 1991; Risau *et al.*, 1992).

The precise subcellular localization of γGTP at the BBB still remains controversial. Some investigators reported that γGTP was localized at the luminal membrane of ECs (Ghandour *et al.*, 1980; Sanchez del Pino *et al.*, 1995; Ogawa *et al.*, 1998). However, other studies reported that the main activity of γGTP is at the abluminal membrane of the capillaries and is found at higher concentration in pericytes (Frey *et al.*, 1991; Risau *et al.*, 1992). This enzyme catalyzes the transfer of gamma-glutamyl residue from the glutathione to amino acids and is possibly also involved in BBB amino acid transport (Tate and Meister, 1985; Wolf and Gassen, 1997). γGTP has a high affinity to cystine (Thompson and Meister, 1975, 1976). However, a recent study showed that inhibition of γGTP activity in isolated adult porcine brain vessels did not affect the uptake of cystine (Wolff *et al.*, 1998). Another possible function of γGTP at the BBB is detoxification (Wolf and Gassen, 1997). γGTP is involved in the mercapturic acid pathway. As brain ECs are not able to exclude lipophilic xenobiotic substances, the mercapturic acid pathway can detoxify these potentially harmful substances (Wolf and Gassen, 1997). Further studies are needed to clarify the subcellular localization of this enzyme at the BBB. The precise subcellular localization of γGTP may provide information on the functional role of γGTP at the BBB.

1.5.6 Molecular markers of tight junctions

The molecular anatomy of the TJ is not fully understood. A few TJ-associated proteins have been identified. The TJ components occludin (Ando-Akatsuka *et al.*, 1996), claudin 1 and 2 (Furuse *et al.*, 1998), ZO-1 (Stevenson *et al.*, 1986), ZO-2 (Jesaitis and Goodenough, 1994), ZO-3/p130 (Haskins *et al.*, 1998), 7H-6 (Zhong *et al.*, 1993) and

cingulin (Citi and Kendrick Jones, 1988) were detected in epithelial as well as in the endothelial BBB TJs, whereas symplekin was exclusively found at the junctional zone in epithelial cells (Keon *et al.*, 1996).

Occludin is a 65-kDa protein identified by a monoclonal antibody. Occludin is the first and best-known integral membrane protein of TJs that is believed to be directly involved in their barrier and defence functions. This protein localizes precisely and exclusively to TJ contact sites as determined by immunogold labelling at the electron microscopic level (Tsukita *et al.*, 1997). It is expressed in the TJs of both epithelial cells and endothelial cells.

ZO-1 is a TJ associated-protein, a 220 kDa phosphoprotein that is present in both epithelial cells and ECs (Stevenson *et al.*, 1986). It is localized to the tight junction, although not exclusively, and is present in all types of TJs (Howarth *et al.*, 1992; Itoh *et al.*, 1993; Aaku-Saraste *et al.*, 1996). ZO-2, a 160 kDa protein is considered as an ubiquitous component of epithelial and endothelial TJs (Jesaitis and Goodenough, 1994). The functional significance of ZO-2 is not clear.

Two additional tight junction proteins, cingulin (140 kDa) and the 7H 6 antigen (155 kDa) are yet to be cloned and sequenced. The exact role of these proteins in TJ permeability regulation is not clear. The modification of adherens junctions can alter the permeability of TJs. Adherens junctions are formed by a class of membrane proteins termed cadherins and their cytoplasmic plaque proteins α-, β- and γ-catenin. The cadherins/catenins system at the adherens junction is sensitive to calcium levels.

Removal of Ca^{2+} leads to the disruption of adherens junctions and the opening of TJs (Pitelka and Taggart, 1983; Gumbiner and Simons, 1986). The level of cAMP in cultured brain ECs can also regulate the TJ formation. Elevation of cAMP levels causes a striking elevation of TJ resistance and reorganisation of the actin cytoskeleton (Rubin *et al.*, 1991).

1.6 The blood-brain and blood-spinal cord barriers after injury

1.6.1 Vascular damage after brain and spinal cord injury

Vascular damage after brain injury has been extensively studied. Vasogenic brain oedema can occur following mild, moderate, or severe head injury. Leakage of macromolecular tracers, such as endogenous plasma proteins and/or exogenous protein, such as HRP or albumin has been observed by numerous studies on experimental brain injury (Povlishock *et al.*, 1979; Schmidt and Grady, 1993; Lammie *et al.*, 1999) and human brain injury (Citi and Kendrick Jones, 1988; Cornford *et al.*, 1996). The opening of the blood brain barrier (BBB) occurs several minutes after the injury. However, different experimental models have demonstrated different time frames of cerebral oedema. Study of cortical impact brain injury in rats showed a biphasic opening of the BBB (Baskaya *et al.*, 1997). Recent studies have also shown that cytotoxic oedema may play a major role in the development of brain oedema (Ito *et al.*, 1996; Barzo *et al.*, 1997). Based on the measurement of the apparent diffusion coefficient (ADC) by diffusion-weighted imaging, Barzó and co-workers (1997) reported a transient opening of the BBB and a prolonged cytotoxic oedema (mainly in astrocytes) after experimental brain injury. In addition to the vasogenic and cytotoxic oedema mainly in astrocytes, neurotoxic oedema is also considered to occur after

traumatic brain injury. Significant increases in extracellular potassium and excitatory amino acids such as glutamate have been reported in experimental traumatic brain injury (Katayama *et al.*, 1990). Therefore, at least three forms of oedema, vasogenic, cytotoxic, and neurotoxic may contribute to brain oedema formation following trauma.

The subcellular passage way for large molecules through the BBB following traumatic brain injury is not fully understood. There is little evidence to indicate that disruption of TJs occurs after traumatic brain injury. EM studies showed that TJs appear to remain intact after head injury in humans (Castejon, 1998) and experimental animals (Foda and Marmarou, 1994). However, there is abundant evidence which demonstrates increased pits and vesicle density in ECs in both human and experimental traumatic brain injury, indicating activation of ECs (Castejon, 1998). When the exogenous tracer HRP was used in an experimental brain injury model, vesicles were shown to contain HRP following injury (Povlishock *et al.*, 1979). However, the role of vesicles in transendothelial transportation remains controversial (Broadwell, 1989).

The disruption of the blood-spinal cord barrier (BSB) after injury has also been investigated in different animal models, such as transection, contusion and compression injury and experimental allergic encephelomylitits (EAE) models (Noble and Maxwell, 1983; Juhler *et al.*, 1984; Noble and Wrathall, 1987, 1988, 1989; Noble and Ellison, 1989). In all these models, remarkable changes in the permeability to endogenous and exogenous tracers have been demonstrated. The breakdown of the BSB may occur as early as 10 min after transection injury with the maximum

breakdown at 3 days after injury (Noble and Wrathall, 1987). Vascular damage can extend to several segments remote from the epicentre of trauma. It was also reported that the extent of damage to the BSB in the tissue rostral and caudal to the trauma sites are different with more severe damage to the area caudal to the injury (Noble and Wrathall, 1987). An EM study also revealed that the breakdown of the BSB mainly resulted from an increase in transendothelial vascular transport rather than the interendothelial passage of tracer across the compromised TJs (Noble and Wrathall, 1988). The breakdown of the BSB in the peritraumatic areas caudal and rostral to the trauma sites demonstrated a similar mechanism (Noble and Wrathall, 1988). Using quantitative autoradiography following contusion injury to the rat spinal cord, Popovich *et al.* (1996a) measured BSB permeablity. BSB permeability was assessed by calculating blood-to-tissue transfer constants (K-i values) for the vascular tracer alpha-aminoisobutyric acid (AIB) in injured (3, 7, 14, and 28 days post injury), laminectomy control, and uninjured control animals (Popovich *et al.*1996a). Regardless of the type of analysis used, increased permeability was noted at all survival times in all tissue regions compared to both uninjured and laminectomy control groups, with a remarkable increase in the permeability 3 days post injury. By 7 days, the increase in the permeability in all regions was not so remarkable compared with 3-day tissues. In subsequent time intervals, circumferential white matter tracts showed a secondary increase in permeability compared to 7-day tissue. Permeability in the white matter at 14-28 days post injury was comparable to that at 3 days post injury. Increased BSB permeability occurred over several segments rostral and caudal to the lesion epicenter (3 cm in both directions). These results suggest that the spinal white matter at later survival times (14-28 days post injury) is an area of dynamic vascular

and/or axonal reorganisation. However, the detailed mechanism accounting for the opening of the BSB is still not fully understood.

1.6.2 Expression of BBB markers after injury.

1.6.2.1 EBA expression after brain and spinal cord injury

As described in the previous section, in brain pathology associated with the formation of oedema, the expression of BBB molecular markers is altered. The level of EBA expression is reduced in experimental encephalomyelitis (Sternberger *et al.*, 1989), stab-wound brain injury (Rosenstein *et al.*, 1992) and in the cerebral infarction injury model (Lin and Ginsberg, 2000). However, the EBA expression is restored along with recovery from the acute state of the above diseases. Interestingly, these models demonstrated almost the same time frame for the disappearance and re-expression of EBA. In all these models, EBA appeared to show a reduction at 1 day after the injury, with the maximum reduction at approximately 3 days after injury. By two weeks after these pathological insults, the expression of EBA started to recover to normal levels.

The blood-spinal cord barrier (BSB) is similar to the BBB in structure and is also characterized by the expression of certain endothelial cell markers including EBA, GLUT1 and γGTP. A recent study reported that the spinal cord after compression injury, like injured brain tissues, showed remarkable temporal reduction of EBA immunoreactivity in the BSB at the injured area. The reduction of EBA reached lowest level at 4 days after injury. The reduced EBA IR was restored at two weeks after injury (Perdiki *et al.*, 1998). Thus, it has been suggested that EBA IR can be used

to detect sites of barrier dysfunction and recovery after trauma to rat brain or spinal cord (Perdiki *et al.*, 1998).

However, the above study (Perdiki et al., 1998) addressed only changes at the injury site subjected to the direct mechanical trauma employing light microscopy. Also it did not investigate changes in EBA IR in the peritraumatic areas, such as the area caudal and rostral to the injury sites. The study also did not address why EBA IR is dramatically reduced during certain time periods after injury. As yet, it is also not evident whether the expression of EBA by the ECs is related to the function of the BSB and what factors mediate the expression of EBA after injury. Furthermore, it is not known whether the expression of the BBB markers is related to the pathological evolution of lesioned axons and the plasticity of the astrocytes and other glial cells in the traumatic and peritraumatic areas. The factors that down-regulate EBA expression after injury are still not clear.

1.6.2.2 GLUT1 expression after injury

Since the metabolism of glucose is a major energy source in the CNS, glucose transporter proteins, which regulate the transport of glucose, may also be involved in the pathological evolution of spinal cord injury. A recent study investigated GLUT1 expression in the normal and injured spinal cord (Stark *et al.*, 2000). It was found that GLUT1 IR and the mRNA signal for GLUT1 can be detected in the microvessels of the spinal cord of both embryonic and adult animals (Stark *et al.*, 2000). However, no labelling was found in the pia matter of the spinal cord. A strong immunolabelling was present in blood vessels that were directly injured by the spinal cord lesion. This result

seems to be in agreement with a previous report that GLUT1 expression is still present in the microvessels in the injured tissues after stab wound injury to the brain (Rosenstein and More, 1994). However, previous early studies reported a reduction in energy metabolism in the traumatic area of the injured spinal cord. For example, Noble and Wrathall (1987) reported that after injury the level of ATP in the trauma site of the spinal cord was decreased with time compared to that in the peritraumatic sites. Currently no reports exist on alterations in the expression of GLUT1 at different time intervals after injury. It is also not clear whether the GLUT1 expression is correlated with the pathological changes and the function of the BSB after injury. The underlying mechanisms by which the GLUT1 is up-regulated or down-regulated are also not clear.

1.6.2.3 What factors mediate the expression of BBB molecular markers?

The regulatory mechanism for EBA and other molecular markers expression is still unknown. As reviewed in previous sections, there are several lines of evidence suggesting that extracellular micro-environments play a role in induction and maintenance of the BBB. Thus, it has been hypothesized that astrocytes may play a role in expression of BBB markers. Indeed, some previous studies have suggested that astroglial cells not only directly or indirectly induce BBB properties such as increased TJ complexity, but also regulate the expression of barrier-specific markers (Bouchaud *et al.*, 1989; Meyer *et al.*, 1991; Tontsch & Bauer, 1991; Rauh *et al.*, 1992; Frank & Wolburg, 1996). Since EBA expression seems to be related to BBB integrity, it has been hypothesized that astroglial cells may also exert regulatory effects on EBA and other molecular markers' expression by the ECs. However, a recent in vivo study

reported conflicting results that astroglial degeneration appears not to affect the expression of BBB markers (Krum et al, 1997). In that study, after systemic application of 6-aminonicotinamide (6-AN), an anti-metabolite, to the neonatal rats, the brain microvasculature was examined at postnatal days 6-12 and the histochemical and immunohistochemical expressions of EBA, γ -GTP and GLUT1 were quantitatively analyzed. Despite the apparent perivascular astroglial degeneration, all of the BBB markers examined were robustly expressed throughout the CNS and comparable to the age-matched control. The author claimed that, in contrast to the majority of in vitro studies (Krum, 1994), the postnatal brain microvasculature continues to express GLUT-1, γGTP and EBA in situ without the influence of continuously manufactured, astrocyte-derived substance. However, in that study, the regulation of the release of astrocyte-derived factors after systemic injection of the 6-AN was not studied. It is most likely that the astrocytic responses induced by this model are different from those induced by traumatic injury.

1.7 Other blood-tissue barriers

Blood-tissue barriers exist in some peripheral body organs including blood-nerve barrier, blood-testis barrier, blood-ocular barrier and blood-thymus barrier. These barriers have different morphological properties compared to that of the BBB although they share some similarities. The anatomical basis of these barriers is also located in the ECs although in the testis the blood-testis barrier is mainly constituted by Sertoli cells. These barriers may also express some molecular markers that are specifically expressed by the BBB. This review will focus on the blood-nerve barrier and blood-testis barrier.

1.7.1 The blood-nerve barrier

Numerous previous studies demonstrated that there is also a barrier between blood circulation and the peripheral nerves (Michel *et al.*, 1984; Allt and Lawrenson, 2000) which prevents free entry of some macromolecules such as HRP and other large molecules to the peripheral nerve (Orte *et al.*, 1999). When tracer substances such as ferritin and HRP are injected into the blood, they do not enter the peripheral nerves. Their entry is prevented by TJs in the inner layers of the perineurium and between endothelial cells of endoneurial blood vessels. Thus, these studies have demonstrated that the BNB is constituted of the perineurium and the endothelium of endonurial microvessels. The perineurium of peripheral nerves consists of concentric layers of flattened cells separated by layers of collagen. The number of cell layers varies from nerve to nerve and depends on the size of the nerve fascicle. Electron microscopic studies further showed that perineurial cells have membrane-associated vesicles that appear to open on to the external and internal surfaces of the cell. Basement membrane is usually seen on both sides of each perineurial lamina (Michel *et al.*, 1984; Thomas *et al.*, 1993). There are TJs that join adjacent cells within the same layer of perineurium and between adjacent layers.

Tracer studies in developing animals indicated that the BNB is not formed before 13 days of life, and that its function is established by 16 days (Christopher *et al.*, 2001). These results were further confirmed by electron microscope examinations of nerve sections from animals injected with the tracer HRP, which showed tight junctions preventing the passage of the HRP through the clefts between the endothelial cells of endoneurial vessels. These studies therefore support a functional barrier to protein

tracer at the BNB. Thus it appears that there are morphophysiological similarities between the BNB and the BBB. However, studies using ionic tracers showed that although the perineurium may exclude lanthanum ions, at least some endoneurial blood vessels may allow lanthanum ions through endothelial tight junctions (Mac Kenzie *et al.*, 1987; Ghabriel *et al.*, 1989).

The induction of the BNB has not been studied extensively. In the peripheral nerve, there have been no studies of EC and Schwann cell interaction, analogus to EC and astrocyte interaction in the brain. Recent evidence indicates that Schwann cell signalling is responsible for both the induction and maintenance of the barrier properties of the perineurium. A study on nerve section and grafting showed that the perineurium at the site of the graft contribut to the formation of internal compartment within the nerve, possibly as a mechanism for reconstitution of the blood-nerve barrier, although these compartment and endoneurial blood vessels remain permeable to HRP for at least 24 weeks (Ahmed and Weller, 1979). It was also found that the intact perineurium distal to a graft becomes permeable to HRP in the asbsence of growing axons, but the endoneurial blood vessels could exclude the tracers (Ahmed and Weller, 1979). This suggests an axonal influence on the perineurium but not on ECs of endoneurial blood vessels. A recent study suggested that the endoneurial pericytes play a role in strengthing the BNB in vitro (Iwasaki *et al.*, 1999).

1.7.2 The blood-testis barrier

In the testis, there is both functional and structural evidence for a blood-testis barrier. The observation that only few substances of those present in blood appear in the

testicular fluid suggests the existence of a barrier between the blood and the interior of the seminiferious tubules. Some studies showed that the occluding junctions between Sertoli cells are responsible for this barrier, which is of importance in protecting the germinal cells against noxious agents (Dym and Fawcett,1970., Dym and Cavicchia , 1977).

In previous studies, much attention has been directed to these specialized junctions between pairs of adjacent Stertoli cells, which divide the spermatogenic epithelium into basal and adluminal compartments (Dym and Cavicchia , 1977; Russell, 1977). The diploid, mitotically-dividing spermatogonia are located in the basal compartment and during the leptotene stage of the first meitotic prophase, the spermatocytes move into the adluminal compartment, where the rest of the process of the sperm formation occurs (Dym and Fawcett 1970). There is evidence that the peritubular myoid cells and ECs of the testicular blood vessels also contribute to the barrier (Plöen and Setchell, 1992; Holash *et al.*, 1993).

Testicular capillaries show some similarities to brain vessels. Testicular capillaries are continuous and have intercellular tight junctions (Weihe *et al.*, 1979). However, morphological and physiological studies showed some difference between the two vascular beds in the brain and testis. Albumin, which does not freely enter the brain, is readily detectable in testicular lymph (for a review, see Setchell and Wates, 1975). Also the density of the tight junctions in testicular vessels is lower than those of brain endothelial cells (Holash *et al.*, 1993a; Stewart, 2000). Testicular capillaries are larger and have a thicker wall and higher density of mitochondria than those of brain

capillaries (Holash *et al.*, 1993a; Stewart, 2000). Other studies have provided evidence for the leakage of Evans blue (Caster *et al.*, 1955) and trypan blue (Kormano, 1967) into the interstitial tissues of the testis. HRP can also enter the interstitial tissues of the testis (Weihe *et al.*, 1979) but cannot enter the brain (Brightman and Reese, 1969). The difference in the permeability between testicular and brain vessels may be due to the differences in the structure and function of the TJs between ECs in the two systems. Brain blood vessels have long sinuous intercellular junctions with high electrical resistance. Testicular blood vessels have wide compartments between the series of tight junctional appositions and some intercellular junctions are expanded (> 10nm), indicating patent junctions (Dym and Fawcett, 1970; Holash *et al.*, 1993a; Stewart, 2000). Fifteen per cent of the testicular blood vessels have wide junctions with a higher cleft index (Holash *et al.*, 1993a) which may explain their higher permeability compared with brain vessels.

1.7.3 Expression of molecular markers in the blood-nerve barrier and blood-testis barrier

1.7.3.1 Molecular markers of the Blood-testis barrier

Endothelial cells of testicular microvessels share several molecular markers with those in brain. There is a specific saturable transport system for leucine in ECs of the testis and the kinetic properties of this system are very similar to those found in the brain (Bustamante and Setchell, 2000). Endothelial cells in the testis contain the glucose transporter GLUT1, γGTP and P-gp (Harik *et al.*, 1990; Holash *et al.*, 1993a) which were thought to be specific to the brain. It has also been demonstrated that the Leydig cells, which lie close to the ECs in the testis, contain S-100 protein, the glial fibrillary

acidic protein and glutamine synthetase (Holash *et al.*, 1993a). These are characteristic markers of astrocytes, the cells in the brain that may confer the barrier properties on brain ECs (Risau, 1995). Some early studies have investigated the expression of the barrier marker, glucose transporter, in the testis. The expression of the facilitative hexose transporter was compared in rat and human testes. In rat testis, only GLUT1 and GLUT3 proteins were expressed. By contrast, human testis expressed GLUT1 and GLUT3 in addition to GLUT5. Immunocytochemical studies showed that GLUT3 was expressed in all cells of the seminiferous epithelium of rat testis, including sperm. In human testis, GLUT3 was expressed exclusively in cells juxtaposed to the lumen of the seminiferous tubule and in ejaculated sperm, a pattern of expression that was identical to that of GLUT5. Induction of insulin dependent diabetes mellitus in the rat did not alter the levels or the distribution of GLUT3 protein or mRNA in the testis. Moreover insulin treatment of the diabetic rats did not produce changes in GLUT3 mRNA or protein levels. The results show that rat and human testes express the high-affinity glucose transporter GLUT3, which allows for the efficient uptake of glucose. In addition, the testis may be protected from changes in glucose transporter expression in experimental diabetes.

Although testicular blood vessels share many biochemical markers with brain vessels, there are some differences. Unlike brain vessels, those of the testis do not express the transferin receptor (Holash *et al.*, 1993a). Although ECs of the brain vessels and testis express the P-gp, the distribution of this marker is different in the two systems. P-gp is localized to the luminal membranes in brain ECs but to both luminal and abluminal membranes in testicular endothelial cells (Stewart *et al.*, 1996). The biological

significance of the difference in the distribution of P-gp in the two systems is not understood (Stewart *et al.*, 1996).

1.7.3.2 Molecular markers of the blood-nerve barrier

A number of enzymes, transporters, and receptors have been investigated in the BNB and compared to the BBB (See review by Allt and Lawrenson, 2000). Immunocytochemistry showed that GLUT1 was uniformly and strongly represented in brain ECs, nerve ECs and the perineurium. OX-26 antibody, which detects the transferrin receptor, strongly labelled brain EC but only weakly labelled nerve ECs and the perineurium. Anti-EBA similarly showed strong positivity in brain ECs but weak staining of nerve ECs, and was absent from the perineurium. OX-47 antibody moderately labelled brain ECs and the perineurium but not nerve ECs. Quantitative immunoblotting of brain and sciatic nerve homogenates showed statistically significant differences in the level of expression of EBA and transferrin between the two tissues. Enzyme cytochemistry showed that γGTP was strongly positive in brain ECs but absent from nerve ECs and perineurium. Alkaline phosphatase was strongly detected in nerve ECs but was absent from the perineurium. Alkaline phosphatase is of special interest because it is abundant in brain ECs and is used as a marker for the BBB, and the expression of this enzyme is astrocyte-dependent. The P-gp is expressed by ECs at the BNB similar to the BBB but not by ECs of peripheral tissues. It appears therefore that there are immunocytochemical differences between the BNB and the BBB. These differences cannot simply be accounted for by the absence of astrocytes and their inductive influences in the PNS.

The expression of some markers may change in the BNB after injury (Hirakawa *et al.*, 2003). The intercellular junctional proteins can change after injury. The breakdown and ensuing recovery of the blood-nerve barrier are closely associated with changes in the expression of claudins, occludin, VE-cadherin, and connexin 43 and the recovery time course is similar but nonidentical among the different markers (Hirakawa *et al.*, 2003).

1.8 Summary

The morphological and molecular properties of the BBB have been extensively studied since the turn of the twentieth century. Considerable progress has been made in understanding the biology of the BBB. It is now clear that the TJs between adjacent ECs form the morphological basis of the BBB. The TJs of ECs of the BBB are characterized by their high electrical resistance. Also ECs contain very few pinocytotic vesicles, and the paucity of the vesicles contribute significantly to the barrier properties of the BBB.

In past decades, numerous molecules specifically expressed by the BBB have been identified. The functional roles of most of these molecules are still not clear with the exception of GLUT1. These proteins have been defined as BBB markers. EBA has been regarded as a sensitive indicator for vascular damage in the CNS because a sensitive and remarkable reduction of its expression has been consistently observed in pathologies associated with oedema. However, the precise functional role of EBA is still unclear.

The barrier function of the ECs in the CNS is mirrored to some extent by barriers in other tissues. Blood-tissue barriers are also present in the PNS and the testis. These barriers like the BBB, also have the capacity of preventing the free exchange of some molecules and maintaining tissue homeostasis. These barriers in the PNS and the testis also express some special molecular markers. Comparative studies of the BBB, BNB and BTB are of special significance for understanding the function and physiology of the BBB and its special markers.

Under pathological conditions such as trauma and ischaemia associated with brain oedema, the expression of these molecular markers is altered. The TJs may also change after pathological insults. The reduction of EBA has been reported in a few animal models of pathological conditions. The alteration of GLUT1 expression has also been reported in brain trauma. However the significance of the alteration of these molecular markers has not been completely revealed. Detailed study of the expression of these makers in normal and pathological conditions may provide further insights into the physiology of the BBB, BNB and BTB.

CHAPTER 2

AIMS

Chapter 2 Aims of the thesis

Microvessels in the CNS (brain and spinal cord) have special barrier properties, which prevent free transport of some molecules from the blood to the neural tissues and vice versa. The barrier function of these vessels maintains tissue homeostasis, which is vital for the normal function of the CNS. Endothelial cells of these vessels are responsible for the barrier function and thus form the blood brain (BBB) and blood-spinal cord barrier (BSB). Endothelial cells at the BBB and BSB express certain biochemical markers, such as the endothelial barrier antigen (EBA) and the glucose transporter protein GLUT1. The first aim of this study is to investigate quantitative and qualitative changes in EBA and GLUT1 in the BSB after compression spinal cord injury, and correlate any changes with permeability of the BSB to endogenous albumin. The hypothesis is that the expression of EBA and Glut-1 will be reduced after spinal cord injury, in correlation with increased vascular permeability.

It has been suggested that testicular blood vessels contribute to the blood-testis barrier, since they share the expression of some markers with the BBB, including GLUT1. Therefore the second aim of this project is to investigate if testicular blood vessels in normal rats express EBA similar to the BBB and BSB. Furthermore, the expression of EBA and GLUT1 in the testicular vessels will be investigated following spinal cord compression injury. The hypothesis is that EBA, like other barrier proteins, will also be detected in testicular blood vessels, and the expression of EBA and GLUT1 will be reduced in testicular vessels after spinal cord injury.

There is experimental evidence that EBA plays an important role in maintaining the functional integrity of the BBB. Therefore, the third aim of this project is to further elucidate the function of EBA at the BSB and BBB using an immunological targeting approach to investigate the temporal pattern of opening and closure of the BBB and BSB following in vivo administration of an antibody to EBA. It is hypothesized that sysytemic administration of an antibody to EBA will selectively alter the intergrity of the BBB.

CHAPTER 3

MATERIALS AND METHODS

Chapter 3 Materials and methods

3.1 The study of the blood-spinal cord barrier in spinal cord trauma

3.1.1 Animals

Sixty-four male Sprague Dawley rats (350-380g) were used in this study. Animals were divided into four groups including severe trauma (n=13), moderate trauma (n=30), sham control (n=15) and non-operated normal groups (n=6). Animals were supplied and maintained under standard conditions by the Animal Services of the University of Adelaide. The experiment was approved by the Animal Ethics Committee of the University of Adelaide (S/37/1999) and conducted under the guidelines of the NH&MRC of Australia.

3.1.2 Compression spinal cord injury

Rats were deeply anaesthetized by inhalation of isofluorane or Halothane. Rectal temperature of the animals was measured and kept at 36.5-37.5°C by keeping the animal under a heating lamp. An incision was made on the dorsal skin and laminectomy was performed at the thoracic (T) 10-11 level. The spinal cord and its dural sheath were exposed and the dura mater was kept intact so that the CSF compartment was not compromised. The spinal column was immobilized by two clamps fixed to the spinous processes at T7 and L3 levels to minimise the movement of the spinal column and spinal cord during the procedure (Fig 3.1). A sustained compression injury was induced by applying a weight to the dorsal surface of the spinal cord through the intact dura mater using a compression device. The device is formed of (a) a lower curved plate (2x4 mm) representing a half of a cylinder to fit over the spinal cord, (b) a vertical stem, and (c) an upper flat platform. The device was lowered gently on the cord using a

micromanipulator. Metal discs were loaded on the upper platform to a total weight of 50 g including the weight of the device and left for 15 min to induce severe injury, or a total weight of 35 grams for 5 min was used to induce moderate injury. For the sham control animals, only the laminectomy was performed to expose the dura over the dorsal surface of the spinal cord but the device was not applied. All experimental and sham animals were injected with a daily dose of a broad-spectrum antibiotic (Gentamicin 4mg/kg) for 5 days post-injury, and Buprenorphine (0.05mg/Kg) was injected subcutaneously 12 hourly for 5 days for post-operative analgesia. In the severe trauma group, animals were allowed to survive for 1d (n= 3), 3d (n=4), 7d (n=3) and 14d (n=3). In the moderate trauma group, animals were allowed to survive for 1 d (n=6), 3 d (n=6), 7d (n=6), 14d (n=6) and 28d (n=6). In the sham control group animals were allowed to survive for 1d (n=3), 3d (n=3), 7d (n=3), 14d (n=3), and 28d (n=3).

3.1.3 Motor function test after spinal cord injury.

Motor function was tested with an incline plane as described by (Rivlin and Tator, 1977) (Fig. 3.2 and Fig.3.3). The plane consisted of a rectangular plywood board hinged at one end to a lower horizontal board. The lower board served as the base and the upper board as the moveable incline plane. Two protractor-like side panels with degrees marked on their faces were fixed on the base. A rubber mat with ridges, 0.6 mm in height, was fixed to the surface of the moveable plane. For clinical assessment, rats were placed in such a position on the mat that their body axis was perpendicular to the axis of the incline board. The maximum inclination of the plane at which a normal rat could maintain its position for 5 seconds was recorded and taken as to represent the rat's functional ability. In the practical test, the angle of the plane was increased or decreased

at 5° increments. The reading was taken for the maximum angle at which the rat could maintain its position on the incline plane for 5 seconds without falling.

Fig. 3.1 Photograph showing the surgery scene to induce compression spinal cord injury. Two clamps were used to immobilize the spinal column. Laminectomy was performed at T 10-11 level. Micrometer device was used to position the curved plate at the low end of the compression device onto the dorsal surface of the spinal cord through the intact dura.

Fig. 3.1

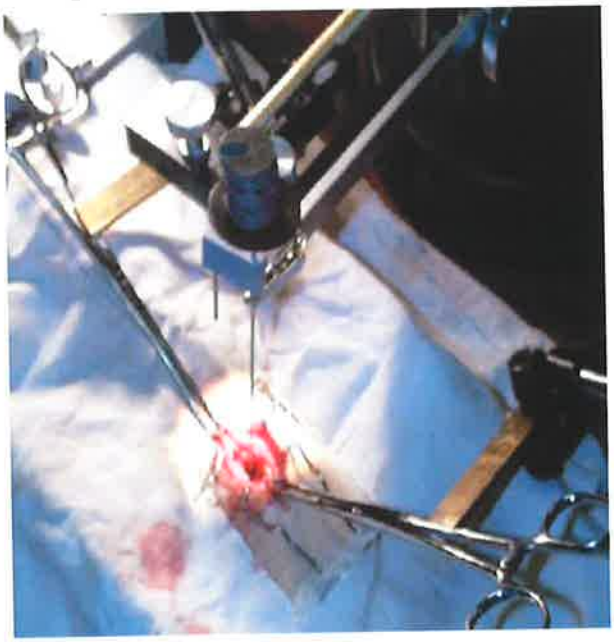

Fig. 3.2 Photograph showing the incline plane used for motor function testing after compression spinal cord injury. The photograph shows an experimental rat with moderate compression spinal cord injury being tested for the motor function immediately after the surgery; the rat can maintain its position on the plane at 45 degrees.

Fig.3.2

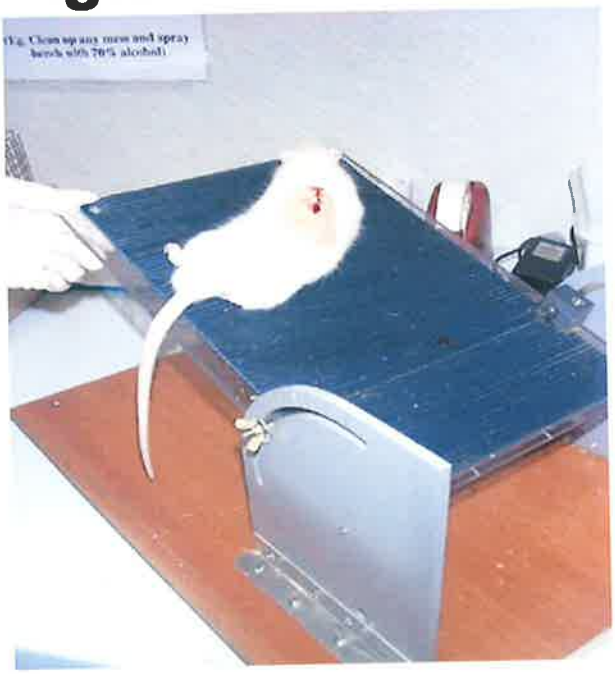

Fig. 3.3 Photograph showing the incline plane used for motor function testing and shows a normal rat being tested. A normal rat can maintain its position on the plane at an angle of approximately 70 degrees.

Fig. 3.3

3.1.4 Animal perfusion

Animals were sacrificed by transcardiac perfusion. Under deep anaesthesia, induced by intraperitoneal injection of pentobarbitone sodium (Nembutal, 60mg/kg) the thoracic cage was quickly opened. A wide bore needle was inserted into the left ventricle and the right atrium was cut. Under constant pressure of 90 mm Hg, the vascular bed was flushed with 37°C Dulbecco's phosphate buffered saline (containing 1% Minimum Essential Medium (Sigma) and gassed with 95%O_2: 5%CO_2) for 30 seconds, followed by perfusion with fixative at 4°C. For the immunocytochemical study, the fixative contained 4% paraformaldehyde in 0.1 M phosphate buffered saline (pH 7.4). For the ultrastructural study, the fixative contained 4% paraformaldehyde and 2% glutaraldehyde in 0.1 M phosphate buffer (pH 7.4). The rate of perfusion was adjusted to allow a fast flow for the first 100 ml of fixative (5 min), followed by 300 ml at a slow rate (30 min), with a total perfusion time of approximately 35 min.

3.1.5 Tissue preparation

The spinal cord was removed and post-fixed in the same fixative used for the perfusion for 3 hours. A 5 mm segment was taken from the trauma site. Ten segments (5mm each) were then taken from the rest of the cord, 5 segments rostral (R1-R5) and 5 segments caudal (C1-C5) to the trauma site. Each segment was cut into two halves (2.5mm), one for paraffin embedding and one for Vibratome cutting. For most of this study, segments R5 and C5 were used unless specified otherwise. Seven micron paraffin sections were cut and mounted on silane-coated slides. One set of paraffin sections from all experimental animals were used for Haematoxylin and Eosin staining. Adjacent sections were used for lectin staining, and immunocytochemistry for EBA and GLUT1. Sixty

micron Vibratome sections were floated in PBS. Vibratome sections were also immunolabelled for EBA and GLUT1 and mounted on slides for light microscopy. For the ultrastructural study, some immunostained Vibratome sections were osmicated, dehydrated and processed for electron microscopy (EM).

3.1.6 Primary antibodies and antisera

(1) Anti-EBA antibody

Anti-EBA antibody (SMI 71) was purchased from Sternberger Monoclonals Inc., MD, USA. The antibody is a mouse anti-rat, IgM monoclonal antibody (mAb), supplied as a high titre mouse ascites fluid. This antibody is species-specific for rat, used at a dilution of 1:3000 in 1% normal horse serum in 0.1 M phosphate buffered saline (PBS).

(2) Anti-GLUT1 antibody

Anti-GLUT1 polyclonal antibody (SC1605) was purchased from Santa Cruz Biotechnology, Inc. CA, USA. It is an affinity purified goat polyclonal antibody raised against a peptide mapping within the carboxy terminal, cytoplasmic domain of the GLUT1 precursor of human origin (identical to corresponding rabbit sequence), used at a dilution of 1:2500 in 1% normal horse serum.

(3) Goat anti-rat albumin antiserum

Goat anti-rat albumin antiserum was purchased from ICN Pharmaceuticals Inc., USA. This antibody is raised in goat, recognises rat endogenous albumin and has been widely used in immunocytochemistry studies. It was used at a dilution of 1:20,000 in 1% normal horse serum.

3.1.7 Secondary antibodies

Biotinylated horse anti-mouse IgG and biotinylated horse anti-goat IgG were purchased from Vector Laboratories (Burlingame, CA, USA). Rabbit anti-goat secondary antibody conjugated to HRP was purchased from Sigma, USA.

3.1.8 Biochemical reagents

Immunochemicals

Peroxidase conjugated Streptavidin was obtained from Rockland Inc., Gilbertsville, PA, USA. Normal horse serum (NHS), normal rabbit serum (NRS) and normal goat serum (NGS) were obtained from Vector Laboratories.

Resins

TAAB resin was obtained from TAAB Laboratories Equipment Ltd, UK.

Immunoblotting reagents

ECL-Plus detection reagents were purchased from Amersham Bioscience Co. Buckinghamshire, England. Tris-base was obtained from Bio-Rad. SDS, Mercaptomethanol and N,N,N',N'-Tetramethylenediamine (TEMED) were all purchased from Sigma. Protease inhibitor cocktail was obtained from Roche Diagnostic GmbH, Roche Molecular Biochemicals, Germany. The Bradford protein assay reagent was obtained from Bio-Rad, CA, USA.

Lectin

Fluorescein *Lycopersicon esculentum* (Tomato) lectin was used as a marker to label the endothelial cells of spinal cord blood vessels. This lectin is obtained from Vector

Laboratory, Inc., Burlingame, CA, U.S.A. (Cat. No FL-1171). It specifically labels the endothelial cells of microvessels and has been widely used as a marker for microvessels (Thurston *et al.*, 1998; Ezaki *et al.*, 2001).

3.1.9 Electrophoresis equipment and materials

The SE 250 Mini-vertical gel electrophoresis unit, Hyper film and Hybond-P PVDF membrane used for electrophoresis were all purchased from Amersham Pharmacia Biotech, Buckinghamshire, England.

3.1.10 Light and electron microscope immunocytochemistry for EBA

The indirect immunoperoxidase method was employed. Paraffin sections were deparaffinised and hydrated. Both paraffin and Vibratome sections were rinsed in PBS. To eliminate endogenous peroxidase activity, paraffin sections were incubated in 0.3% hydrogen peroxide in 70% methanol for 30 min whereas Vibratome sections were incubated in 0.3% hydrogen peroxide in 50% ethanol for 30 min. After washing in PBS, sections were incubated in 10% NHS for 60 min to reduce non-specific protein binding. Sections were then incubated in the anti-EBA monoclonal antibody diluted 1:3000 in 1% NHS overnight with slow agitation. Thereafter, sections were washed in PBS (3 x 10 min) and incubated in a biotinylated horse anti-mouse IgG secondary antibody diluted 1:200 in 1% NHS, 60 min for Vibratome sections and 30 min for paraffin sections. Following thorough washing in buffer, the bound secondary antibody was detected by one of the following two methods.

1) Avidin-biotin peroxidase method. The peroxidase reaction product was visualised by using 3, 3'-diaminobenzidine tetrahydrochloride as chromogen (DAB, Sigma). Sections were incubated in 0.05% DAB in Tris buffer or Phosphate buffer (pH 7.4) for 10 min then in 0.05% DAB containing 0.01% H_2O_2 for 7 min. The reaction was stopped by washing the sections in PBS.

2) Streptavidin-biotin peroxidase method. Sections were incubated in peroxidase conjugated streptavidin diluted 1:1000 in 1% NHS for 60 min. After washing, the sections were incubated in 0.05% DAB in phosphate buffer (pH 7.6) containing 0.01% H_2O_2 for 7 min. The reaction was stopped by washing the sections in PBS.

Controls for the specificity of the immunostaining consisted of staining some sections without the primary antibody and others without both the primary and secondary antibodies. After thoroughly washing in PBS, paraffin sections were dehydrated, cleared in Histolene or 100% Xylene and covered with coverslips. Some sections were counterstained lightly with haematoxylin.

Immunostained Vibratome sections used for light microscopy examination (LM) were mounted on albumen- or gelatin-coated slides. After air-drying overnight, sections were placed in 100% ethanol, cleared in Histolene, an organic soluent, and covered with coverslips. Immunostained Vibratome sections of the spinal cord used for EM examination were cut into quadrants, osmicated, dehydrated and processed in TAAB resin. These tissue blocks were embedded in TAAB resin and polymerised. Sections were embedded horizontally in the block. Ultrathin sections (approximately 90 nm)

were cut at a plane perpendicular to that of the Vibratome plane. Sections, counterstained with uranyl acetate for 3 min or without counterstaining, were viewed in a Philips CM 100 electron microscope.

3.1.11 Light and electron microscope immunocytochemistry for GLUT1

The biotin-streptavidin-perioxodase method was employed. Paraffin sections were deparaffinised and hydrated. Both paraffin and Vibratome sections were rinsed in PBS. To eliminate endogenous peroxidase activity, sections were incubated in 0.3% hydrogen peroxide in 70% methanol for paraffin sections or in 50% ethanol for the Vibratome sections for 30 min. After washing, sections were incubated for 60 minutes in 10% normal goat serum (NGS) or 10% NHS to block non-specific protein binding. Then, sections were incubated in the anti-GLUT1 goat polyclonal antibody (1:2500 in 1% NHS) at room temperature overnight with slow agitation. Thereafter, sections were washed in buffer and incubated in a biotinylated horse anti-goat IgG secondary antibody diluted 1:200 in 1% NHS (60 min for Vibratome sections and 30 min for paraffin sections). Following thorough washing in buffer, the bound secondary antibody was detected as described in section 3.1.10. Paraffin and Vibratome sections were prepared for LM and EM examination as described in 3.1.10.

3.1.12 Light and electron microscope immunocytochemistry for endogenous albumin

The biotin-streptavidin-perioxidase method was employed. Paraffin sections were deparaffinised and rehydrated. Both paraffin sections and Vibratome sections were rinsed in PBS. To eliminate endogenous peroxidase activity, sections were incubated in 0.3% hydrogen peroxide in 70% methanol for paraffin setions or 50% ethanol for

Vibratome sections for 30 min. After washing in PBS, sections were incubated in 10% NHS to reduce non-specific protein binding, 60 min for Vibratome sections and 30 min for paraffin sections. Then, sections were incubated in the goat anti-rat albumin 1:10,000 in 1% NHS, for paraffin sections, or 1:20,000 for Vibratome sections at room temperature overnight with slow agitation. Thereafter, sections were washed in buffer and incubated in a biotinylated horse anti-goat IgG secondary antibody diluted 1:250 in 1% NHS, 60 min for Vibratome sections and 30 min for paraffin sections. Following thorough washing in buffer, the bound secondary antibody was detected as described in section 3.1.10.

3.1.13 Quantitative assessment of fluorescein Lycopersicon esculentum tomato (LET) lectin labelling at the LM level

In the group with moderate trauma, spinal cord sections obtained from the trauma, rostral and caudal sites were stained with fluorescein *Lycopersicon esculentum* tomato (LET) lectin (Vector Laboratories, Inc., Burlingame, CA), which has an affinity for N-acetyl-β-D-glucosamine oligomers. This lectin binds to endothelial cells and is used to visualise the microvasculature (Thurston *et al.*, 1998, Ezaki *et al.*, 2001). After dewaxing, the slides were incubated in 1% BSA in Tris-buffered saline (TBS) for 30 min followed by incubation for 60 min in the lectin at a concentration of 5 µl in 1 ml. Slides were washed in TBS, mounted with anti-fade and examined in an Olympus BX50 microscope fitted with an FITC filter. The microvessels showed green fluorescence. The grey matter was photographed using x 20 or x 40 objective lens at four regions in each section, right and left dorsal horns, and right and left ventral horns, using an Oplympus DP 11 digital camera. The area of the images was calculated with reference to a

graticule photographed at the same magnification. The images were projected on a computer screen in Adobe photoshop and the number of blood vessels was counted in each image. The density of blood vessels/mm^2 was calculated for each region and the mean number was calculated for each section. The mean number of blood vessels in the trauma, roatral and caudal sites for three animals killed at each of 1, 3, 7, 14, and 28 day were compared to three corresponding regions from normal control animals using Student's *t* test. P values less than 0.05 were considered significant. The mean numbers of blood vessels obtained from the three animals killed at each time interval were plotted in a graph and compared to the means in three normal animals.

3.1.14 Quantitative assessment of EBA and GLUT1 immunoreactivity at the LM level

Light microscope sections stained for EBA and others stained for GLUT1 were viewed in an Olympus microscope equipped with an Olympus digital camera (DP11). Four microscopic fields from the grey matter of transverse cord sections, as for the lectin study, from trauma site and segments rostral and caudal to the trauma site were photographed using x 20 or x 40 objective lens as described in the previous section. The digital images were transferred to a computer, enlarged and analyzed using a computer software program for image analysis (Measure Master, Leading Edge Technology, SA, Australia). The field area of each image was 0.149 mm^2 and 0.0352 mm^2 respectively. The number of EBA-immunoreactive blood vessels contained in this area was counted. The mean number of vessels was calculated for normal and experimental animals (Mean $\pm$ SD per mm^2). Student's *t* test was employed to statistically compare the number of immunoreactive vessels in experimental animals and control animals. Differences were rated significant if the P value was less than 0.05.

3.1.15 Quantitative assessment of GLUT1 using Western blot protein analysis

Protein extraction

Normal and experimental rats subjected to moderate trauma were used for protein extraction and Western blotting. Under anesthesia, experimental and normal control animals were first perfused with 0.9 % sterile physiological saline via the left ventricle. Spinal cord segments (1.5 cm) from control animals, and similar segments from experimental animals containing the epicenter of the trauma site were taken. Tissues were washed with 0.1 M PBS three times. Tissues were then homogenized with a Tefflon glass homogenizer in 5 times (w/v) homogenization buffer, 1% NP 40 (Sigma Co. USA) supplemented with 0.0016% protease inhibitor (Roche Diagnostic GmbH, Roche Molecular Biochemicals, Germany) and allowed to stand for 1 hour on ice. The homogenates were then centrifuged at 14000 rounds per minute (rpm) for 15 min. The supernatant was collected and kept at - 70°C for future use. A standard Bradford protein assay method was used to determine the protein concentration in each lysate.

Immunoblotting

Protein lysate was spun at 15000 rpm for 10 min at 4°C. Equal amounts of protein lysate was resuspended in reducing sample buffer. Equal amounts of protein lysate were loaded and separated using 12% sodium dodecyl sulfate-polyacrylamide gel electrophoresis (SDS-PAGE). Experimental and normal control animals were used in parallel lanes for comparison. The separated proteins were transferred onto polyvinylidene difluoride (PVDF) membranes overnight by standard methods and immuno-blotted using a primary antibody directed against GLUT1, followed by an HRP conjugated rabbit anti-goat secondary antibody. Immunoreactive proteins were detected

using the ECL-plus substrate and Hyper X-ray film. The levels of GLUT1 expression in normal and experimental animals were thereafter quantified. The immunoblotting bands were scanned, transferred to a PC computer screen and enlarged. The density of bands was analyzed with Measure Master Image Analysis program. The mean volume of the density of blotting bands was obtained from three animals of each survival interval. The normal and the experimental animals were compared and the difference was examined for significance using Students' *t* test.

3.2 In vivo immunological targeting of EBA model

3.2.1 Animals

Sixty–four adult male Sprague-Dawley rats (180g-350g) were used. Animals were supplied and maintained under standard conditions by the Animal Services of the University of Adelaide. The experiment was approved by the Animal Ethics Committee of the University of Adelaide (S/06/2001) and conducted under the guidelines of the NH&MRC of Australia.

3.2.2 Antibodies

The primary antibodies, monoclonal mouse anti-EBA and polycolonal goat anti-rat albumin antibody were as described previously (sections 3.1.6). Secondary antibodies used for this study were as described previously (section 3.1.7). A mouse IgM (MGMOO, Caltag Laboratories, Burlingame, California, USA) was used as isotype control for anti-EBA

3.2.3 Biochemical reagents

BBB tracers
Horseradish peroxidase type II (HRP, MW 40,000) was purchased from Sigma, USA. HRP is a glycoprotein, which is widely used as a macromolecular tracer for barrier studies. Other biochemical reagents used for this study were as described previously (section 3.1.8).

3.2.4 Animal Model

Experimental animals were divided to two groups; group 1 for HRP leakage study, and group 2 for immunocytochemistry study. Rats were injected intravenously with one of three doses, (50, 40, or 25 µl/kg equivalent to 50, 40, 25 µg/kg respectively) of mouse monoclonal antibody to EBA (anti-EBA) or with an isotype antibody (mouse IgM, 40 µl/kg bw). Antibodies were injected under general anaesthesia. The experiment was terminated by cardiac perfusion at various time intervals following the injection. For the HRP leakage study, animals (group 1) were injected intraperitoneally with an antihistaminic drug, promethazine theoclate (1%) to prevent any allergic reaction to HRP. Ten min prior to perfusion, animals were injected intravenously with HRP (type II, Sigma, 200mg/Kg) and then perfused with 300 - 400 ml 4% paraformaldehyde and 2% glutaraldehyde fixative in 0.1 M phosphate buffer, pH 7.4. Vibratome sections were cut and used for HRP reaction development. In group 2, for the immunocytochemistry study, animals were perfusion fixed with 4% paraformaldehyde only. Vibratome sections were cut and used for immunostaining for EBA and albumin. The brain areas that showed leakage of HRP and immunolabelling for EBA and albumin as detected by LM, were selected and processed for EM as described previously (section 3.1.10).

3.2.5 Animal Perfusion

The detailed procedure for animal perfusion in this study was as described previously (section 3.1.4.). Briefly, following washing of the circulation with PBS gassed with 95%O_2:5%CO_2) for 30 seconds, animals were transcardially perfused with 4% paraformaldehyde and 2% glutaraldehyde in 0.1 M phosphate buffer (group1) or 4% paraformaldehyde only in 0.1 M phosphate buffer (group 2).

3.2.6 Tissue preparation and staining for HRP study

In group 1, after perfusion, the brain and spinal cord were removed and immersed in the same fixative as that used for perfusion, for 3 hours at 4°C. The brain was divided in the median plane. Vibratome sections (60μm) were cut from the brain (Sagittal plane) and from the spinal cord (horizontal plane) were reacted with DAB to detect HRP leakage. The sections were incubated in 0.05% DAB containing 0.01% H_2O_2 for 7 min. After the reaction, sections for LM were mounted on gelatine-coated slides, air-dried overnight, dehydrated, cleared and covered with coverslips. For electron microscopy, rectanglar 2x1mm pieces were cut out of some Vibratome sections, from the cerebral cortex, white matter, brainstem and spinal cord. These were osmicated, dehydrated and embedded in TAAB resin. Ultrathin sections were examined by electron microscopy for HRP leakage in the brain and spinal cord.

3.2.7 Tissue preparation and immunocytochemistry for EBA and Albumin

In group 2 of animals used for immunocytochemistry, a 2 mm thick sagittal block of the brain and a 2 mm thick transverse section of spinal cord were embedded in paraffin. Paraffin sections of 7 μm thickness were cut and mounted on silane-coated slides. These

sections used for immunocytochemical detection of Albumin. Sections of 60 μm thickness were cut from the other half of the brain and from part of the spinal cord, using a Vibratome (Lancer Laboratory Supply, FL, USA). Vibratome sections were floated in PBS and used for immunolabelling for EBA and albumin.

For the EM study, immunolabelling for EBA and endogenous albumin was carried out as described in section 3.1.10 and 3.1.12 respectively. Some sections were immunostained with omission of the primary antibody, and others with omission of both the primary and secondary antibodies. After immunolabelling, small rectangles 2x1 mm were cut from different parts of the brain including the cortex, brainstem and the projection tracts/corpus striatum regions were post-fixed with 1% osmium tetroxide for 1 hour, followed by graded alcohol dehydration and finally embedded in TAAB resin. Ultrathin sections were cut using a diamond knife on a Leica ultracut microtome. Sections were examined either unstained or after counterstaining with uranyl acetate and lead citrate.

3.3 Expression of EBA and GLUT1 in the male reproductive tract after compression *injury of the spinal cord*

3.3.1 Animals

Five normal male Sprague Dawley rats of 300-350g body weight were used for the study of the expression of EBA in the normal male reproductive tracts. The tissues of reproductive tract used for the study of the expression of EBA and GLUT1 after compression spinal cord injury, were collected from the same experimental animals used for the moderate compression spinal cord injury study described in sections 3.1.1

and 3.1.2. All experimental procedures were approved by the Animal Ethics Committees of the University of Adelaide (S-06-2001 and S-37-1999) and conducted under the guidelines of the NH & MRC of Australia.

3.3.2 Antibodies

The primary anti-EBA and anti-GLUT1 antibodies and secondary antibodies used for immunocytochemistry in this study were as described previously (sections 3.1.6 and 3.1.7)

3.3.3 Biochemical reagents

The biochemical reagents used for this study were as described in section 3.1.8

3.3.4 Animal perfusion

The perfusion method used for this study was as described in section 3.1.4. Briefly, the vascular bed was first flushed with 0.1 M Delbecco phosphate buffered saline and then perfusion fixed with 4% paraformaldehyde in 0.1 M phosphorate buffer. The tissues were removed and post-fixed in the same fixative for 3 hours.

3.3.5 Tissue preparation

The testis, epididymis, spermatic cord, seminal vesicles with the associated coagulating gland, ventral prostate, dorsolateral prostate, membranous urethra, the bladder-neck region and the bulbourethral gland from normal and experimental animals were removed. The brain, spinal cord, suprarenal gland, liver, kidney, spleen, intestine, skin, skeletal muscle, and the heart were also removed and used as positive and negative

control tissues for EBA expression. Segments were then taken from the spinal cord of experimental animals; trauma site and rostral and caudal to the trauma site as described in section 3.1.5. Comparable segments were taken from control non-injured animals. Tissues were immersed for 3 h in the same fixative, then processed and embedded in paraffin wax and 7μm sections were cut and collected on silane-coated slides.

3.3.6 Immunohistochemistry

The anti-EBA and anti-GLUT1 antibodies and the methods for EBA and GLUT1 immunocytochemistry at the light microscope level used in this study were as described previously (sections 3.1.10 and 3.1.11).

CHAPTER 4

RESULTS

Chapter 4 Results

4.1 Blood-spinal cord barrier after compression spinal cord injury

4.1.1 General conditions of experimental animals

After surgery, animals recovered from the anaesthesia about 5-10 min after cessation of inhalation anaesthesia. During the surgery, the rectal temperature of experimental and sham control animals was monitored and maintained at 36.5-37.5 °C. Nearly all animals survived after the injury, apart from three animals which are not reported here. After injury, animals sustained a mild drop in their body weight (5-10g) for four days and thereafter regained their body weight steadily (5-10g per day). Sham control animals that had only a laminectomy also suffered a mild drop in body weight (~5g). Experimental animals maintained their interest in the environment. Their eating and drinking habits were similar to those of the controls throughout the experiment.

4.1.2 Motor function of experimental animals

Moderate injury group

Motor function was tested with an incline plane (Rivlin and Tator, 1977). Normal animals (n=6) could maintain their position on the plane with an inclination of 70 ± 5°. Sham operated animals (n=15) showed slight decrease (2-5 degree) in the test angle of incline plane. Animals with moderate injury (n=30) showed transient paraparesis. Immediately after surgery, animals with moderate injury could only keep their normal position on the plane at an angle of 45 ± 2.4°. At one day post-injury, the angle increased to 50 ± 2.3°. Animals started to recover their motor function at 3 days post injury and could stay on the plane at 52 ± 8° inclination. At 1 week post-injury, the

motor function of the moderate injury animals showed a degree of deficit in the movement of the hind limbs. The incline plane test showed 65 ± 3.4°. Two weeks post-injury, the motor function of the moderate injury animals were normal as the test angle increased to 70 ±3.4°, which is similar to the normal animals.

Severe injury group

In the severe injury animals (n=13), there was pronounced loss of motor function of the hind limbs that was maintained throughout the experiment. The animals could not stay on the plane at 45± 2° immediately after injury with no improvement during the post injury period.

4.1.3. General pathological changes in the spinal cord

Moderate injury

Moderate injury was induced by the sustained compression of a 35g of weight on the cord for 5 min. At the trauma site, 1 day post injury, localized haemorrhage, predominantly asymmetric, was observed in the dorsal white column and dorsolateral part of the cord (Fig. 4.1.1A and B). Some inflammatory cells such as macrophages, neutrophils and lymphocytes were seen in the grey and white matter 3 days post injury (Fig 4.1.1C and D). At 7 days post injury, inflammatory cells were still present in the dorsal and central parts of the cord. At 14 days post injury, in the trauma site, the dorsal, lateral and anterior white columns showed axonal swelling, microvacuolation and glial cell proliferation were obvious. At 28 days post-injury, loss of neural tissue was evident with large cavity formation observed in the dorsal column, but most neurons in the grey matter appeared to be normal. Abundant vessels were present in the grey and white

matter with vascular in-growth. Cellular proliferation in the grey and white matter was obvious in the trauma site at this time interval.

Sections rostral and caudal to the trauma site in moderate injury showed minimal morphological changes at 1 day post-injury. A few hyperchromatic neurons could be seen in the grey matter (Fig. 4.1.2A). Some axonal degeneration and necrosis could be observed in the dorsal column and dorsolateral parts of the cord (Fig. 4.1.2B). At 3 days post injury, some inflammatory cells could be seen in the grey and white matter of sections rostral and caudal to the trauma site. At 7 days post injury, a few hyperchromatic neurons and inflammatory cells could still be seen in the rostral and caudal sections. At 14 days and 28 days post-injury, the morphology was similar to that of 7 days animals with predominant white matter vacuolation.

Severe injury group

Severe injury was induced by the sustained compression of a 50 g weight for 15 min on the dorsal part of the cord. Animals with severe injury showed an extensive haemorrhagic necrosis in the grey matter as well as in the white matter in the trauma site. The necrosis occurred as early as 1 day post injury, the shortest survival time period, and was sustained for 2 weeks, the longest survival period (Fig.4.1.1E and F). Haemorrhage was visible even macroscopically in a few animals. In some animals, the normal structure of the central canal could not be observed or the walls of the canal were collapsed. Very few vessels could be seen in the trauma site. At 3 days after injury, haemorrhage was still present. Occasionally, some vessels in the grey matter of the trauma site showed peri-vascular oedema with increased peri-vascular space. At 7 days

post-injury, some inflammatory cells could be observed including macrophages and neutrophils. Some foam cells could also be observed in the trauma site. At 14 days post-injury, many blood vessels were detected in the grey matter as well as in the white matter, but predominantly in the grey matter, suggesting angiogenesis. A few vessels could be observed in the trauma site. A few inflammatory cells including macrophages and neutrophils could still be seen in the grey matter.

The sections rostral and caudal to the trauma site, also showed some haemorrhage in the dorsal column, posterior horn of the grey matter and occasionally in the white matter of the dorsolateral part of the cord. At 3 days post injury, haemorrhage could still be observed in the dorsal part of the cord tissue rostral to the trauma site (Fig. 4.1.2C). Dorsal column and ventral column of sections showed degenerative changes at 7 days and 14 days post injury rostral and caudal to the trauma site, but especially caudal to the trauma site (Fig. 4.1.2D).

Fig.4.1.1 Light micrographs showing H and E staining of sections of spinal cord at the trauma site after moderate and severe injury. **A**. Haemorrhage in the dorsal column of a section at the trauma site at 1 day after moderate injury. **B**. High magnification showing haemorrhage (red blood cells) at 1d in the dorsal column. **C**. Inflammatory response in the dorsal column of a section in the trauma site at 3 days after moderate injury. Neutrophils (arrows) and lymphocytes (arrowheads) are seen in the white matter of the spinal cord. **D**. High magnification of an area of the white matter at 3d showing lymphocytes (arrowheads) in the trauma area. **E**. At 7 days after severe injury, extensive necrosis in the dorsal column white matter is seen in the trauma site. **F**. Cellular proliferation in the trauma site at 14 days after severe injury. ***DC***, dorsal column; ***G***, grey matter; ***W***, white matter.

Fig.4.1.1

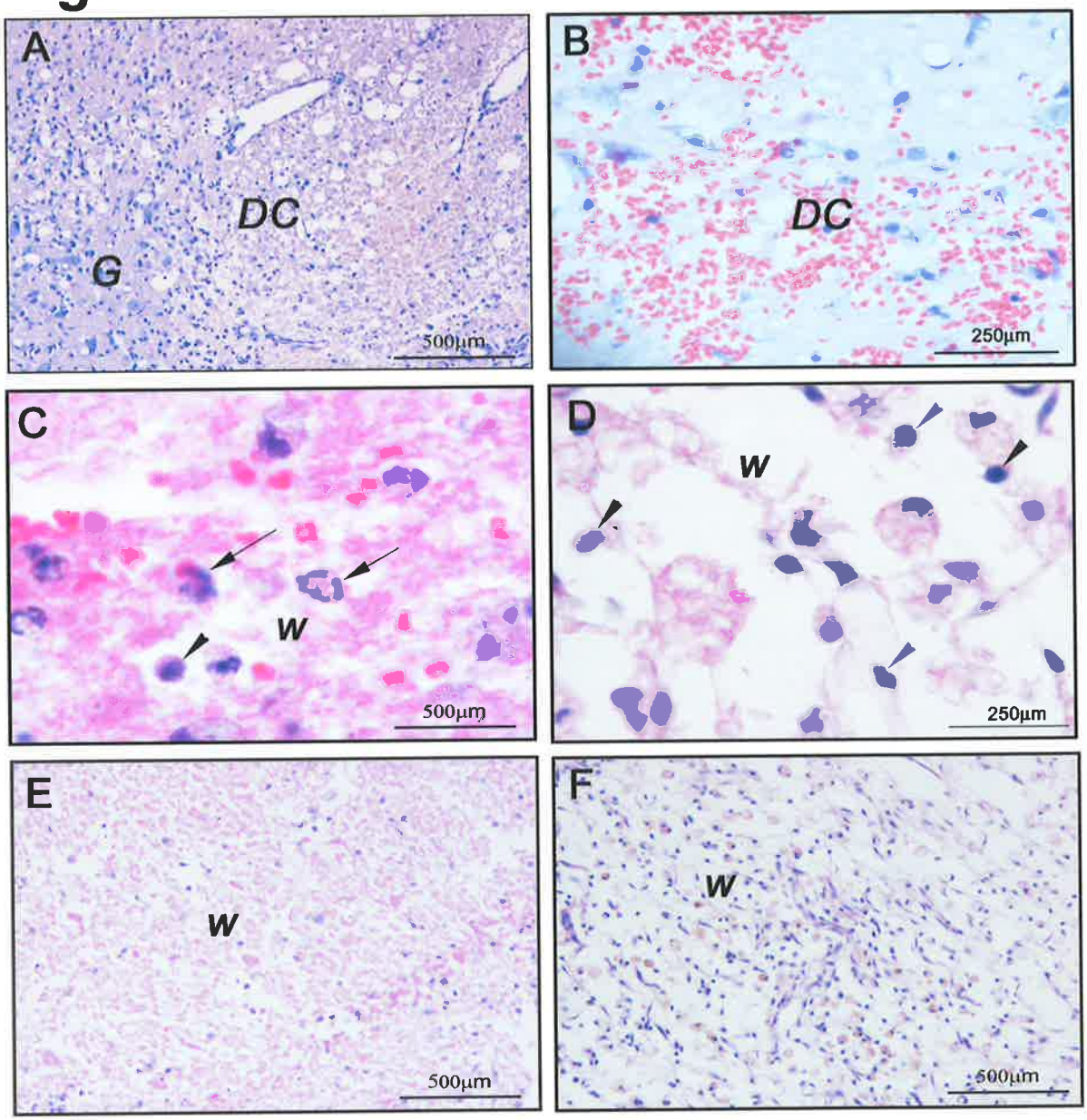

Fig.4.1.2 Light micrographs showing H and E staining of spinal cord sections rostral and caudal to the trauma site after moderate and severe compression spinal cord injury. **A**. hyperchromatic neurons (arrows) in a section from a segment rostral to the trauma site at 1 day after moderate injury. **B**. Axonal degeneration in the dorsal column in a section from a segment rostral to the trauma site at 1 day after moderate injury. **C**. Haemorrhage in a section from a segment rostral to the trauma site at 3 days after severe injury. **D**. Degeneration and haemorrhage in the dorsal column of a section caudal to the trauma site at 7 days after severe injury. ***DC***, dorsal column.

Fig.4.1.2

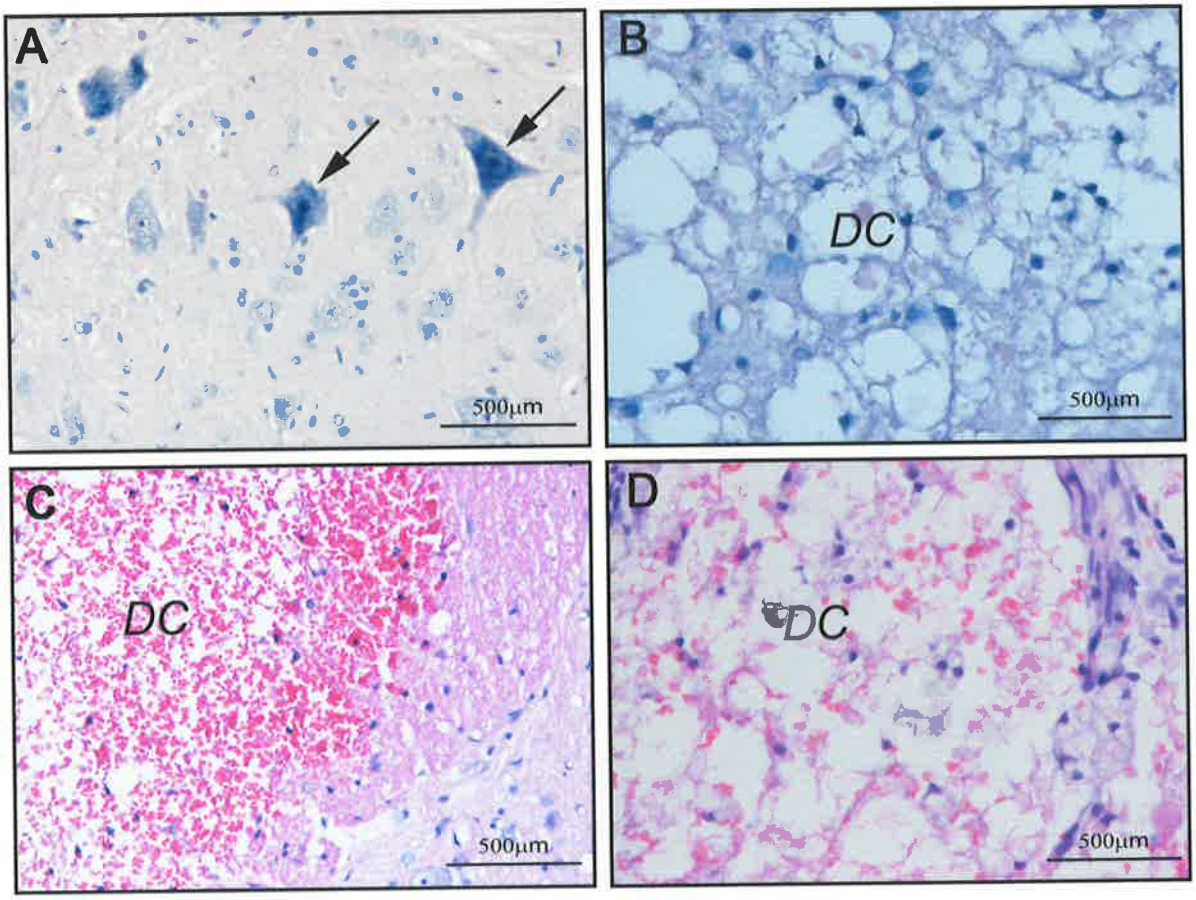

4.1.4 EBA immunocytochemistry after compression spinal cord injury

LM

Normal and sham control animals

In the spinal cord of normal animals, almost all vessels were strongly labelled with anti-EBA. Many vessels in dorsal root ganglia (DRG) and dorsal nerve roots were also labelled. Vessels in the pia mater showed a heterogeneous labelling pattern with complete, partial or no labelling. There was no background staining. Neurons and neuroglial cells were not labelled (Fig. 4.1.3F).

Moderate injury

In the moderate injury animal, at the trauma site, the intensity of EBA labelling was slightly reduced 1 day after injury (Fig. 4.1.3A). A closer examination showed a few non-labelled and partially labelled vessels in the trauma site. The labelling intensity appeared to reach a maximum reduction at 3 days post injury (Fig. 4.1.3B). However, it started to recover at 1 and 2 weeks after injury (Fig. 4.1.3 C and D). The intensity of labelling at four weeks post-injury was comparable to that in normal animals with only few unlabelled vessels (Fig. 4.1.3E).

Spinal cord sections rostral to the trauma site also showed reduction in labelling intensity in the grey matter and white matter at 3 day after injury with some unlabelled vessels, but no reduction in labelling was seen at 1 day post injury. The reduction was maximal at 1 week (Fig. 4.1.4). The labelling was almost similar to that of normal animals at two and four weeks after injury although some unlabelled vessels could be observed. In the ventral part of dorsal column, where in the rat the long descending

tracts are known to exist, the labelling was not obviously affected during all survival time periods in animals of the moderate injury group.

Spinal cord section caudal to the trauma site also showed reduction in the intensity of immunolabelling for EBA. Unlabelled vessels were seen at 1, 3, 7, 14 and 28 days after injury but most frequently at 7 and 14 days (Fig 4.1.5).

Severe injury

In the spinal cord at the trauma site in the severe injury animals, a remarkable reduction of EBA labelling could be observed as early as 1 day after injury (Fig 4.1.6A). Most vessels lost the normal pattern of labelling and the few that retained labelling had a granular appearance to the labelling. Few partially labelled vessels were seen in the trauma site at 3 days post-injury (Fig 4.1.6B). At 7 days post injury, obvious loss of EBA labelling was still apparent, with very few partially labelled vessels being observed in the grey and white matter (Fig 4.1.6C). Two weeks after the injury, the labelling for EBA started to recover in a few vessels (Fig 4.1.6D) but the intensity of labelling was not as strong as in the normal and sham-control animals.

In the segments rostral to the trauma site, some unlabelled vessels could be seen in the grey and white matter at 1 day after injury. At 3 days and 7 days after injury, this reduction was still present (Fig. 4.1.7B and C). At 14 days post injury, the labelling was seen in almost all vessels. In segments caudal to the trauma site, some unlabelled vessels were also seen at 1 and 3 days after injury (Fig. 4.1.8A and B). This reduction was more remarkable at 7 days after injury (Fig. 4.1.8 C). Some unlabelled vessels were still seen at 14 days after injury (Fig. 4.1.8D) whereas most vessels were strongly labelled.

Fig.4.1.3 Light micrographs showing EBA immunoreactivity in spinal cord sections of the trauma site at different time intervals after moderate injury (**A-E**). Note the intensity of the EBA immunolabelling is reduced at 1, 3 and 7 days after injury compared to the immunolabelling in a normal animal (**F**). Many non-labelled or weakly labelled vessels are observed at 1, 3 and 7 days (arrowheads) while other vessels are positively labelled (arrows). At three days animals showed maximal reduction in the labelling. The EBA immunolabelling is pronounced at 14 days after injury; most vessels are positively labelled although some unlabelled vessels are still seen (arrowheads). At four weeks after injury, the intensity of labelling is comparable to that of the normal with only few vessels unlabelled (arrowheads). Sections were lightly stained with haematoxylin. ***G***, grey matter; ***W***, white matter.

Fig. 4.1.3

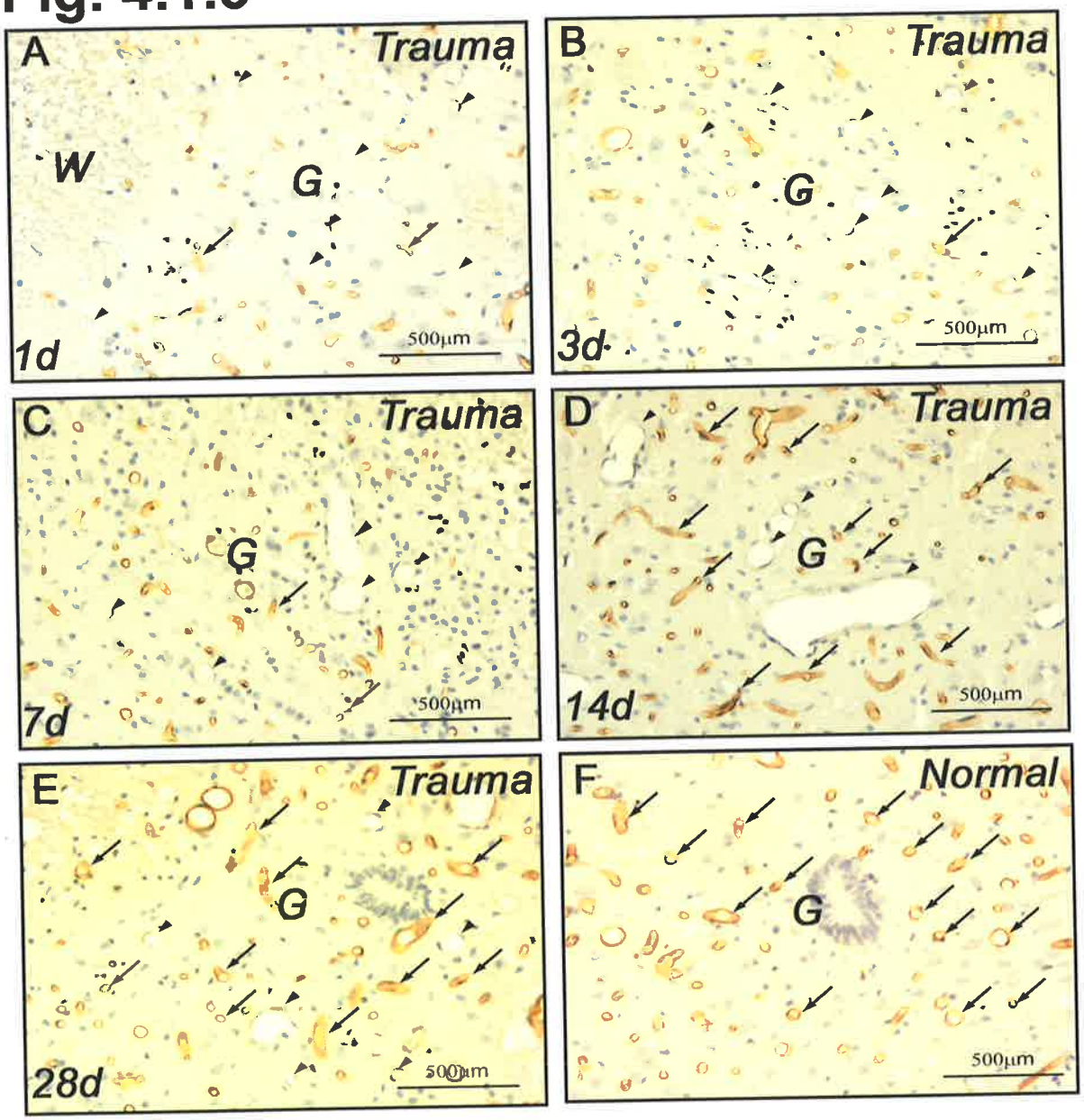
A
Trauma
W
G
1d
500μm
B
Trauma
G
3d
500μm
C
Trauma
G
7d
500μm
D
Trauma
G
14d
500μm
E
Trauma
G
28d
500μm
F
Normal
G
500μm

Fig.4.1.4 Light micrographs of paraffin sections of spinal cord segments rostral to the trauma site after moderate injury showing EBA immunolabelling of blood vessels (arrows). **A,** 1 day; **B,** 3 days; **C,** 7 days; **D,** 14 days and **E,** 28 days after injury, and **F**, Normal control. Note the reduction of EBA expression at 1 day post injury is unremarkable in the sections rostral to the trauma site. However, some unlabelled vessels (arrowheads) are seen at 3 days, but more so at 7 days after injury. Almost all vessels are labeled at 2 weeks and 4 weeks after injury and the intensity appears similar to that in the normal. Sections were lightly stained with haematoxylin. ***G,*** grey matter; ***W,*** white matter.

Fig.4.1.4

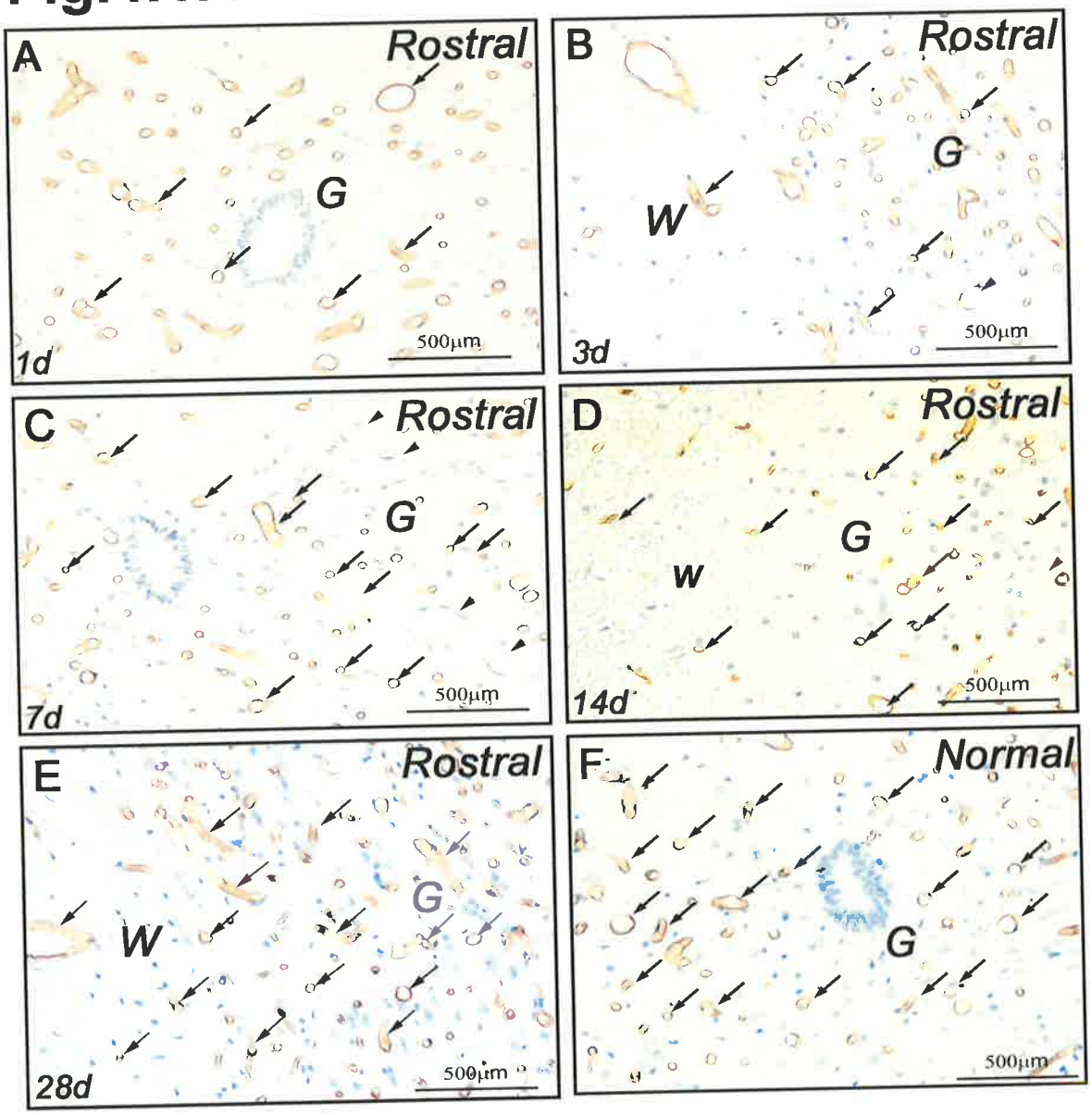
A
Rostral
G
500μm
1d
B
Rostral
G
W
500μm
3d
C
Rostral
G
500μm
7d
D
Rostral
G
W
500μm
14d
E
Rostral
G
W
500μm
28d
F
Normal
G
500μm

Fig.4.1.5. Light micrographs of sections from segments caudal to the trauma site showing EBA immunoreactive vessels (arrows) at different time intervals after moderate injury. **A,** 1 day; **B**, 3 days; **C,** 7 days; **D,** 14 days; **E,** 28 days after injury, and **F,** normal control. Note some unlabelled vessels are seen at 1, 3, 7, 14 and 28 days after injury (arrowheads) but particularly at 7 and 14 days. The intensity of immunolabelling is almost normal at 28 days after injury. Sections were lightly stained with haematoxylin. ***G***, grey matter; ***W***, white matter.

Fig.4.1.5

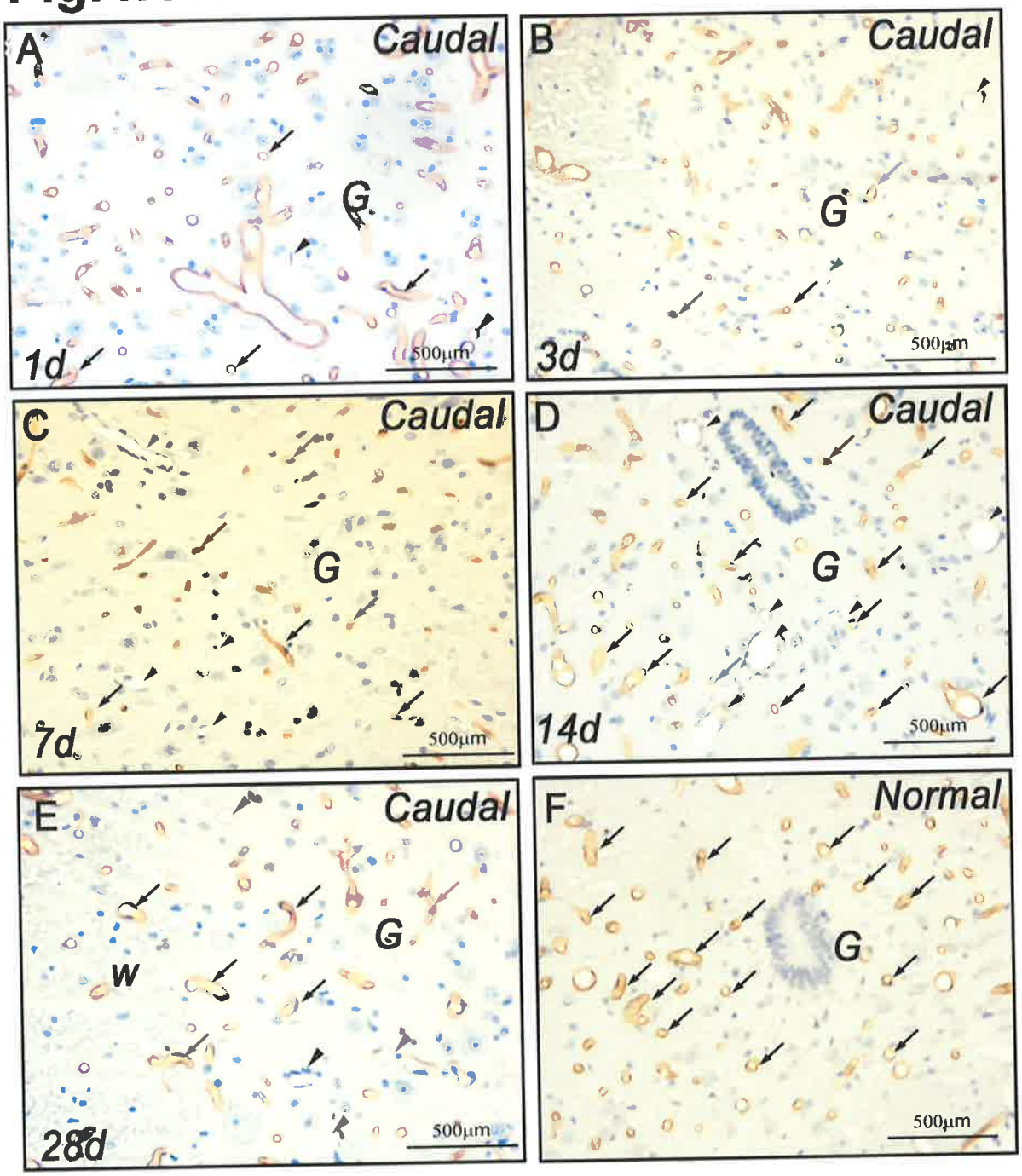
A
Caudal
G
1d
500μm
B
Caudal
G
3d
500μm
C
Caudal
G
7d
500μm
D
Caudal
G
14d
500μm
E
Caudal
G
w
28d
500μm
F
Normal
G
500μm

Fig.4.1.6. Light micrographs of sections of the trauma site showing EBA immunoreactive vessels at different time intervals, 1-14 days after severe compression injury.

Remarkable reduction in EBA labelling is seen at all time intervals after injury. Most vessels were weakly labelled or completely unlabelled (arrowhead) and the vessels show granular appearance of the labelling with loss of the tubular appearence of microvessels. Very few vessels are labelled (arrows), and show normal tubular appearance.

Fig.4.1.6

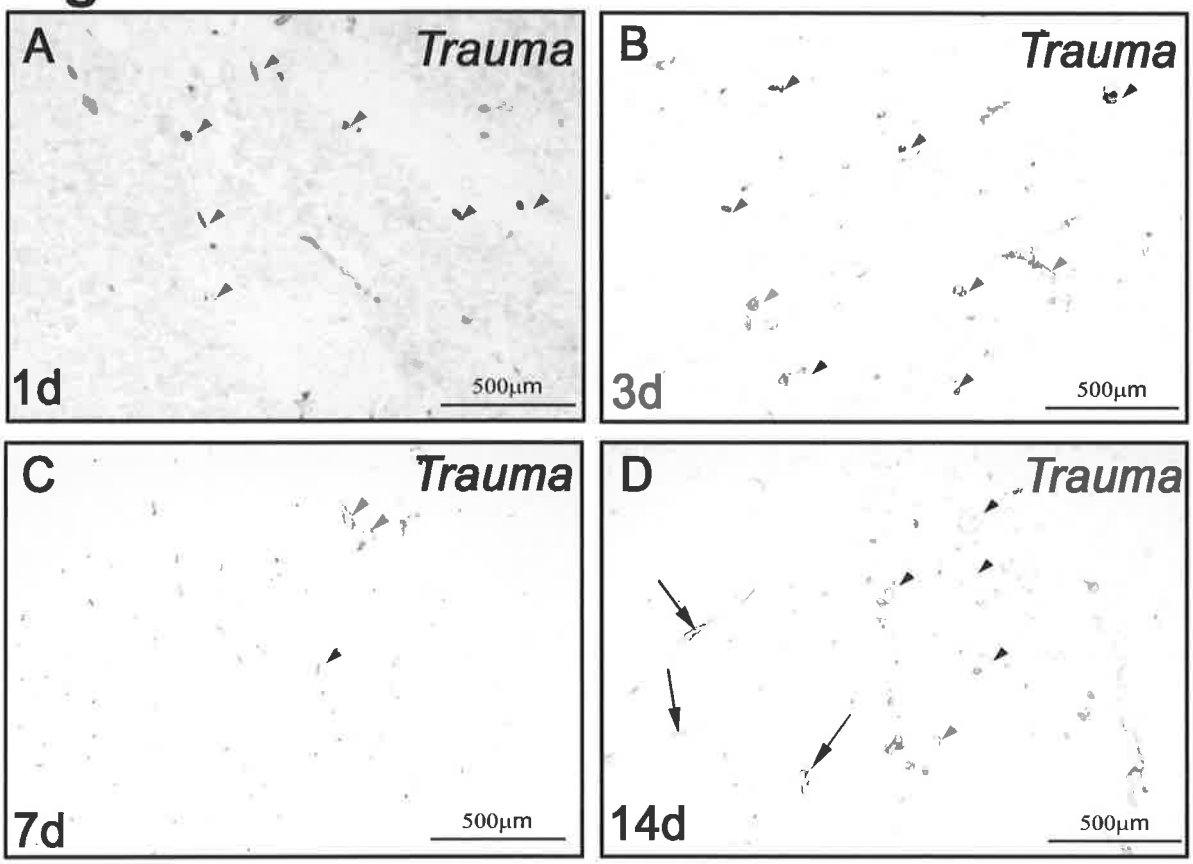
A
Trauma
1d
500μm
B
Trauma
3d
500μm
C
Trauma
7d
500μm
D
Trauma
14d
500μm

Fig. 4.1.7 Light micrographs of sections rostral to the trauma site showing EBA immunoreactivity after severe compression injury. **A,** 1 day; **B,** 3 days; **C,** 7 days and **D,** 14 days. Some unlabelled vessels are seen at 1 and 3 days after injury (arrowheads), but most vessels are positively labelled (arrows). At 7 days and 14 days after injury noticeable recovery occurred but some unlabelled and weakly labelled vessels are still seen (arrowheads). Sections were lightly counterstained with Haematoxlin. ***G***, grey matter; ***W***, white matter.

Fig.4.1.7

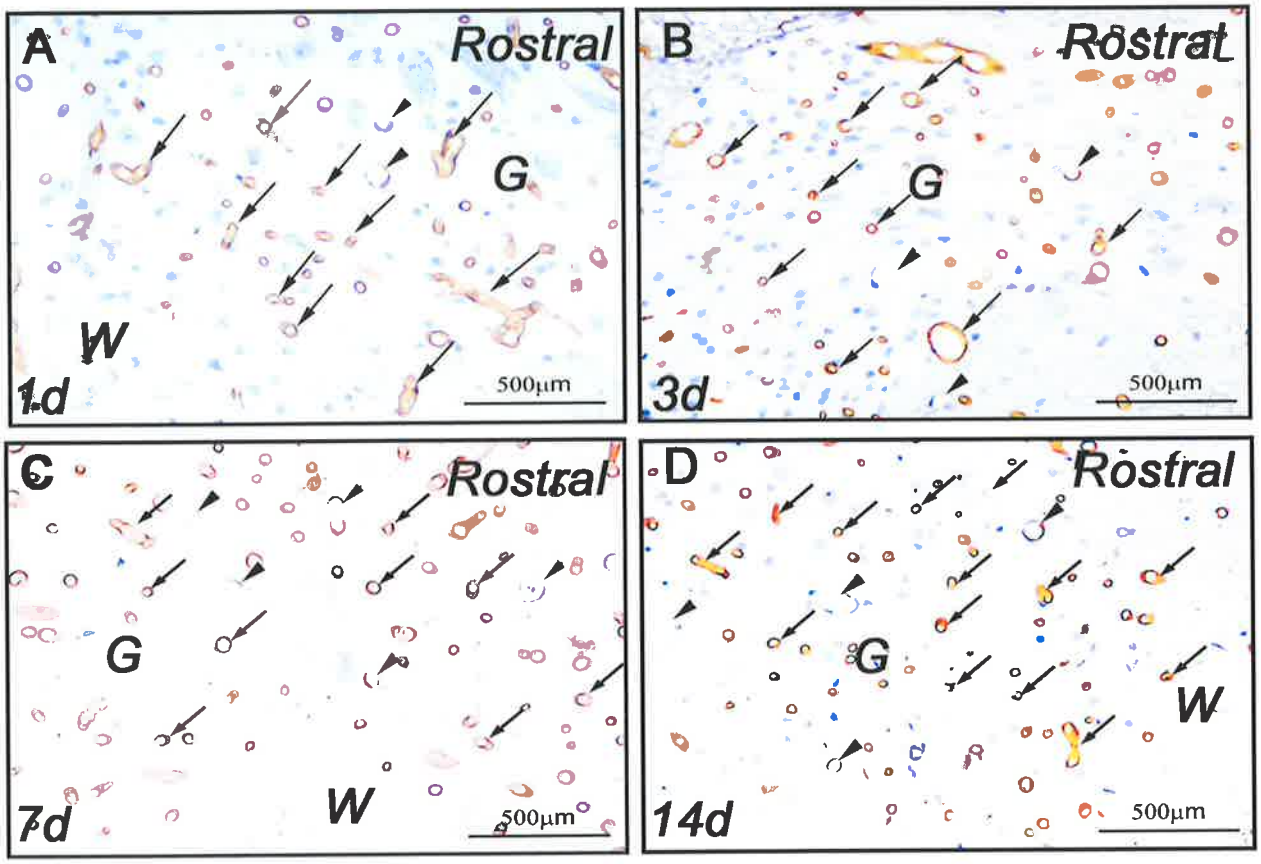
A
Rostral
G
W
1d
500μm
B
Rostral
G
3d
500μm
C
Rostral
G
W
7d
500μm
D
Rostral
G
W
14d
500μm

Fig. 4.1.8 Light micrographs of sections from segments caudal to the trauma site showing EBA immunoreactive vessels after severe compression injury, 1 day to 14 days after injury. Some unlabelled or partially labelled vessels are seen at 1, 3, 7, 14 days after injury (arrowheads), particularly at 7 days after injury. Most vessels are strongly labelled (arrows). Sections were lightly counterstained with Haematoxlin. ***G***, grey matter; ***W***, white matter.

Fig.4.1.8

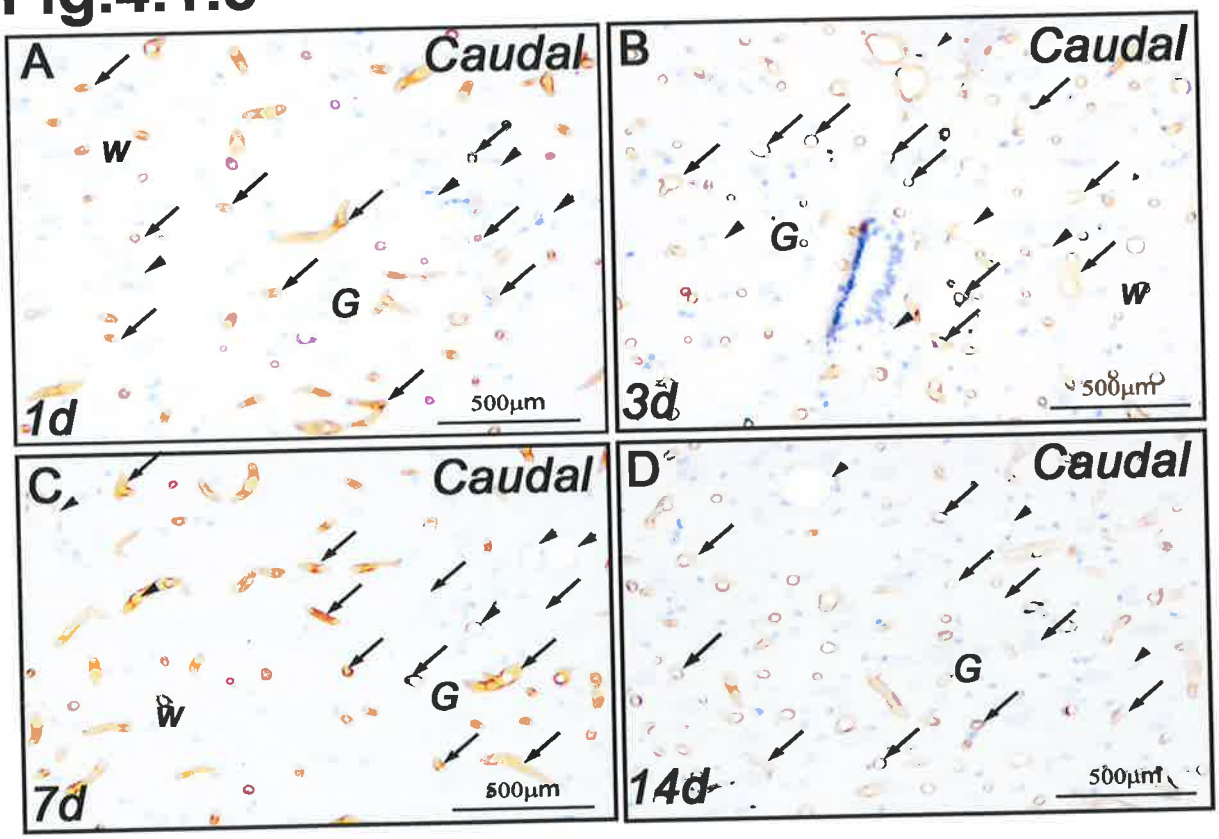
A
Caudal
W
G
1d
500μm
B
Caudal
G
W
3d
500μm
C
Caudal
W
G
7d
500μm
D
Caudal
G
14d
500μm

EM studies

Normal animals

In normal animals, EM of microvessels showed a distinct labelling pattern; anti-EBA labelled not only the luminal surface but also to some extent the cytoplasm of EC. However, the reaction product was essentially located at the luminal membrane of ECs. In most vessels the reaction product was seen at the luminal membrane along the entire circumference of the vessels. However, the density of the reaction was not uniform in all ECs around the vessel circumference. A few ECs showed focal absence of the reaction product. In addition to luminal membrane staining, the cytoplasm of many ECs showed staining which involved the full thickness of the cytoplasm between the luminal and the abluminal membranes. Other ECs showed a gradient of staining fading away towards the abluminal membrane. Endothelial cell vesicles were not stained and appeared electron lucent against the darkly stained cytoplasm. Some EC nuclei showed immunoreactivity on the side of the nucleus facing the lumen. The astrocytes and other perivascular structures were not labelled (Fig 4.1.9A, B and C).

Experimental animals

Moderate injury

In moderate injury animals, at all time intervals, there was a spectrum of EBA labelling. The reduced labelling was in two forms. (a) A reduction in labelling intensity in luminal membranes and the cytoplasm. (b) A reduction in the percentage of labelled luminal membranes in relation to total circumference of the vessel. At all time intervals a mixture of unlabelled, partially labelled or fully labelled vessels were seen. However,

there was a trend of partially labelled and unlabelled vessels being present at 1 day and 3 days after injury (Fig.4.1.10A and B). The recovery of labelling started 1 week after injury. The intensity of labelling appeared to increase in terms of the proportion of the circumference labelled and the intensity of the immunolabelling. The labelling became almost normal in most vessels seen 2 weeks after injury (Fig.4.1.10 C and D). Sections rostral and caudal to the trauma site showed reduction of labelling with a similar labelling pattern. Sections rostral to the trauma site also showed a maximum reduction at 3 days after injury. The inmunolabelling started to recover at 7 days after injury. Sections caudal to the trauma site showed slight difference in the time frame of EBA reduction with a remarkable reduction in the immunostaining intensity at 7 days after injury. Vessels in spinal cord sections caudal to the trauma sites started to recover at 14 days after injury. Most vessels were completely labelled in terms of luminal circumference.

Severe injury

At 1 day after injury, there was obvious reduction of EBA labelling, with a few vessels showing partial labelling. One week post injury, there was no apparent recovery of EBA immunoreactivity, as most vessels were still not labelled. However, two weeks post-injury almost all vessels showed complete or partial labelling of the vessel circumference (Fig.4.1.11 A and B). Some vessels showed vacuoles in the cytoplasm of endothelial cells and these vacuoles were not labelled (Fig.4.1.11B).

Sections rostral and caudal to the trauma site also showed reduction of EBA labelling. The reduction showed a similar pattern to that seen in the trauma site. Most vessels

completely or partially lost electron dense immunolabelling for EBA in endothelial cells. This reduction was seen as early as 1 day after injury and was sustained for 1 week. The recovery of labelling occurred at two weeks and most vessels were completely labelled.

Fig. 4.1.9 Electron micrographs showing vessels from normal control animals labelled with anti-EBA (**A - C**). Anti-EBA antibody labelled not only the luminal surface (arrows in A and B) but also to some extent the cytoplasm of EC between the luminal membranes (single arrows) and abluminal membranes (double arrows) in **C**. Note the astrocytes and other perivascular structures are not labelled (asterisks). Cytoplasmic vesicles (V) are not labelled.

All micrographs are from grids not counterstained with heavy metals.

Fig.4.1.9

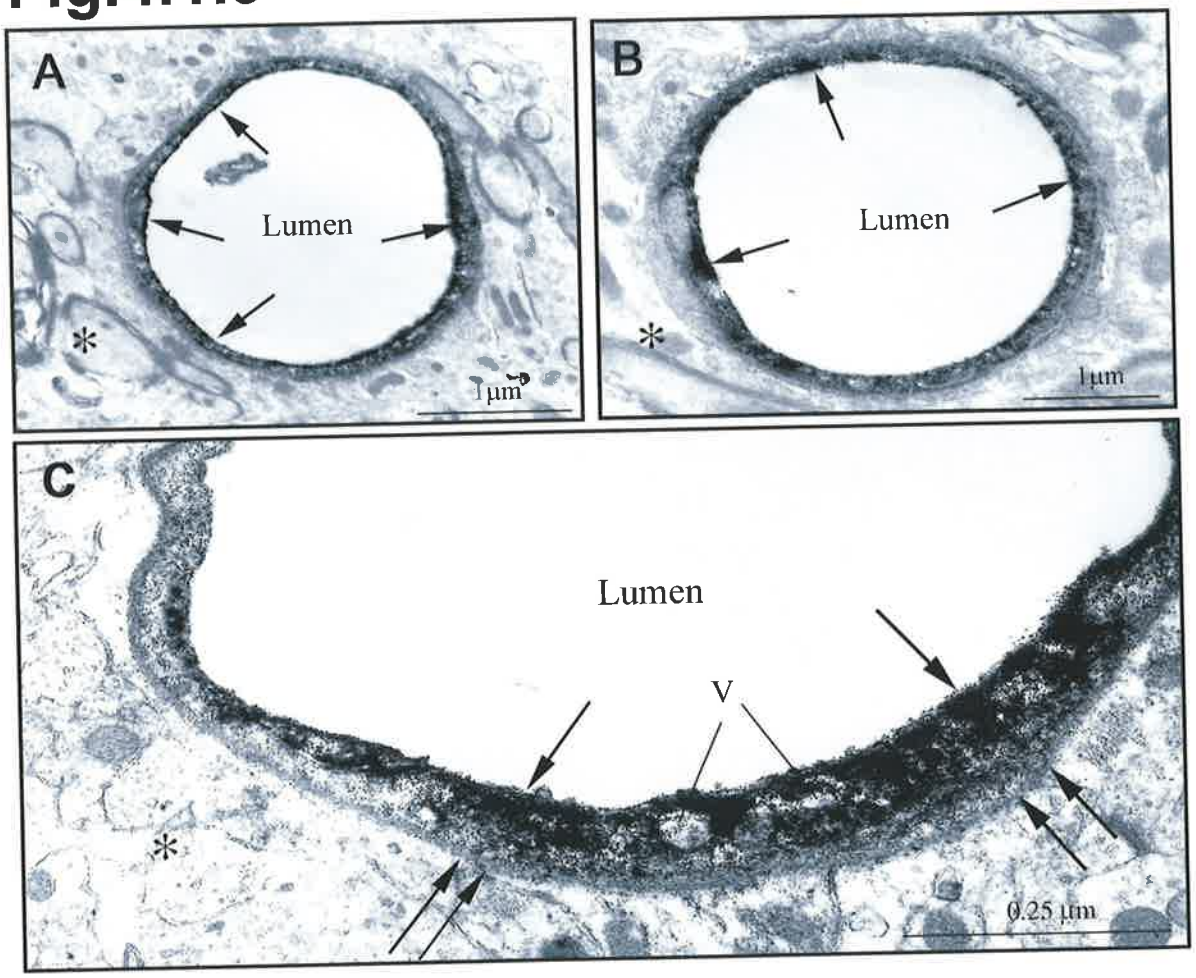

Fig. 4.1.10 Electron micrographs showing vessels labelled with anti-EBA at the trauma site after moderate compression injury. **A.** Luminal membranes (arrowheads) show absence of EBA-labelling in most of the vessel circumference (arrowheads) at 3 days after injury. **B.** A labelled vessel at 7 days after injury (arrowheads) showing luminal membrane labeling, but one part of the vessel circumference is not labelled (arrowheads) and show blebing. **C.** Two weeks after injury, part of a vessel showing strongly labelled luminal membranes (arrows). **D.** A vessel partially labelled with anti-EBA at 14 days after injury. Parts of the endothelial luminal membrane are strongly labelled (arrows) while other parts of luminal surface show weakly labelled or unlabelled membranes (arrowheads).
All micrographs are from grids not counterstained with heavy metals.

Fig.4.1.10

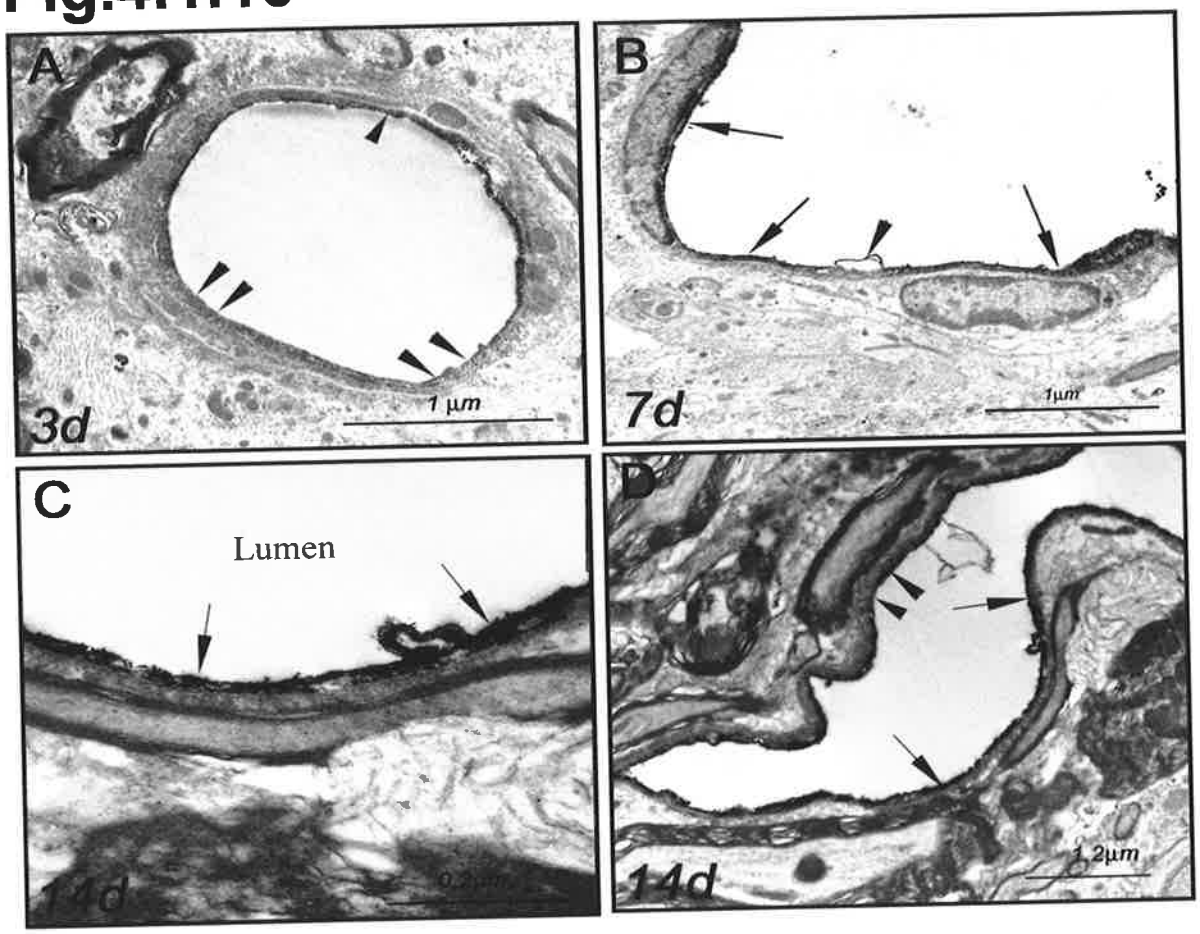

Fig. 4.1.11. Electron micrographs of vessels immunolabelled for EBA from the trauma site at 14 days after severe injury. **A.** A vessel showing very strong labelling of the luminal membranes (arrows) and cytoplasm (double arrows), but endothelial cell vacuoles in the cytoplasm (arrowheads) are not labelled. **B.** a high magnification electron micrograph of a part of a vessel wall showing faint labelling of the luminal membranes 2 weeks after injury (arrowheads). A vacuole (asterisk) adjacent to an intercellular tight junction lacks any labelling.

Both micrographs are from grids not counterstained with heavy metals.

Fig.4.1.11

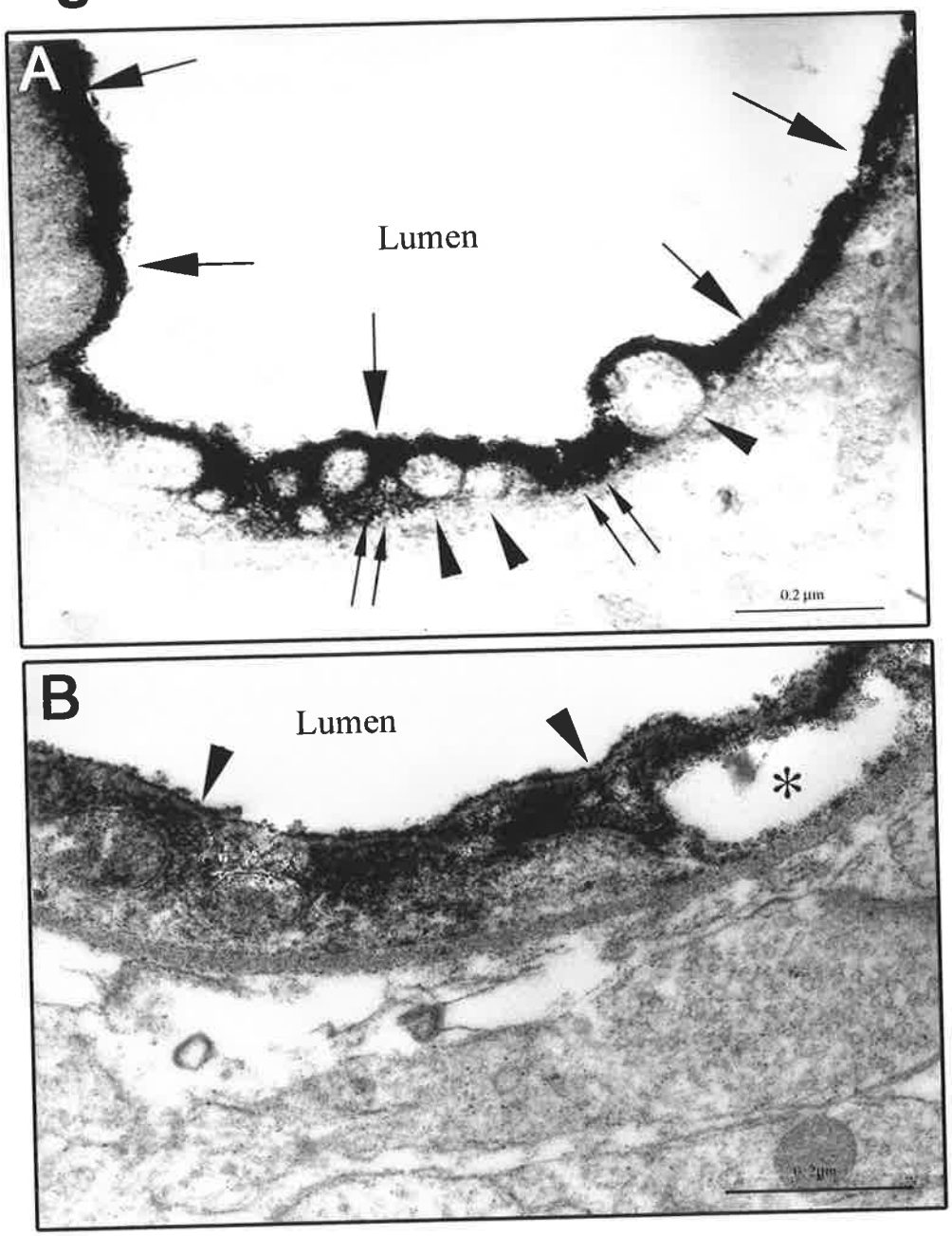

4.1.5 GLUT1 transporter immunocytochemistry after compression spinal cord injury

LM study

Normal control and sham control animals

Vibratome and paraffin sections from normal and sham control animals showed an intense and uniform distribution of GLUT1 immunoreactivity in microvessels throughout the spinal cord. Blood vessels of various sizes showed positive staining (Fig. 4.1.12F). Nearly all vessels in the grey and white matter were labelled with GLUT1 and almost all pial vessels were also labelled. Some vessels in the dorsal roots and dorsal root ganglia (DRG) were also labelled.

Moderate injury

At the trauma site, most vessels showed reduction in labelling after moderate injury. Light microscopy of immunostained sections showed noticeable difference in the intensity of labelling at different time intervals after injury compared to the normal control. Some unlabelled and partially labelled vessels in the grey and white matter were seen particularly at 3 and 7 days (Fig.4.1.12A, B, and C). At 2 weeks post injury, there were still many vessels in the grey matter, which were only partially labelled or unlabelled (Fig.4.1.12D and E). There was some increase in the background labelling mainly in the grey matter of the cord (Fig.4.1.12). At 4 week after injury, the labelling was not different from that in the normal control.

Sections rostral and caudal to the trauma site showed a reduction in GLUT1 labelling, especially in the dorsal part of the cord and the grey matter (Fig. 4.1.13), and some unlabelled vessels could be observed as early as 1 day post injury rostral to the trauma

site. The reduction reached a maxium at 14 days after injury, but the immunolabelling was pronounced at 28 days after injury although numerous vessels were unlabelled. In the caudal site, there was reduced labelling which started at 1 day after injury with maximal reduction at 7 days. The intensity of labelling at 28 days after injury was still less than that of controls (Fig.4.1.14) with numerous unlabelled vessels.

Severe injury

In animals with severe injury there was a remarkable loss of labelling for GLUT1, particularly in the trauma site. The reduction of labelling started as early as 1 day post injury. This reduction was sustained for the 2 weeks of the experiment (Fig. 4.1.15). Very few labelled vessels could be observed in the grey and white matter especially in the dorsal part of the cord at 3 days and 7 days after injury.

Segments rostral and caudal to the trauma site also showed remarkable reduction in the GLUT1 labelling, in the grey and white matter 1 day post injury and the reduction was sustained for 2 weeks (Fig 4.1.16 and Fig 4.1.17). Many unlabelled or weakly labelled vessels were observed at all time intervals, particularly at 3 and 7 days after injury.

Fig.4.1.12 Light micrographs showing GLUT1 immunoreactivity at the trauma site at different time intervals 1 day to 14 days (**A-E**) after moderate compression injury, and a normal control (**F**). Note a reduction of GLUT1 immunoreactivity in the trauma site at different time intervals after moderate injury compared to the normal. In **A-E**, most vessels are unlabelled (arrowheads) or weakly labelled (arrows) for GLUT1. **E**, High magnification of an area in **D** showing microvessels which are unlabelled (arrowheads) and partially labelled (arrows). The grey matter shows some increase in background labelling. Sections were lightly counterstained with Haematoxlin. ***W***, white matter; ***G***, grey matter.

Fig.4.1.12

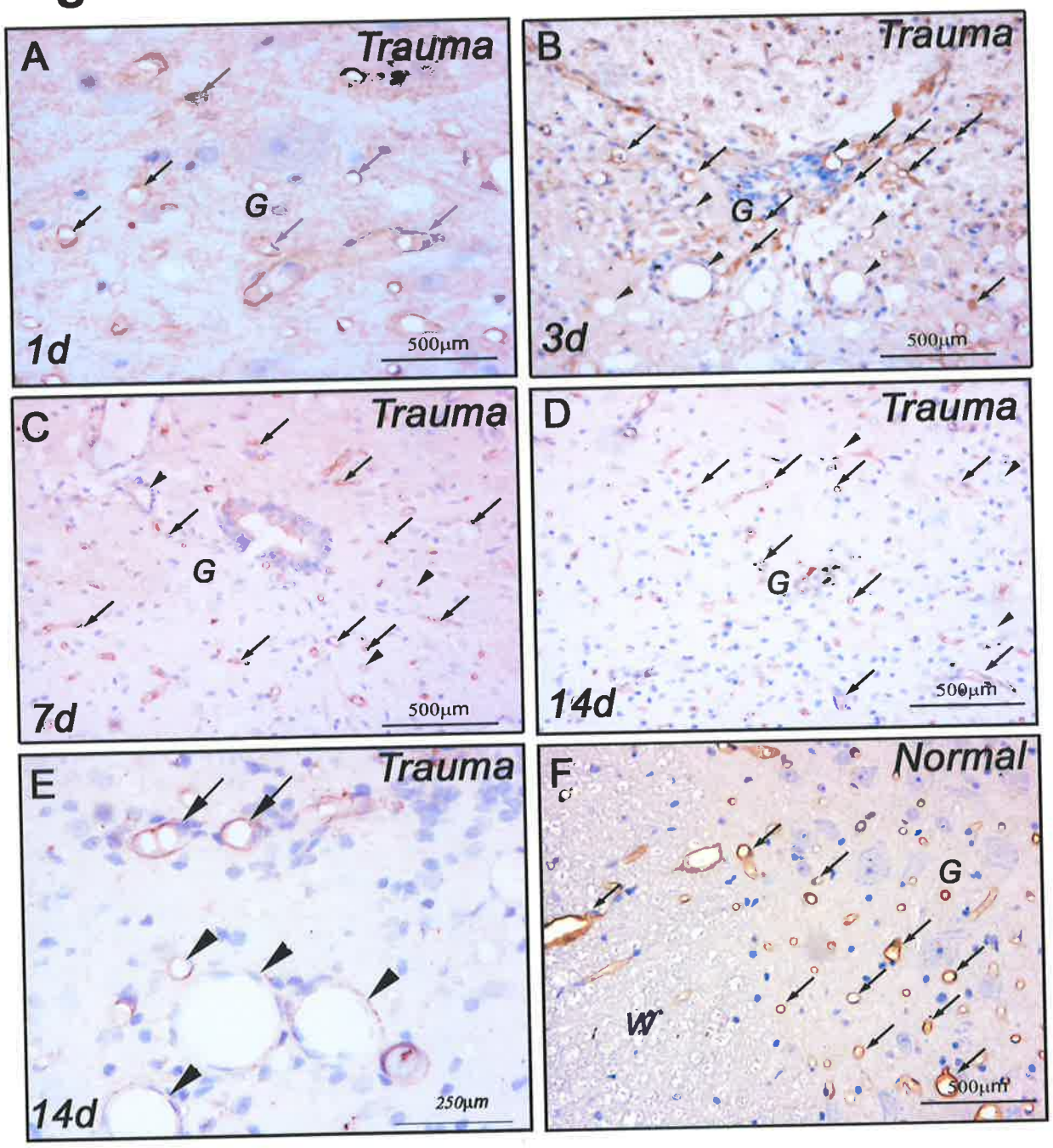
A
Trauma
G
1d
500μm
B
Trauma
G
3d
500μm
C
Trauma
G
7d
500μm
D
Trauma
G
14d
500μm
E
Trauma
14d
250μm
F
Normal
G
W
500μm

Fig. 4.1.13 Light micrographs showing GLUT1 immunoreactivity of spinal cord sections rostral to the trauma site at different time intervals after moderate compression injury (**A-E**) and from a normal control animal (**F**). Note apparent reduction of GLUT1 labelling after injury at all time intervals after moderate compression injury. Many vessels are unlabelled (arrowheads) and most labelled vessels in **A-D** (arrows) show weak staining in part of the circumference. At 28d (E) although many vessels show strong immunolabelling (arrows) many other microvessels are unlabelled (arrowheads). Sections were lightly counterstained with Haematoxlin. ***G***, grey matter; dh, dorsal horn.

Fig.4.1.13

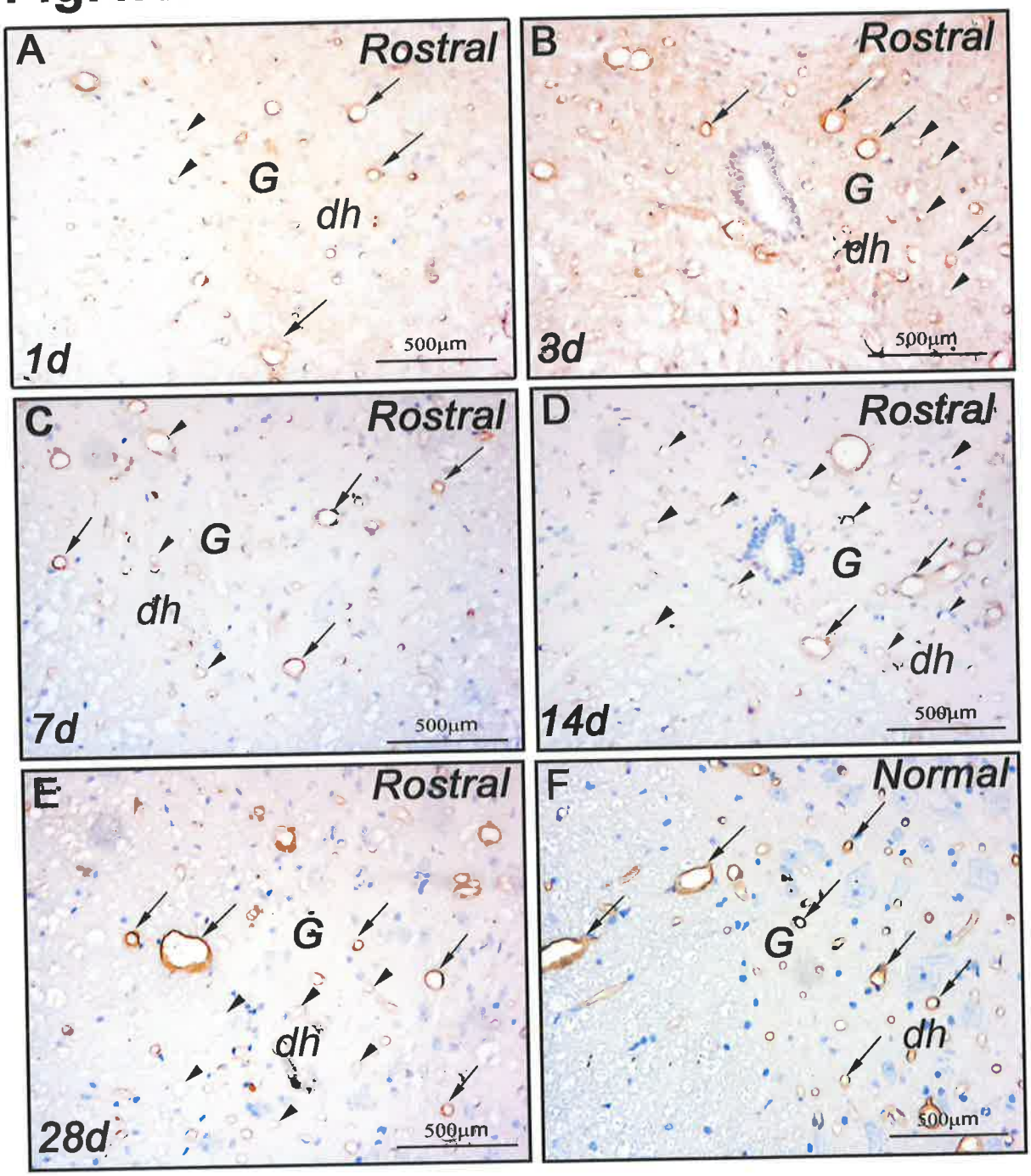
A
Rostral
G
dh
1d
500μm
B
Rostral
G
dh
3d
500μm
C
Rostral
G
dh
7d
500μm
D
Rostral
G
dh
14d
500μm
E
Rostral
G
dh
28d
500μm
F
Normal
G
dh
500μm

Fig. 4.1.14 Light micrographs showing GLUT1 immunoreactivity in the segments caudal to the trauma site at different time intervals (**A-E**) after moderate compression injury and from a normal control (**F**). Labelled vessels (arrows) are less apparent at all experimental time intervals than in the controls. Unlabelled vessels are seen in all experimental time points. The reduction of GLUT1 staining is seen at 1, 3, 7 and 14 days but most apparent at 7 days post injury. At 28 days labelling intensity is still less than that in the control with numerous unlabelled vessels. Sections were lightly counterstained with Haematoxlin. ***G***, grey matter; ***W***, white matter; dh, dorsal horn.

Fig.4.1.14

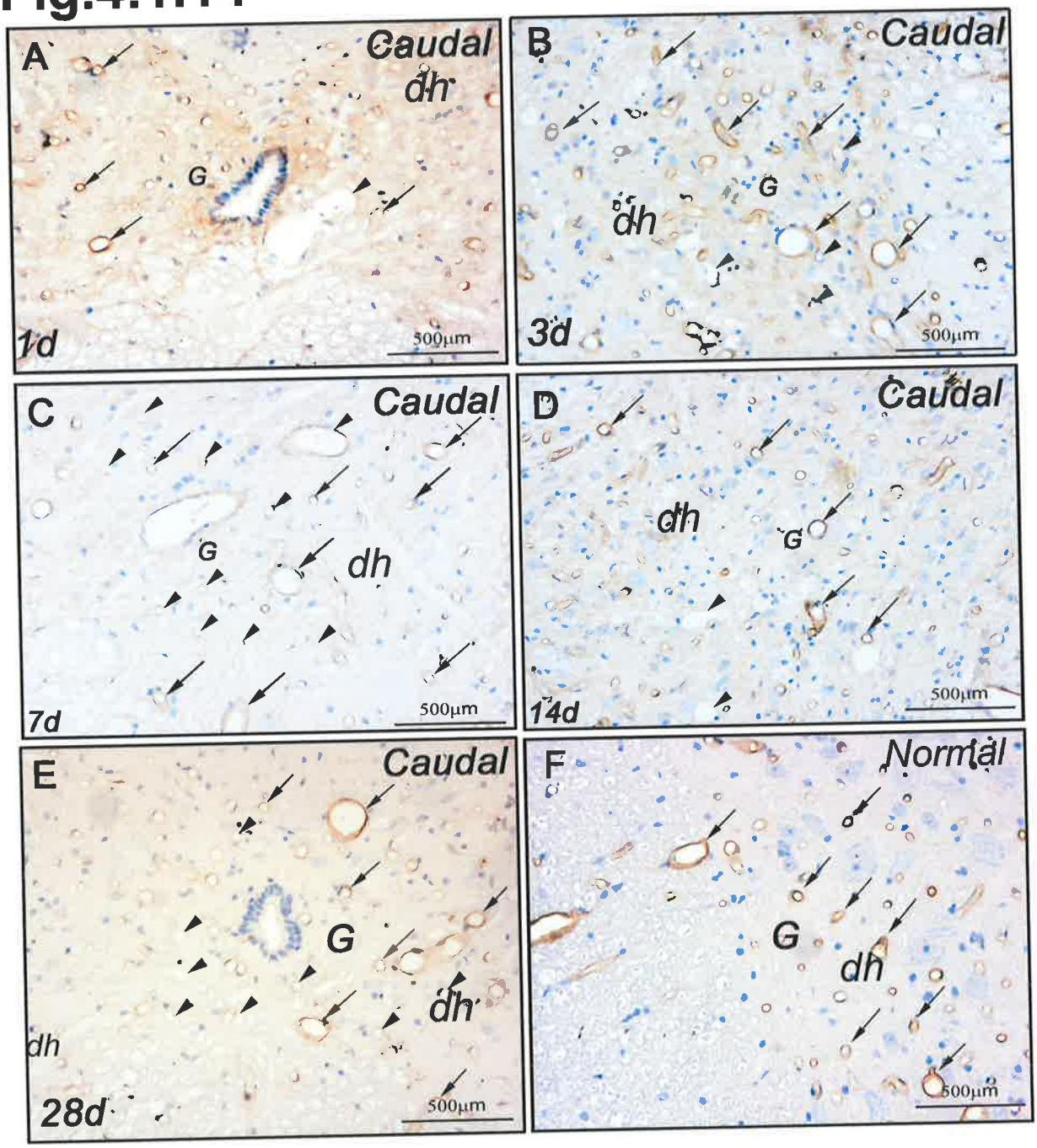
A
Caudal
dh
G
1d
500μm
B
Caudal
G
dh
3d
500μm
C
Caudal
G
dh
7d
500μm
D
Caudal
dh
G
14d
500μm
E
Caudal
G
dh
dh
28d
500μm
F
Normal
G
dh
500μm

Fig. 4.1.15. Light micrographs showing GLUT1 immunoreactivity in sections from the trauma site at different time intervals (1d-14d) after severe compression injury to the spinal cord and from a normal animal. Note obvious reduction of the GLUT1 immunoreactivity at the trauma site (arrowheads). Most vessels are not labelled at the trauma site from 1 day to 7 day (arrowheads). The immunolabelling for GLUT1 shows partial recovery at 14 days after injury with many labelled vessels (arrows). **E.** A section from a control spinal cord showing labelled vessels (arrows). Sections were lightly counterstained with Haematoxlin. ***G***, grey matter; dh, dorsal horn.

Fig.4.1.15

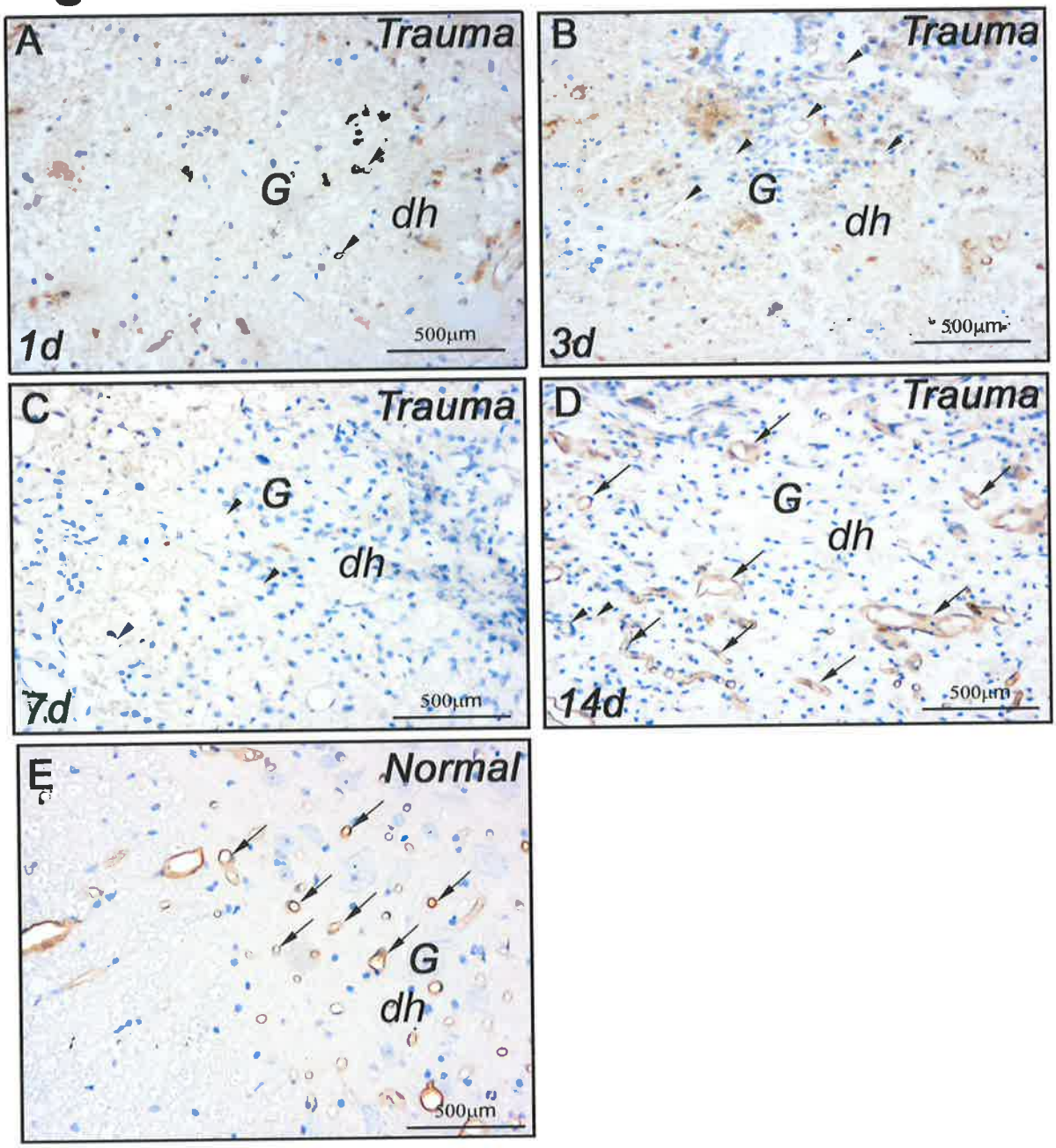
A
Trauma
G
dh
1d
500μm
B
Trauma
G
dh
3d
500μm
C
Trauma
G
dh
7d
500μm
D
Trauma
G
dh
14d
500μm
E
Normal
G
dh
500μm

Fig. 4.1.16. Light micrographs showing GLUT1 immunoreactivity in spinal cord sections rostral to the trauma site at different time intervals (1d-14d) after severe compression injury and from a normal control (**E**).

The reduction of GLUT1 is particularly apparent at 3 days after injury. At 1 and 7 days post injury, many unlabelled vessels (arrowheads) are seen. At 14 days labelled vessels (arrows) are comparable to normal but many vessels are unlabelled (arrowheads). Sections were lightly counterstained with Haematoxlin. ***W***, white matter; ***G***, grey matter; dh, dorsal horn.

Fig.4.1.16

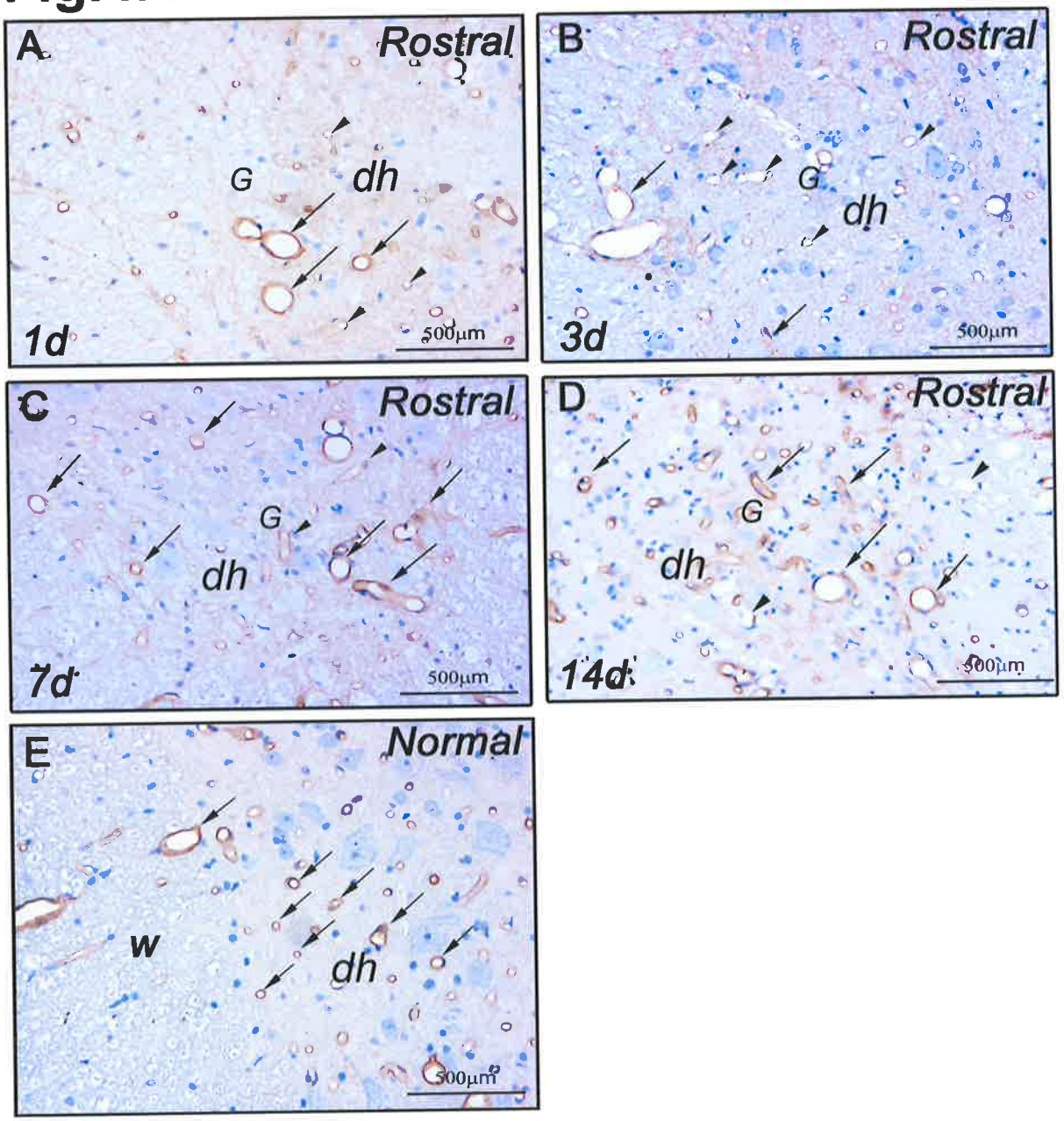
A
Rostral
G
dh
1d
500μm
B
Rostral
G
dh
3d
500μm
C
Rostral
G
dh
7d
500μm
D
Rostral
G
dh
14d
500μm
E
Normal
w
dh
500μm

Fig. 4.1.17. Light micrographs showing GLUT1 immunoreactivity in spinal cord sections caudal to the trauma site at different time intervals (1d-14d) after severe compression injury, and from a normal control (**E**).

At 1 day-14 day post injury there is obvious reduction in GLUT1 labelled vessels (arrows), more so at 3 and 7 days after injury and many unlabelled vessels (arrowhead) are seen. **D**. Labelled vessels are seen (arrows) at 14 day postinjury, but many unlabelled vessels (arrowheads) are also apparent. **E**. shows GLUT1 immunolabelled vessels (arrows) in the grey and white matter of normal control spinal cord. Sections were lightly counterstained with Haematoxlin. ***G,*** grey matter; ***W,*** white matter; dh, dorsal horn.

Fig.4.1.17

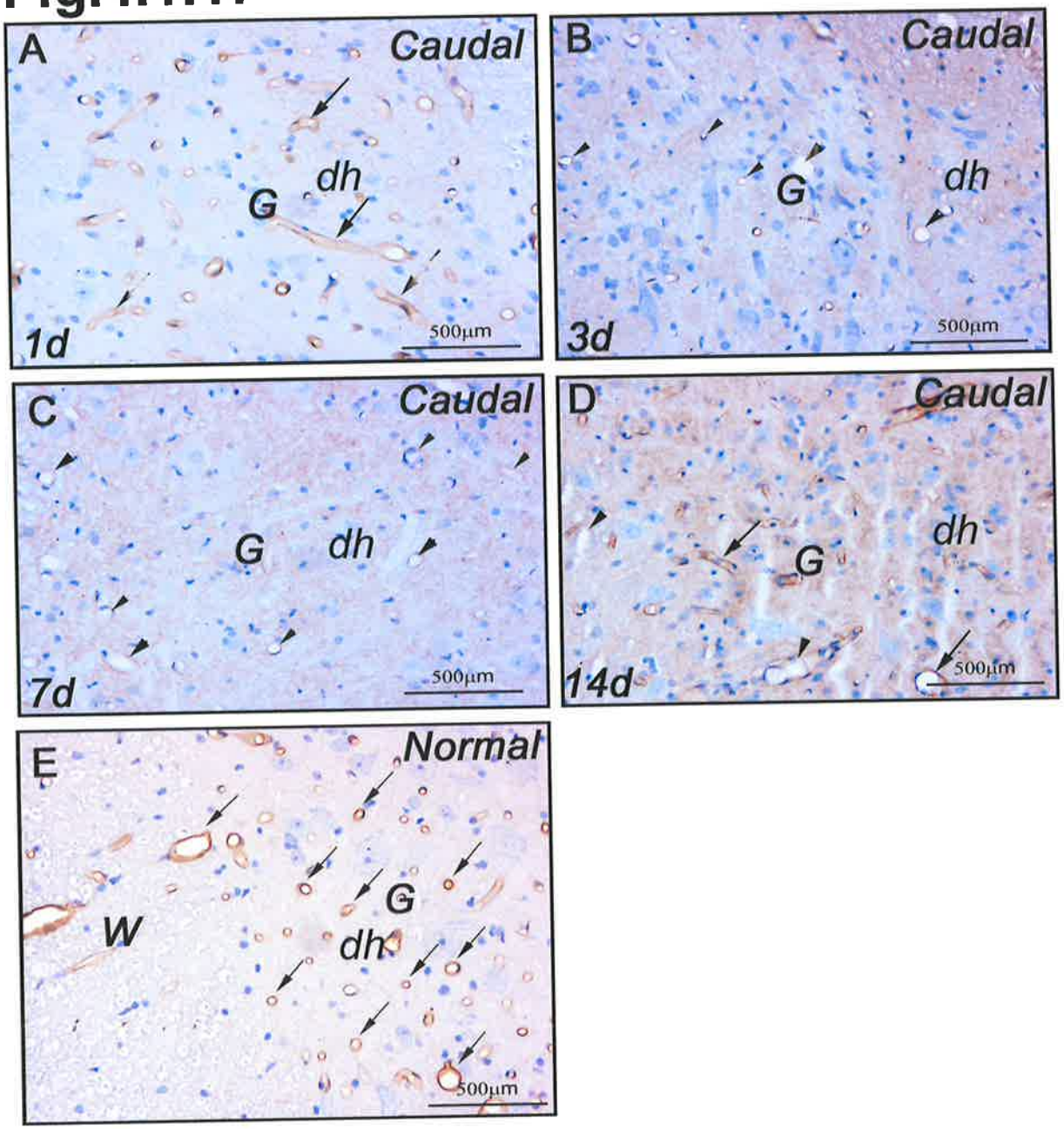
A
Caudal
G
dh
1d
500μm
B
Caudal
G
dh
3d
500μm
C
Caudal
G
dh
7d
500μm
D
Caudal
G
dh
14d
500μm
E
Normal
W
G
dh
500μm

EM study

Normal and sham controls

Immunoelectron microscopy for GLUT1 in normal and sham control animals showed luminal labelling of vessels in the grey and white matter. The immunoreactivity for GLUT1 appeared as electron dense deposits representing the peroxidase reaction product. GLUT1 immunoreactivity was mainly localized to the luminal membrane of ECs. The abluminal membranes were also stained, but the staining appeared less intense (Fig. 4.1.18A). The cytoplasm of some ECs was also labelled, but vesicles in the cytoplasm of ECs were unlabelled (Fig.4.1.18A and C). GLUT1 staining was present at the entire luminal circumference of most microvessels. Few vessels showed sectoral absence of GLUT1 labelling (Fig.4.1.18B). No GLUT1 immunoreactivity was localized to pericytes or astrocytic endfeet. In the neuropil, neurons and axons were not labelled.

Experimental animals

Moderate injury

At the trauma site, a spectrum of strong staining-to-complete loss of staining was seen at all time points in experimental animals, but there was an obvious predominence of unlabelled or partially labelled vessels (Fig 4.1.19A). The reduction started at 1 day after injury and continued for 2 weeks. Most vessels completely or partially lost immunolabelling. After 2 weeks post injury, the labelling started to recover. Most vessels then were completely labelled with electron-dense peroxidase reaction deposits in terms of luminal circumference.

Segments rostral and caudal to the trauma site also showed reduction of GLUT1

labelling. By EM (Fig. 4.1.19B), at one day after the injury, most blood vessels examined in the segment rostral to the trauma site showed partial staining for GLUT1. Some blood vessels showed no immunoreactivity for GLUT1. Three days after the injury, animals showed maximum loss, the majority of blood vessels in segments both rostral and caudal to the trauma site showed sectoral or complete loss of GLUT1 (Fig. 4.1.19C) whereas very few vessels were completely labelled. However, after 1 week, the labelling started to recover with many vessels showing complete labelling although some unlabelled vessels were seen.

Severe injury

In the trauma site, obvious loss of the GLUT1 labelling could be observed. The entire circumference of the vessels was completely unstained or only partially immunostained especially in the dorsal part of the cord tissue. The loss occurred as early as 1 day after injury and was sustained for 2 weeks. However, the expression of GLUT1 was partially recovered at 2 weeks post injury.

Sections rostral and caudal to the trauma site also showed loss of GLUT1 labelling. The reduction started as early as 1 day after injury. Some vessels were only partially or completely unlabelled (Fig. 4.1.19D and E) at 3 and 7 days after injury. The labelling pattern was similar to that seen in the trauma site. At 2 weeks post injury, the intensity of immunlabelling in labelled vessels was similar to that of normal controls but many vessels were still unlabelled.

Fig. 4.1.18 Electron micrographs of spinal cord microvessels showing pre-embeding immunoperoxidase labelling for GLUT1 in the normal rat spinal cord. (**A**) A microvessel shows electron dense reaction product along the entire circumference. Endothelial cells show immunoreactivity in the cytoplasm involving the full thickness between the luminal and abluminal membranes (between single and double arrows). (**B**). A high magnification of the rectangle "B" in Figure "A" shows an unlabelled sector (arrowhead). (**C**). A high magnification of the rectangle "C" in Figure "A" shows that cytoplasmic vesicles are unstained. No labelling is seen in perivascular astrocytes or pericytes **V,** vesicle.

All micrographs are from a grid not counterstained with heavy metals.

Fig.4.1.18

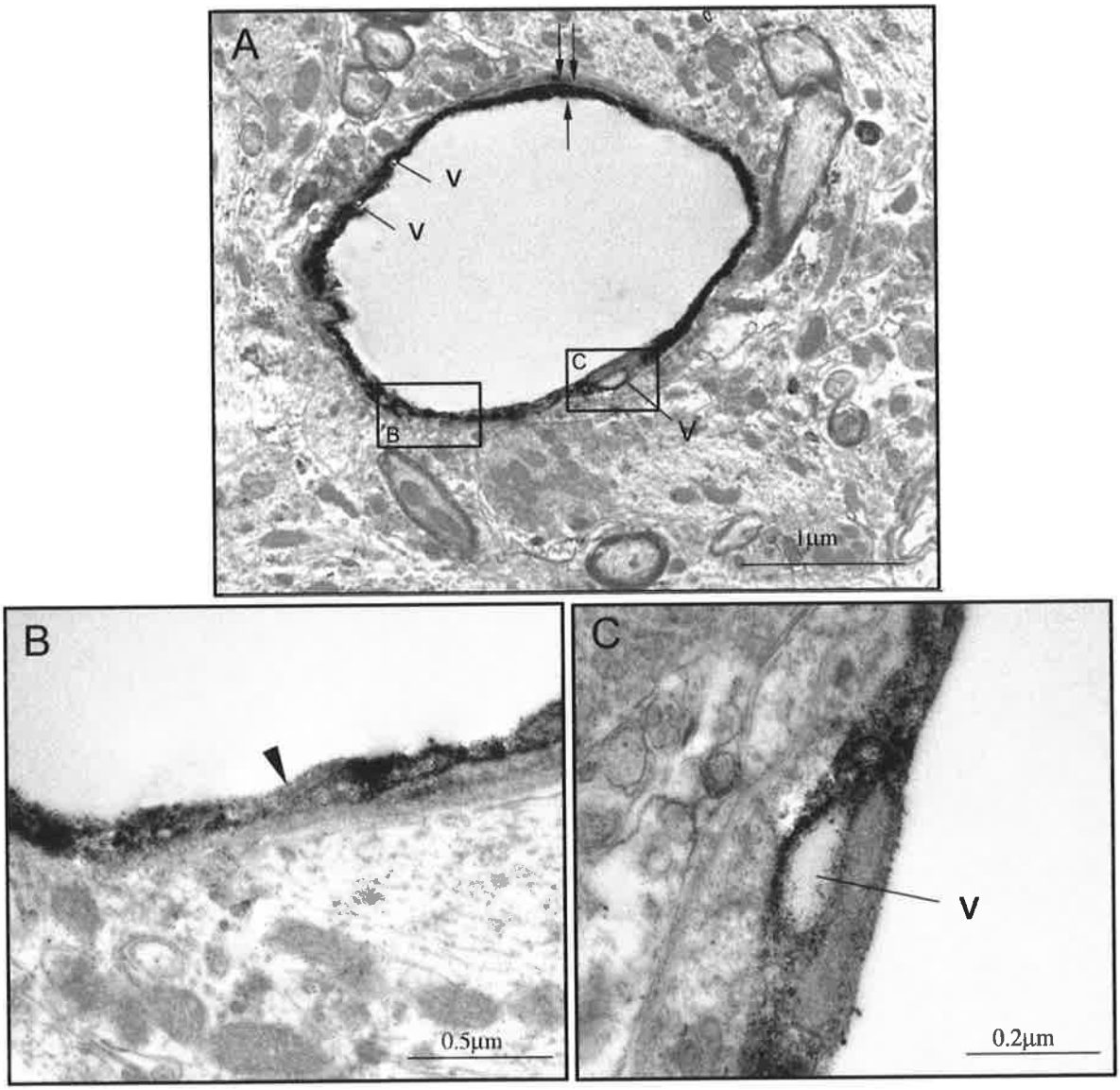

Fig. 4.1.19 Electron micrographs showing GLUT1 immunoreactivity at different time intervals after moderate and severe compression injury. Various degrees of loss of immunolabelling is seen at different time intervals. **A.** GLUT1 labelling in a section from a segment at the trauma site at 3 days after moderate compression injury. A small part of the vessel circumference is strongly labelled (arrow) while other parts of the vessel circumference are not labeled (arrowheads). **B.** GLUT1 immunolabelling in a section from a segment at the caudal site 1 day after moderate injury. **C.** Remarkable reduction of GLUT1 labelling in a section rostral to the trauma site 3 days after moderate injury. **D.** Remarkable loss of GLUT1 labelling at the caudal site 3 days after severe injury. Wide perivascular space is seen (asterisk). **E.** A microvessel from a segment caudal to the trauma site is partially labelled at 7 days after severe injury. Arrows indicate electron dense immunolabelling in the luminal membranes. Arrowheads indicate areas lacking immunolabelling. All images are from sections not conterstained with heavy metals.

Fig.4.1.19

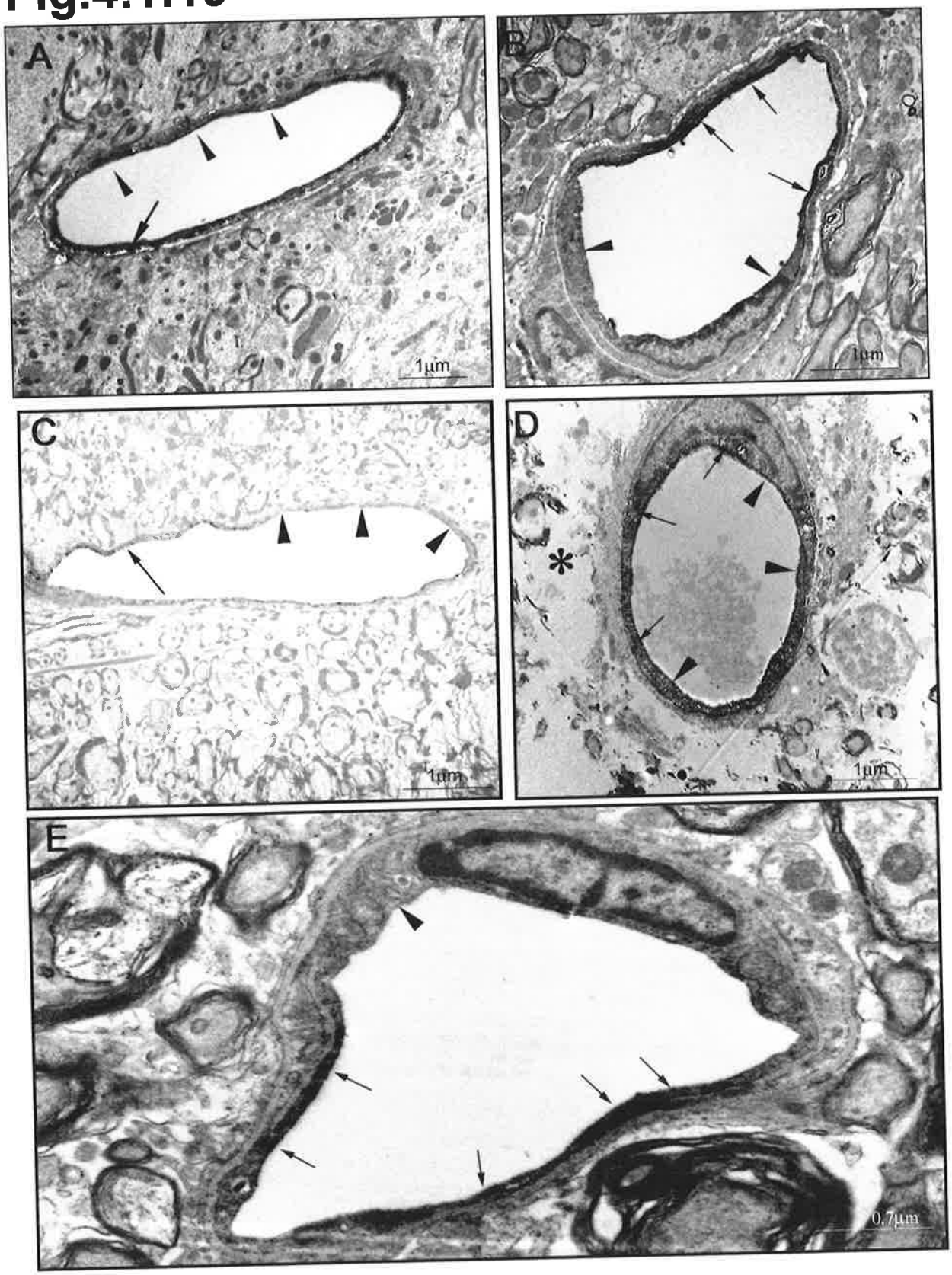

4.1.6 Albumin permeability changes at the BSB after compression spinal cord injury

Normal animals

Permeability changes of the BSB after compression was assessed by immunocytochemical detection of the leakage of endogenous albumin. In normal animals, albumin immunoreactivity was found only in the dorsal root ganglia and dura mater. No albumin immunoreactivity could be observed in the white matter, grey matter or pia mater of the spinal cord (Fig.4.1.20A and B).

Experimental animals

Moderate injury

In moderate injury animals, albumin leakage occurred in the trauma site in the dorsal part of the spinal cord particularly in the posterior grey horn. The leakage was seen one day after the injury, the shortest survival time period in this study, and 3 days (Fig.4.1.20C) and was sustained for 1 week. After the first week, the intensity of albumin immunolabelling started to diminish (Fig 4.1.20D). At 4 weeks post-injury, no leakage was detected in the injury site.

Segments rostral and caudal to the trauma site also showed albumin immunolabelling, which started from 24 hours after injury and continued for 2 weeks. At four weeks after injury, there was no obvious detectable immunoreactivity for albumin rostral and caudal to the trauma site.

Severe injury

At the trauma site in the severe injury animals, diffuse leakage of albumin was found 24 hours post-injury and was sustained for 2 weeks. The leakage was predominantly present in the grey matter but was also found in the white matter of the cord in the trauma site.

Rostral and caudal sites also showed albumin immunoreactivity 1 day post-injury and was mainly present in the dorsal white column, but not in the grey matter. At 2 weeks post-injury, there was no obvious albumin immunoreactivity in the rostral segments. However, in the segements caudal to the trauma site, some albumin immunoreactivity could be seen in the areas where corticospinal tracts decend (Fig 4.1.20 E and F).

Fig.4.1.20 Light micrographs showing albumin immunoreactivity in spinal cord sections of normal and experimental animals. **A**. A section from a normal animal, showing no albumin immunoreactivity, but occasionally some peroxidase reaction product for blood-born albumin is observed inside the vessels (arrow) indicating successful immunolabelling. **B**. Immunolabelling for albumin in a normal animal showing immunoreactivity in the dura (small arrows) and nerve roots (large arrows) but not in the pia matter (**P**) and the neuropil of the spinal cord (SC). **C**. Diffuse immunoreactivity for albumin in the trauma site 3 days after moderate compression injury. Labelling appears as moderate brown reaction product in the grey matter around the central canal. The section was counterstained with haematoxylin. **D**. At 14 days after moderate injury, there is moderate albumin immunoractivity. **E**. At 14 days after severe injury, albumin immunoreactivity is seen in the ventral part of the dorsal column (arrow) where in the rat the corticospinal tract descends. This section is caudal to the trauma site. **F**. A high magnification of the area of increased albumin immunolabelling seen in **E.**

G, grey matter; ***DH***, dorsal horn; ***DC***, dorsal column. **C** & **D** are lightly counterstained with haematoxylin.

Fig.4.1.20

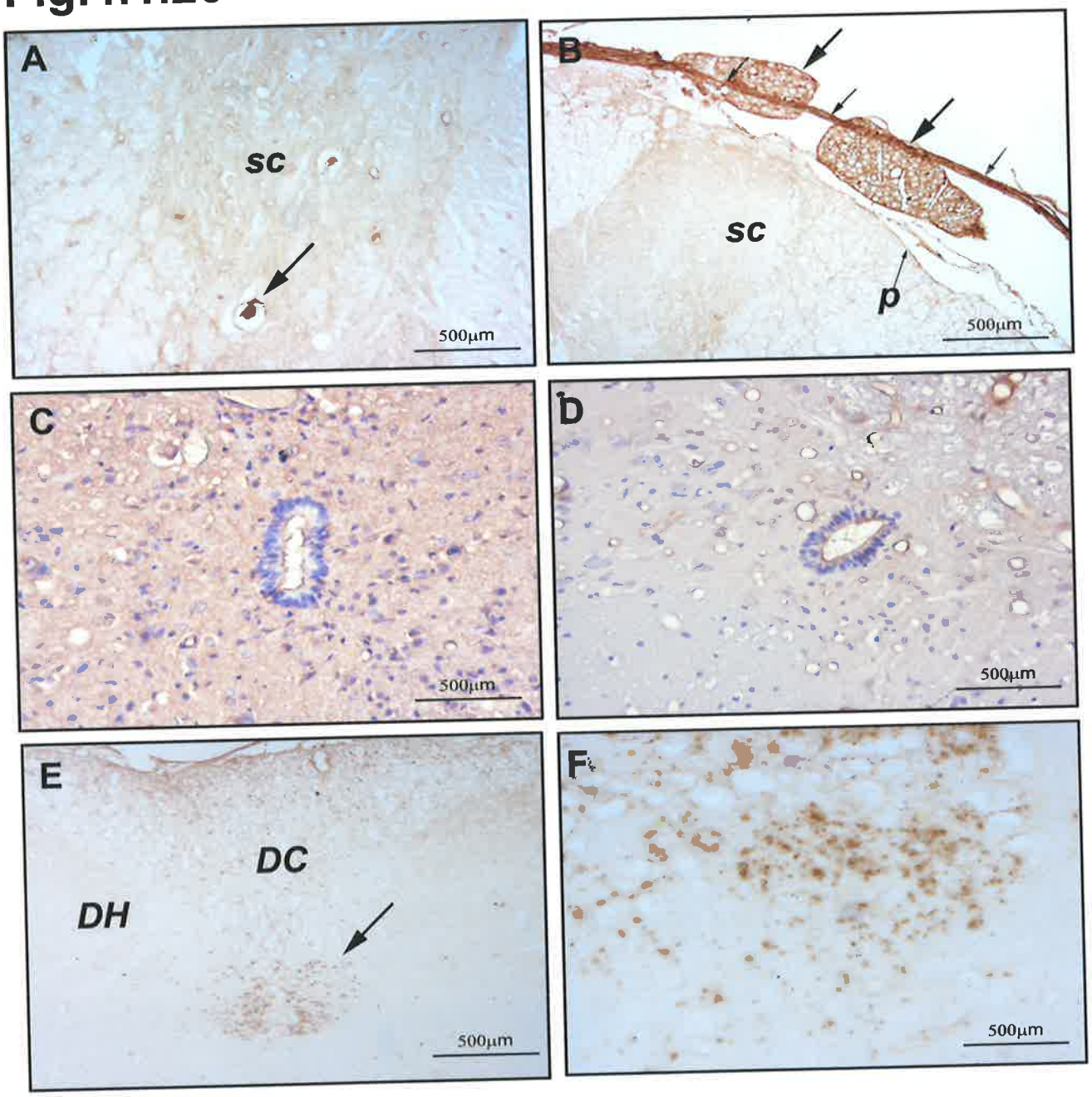

4.1.7 Quantitative study of the total profile of microvessels in normal and experimental animals

LET Lectin was used as a marker to label all microvessels in the rat spinal cord (Fig.4.1.21). Microvessels labelled with LET lectin in normal and experimental animals were quantified by counting the labelled vessels in four areas including one area in each dorsal horn and one area in each ventral horn at the trauma site, and in the segments rostral and caudal to the trauma site. The results (Table 4.1, Fig 4.1.22) showed a general trend of increase in the number of lectin-labelled blood vessels at all time intervals from 1 day to 28 days following trauma, at the trauma site and rostral site, when compared to the normal controls. However, in the caudal segments, most time intervals showed a slight reduction in the mean number of vessels when compared to controls. The total profiles of vessels in the normal and experimental animals were statistically analysed using Student's *t* test. The analysis however, showed that the numbers of lectin-labelled vessels at the trauma and caudal sites were not significantly different from the normal control (Table 4.1). Also there was no significant difference between the number of labelled vessels at rostral segments at 1d, 3d, 7d as compared to the normal, but at 14 and 28 days after injury the numbers were significantly higher than the normal (Table 4.1).

4.1.21. Light Microphotographs showing the fluorescein *Lycopersicon esculentum* tomato (LET) lectin labelling of mcirovessels (arrows) in the normal (**A**) and at the trauma sites of experimental spinal cord at 3 days (**B**), 14 days (**C**) and 28 days (**D**) after moderate injury. Scale bars, 500 μm.

Fig.4.1.21

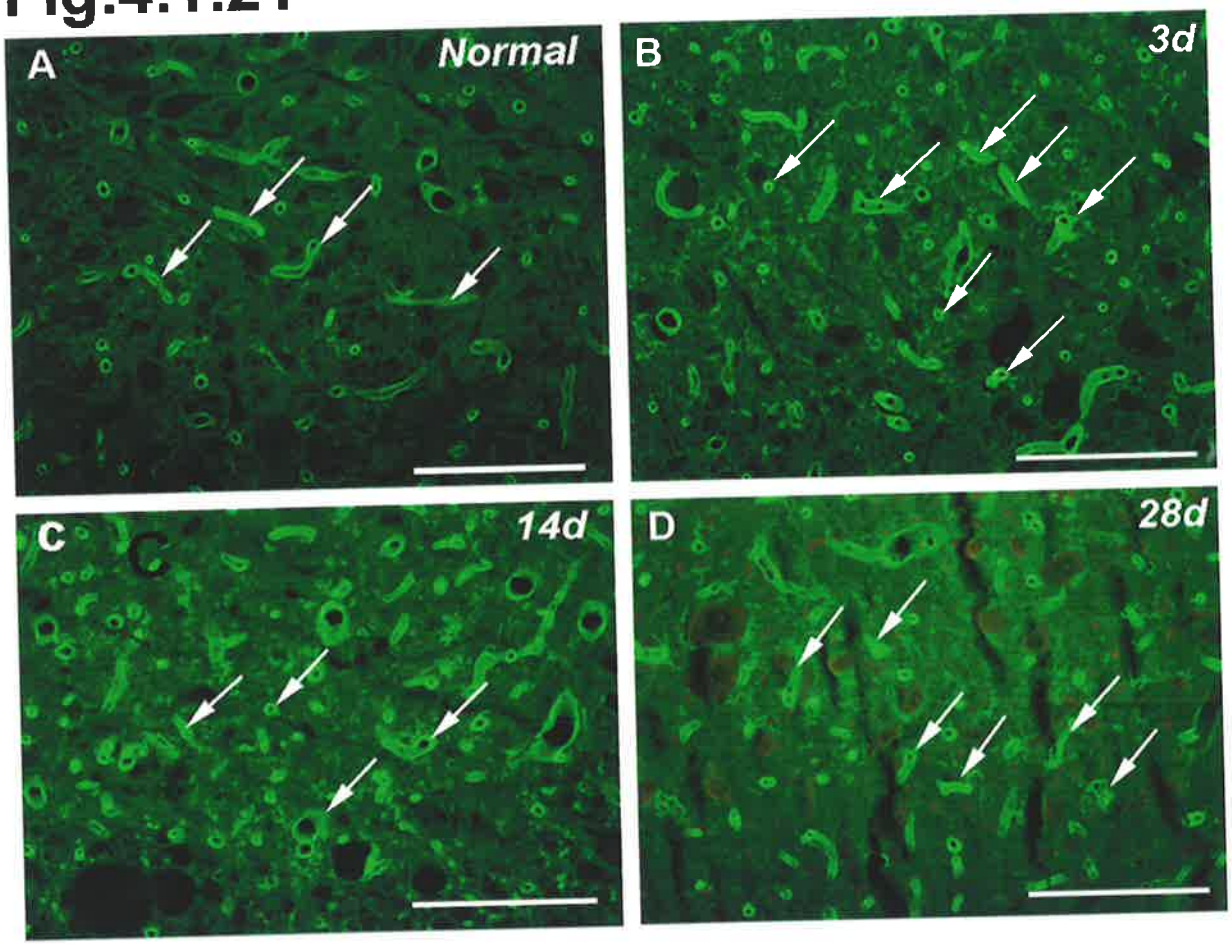

Table 4.1. The mean number of lectin labelled blood vessels in the spinal cord of normal control and moderate spinal cord injury (SCI) rats

	Rostral site (n/mm^2)	Trauma site (n/mm^2)	Caudal site (n/mm^2)
1d SCI	653±182 (522-860)	643 ± 135 (545-797)	473±78 (440-562)
3d SCI	633±95 (541-730)	824 ±335 (593-1208)	593±177 (431-781)
7d SCI	554±104 (448-565)	610± 223(477-867)	458±140 (478-587)
14d SCI	693±101* (596-808)	845±343 (634-357)	484±75 (416-586)
28d SCI	719 ±65* (644-760)	696 ±72 (645-747)	471 ±75(414-556)
Normal	507 ±64 (463-599)	560± 49 (497-611)	501 ± 35 (486-552)

Data shown represent the mean value ± SD (range).

n/mm^2, number of lectin labelled blood vessels per mm^2.

**Significantly different from the mean value of the normal control, $P < 0.05$.*

4.1.8 Quantitative study of the expression of EBA and GLUT1 after compression spinal cord injury

4.1.8.1 Quantitative study of EBA immunoreactive vessels

Moderate injury

EBA expression in normal and experimental animals was quantified by counting the immunoreactive vessels in four areas in the trauma site as well as in the segments rostral and caudal to the trauma site (Fig 4.1.22, Table 4.2). The four areas of each spinal cord section included one area from each ventral horn and one area from each dorsal horn. The mean number of the immunolabelled vessels in the trauma site 1 day after injury was 444±71/mm^2. Three days after injury, the number of labelled vessels was reduced to 405±84/mm^2 in the trauma site. Seven days after injury, the number of vessels was further reduced to 337±166/mm^2, which was significantly lower than normal control (P=0.02). Two weeks post injury, the number of labelled vessels increased to 517±163/mm^2 but was not significantly different from the normal animals (P= 0.4). Four weeks after injury, the number of EBA immunoreactive vessels was further increased to 577±180 which was also not significantly different from normal control (P=0.45).

In the segments rostral and caudal to the trauma site, there was also reduction in EBA labelled vessels from 1 day to 7 days after injury. However, at 2 weeks after injury there was an increase in the number of EBA labelled vessels. At 1 day post injury there were 441 ±112/mm^2 EBA labelled vessels. Three days after injury, the mean number of labelled vessels was further reduced to 349±116. At 7 days after injury, the number of

labelled vessels was still below the normal (430 ± 136/mm^2 ; P= 0.08). At 14 days and 28 days after injury, There were 553±194 /mm^2 and 506±112/mm^{2}vessels positive for EBA respectively. Statistically, in the segments rostral to the trauma site, there were no significant changes in the number of EBA-labelled vessels in most of the time intervals after injury except at 3 days after injury (P=0.04). In the segments caudal to the trauma site, there were no significant changes in the EBA labelling at all time intervals after injury when compared to normal controls. There were 376 ± 66 labelled vessels at 1 day, 366 ± 159 at 3 days, 366± 131 vessels at 7 days, and 391± 62 and 373±64 at 14 and 28 days respectively (Fig 4.1.22, Table 4.2).

Table 4.2 The mean number of EBA-immunoreactive blood vessels in the spinal cord of normal control and moderate spinal cord injury (SCI) rats

	Rostral site (n/mm^2)	Trauma site (n/mm^2)	Caudal site (n/mm^2)
1d SPI	441±112 (269-624)	444±71 (235-544)	376±66 (268-517)
3d SPI	349±116 * (107-517)	405±84 (242-477)	366±159 (174-607)
7d SPI	430 ±136 (289-705)	337±166 * (131-604)	366±131 (208-631)
14d SPI	553±194(168-664)	517±163 (396-846)	391± 62 (302-497)
28d SPI	506±112 (348-624)	577±180 (283-1046)	373±65 (308-470)
Normal	497±127 (161-591)	478±88 (255-477)	469±42 (463-537)

Data shown represent the mean value ± SD (range).

n/mm^2, number of EBA-immunoreactive blood vessels per mm^2.

**Significantly different from the mean value of the normal control, $P < 0.05$.*

The percentage of vessels labelled for EBA was calculated in relation to the mean number of blood vessels, stained with LET lectin, at each time interval and in normal controls (Table 4.3), with three animals being used for each group. In normal animals, 87%-98% of the blood vessels showed labelling for EBA. The percentage of EBA positive blood vessels in experimental animals at the trauma site ranged from 55% to 83%, in the rostral site from 66% to 78% and in the caudal site the range was 71% to 81% (Table 4.3).

Table 4.3 The percentage of mean number of EBA-immunoreactive blood vessels in the spinal cord of normal control and moderate spinal cord injury (SCI) rats, in relation to the mean number of vessels as detected by the lectin labelling.

	Rostral (%)	**Trauma site (%)**	**Caudal site (%)**
1d SPI	**68(441/653)**	**69(444/643)**	**80 (376/473)**
3d SPI	**55 (349/633)**	**49 (405/823)**	**62 (366/593)**
7d SPI	**78 (430 /554)**	**55 (337/610)**	**80 (366/458)**
14d SPI	**80(553/693)**	**61 (517/845)**	**81(391/484)**
28d SPI	**70 (506/719)**	**83 (577/696)**	**79 (373/471)**
Normal	**98 (497/507)**	**85(478/560)**	**94 (469/501)**

Severe injury

The density of EBA-immunoreactive vessels was also assessed quantitatively after severe spinal cord compression using the method described for the moderate injury group. In the severe injury group, in the trauma site, there was a remarkable reduction in EBA labelling. At one day post injury, the mean number of labelled vessels was reduced to 151 ± 92/mm^2 vessels which was significantly less than the normal control animals (P=0.0005). Three days after injury, the mean number of labelled vessels was further reduced to 145 ± 73/mm^{2,} which was also significantly less than the control animals (P= 0.0001). At seven days after injury, there was still obvious reduction in the labelling density; 88 ± 46/mm^2 vessels were labelled. At 14 days after injury, the EBA labelling started to recover; the number of labelled vessels was increased to 200 ± 57, but was still significantly reduced compared to the normal animals (Table 4.4).

In the rostral segments EBA expression was reduced at 1 day post-injury. The mean number of labelled vessels was reduced to 309 ±83 /mm^2. The number of labelled vessels gradually increased after this time point. At 3 and 7 days after injury, the number of labelled vessels was increased to 362±125 /mm^2 and 402±44 /mm^2 respectively. The number of labelled vessels at 1, 3 and 7 days after injury was significantly reduced compared to the normal controls (P=0.006, 0.02 and 0.03 respectively). However, at 14 days after injury, the number of vessels was increased to 514±184 which was not significantly different compared to the normal animals (Table 4.4.).

In the segments caudal to the trauma site, there was a remarkable reduction in EBA

labelling which was significantly less compared to the number of labelled vessels in normal control animals. At one day post-injury, the mean number of labelled vessels was 278 ±75 /mm^2 which was significantly less than normal animals (P=0.006). Three days after injury, the mean number of vessels labelled for EBA was 267±30 which was also significantly less than the normal animals (P=0.007). At 7 days after injury a mean of 253 ± 101 /mm^2 vessels were labelled which was also significantly less than the normal animals (P=0.004). At 14 days the number of labelled vessels was (248±99) but was not significantly different from the normal control animals (P=0.8) (Table 4.4).

Table 4.4 The mean number of EBA-immunoreactive blood vessels in the spinal cord of normal control and severe spinal cord injury (SCI) rats

	Rostral (n/mm^2)	Trauma site (n/mm^2)	Caudal site (n/mm^2)
1d SCI	309±83 * (97-469)	151 ± 92 * (69-293)	278±75 * (69-393)
3d SCI	362±125 * (83-547)	145 ± 73 * (55-255)	267±30 * (41-345)
7d SCI	402±44 * (117-483)	88± 46 * (34-214)	253±101 * (55-372)
14d SCI	514±184 ((273-759)	200± 57 * (21-262)	248±99 (131-448)
Normal	497±127 (166-607)	478±88 * (55-573)	469±42 (221-483)

Data shown represent the mean value ± SD (range).

n/mm^2, number of EBA-immunoreactive blood vessels per mm^2.

**Significantly different from the mean value of the normal control, $P < 0.05$.*

4.1.8.2 Quantitative study of GLUT1 immunoreactivity after moderate compression injury at LM level.

Three experimental animals from each time interval and three normal controls were used for the quantitative study. Four areas from each section in the trauma, rostral and caudal to the trauma sites including one area from each dorsal horns and one area from each ventral horn, were selected for counting. Comparisons of GLUT1 expression at different time intervals were then performed using the Students's *t* test.

In the trauma site (Fig.4.1.22, Table 4.5), as early as 1 day after injury, the number of vessels labelled for GLUT1 was reduced to 205± 77 which was significantly less than normal animal (P=0.001). Three days after injury, the number of GLUT1 labelled vessels was further reduced to 187±66 (P=0.0006). Seven days after injury, the number of vessels was slightly increased to 308±101 and was not significantly reduced compared to the normal animals (P=0.06). Fourteen days and 28 days after injury, density of labelled vessels were still very low (273 ±86 and 263± 65 respectively), and were significantly less than the normal animals (P=0.001).

Sections rostral to the trauma site also showed a reduction of GLUT1 labelling (Fig 4.1.22, Table 4.5). 1 day after injury, the number of vessels was reduced to 255± 55 (P=0.0004). At 3 days after injury, it was 293± 86 (P=0.0001). At 7 days, 14 days and 28 days after injury, the numbers of vessels were 334±109 (P=0.003), 315±67 (P=0.003) and 237±91 (P=0.002)respectively which were also significantly reduced compared to the normal animal. In sections caudal to the trauma site, the number of vessels

immunoreactive for GLUT1 was also significantly reduced at 1 to 28 days after injury compared to the normal controls. The mean numbers were 274 ± 57 labelled vessels at 1 day (P=0.0004), 261 ± 79 at 3 days (P=0.002), 255± 89 vessels at 7 days (P=0.0001), 252± 89 (P=0.0003) at 14 day and 237± 55 (P=0.008) at 28 days (Fig 4.1.22, Table 4.5).

Table 4.5 The mean number of GLUT1 immunoreactive blood vessels in the spinal cord of normal control and moderate spinal cord injury (SCI) rats

	Rostral (n/mm^2)	Trauma site (n/mm^2)	Caudal site (n/mm^2)
1d SCI	255±55 * (175-322)	205± 77 * (74-322)	274±57 * (194-369)
3d SCI	293±86 * (87-450)	187±66 * (128-329)	261±79 * (148-389)
7d SCI	334±109 * (134 -456)	308± 101 (74-490)	255±89 * (101-376)
14d SCI	315±67 * (184-524)	273±86 * (74-396)	252±89 * (134-376)
28d SCI	237 ±91 * (181-604)	263±65 * (141-369)	237 ±55 * (201-322)
Normal	475 ±122 (322-731)	428± 174 (215-678)	475 ± 142 (235-678)

Data shown represents the mean value ± SD (range).

n/mm^2, number of GLUT1 labelled blood vessels per mm^2.

**Significantly different from the mean value of the normal control, $P < 0.05$.*

The percentage of vessels labelled for GLUT1 was calculated in relation to the mean number of blood vessels, stained with LET lectin, with three animals being used for each group. In normal animals, 83% to 95% of the blood vessels showed labelling for GLUT1. The percentage of GLUT1 immunoreactive blood vessels in experimental animals at the trauma site ranged from 32% to 51%, in the rostral site from 33% to 60% and in the caudal site the range was 51% to 58% (Table 4.6).

Table 4.6 The percentage of the mean number of GLUT -immunoreactive blood vessels in the spinal cord of normal control and moderate spinal cord injury (SCI) rats in relation to the mean number of vessels detected by lectin labelling.

	Rostral (%)	**Trauma site (%)**	**Caudal site (%)**
1d SPI	**39 (255/653)**	**32 (205/643)**	**58 (274/473)**
3d SPI	**46 (293/633)**	**32 (187/824)**	**51 (261/593)**
7d SPI	**60 (334 /554)**	**51 (308/610)**	**56 (255/458)**
14d SPI	**46 (315/693)**	**32 (273/845)**	**52 (252/484)**
28d SPI	**33 (237/719)**	**36 (263/696)**	**58 (237/471)**
Normal	**94 (475/507)**	**83 (428/560)**	**95 (475/501)**

4.1.8.3 Quantitative study of GLUT 1 expression in the spinal cord by immunoblotting after moderate compression injury

Three animals were used for each time point. The relative level of expression of GLUT1 was determined by normalization of band intensity determined in injured spinal cord relative to band intensity determined in control non-injured spinal cords. Comparisons of GLUT1 expression at different times after injury were then perfomed using the *Student's t* test.

Two bands migrating at approximately 45 and 55 kDa, consistent with the glial and endothelial forms of GLUT1 respectively, were detected in control non-injured tissues and at all time points following induction of injury. A typical blot of GLUT1 immunoreactivity in control and injured cords is shown in Figure 4.1.23. Analysis of the level of GLUT1 expression showed that there was a tendency for a decrease in GLUT 1 expression following injury, especially in the first two weeks. The intensity of the 55 kDa immunoblot band was assessed using the computer program Measure Master. The mean intensity of bands immunolabelled in normal non-injured animals was 0.95. The mean intensities of the bands were 0.95 at 1 day, 0.72 at 3 days, 0.83 at 7 days and 0.99 at 14 days after injury. However, *Student's t* test showed that all changes in these time intervals were not significant. On the other hand, at 28 days post injury the mean density was 1.44, which was significantly higher compared to the normal animal.

Fig 4.1.22 Histograms showing the density of EBA, GLUT1 immunoreacitve and LET lectin-positive vessels in the trauma, rostral and caudal sites after moderate compression injury. The density of vessel is shown as mean /mm^2± SD.

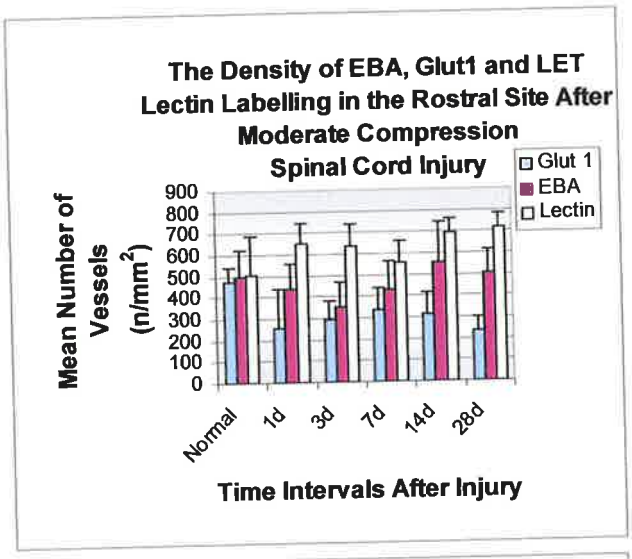
The Density of EBA, Glut1 and LET Lectin Labelling in the Rostral Site After Moderate Compression Spinal Cord Injury
Glut 1
EBA
Lectin
Mean Number of Vessels (n/mm2)
900
800
700
600
500
400
300
200
100
0
Normal
1d
3d
7d
14d
28d
Time Intervals After Injury

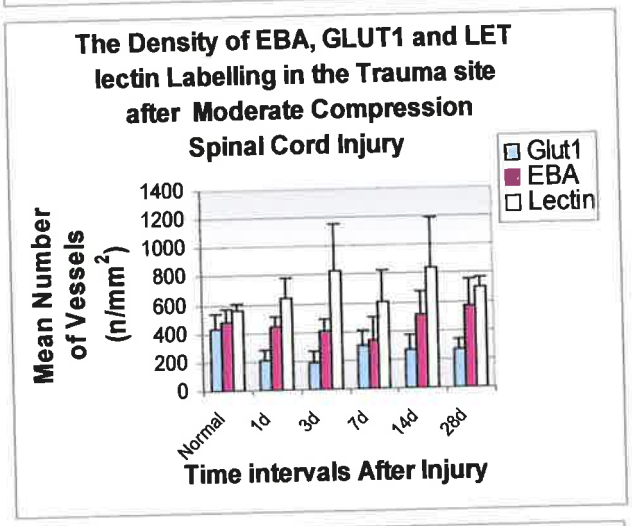
The Density of EBA, GLUT1 and LET lectin Labelling in the Trauma site after Moderate Compression Spinal Cord Injury
Glut1
EBA
Lectin
Mean Number of Vessels (n/mm2)
1400
1200
1000
800
600
400
200
0
Normal
1d
3d
7d
14d
28d
Time intervals After Injury

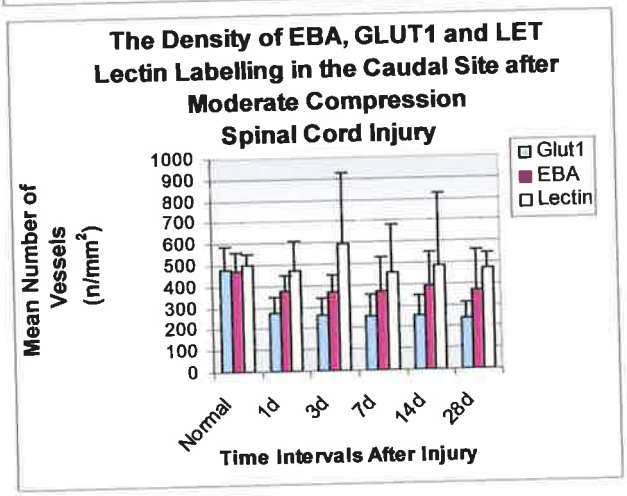
The Density of EBA, GLUT1 and LET Lectin Labelling in the Caudal Site after Moderate Compression Spinal Cord Injury
Glut1
EBA
Lectin
Mean Number of Vessels (n/mm2)
1000
900
800
700
600
500
400
300
200
100
0
Normal
1d
3d
7d
14d
28d
Time Intervals After Injury

Fig.4.1.23 Photographs showing Western immunoblots of normal and experimental animals. There are two bands in the normal and experimental animals of 45 and 55 kDa representing astrocytic and endothelial GLUT1 isoforms respectively in the spinal cord tissue. The intensity of the 55 kDa GLUT1 isoforms detected by the antibody used in this study is reduced particularly at 7 days after moderate compression injury, but its intensity is higher at 14 days and 28 days post injury compared to the normal. The 45 kDa GLUT1 isoform also shows a reduction maximally at 7 days postinjury.

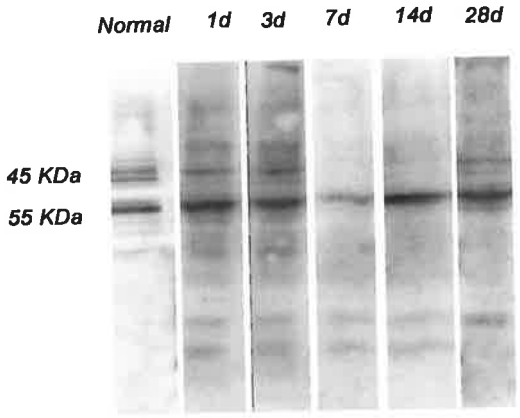
Normal
1d
3d
7d
14d
28d
45 KDa
55 KDa

4.2 The blood-testis barrier after compression spinal cord injury

4.2.1 EBA expression in the blood-testis barrier and the male reproductive tract of normal animals.

In the male reproductive tract of normal animals, positive immunolabelling for EBA was detected in two cell types, ECs of microvessels and epithelial cells of some accessory sex organs.

Strong labelling for EBA was seen in ECs in most microvessels of the testis, in the tunica albuginea, in the subcapsular tissues and in the interstitial compartment in all the normal animals examined (Figs. 4.2.1 A-C). However, endothelial cells of lymphatic channels of the testis were not labelled (Fig.4.2.1A and B). Capillaries in the wall of the ductus deferens were labelled (Fig.4.2.1.D). ECs lining the artery and arterioles of the ductus deferens also showed moderate immunoreactivity but large veins in the spermatic cord were not labelled (Fig 4.2.1E). Many microvessels among the striated muscles and the connective tissue surrounding the membranous urethra showed moderate EBA labelling (Figs.4.2.1F, 4.2.2A). A few microvessels in the seminal vesicle (Fig 4.2.2B), epididymis (Fig. 4.2.2C), coagulating gland, ventral prostate (Fig. 4.2.2D) and the dorsolateral prostate were labelled.

Labelling of epithelial cells was seen in the rete testis (Fig.4.2.3A). The labelling was pronounced in the sector of rete testis tubules closest to the seminiferous tubules (Fig. 4.2.3A). No staining was seen in the Sertoli cells or any of the spermatogenic cells in the seminiferous tubules (Figs. 4.2.1A and B). Apart from ECs of testicular vessels, other cells in the interstitial compartment of the testis and the peritubular myoid cells were

EBA-negative (Figs. 4.2.1A and B). No consistent or reproducible staining was seen in epithelial cells in the epididymis or vas deferens. However, strong granular cytoplasmic staining for EBA was seen in the epithelium of the dorsolateral prostate (Figs. 4.2.3B and C), especially in the acini near to the urethra, whereas cells in the connective tissue stroma of the prostate were negative. The epithelium of the coagulating gland (Fig. 4.2.3D), the ventral prostate (4.2.3E) and seminal vesicle (Fig.4.2.3F) showed labelling in only a few epithelial cells in each tubular profile. No labelling was seen in the epithelium of the bulbourethral gland. All the positive labelling seen in cellular elements in the male reproductive tract was eliminated in control slides in which the primary antibody was omitted from the staining protocol (Fig.4.2.4A). Control tissue sections stained with haematoxylin and eosin for general histology did not show any similar brown deposits in epithelial or endothelial cells.

Examination of other tissues of the rat body including the intestine (Fig.4.2.4 B), skin of footpad, liver, kidney, adrenal cortex, skeletal muscles and cardiac muscle did not show any labelling for EBA. The brain and spinal cord (Fig.4.2.4C) used as positive control for EBA staining showed strong labelling of vessels throughout the grey and white matter. The spleen showed labelling of some ECs of sinsoids in the red pulp. However, the central arterioles of the white pulp (Fig.4.2.4.D) and the splenic artery and vein at the hilum were not labelled. All the above findings were consistent in all the five normal animals examined and were reproducible in several staining sessions.

Fig.4.2.1. Light micrographs showing immunostaining for the endothelial barrier antigen (EBA) in endothelial cells of microvessels in various tissues of the reproductive tract of normal control male rats. Positive immunolabelling appears as brown reaction product, except when nickel enhancement was used, in which case a black reaction product is seen (C). All figures are from sections counterstained with haematoxylin, except for **C**. **A** and **B** show strong immunoreactivity in endothelial cells of interstitial testicular blood vessels (arrows). No labelling is seen in Sertoli and germinal epithelial cells in the seminiferous tubules (ST), interstitial cells (IC), endothelial cells (arrowhead) of the wide lymphatic channels (LC) surrounding the seminiferous tubules or myoid cells (MC). **C**. Nickel-enhanced immunostaining of interstitial vessels of the testis (arrows). **D** and inset. Immunostained endothelial cells of capillaries (arrows) located in the subepithelial connective tissues of the ductus deferens. Epithelial cells lining the lumen do not show labelling for EBA. **E**. Immunoreactivity is seen in endothelial cells lining the artery of the ductus deferens (arrows) and in a smaller adjacent arteriole (double arrows), but not in the venous plexus of the spermatic cord (arrowheads). Inset shows enlargement of the area within the rectangle shown in **E** and shows labelling (arrow) of endothelial cells. **F** and inset. Moderate immunoreactivity is seen in most microvessels (arrows) among the striated muscles surrounding the membranous urethra. Scale bars in A, B, D and inset in E, 20 μm; C, F and inset in D, 50μm; E, 100μm.

Fig.4.2.1

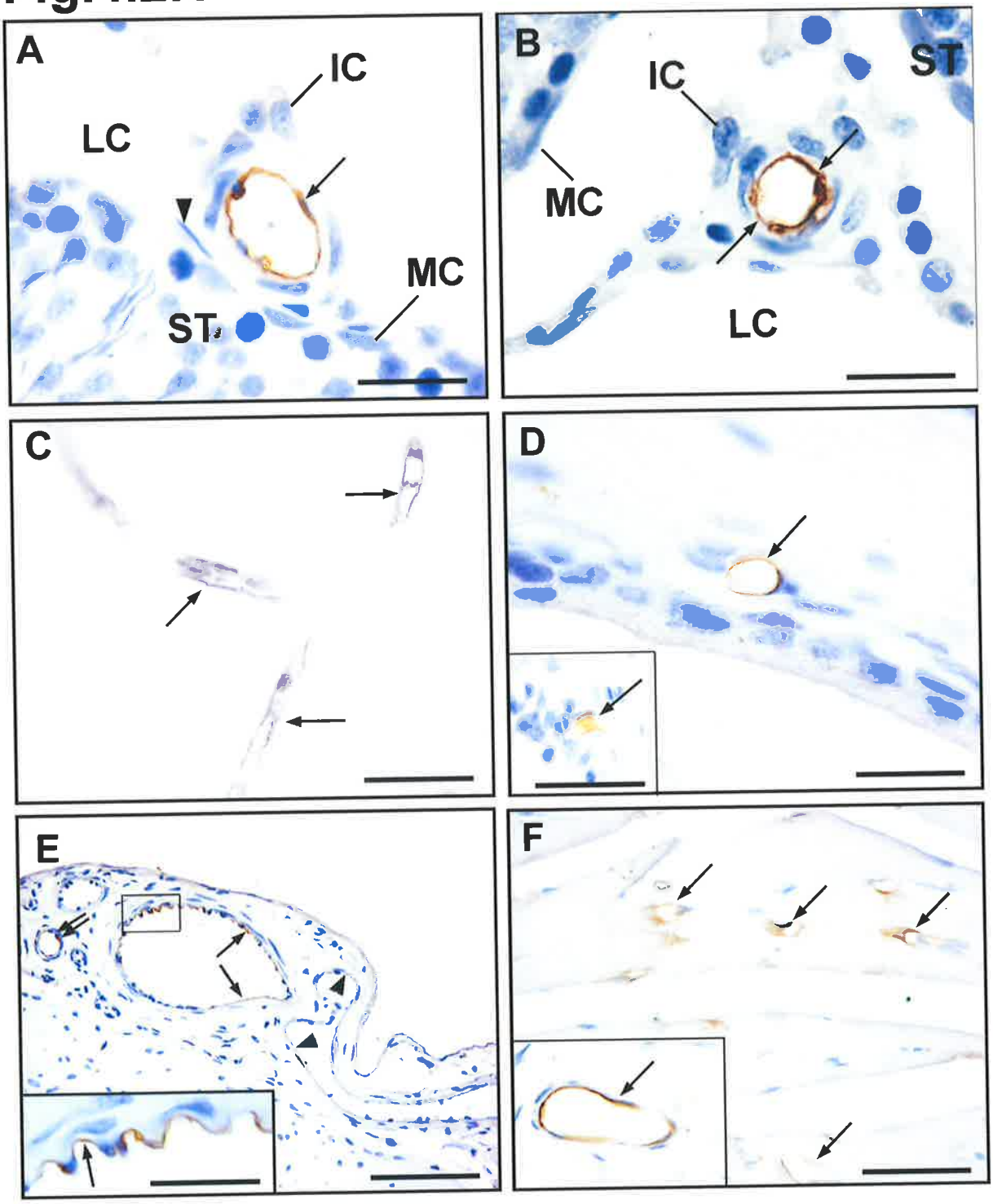

Fig.4.2.2. Light micrographs showing immunostaining for the endothelial barrier antigen (EBA) in endothelial cells of microvessels in various tissues of the reproductive tract of normal control male rats. All figures are from sections counterstained with haematoxylin. (**A**) Immunostained endothelial cells (arrows) in blood vessels located in the connective tissue surrounding the membranous urethra. (**B**) EBA-positive microvessel (arrow) in the seminal vesicle, seen in an oblique section. The staining appears at the plane of endothelial cells. (**C**) EBA-positive vessels (arrows) in the head of the epididymis. (**D**) EBA-positive vessels (arrows) in the ventral prostate gland. Double-arrows indicate EBA-positive regions of endothelial cells cut tangentially. Arrowheads indicate regions devoid of EBA staining, demonstrating regional variability in EBA expression in endothelial cells. Scale bars represent 50μm (**A**, **C**) and 20 μm (**B**, **D**).

Fig.4.2.2

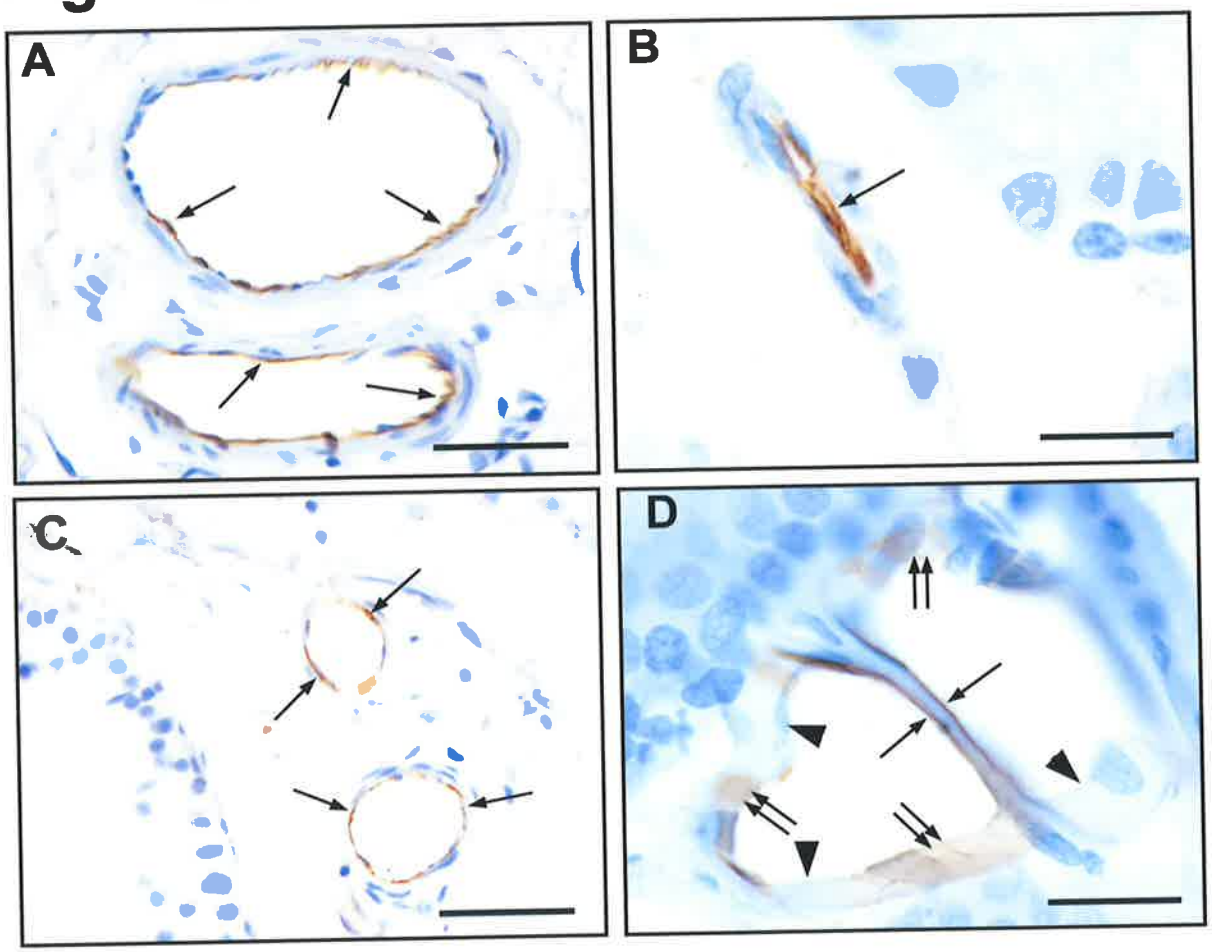

Fig.4.2.3. Light micrographs showing immunolabelling for the endothelial barrier antigen (EBA) in epithelial cells of various tissues of the reproductive tract of normal control male rats. All sections were counterstained with haematoxylin. **A.** EBA immunoreactivity is seen as a brown reaction product in the epithelium of the rete testis tubules (arrows) located close to the seminiferous tubules (ST), whereas rete testis profiles located further away are EBA-negative (arrowheads). (**B - D**) Positive labelling is seen in the cytoplasm of the dorsolateral prostate gland (**B** and **C**) and the coagulating gland (**D**). In the ventral prostate gland (**E**) and seminal vesicle (**F**) weak immunolabelling is seen in the cytoplasm of only a few cells (arrows). Scale bars represent 200 μm (**A**), 100 μm (**B**), 20 μm (**C**, **E**, **F**) and 50 μm (**D**).

Fig.4.2.3

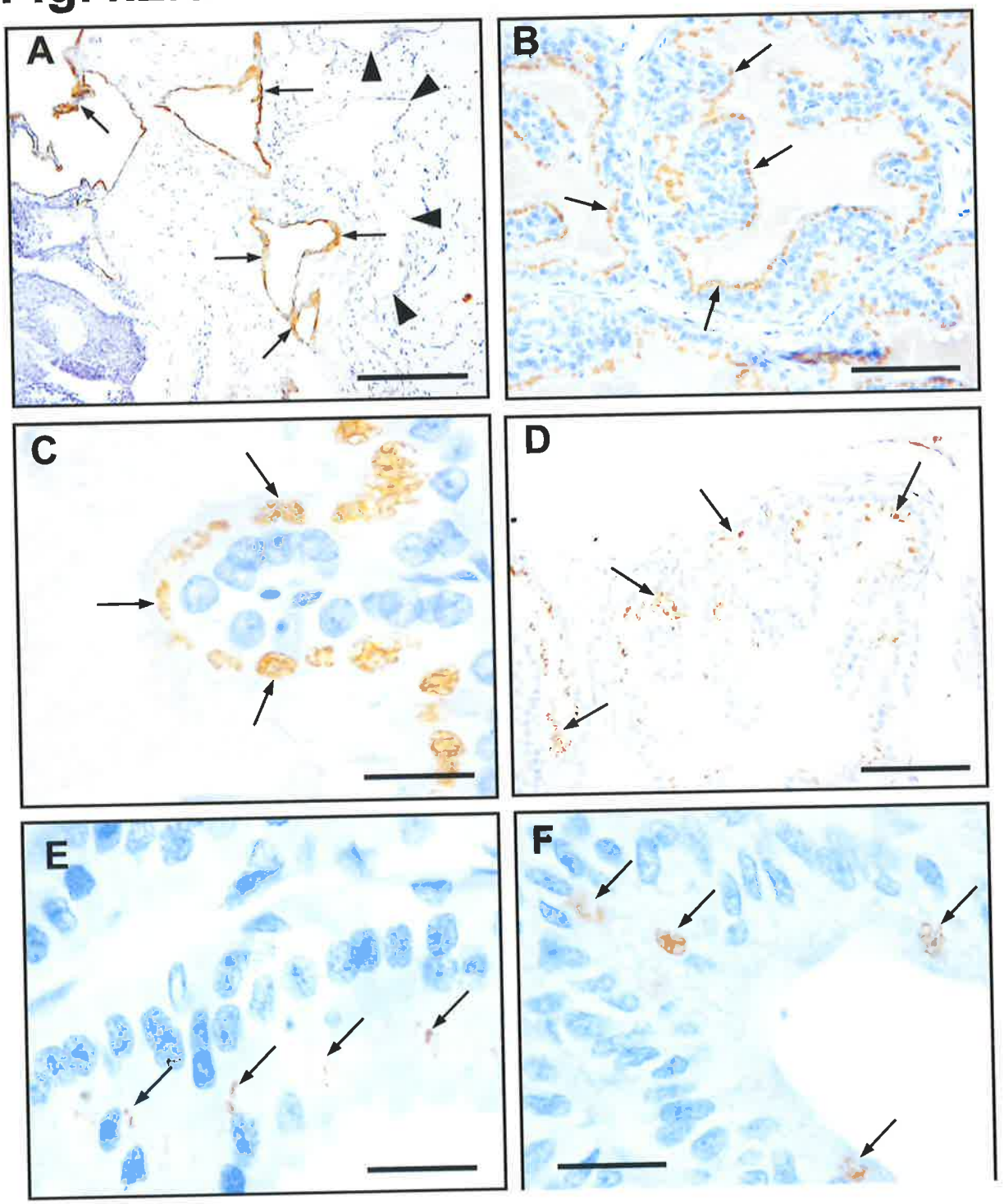

Fig.4.2.4. Light micrographs showing negative and positive control for the endothelial barrier antigen (EBA) immunolabelling in control animals. All sections are counterstained with haematoxylin. **A.** Dorsolateral prostate gland from a section in which the primary anti-EBA antibody was omitted in the staining protocol, as negative control, showing absence of immunoreactivity (compare with Figs. 4.2.3 B and C). **B.** A section from the small intestine immunostained for EBA, the intestinal epithelium does not show any EBA labelling. The intestine was used as negative control tissue. **C.** EBA-positive microvessels in the grey matter of the spinal cord (arrows). The spinal cord was used as positive control tissue for EBA labelling. **D.** The red pulp of the spleen shows EBA-positive endothelial cells (arrows) seen also at a higher magnification (left inset). The central arteriole of the white pulp (main figure and right inset) is not labelled. Scale bars represent 100 μm (A, D), 50 μm (B, C) and 20 μm insets.

Fig.4.2.4

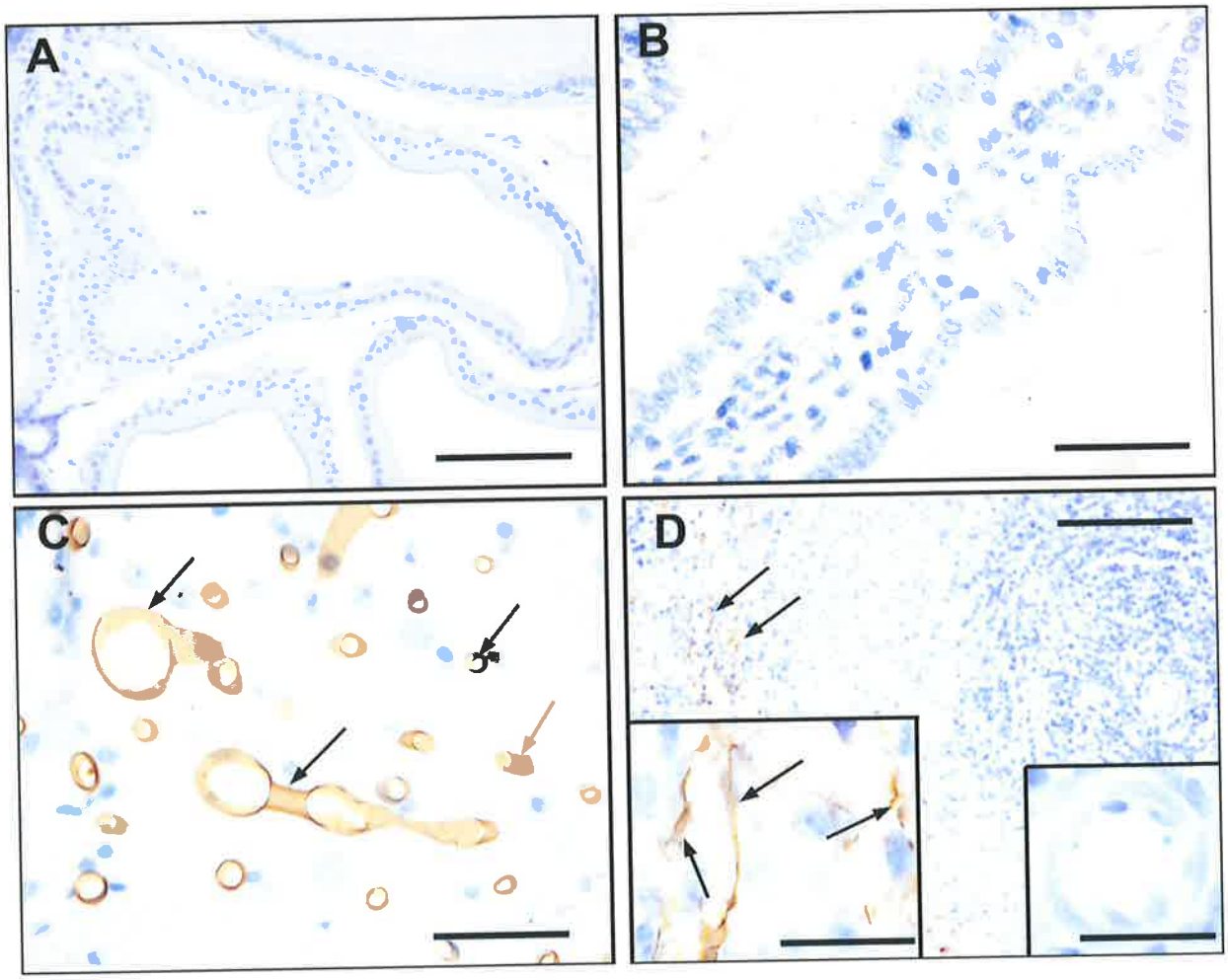

4.2.2 EBA expression in the male reproductive tract following compression spinal cord injury

In the group of experimental animals with moderate compression spinal cord injury, the testis and prostate gland were examined for EBA expression. After moderate compression spinal cord injury there was a remarkable reduction in EBA labelling in endothelial cells of the testis and epithelial cells of the prostate gland compared to the normal and sham control animals. In the testis, the reduction occurred as early as 1 day after compression injury. The ECs of testicular vessels showed very faint staining at 1 day after injury whereas some vessels showed complete loss of EBA labelling. At 3 and 7 days after injury, ECs in the testis still showed a reduction in the intensity of EBA labelling. Some unlabelled and weakly immunolabelled vessels could be observed. This reduction continued up to 4 weeks. At four weeks after injury, the longest time interval investigated in this study, EBA expression was still not completely recovered. Although most vessels were labelled for EBA, the labelling was partial in many vessels and others where not labelled (Fig 4.2.5).

Epithelial cells in the dorsal, lateral and ventral prostate gland also showed reduction in EBA labelling. The reduction started at 1 day after injury and continued for 4 weeks, (Fig.4.2.6B-F) compared to the normal labelling of control animals (Fig4.2.6A). The acini of the prostate were distended and the luminal content of the acini in dorsal and lateral prostate showed increased brown staining, suggestive of positive labelling of prostatic secretion for EBA (Fig.4.2.6F). This increased labelling of the luminal secretions occurred as early as 3 days after injury and continued for 2 weeks. The increased labelling was obvious compared to the faint discoloration of the luminal

content of prostatic acini in normal animals (4.2.6A) which showed narrow lumen and folded walls.

Fig 4.2.5 Light micrographs showing EBA immunostaining in testicular vessels at different time intervals after spinal cord injury. **A.** Faint labelling is seen in a testicular vessel at 1 day after compression spinal cord injury. **B.** Two testicular vessels show weak labelling (arrows) or sectoral absence of labelling (arrowheads) at 3 days after injury. **C.** At 7d after injury, a testicular vessel shows complete loss of EBA labelling (arrowheads). **D.** At 28 days, a testicular vessel still shows complete absence of EBA labelling in most of the vessel circumference (arrowheads) and only weak labelling of one sector (arrow). Scale bars, 50μm.

Fig.4.2.5

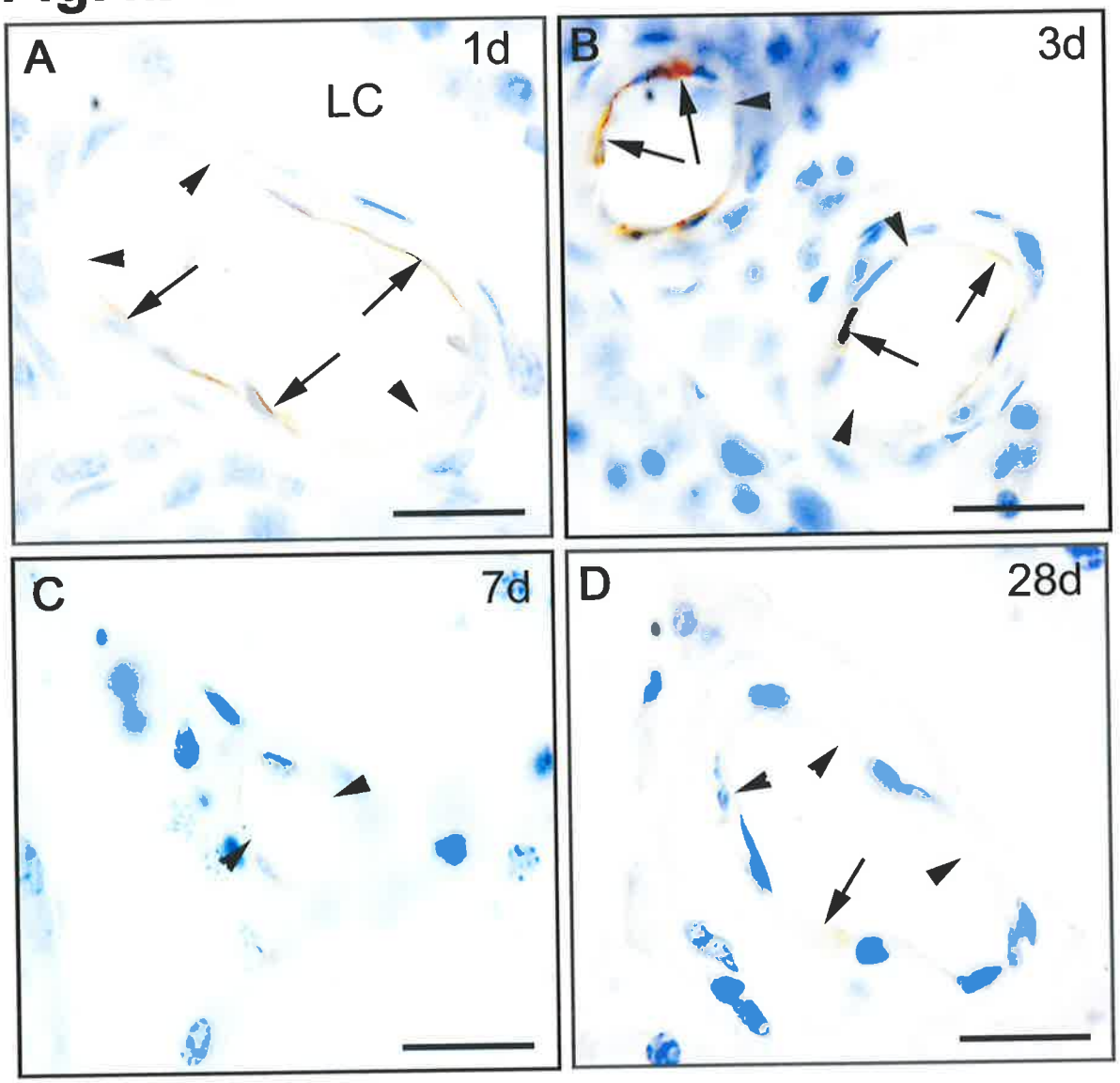

Fig 4.2.6 Light micrographs showing EBA staining in the lateral prostate glands in normal control and experimental animals. **A.** Strong labelling for EBA in the apical cytoplasm of epithelial cells in the lateral prostate gland in a normal rat. **B.** EBA immunoreactivity is seen in the apical cytoplasm of epithelial cells of the lateral prostate. The acini are distended with luminal secretions (asterisks) that show a slight brown reaction product at 1 day after injury.**C.** Lateral prostate showing reduction in EBA labelling in many epithelial cells (arrowheads) while others show apical labelling (arrows) as in controls. The luminal secretions show a brown reaction product (asterisks) at 3 days after injury. **D.** Lateral prostate showing pronounced reduction of EBA labelling in epithelial cells (arrowheads). Only few epithelial cells show apical labelling (arrows). The lumina of the acini are distended with secretions that show a brown reaction product (asterisks) at 7 days after injury. **E** Lateral prostate showing reduced EBA immunolabelling (arrowheads) in many epithelial cells, while some other epithelial cells of acini are well labelled (arrows) at 14 days after injury. **F**. Epithelial cells of the prostate gland shows no immunoreactivity for EBA at 28 days after injury (arrowheads). Scale bars, 20μm.

Fig.4.2.6

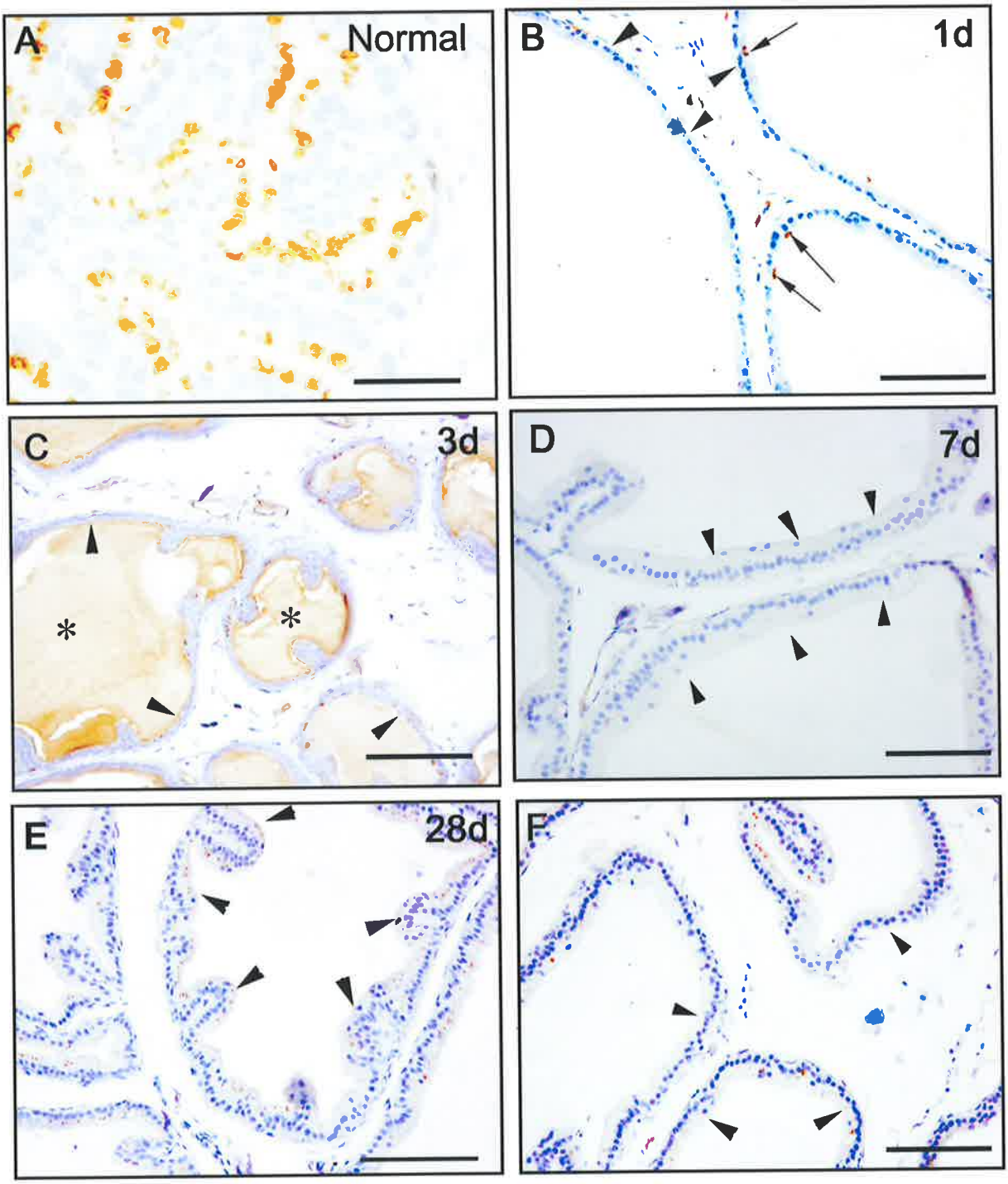

4.2.3 GLUT1 expression in the male reproductive tract following compression spinal cord injury

In normal and sham control animals, strong labelling of GLUT 1 could be seen in testicular vessels but not in vessels of other accessory organs (Fig 4.2.7A). LM showed that GLUT 1 immunostaining in endothelial cells was evenly distributed throughout the entire circumference of testicular ECs. Survey of other reproductive accessory organs did not show any positive labelling for GLUT1 in the ECs. The epithelial cells of dorsal lateral and ventral prostate and other accessory reproductive organs also did not show any labelling. Small arteries and veins were not labelled.

4.2.4. Experimental animals

In the group of experimental animals with moderate compression spinal cord injury, the testis and prostate gland were examined for GLUT1 expression. At 1 day after compression injury to the spinal cord, there was obvious reduction in the expression of GLUT1 in most testicular vessels. Some testicular vessels showed very faint labelling (Fig 4.2.7B) while some labelled vessels showed granular and faint staining. At 3 days after injury, the reduction in the labelling was most pronounced. At one week after injury, the reduction in GLUT1 labelling in the testis persisted, where most vessels were not labelled or partially labelled. At two weeks, the labelling started to recover and more vessels were positively labelled compared to those seen at 1 week after injury. At four weeks after injury, the majority of vessels were labelled but a few unlabelled vessels were still seen (Fig.4.2.7D).

Fig 4.2.7 Light micrographs showing GLUT1 staining in the testicular vessels in normal rats and after compression spinal cord injury. **A.** Strong labelling for GLUT1 in a testicular vessel (arrows) in a normal animal. **B.** Weak labelling (arrowheads) for GLUT1 at 1 day after injury **C.** Weak labelling (arrowheads) for GLUT1 at 14 days after injury **D.** 28 day after injury two interstitial testicular vessels, one shows immunolabelling (arrow) for GLUT1. The other is not labelled (arrowhead). Scale bars, 20μm.

Fig.4.2.7

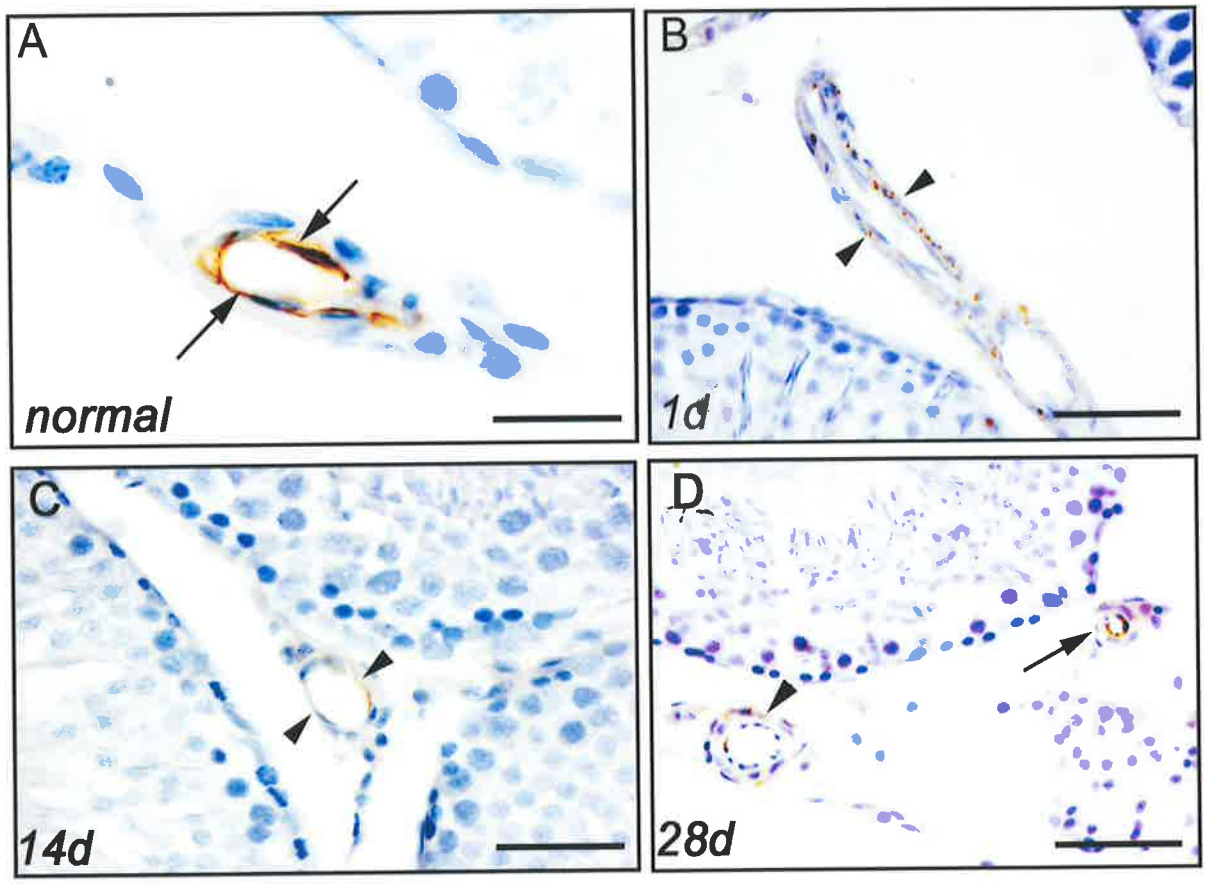

4.3 Time course of opening and closure of BBB after immunological targeting of EBA.

4.3.1 The temporal pattern of EBA expression after immunotargeting of EBA

This experiment was undertaken to further elucidate the role of EBA in blood vessels of the brain and spinal cord

Control animals

Control animals injected intravenously with the isotype mouse IgM did not show any staining in brain or spinal cord vessels for EBA, when vibratome sections were exposed to the secondary antibody and tertiary reagents only, but showed very intense labelling after inclusion of the primary antibody in the staining protocol at all time intervals after isotype injection (Fig 4.3.1).

Experimental animals

Experimental animals were injected with anti-EBA antibody. Microvessels of the brain and spinal cord of experimental animals, which have survived for different time intervals from 30 min to two weeks, showed very strong immunolabelling for EBA after routine immunocytochemical labelling, in which the primary anti-EBA was included in the protocol. Surveying the sections which have been immunolabelled without primary anti-EBA antibody showed that only those animals surviving for short time intervals from 30 min to six hours were positively labelled. Generally, the shorter the time intervals after anti-EBA injection, the more intense the labelling. Using the same immunolabelling method without exposure of the sections to the primary antibody, animals which survived longer than six hours did not show any positive labelling for EBA (Fig.4.3.2).

Fig 4.3.1 Light microphotographs showing EBA labelling in the brain 1 hour after isotype IgM injection. **A.** Vibratome section of brain labelled with both primary and secondary antibodies: strong EBA labelling is observed in blood vessels. **B.** A Vibratome section labelled with omission of the primary anti-EBA antibody. No labelling for EBA is observed. Scale bars, 200μm

Fig.4.3.1

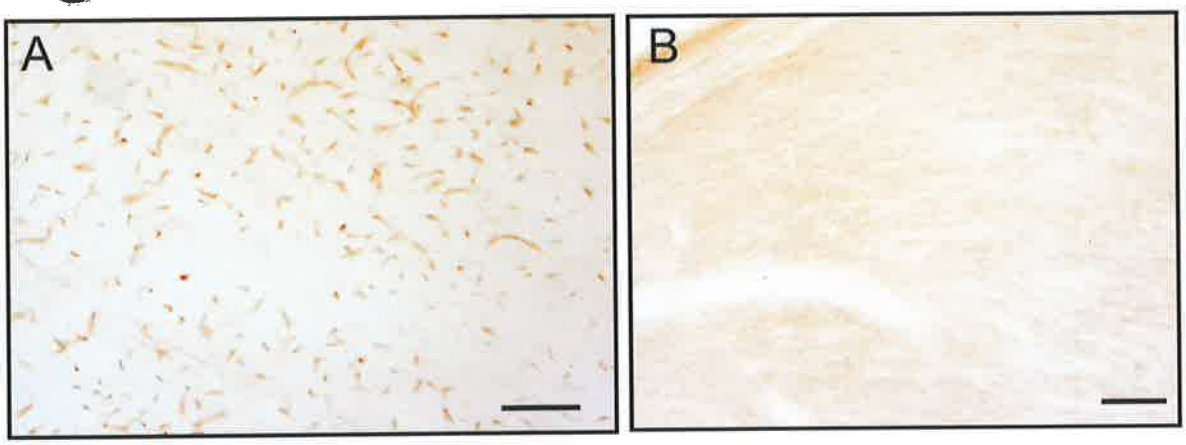

Fig 4.3.2 Light micrographs showing EBA labelling in Vibratome section of brains at different time intervals after anti-EBA injection. **A.** A section labelled with both primary and secondary antibodies. Blood vessels show very strong labelling. All sections in B-E were immunolabelled with omission of the primary anti-EBA antibody in the staining protocol. **B.** One hour after antibody injection: strong labelling is seen. Inset shows high magnification of B. **C.** Three hours after anti-EBA injection: moderate labelling is observed in the microvessels. **D.** Six hours after anti-EBA injection, mild to moderate labelling is seen; Inset shows high magnification of D. **E.** One day after anti-EBA injection, no EBA labelling is seen.

Fig.4.3.2

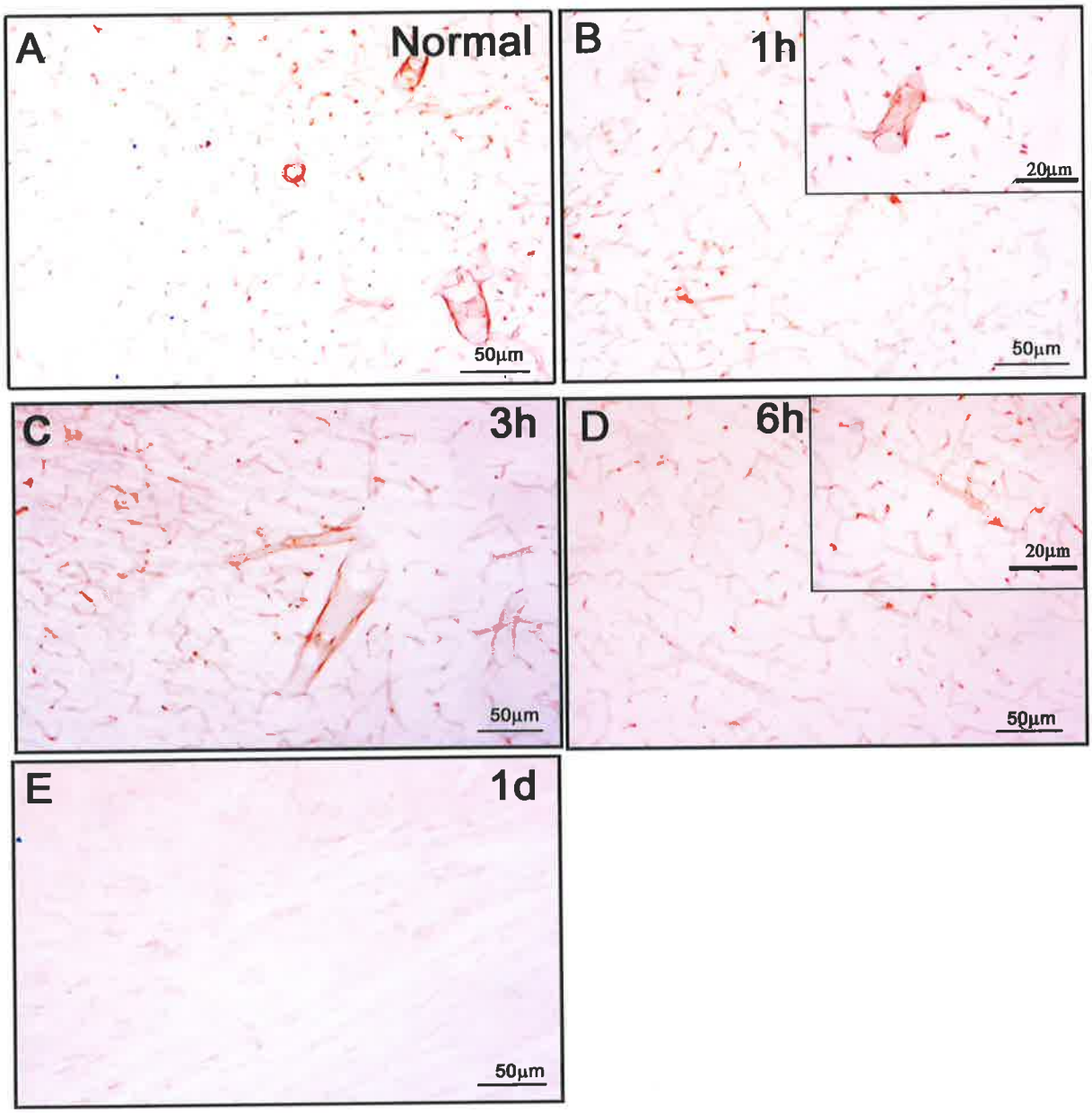

4.3.2 Permeability of HRP following immunological targeting of EBA

Control animals

None of the control animals, injected intravenously with isotype control antibody showed leakage of HRP. Light microscopy of Vibratome sections showed clear parenchyma throughout the brain and spinal cord. Occasional RBCs seen in the lumina of some vessels showed dark staining due to their content of endogenous perioxidase, indicating the successful development of peroxidase reaction product. The choroid plexus and pineal gland showed HRP distribution in the tissues. In all experimental and control animals, Vibratome sections of the liver showed HRP in the liver sinusoids, indicating the successful intravenous injection of the tracer, its circulation throughout the body and the successful development of HRP reaction product (Fig. 4.3.4).

Experimental animals

Experimental animals were injected with three doses of anti-EBA, low, medium and high doses (Fig.4.3.3 and 4.3.4). In the initial phases of the study, animals were injected with the high dose of 50 μg/kg body weight. However, this dose resulted in a high mortality rate. Fifty percent of the injected animals died, either soon after the injection or within 3h, irrespective of the type of anaesthesia. Subsequently this dose was reduced to 25 μg/kg body weight. However, this low dose did not produce significant BBB opening. Thereafter the medium dose of 40 μg /kg body weight was preferentially used. This medium dose gave consistent and widespead opening of the BBB although three animals died in this group. Retrospectively these animals were found to have had faster injections of the antibody. Therefore, the respiratory rate and depth were monitored and

the rate of antibody injection was adjusted in response to the respiratory pattern. The following description applies to the medium dose unless stated otherwise.

Surveying the sections at low magnification gave a clear indication of the pattern of HRP leakage, which rapidly reaches a maximum level by 30 min with progressive reduction in subsequent time intervals (Fig.4.3.3). Seventeen min after anti-EBA injection the brains showed weak staining in a few foci in the striatum and brainstem and the grey matter of the spinal cord showed similar weak HRP staining. At 30 min after antibody injection the brain showed extensive leakage of HRP. The tracer was widely distributed in the grey and white matter, being present in the cerebral cortex, subcortical white matter, striatum, diencephalon, brainstem and cerebellum. The spinal cord showed HRP in the dorsal and ventral grey horns and white matter. In the animals killed 45 min after anti-EBA injection, HRP distribution in the brain and spinal cord was almost identical to that seen at 30 min, although the intensity of staining and the areas of leakage appeared to be fractionally less than in the 30 min animals. At 1 h after anti-EBA injection, the brain and spinal cord showed a dramatic decline in the amount of HRP leakage, although this was still greater than the amount of the tracer seen in the earliest time interval of 17 min. A further reduction in the amount and distribution of HRP in the brain was seen at 2 h after anti-EBA injection, where in one animal no leakage was seen and in others few foci of weak staining were seen in the frontal lobe, dorsal thalamus and brainstem. Of the 5 animals killed at 3 hours after anti-EBA injection, 3 animals showed completely clear parenchyma in the brain and spinal cord, and 2 animals had one or two spots of HRP leakage in the striatum and brainstem. No HRP leakage was seen in the animals killed at 6 h and 1d after anti-EBA injection

(Fig.4.3.3). In all the above animals HRP was regularly seen in the parenchyma of the choroid plexus and the pineal gland.

Examination of the sections from experimental animals, injected with the medium dose, at a higher magnification revealed the pattern of distribution of the tracer, in the cerebrum and brainstem. HRP appeared as multifocal large circumscribed areas of brown staining, or as homogeneous staining affecting large regions, such as the striatum and ventral part of the frontal lobe (Fig. 4.3.3 A-E). Some neurons showed cytoplasmic distribution of HRP reaction product. In many animals irrespective of the time interval of their survival, many phagocytic cells in the pia mater contained HRP reaction product in their cytoplasm. Also intravascular phagocytic cells containing HRP reaction product were seen. Many experimental animals showed numerous red blood cells remaining in the vascular bed which showed brown reaction product due to endogenous peroxidase.

Fewer animals and time intervals were tested with the high and low doses (Fig 4.3.4). The animals injected with the high dose showed similar results to the medium dose. The animals injected with the low dose, showed weak staining for HRP even at the 30 min and 45 min time intervals (Fig 4.3.4), which showed maximun leakage in the medium and high doses (Fig 4.3.3 and 4.3.4).

Fig 4.3.3 Low magnification digital images of sagittal Vibratome sections of brains from experimental animals treated with the medium dose (MD) of anti-EBA and killed at various time intervals ranging from 17 min to 1 d. Horseradish perioxidase (HRP) was injected intravenously 10 min before perfusion fixation. Dark brown HRP reaction product (arrows) is seen in the brains as round patches or homogenous areas of variable sizes. Mild leakage is seen at 17 min (A) mainly in the ventral part of the frontal lobe. The heaviest leakage is seen at 30 min post–injection throughout the brain (B), with less at 45 min (C) and much less at 1 h (D) and 2h (E). No HRP is seen at 3 h (F), 6 h (G) or 1 day (H). The outline of the brain was traced with a thin black line for clarity. Magnification bars, 0.5 cm.

Fig.4.3.3

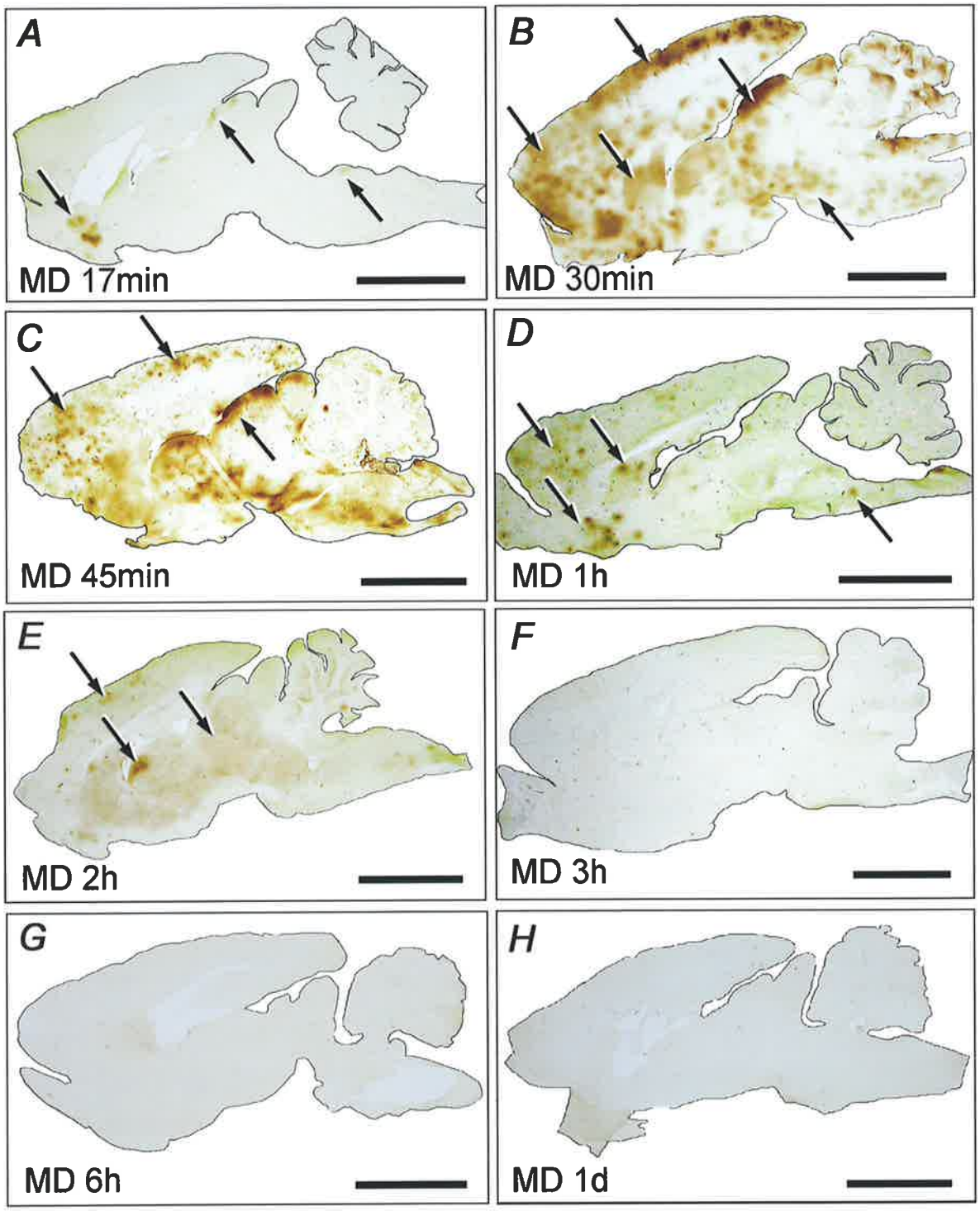

Fig 4.3.4 Low magnification digital images of sagittal Vibratome sections of brain from experimental (A-D) and control (E and F) animals. All animals were injected with HRP 10 min prior to perfusion fixation. **A** shows the brain of an experimental animal injected with the high dose (HD) of anti-EBA and killed at 30 min after antibody injection. There is extensive distribution of HRP reaction product (arrows) in the frontal, pariental and occipital lobes, hippocampus, striatum, diencephalons, brainstem and cerebellum. **B** shows the brain of an experimental animal injected with high dose (HD) of anti-EBA and killed 3 h after the injection. No HRP leakage is seen at this time intervals. Figs. C and D show brains from experimental animals injected with the low dose (LD) of anti-EBA and killed at 30 min and 3 h post-injection, respectively. Fig. **C** shows mild distribution of the tracer in frontal lobe, diencephalon and brainstem. No reaction product is seen in D. Figs. **E** and **F** show brains of control animals killed at 30 min and 45 min after injection of a control isotype antibody. No HRP reaction product is seen. Magnification bars = 0.5 cm.

Fig.4.3.4

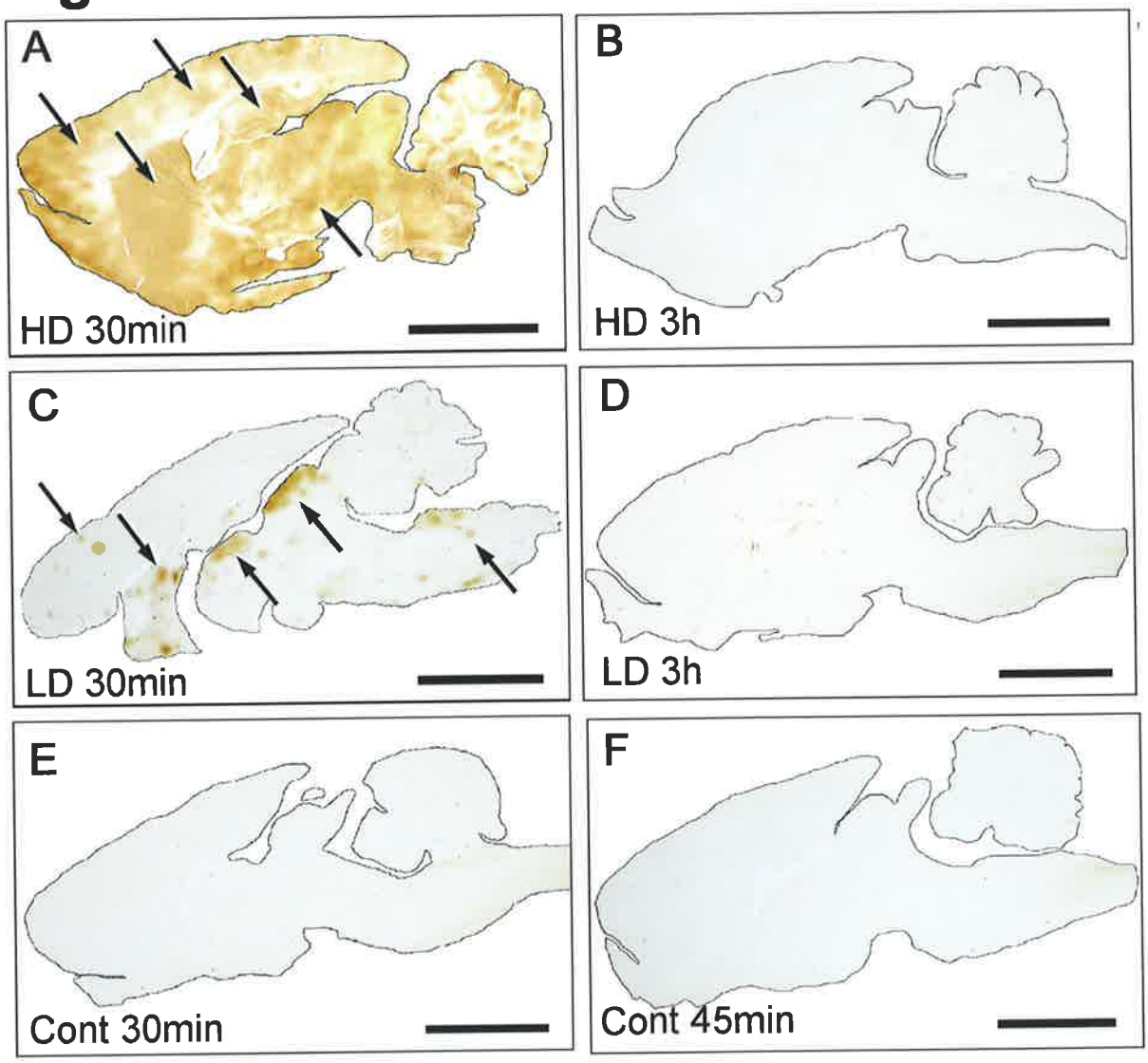

CHAPTER 5

DISCUSSION

Chapter 5. Discussion and Conclusion

5.1 Blood-spinal cord barrier (BSB) after compression spinal cord injury

5.1.1 The integrity of BSB barrier after compression spinal cord injury

In the present study, the integrity of BSB was assessed by the detection of albumin immunoreactivity as an indicator of albumin leakage in the spinal cord after injury. Endogenous albumin is a natural component of the plasma and has been widely used to detect tissue oedema (Fukuhara *et al.*, 1994). Diffuse albumin immunoreactivity could be observed in the trauma site of all moderate and severe injury animals suggesting a wide opening of the BSB. Albumin leakage was sustained for two weeks after injury. The moderate and severe injury models showed a similar pattern of albumin immunolabelling at the trauma site. However, the intensity of albumin immunoreactivity in moderate injury animals was less than that in severe injury animals. The difference in the intensity of albumin leakage between the severe and moderate injury group might be due mainly to the difference in the severity of the injury, reflecting that opening of the BSB after compression injury is dose dependent. Consistent with this observation, there was faster clearance of albumin in moderate injury animals than in those with severe injury. Segments rostral and caudal to the trauma site also showed albumin leakage which was diffusely distributed, but showed a more intense presence in the grey matter. In the present study the leakage of albumin also appeared to correlate with the neurological evolution based on motor function tests after injury. The extent and area of albumin extravation also seemed to coincide with the haemorrhage and necrosis in the trauma site and areas remote from

the trauma site as revealed by the H and E histological studies. The pattern and distribution of albumin leakage observed in the present study is consistent with previous reports on the extravation of albumin after spinal cord injury and brain injury. In previous studies, albumin leakage was reported to be diffusely distributed and to extend for several segments remote from the trauma site (Farooque *et al.*, 1992 ; von Euler *et al.*, 1997). It was also reported that with more severe trauma and longer survival periods extravascular albumin was more extensively distributed along the cord (Farooque *et al.*, 1992). In cryoinjury of the brain, the BBB is compromised and albumin enters the neuropil (Vorbrodt *et al.*, 1993). Albumin leakage was also reported in osmotic opening of the BBB (Vorbrodt *et al.*, 1993).

There are several possible mechanisms that may account for the albumin extravation after spinal cord injury. Firstly, albumin may originate from plasma escaping through the disrupted BSB, from ruptured blood vessels directly damaged by the trauma. Secondly, from the cytoplasm of disrupted cells in the lesion. Thirdly, by leakage through capillaries compromised secondary to tissue damage. Fourthly, from the CSF flowing the subarachnoid space across the spinal cord surface although normally the CSF has low proteincontent (1.0-2.0g/l), this may increase in cases of spinal cord compression (Bannister, 1978). Furthermore, previous studies on the CSF flow in an animal model of post-traumatic syringomyelia have shown that the CSF in the spinal canal has a directional flow towards the syrinx through the perivascular space of the central penetrating brances of the anterior spinal artery in

the grey matter (Brodbelt *et al.*, 2003a, b). The same mechanism of CSF flow after injury may be also applied in this compression injury model. However, in the present study, in the severe injury, the opening of BBB might be primarily caused by the mechanical insults to the cord tissue leading to the disruption of the microvessels and their tight junctions at the trauma site. It is likely that blood vessels were ruptured, because bleeding was observed in the histological study.

In segments rostral and caudal to the trauma site, the mechanisms accounting for albumin leakage might be different from those operating at the trauma site, and the opening of the BSB may be caused mainly by secondary injury and not by the mechanical insults. In the segments remote from the trauma site, several mechanisms may be involved in albumin extravation. Firstly, leakage might be caused by the direct spread of albumin from the trauma site. Secondly, the leakage might be caused by secondary injury, caused by ischeamia and the release of neurotoxic materials from the trauma site and spreading to adjacent segments. A previous study on the blood-nerve barrier following nerve grafting showed that blood vessels and the cell layers forming compartment at the graft junctions remain permeable to HRP for at least 6 months and the intact perineurium around the distal stump of a denervated nerve is permable to HRP but the endoneurial blood vessels are not (Ahmed and Weller, 1979). Interestingly, in the present study, there was also a leakage of albumin in the segments remote from the trauma site at two weeks post severe injury in the dorsal column where axonal degeneration occurred. In the moderate injury

group in the present study, two weeks after the injury, albumin immunolabelling disappeared in the segments remote from the trauma site suggesting that the leaked albumin had been cleared up perhaps by macrophages or activated microglia.

The mechanism of clearance of protein from the interstitial fluid in the brain parenchyma and its relationship to the CSF are complex and not fully understood (Weller, 1998). While insoluble peptides such as β–amyloid protein and prion protein, which are deposited in the brain parenchyma in Alzheimer's and Creutzfeldt-Jakob diseases respectively, appear not to enter the CSF (Weller, 2001), this route may be available for the clearance of albumin. In the rat, it is thought that brain interstial fluid particularly from the grey matter circulates through the narrow extracellular spaces and joins the bulk flow in pericapillary and periarteriolar spaces before entering the CSF (Zhang *et al.*, 1992). Extracellular fluid form the white matter may preferentially drain to the CSF (Weller, 1998) On the other hand under the experimental condition of arachnoiditis (Brodbelt *et al*, 2003) and in human arachnoid web formation (Brodbelt and Stoodly, 2003a, b), CSF has a tendency to drain towards the centre of the spinal cord, preferentially via perivascular spaces (Broadbelt *et al* 2003a, b).

In a previous study, albumin-gold complexes were used to study the cellular mechanism of BBB opening after injury (Vorbrodt *et al.*, 1993). It was suggested by the authors that there are four ways of BBB opening. (1) Opening of a part of the

junctional complexes. (2) The formation of transendothelial openings (endothelial gaps or penetrating crater-like excavations. (3) The uncontrolled passage of tracer particles through the cytoplasm of the injured endothelial cells. (4) Segmental denudation of the endothelial lining (Vorbrodt *et al.*, 1993). These routes of leakage of albumin have also been suggested after compression spinal cord injury (Van Euler *et al.*,1997). Since compression injury was used in present study it is reasonable to suggest that the routes of albumin leakage in the present study are similar to those reported previously. However, further EM studies are needed to investigate the route of albumin leakage in the current model.

The basement membrane appears to represent one of the main obstacles to the passage of blood-borne albumin-gold complexes to the extracellular space in the brain neuropil (Vorbrodt *et al.*, 1993) suggesting that the basement membrane can also serve as a barrier. Once albumin leaks into the neuropil, it promptly moves into the neuronal and astrocytic processes (Vorbrodt *et al.*, 1993). It was suggested that extravasated plasma proteins subsequent to their uptake and processing by the glial cells, may serve some important physiological function in wound healing (Liu and Sturner, 1988; Li *et al.*, 2001). The glial cells are probably the major cell types where the leaked albumin is broken down.

In a previous study of rat spinal cord contusion injury, it was demonstrated that after injury, the compromised microvessels remain permeable to tracers for up to 1 week

after injury. However, by 2 weeks, the barrier is re-established (Popovich *et al.*, 1996a). A prolonged abnormal permeability after spinal cord injury has been reported by others. Nemecek reported permeability to Evans Blue albumin up to at least 9 days after contusion injury (Nemecek *et al.*, 1977). It was also reported that after spinal cord transection, restoration of the BSB to protein was not observed until one week after injury (Noble and Wrathall, 1987; 1988). Although the vasogenic oedema is a very important factor in the secondary progression of pathological event after head injury, a similar contribution in spinal cord injury has not been well defined. A direct relationship between the severity of injury and axial spread of barrier breakdown remains unclear. The degree of the vascular injury at the compression injury site reflects the severity of the initial insults. With increasing severity of initial injury it is likely that a greater proportion of the vascular tree is traumatized. This may result in exudation of vasoactive humoral factors, which in turn diffuse along the axis of the spinal cord and subsequently influence permeability along distant vascular sites. In this study, an obvious diffuse leakage of endogenous albumin was observed in the trauma site and in the segments remote from the trauma site.

Apart from the endogenous albumin, several other tracers have been widely used for studies on the morphological route of tracer leakage from the BBB. These include exogenous albumin (chicken albumin), lanthanum, HRP and dextrans (Bouldin and Krigman, 1975; Noble and Wrathall, 1987; Lane *et al.*, 2001). HRP is probably the most widely used tracer in BBB studies. HRP is a 40-kDa plant glycoprotein. HRP,

as a glycoprotein does not bind to plasma membranes and is a fluid-phase maker, entering cells by the process of fluid phase endocytosis. HRP at doses used routinely in morphological studies does not alter the integrity of the BBB to endogenous albumin and therefore is a suitable probe for investigating the permeability characteristics of the BBB to macromolecules. According to a previous study, blood-born HRP can enter the brain faster than other tracers including the blood-born albumin (Banks and Broadwell, 1994). A comparative study is needed to reveal the difference in the extravasation between HRP and endogenous albumin in the present model of spinal cord trauma.

Sufficiency of blood supply is deemed to be critical for tissue repair after injury. However, the relationship between vascular damage and the development of tissue necrosis is still not clear. There are several factors which might be involved in tissue necrosis in spinal cord injury (See review by Taoka and Okajima, 1998). Firstly, in regions where vascular damage exists, the microenvironment might be damaged and thus the cells in that region cannot survive. Secondly, the presence of haemorrhage in the tissue may be harmful. Free radicals might be released from the damaged tissues. Cellular membranes are highly susceptible to free radical-induced peroxidative damage. Thirdly, the distribution of protein extravasation marks potential pathways for the endogenous plasma components, which could contribute to secondary tissue disease.

In summary, after compression injury, there is widespread albumin leakage in the trauma site as well as in the segments remote from the trauma site suggesting the wide opening of the blood spinal cord barrier after compression injury. However, the route of leakage of albumin was not investigated in this study. The leakage of albumin appears consistent with the pathological evolution of cord tissue damage and is also consistent with neurological development.

5.1.2 EBA expression after compression spinal cord injury

In the present study the number of the vessels labelled with lectin, anti-EBA and anti- GLUT1 was counted in the grey matter in preference to the white matter for several reasons. Firstly, the number of blood vessels in the white matter was found to be much less than in the grey matter. For example, in same levels and sections, only a handful of vessels was seen in the distal white column, even in normal animals. Secondly, statistical analysis would have been less accurate if applied to a smaller number of blood vessels. Thirdly, molecular and quantitative changes in the grey matter remote from the trauma site, are more likely to reflect secondary changes due to disturbance of neural input. The white matter tracts rostral and caudal to trauma showed Wallerian degeneration, but the grey matter rostral and caudal to the trauma was morphologically unremarkable. Thus the changes in grey matter blood vessels, particularly in remote areas, reflect altered neural function due to loss of interspinal and supraspinal input from white matter tract, and are less likely to be due to direct mechanical trauma.

In relation to EBA expression in the spinal cord, there are three major findings in this study. Firstly, the anti-EBA labelled almost all vessels in all sizes in the normal and sham control animals. Secondly, EBA expression is reduced not only in the trauma site but also in the segments remote from the trauma site, especially in animals with severe injury. Thirdly, the expression of EBA appears to correlate with the function of the BSB, as assessed by the leakage and the clearance of the endogenous albumin.

There is only one report in the literature that addressed the expression of EBA in spinal cord compression (Perdiki *et al*, 1998). However, that study only addressed changes at the trauma site using a qualitative and semiquantitative approach for the intensity of labelling, but did not relate the number of labelled vessels to the total profile of vessels. In that study, a reduction was reported in EBA immunoreactivity by light microscopy as early as 1 day after injury and reached a maximum at 4 days after injury followed by a gradual recovery from 9 days post injury (Perdiki *et al.*, 1998). The present study confirmed and expanded these findings. The present study showed a similar time frame for EBA reduction at the trauma site where the reduction of EBA reached a maximum 7 days post injury. However, there was a slight increase in the number of vessels immunoreactive for EBA by 2 weeks post moderate injury compared to normal animals. Other studies showed a similar time frame for EBA reduction following other pathological insults to the brain (Lin and Ginsberg, 2000; Nishigaya *et al.*, 2000). Directly injured and adjacent microvessels lacked EBA expression for a period of approximately 2 weeks after stab wound

injury to mature brain, a time frame that is not too different from that in the present study. The alteration of EBA immunoreactivity in the cord remote from the trauma site found in the present study has not been reported previously.

The apparent similarity in the reduction of EBA expression and its recovery in different pathologies of the CNS suggests a functional role for EBA at the BBB and a common mechanism for its down-regulation in a compromised BBB. The alteration of EBA expression may be associated with direct mechanical damage or a secondary damage to ECs. In terms of the evolution of general pathology in spinal cord injury, two mechanisms have been suggested, a primary injury and a secondary injury (see review by Tator, 1991). The primary injury in the trauma site is principally due to direct mechanical damage, whereas the secondary injury may result from post-traumatic ischaemia and other neurotoxic multifactors. Unlike at the trauma site, the segments remote from the trauma site are principally subjected to secondary damage due to the biochemical changes and ischaemia (Noble and Wrathall, 1987). The present study suggests that, similar to the evolution of general spinal cord pathology, the reduction of EBA in the remote sites observed in this study may be mainly associated with secondary vascular damage. Therefore, the results of the present study suggest that the EBA can be used as a sensitive index for secondary vascular damage. The underlying mechanism by which the EBA is down regulated after injury, needs to be addressed in future studies.

EBA appears to be an indicator in characterizing the location and history of brain and spinal cord lesions. The EBA immunostaining is present in capillaries within the periphery of traumatic and inflammatory lesions but is lost in the centre of lesions (Sternberger *et al.*, 1989). EBA immunoreactivity within an injured area is suppressed for approximately two weeks, but gradually returns to normal levels. Therefore, anti-EBA may be used in characterizing the acuteness or chronicity of a lesion in the CNS.

Although the expression of EBA has been suggested to be inversely related to the oedema resulting from the pathological insults induced in several animal models, it is not clear whether the reduction of EBA is the primary event or subsequent to the pathological insults. A recent study in this laboratory demonstrated that after immunotargeting of the EBA, there is a widespread opening of the BBB in the brain, suggesting that the EBA plays an important putative role in upholding the integrity of the BBB and that the reduction of EBA might be the primary event prior to the formation of oedema (Ghabriel *et al.*, 2000). However, whether the reduction of EBA is the primary event in oedema formation or secondary to vascular damage in this model of spinal cord injury is unclear.

As discussed above, in the present study, in the early stages post injury there was a reduction of EBA expression whereas in the late stages post injury, the EBA expression started to recover, especially in animals with moderate injury. On the

other hand, there was an increased number of vessels labelled with LET lectin at the trauma site as well as segments rostral and caudal to the trauma site after injury. Two important issues were considered here. Firstly, whether the alteration of EBA immunoreactive vessels was due to changes in the total microvessel profile, brought about by angiogenesis or loss of vessels. Secondly, if EBA immunoreactivity was independent of the total profile of microvessels. Therefore, the total profile of the microvessels in the normal and experimental animals with moderate injury was quantified by counting the LET lectin-labelled microvessels. Since this lectin specifically labels endothelial cells of all microvessels (Thurston *et al.*, 1998, Ezaki *et al.*, 2001), it was considered a good marker for the total profile of blood vessels. The present quantitative study showed that at the trauma and rostral sites there was an increase in the total number of blood vessels at all time intervals, although statistical significance was only detected at 14 and 28d in rostral segments. Therefore, these results appear to exclude the possibility that the decreased expression of EBA after compression spinal cord injury was due to any reduction or the loss of total profile of microvessels. The lack of statistical significance despite the apparent increase in the total profile of vessels may be due to the wide range in the number of vessels counted in the dorsal horns and the ventral horns. Individual readings are used in the calculations, and dorsal horns were more subject to heamorrhage and gliosis. There was also a slight increase in the number of EBA positive vessels in the trauma site as well as in the segements rostral to the trauma site at the late stage post injury compared to the normal animals athough this increase

was not statistically significant. This increase may be because of an increase in the total vessel number due to angiogenesis. Furthermore, this result suggests that some new vessels may express EBA. The results obtained from the caudal segments indicate that there was loss of EBA positive vessels greater than the loss in the total vessel profiles at all time intervals following moderate trauma. Because of the time limit of this study, the quantitative study was not undertaken to investigate the total profile of LET lectin labelled vessels in the animals with severe injury.

The other very important issue arising here is whether the new vessels from angiogenesis can express EBA. If so, when do they start to express EBA and other BBB specific markers? As discussed above, the number of LET lectin-labelled vessels is increased in the trauma and rostral sites. The number of EBA labelled vessels was also slightly increased at the late stage post moderate injury, suggesting that some new vessels from angiogenesis express EBA. In a previous study using a double labelling method, Loy *et al.* demonstrated that the angiogenesis starts at 7 days after contusion injury to the spinal cord (Loy *et al.*, 2002). In the present study, there is an obvious trend that lectin labelled vessels are increased in the trauma site as well as in the segment rostral to the trauma site as early as 1 day after injury although this increase was not statistically significant. This suggests that there is angiogenesis in the trauma site as as well as in the rostal site even at the very early stages after injury. However, a double labelling method is needed to further clarify whether the

new vessels express EBA and when they start to express this BBB specific protein and other BBB specific markers.

Interestingly, in the caudal site, there was no remarkable increase in the number of LET lectin-labelled vessels suggesting that there may be no obvious angiogenesis in the caudal site. In a previous study, it was reported that breakdown in the barrier is more severe in the caudal site than the rostral site as demonstrated by HRP injection method (Nobel *et al.*, 1988). In the present study, the reduction in EBA expression at caudal sites after moderate injury and the remarkable reduction after severe injury suggest a compromised barrier in the caudal site in this compression injury model. This study also indicates that the alteration of EBA expression after injury is time- and severity dependent. Further studies are needed to correlate the severity of vascular damage, breakdown of the BSB and angiogenesis after injury and to define how these parameters are related in the present model.

The percentage of EBA labelled vessels in relation to the LET-lectin labelled vessels has been also calculated in the normal and experimental animals and provided an overview of the dynamic situation of blood vessel profiles and expression of EBA. The results showed that in the trauma site and rostral site there was an obvious reduction of the percentage of EBA labelled vessels at the first week post injury but a slight increase at 14 days and 28 days post injury. There are two factors which may account for the reduction in the percentage of EBA labelled vessels. Firstly, an

increase in the number of LET lectin due to angiogenesis in the trauma and rostral sites. Secondly, the number of EBA labelled vessels was reduced due to the reduction or loss of EBA expression. Thirdly, both factors may be operating. The quantitative study indicates that there is a relative reduction of the number of EBA-labelled vessels in relation to lectin-labelled vessels as indicated by the percentages. In addition, the absolute number of EBA–labelled vessels were less than those in controls indicating a loss of EBA expression at the early time intervals.

Interestingly, in the caudal site, the percentage of EBA labelled vessels in relation to the total vessel profile is much higher than those in the trauma site and rostral site although there was also a reduction in the number of EBA labelled vessels at all time intervals post injury. This is likely because no obvious increase in the number of total profile occurred post injury. Taken together, these results appear to suggest that changes in EBA expression do not primarily correlate with the angiogenesis.

5.1.3 GLUT1 expression after compression spinal cord injury

The qualitative study showed a remarkable reduction of GLUT1 immunoreactivity after severe injury in all survival time intervals. The quantitative study by immunolabelling and Western Blotting on animals with moderate injury also showed a decrease in the expression of GLUT1 at the trauma site as well as the rostral and caudal sites in the first two weeks after compression injury. These findings have not been reported previously. Despite extensive studies on GLUT1 in normal brain and

traumatic brain injury, limited information is available on GLUT1 activity in spinal cord injury. The current study has shown for the first time that GLUT1 activity is down-regulated following compression injury to the rat spinal cord. This result appears to be consistent with those of previous studies in other pathological conditions that showed a reduction in the expression of GLUT1. For example, a study on GLUT1 activity in human brain injury reported that in the central zone of dense erythrocyte infiltration, representing the traumatic focus, capillaries almost totally lost immunoreactivity for GLUT1 (Cornford *et al.*, 1996). However, in the peripheral zone beyond this traumatized zone, the majority of microvessels were highly reactive for GLUT1. Quantitative immunogold electron microscopic studies also showed microvessels in the peripheral zone were highly positive for GLUT1 activity, which was even higher than that of erythrocytes (Cornford *et al.*, 1996). Tissue hypermetabolism has been reported in several other animal models (Yoshino *et al.*, 1991; Kawamata *et al.*, 1992) and was also pronounced in brain regions adjacent to the trauma site (Yoshino *et al.*, 1991). In the present study, the expression of GLUT1 in the segments remote from the trauma site was reduced. The mechanism by which the GLUT1 is reduced in segments remote from the trauma site in this model is not clear.

There seems to be an apparent difference in the results between the immunocytochemical and Western blot detection of GLUT1 at 3 and 7d after injury in the present study. In the trauma site, the density of GLUT1 labelled vessels per

mm^2 was dramatically reduced in all time intervals, whereas the Western blot analysis showed that there was a reduction in the band density only at the 3 and 7 days post injury, but much higher at 28 days post injury. This discrepancy may be due to the difference in the sensitivity of two methods applied. The Western blot method may be more sensitive than the immunocytochemical method. On the other hand, Western blotting used a whole segment 1.5 cm long that comprised 0.5 cm epicenter of trauma, two 0.5 cm long segments rostral and caudal to the epicenter of trauma. Thus, the Western blotting method reflects the overall level of GLUT1 in the trauma as well as adjacent rostral and caudal regions.

The percentage of GLUT1 labelled vessels in relation to the LET-lectin labelled vessels has also been calculated in the normal and experimental animals. The results showed that in the trauma, rostral and caudal sites there was an obvious reduction of the percentage of GLUT1 labelled vessels at all time intervals post injury. In the trauma and rostral sites there were slight increases at 7 days post injury. These increases may reflect the higher demand for energy metabolism at 7 days. However at 14 and 28 days after injury, the percentage of GLUT1 immunoreactive vessels in relation to the lectin labelled vessels was decreased again. This second decrease after 1 week post injury may be due to an increased number of lectin labelled vessels because of angiogenesis that did not express the GLUT1. However, at the caudal site, the percentage of GLUT1 immunoreactive vessels in experimental animals showed maximum reduction at 3 d, then progressive increase to 58% at 28 days.

Since no obvious angiogensis was seen at the caudal site in experimental animals, the results suggest an actual reduction of GLUT1 follwed by a gradual restoration caudal to the trauma.

In human brain injury, two types of GLUT1-immunoreactive vessels were identified (Cornford *et al.*, 1996). While about 90% of the microvessels showed uniform staining for GLUT1 throughout the entire cross-sectional profile, about 10% of the microvessels showed a markedly lower density of GLUT1 labelling in one sector of the capillary profile. This pattern was not observed in normal primate or rodent brains (Cornford *et al.*, 1996; Cornford *et al.*, 1998a). This bimodal GLUT1 distribution has also been observed in brain tissues from patients suffering from seizures (Cornford *et al.*, 1998b). In interictal seizure resections, the distribution of high and low GLUT1 immunoreactive ECs provided three types of GLUT1-immunoreactive microvessels. Type A capillaries display abundant GLUT1 immunoreactivity throughout the entire capillary circumference on both luminal and abluminal membranes. Type B capillaries have low GLUT1 density in all ECs. Type AB capillaries display both high and low GLUT1 density ECs. In the present study, there were no distinct three types of microvessels observed, which may be due to the different model used.

Two possible mechanisms for the regulation of human BBB endothelial glucose transport protein (Cornford *et al.*, 1994b) have been suggested; (1) redistribution of

GLUT1 between EC membranes and the cytoplasm; and (2) alteration of the total number of the glucose transporter proteins. However, the mechanism by which the GLUT1 is down regulated after spinal cord injury is not known. The down-regulated GLUT1 immunoreactivity may indicate that the synthesis of this protein was reduced, which may be caused by reduced local glucose supply due to the poor microcirculation in the trauma site. The reduced blood circulation and supply may reduce the local recruitment of the GLUT1. It may suggest that the uptake of glucose by spinal cord ECs is reduced in the compression injury model. Alternatively, this may be due to decreased production of this protein as a result of vascular injury caused by the primary mechanical damage and secondary biochemical insults. The opening of the BSB and ruptured vessels observed after the injury might also enable glucose to diffuse freely into the spinal cord interstitial tissue, which reduced the need for GLUT1 transport activity. However, this explanation does not seem to be likely as this may imply a continous blood flow from ruptured vessels. Also impairment of cerebral glucose uptake has been reported in experimental traumatic brain injury (Krishnappa *et al.*, 1999) and in brain trauma in humans (Cruz, 1995). In an experimental traumatic brain injury study cerebral dialysate glucose concentration fell by 50% following severe cortical impact injury while the dialysate lactate concentration significantly increased (Krishnappa *et al.*, 1999). Studies on the fluid percussion injury model also reported a significant reduction of the cerebral dialysate glucose concentration and increased cerebral dialysate lactate following the injury (Chen *et al.*, 2000). In human brain trauma, global cerebral glucose extraction was

significantly reduced as measured by arteriojugular glucose concentration difference, suggesting impaired cerebral glucose uptake (Cruz, 1995). Thus the increase in glucose diffusion in the injured tissue is not likely. The other possibility, which should be considered in this study, is whether the reduction of GLUT1 expression is due to the reduction or loss of the total vessel profile in the trauma site. However, the LET lectin labelling showed no reduction but an obvious increase in the total vessel profile as discussed in the previous section.

The factors involved in GLUT1 expression are not known. Astrocytes have been long suggested to be involved in the induction of BBB characteristics in ECs (Holash *et al.*, 1993b). Most recently, a study showed that the GLUT1 expression after injury is closely associated with the presence of the astrocytes in the trauma site. The study also demonstrated that both injured and regenerating vessels exhibit abnormal permeability and that GLUT1 expression during revascularization is dependent on the presence of astrocytes (Whetstone *et al.*, 2003).

Accumulating evidence suggests that the regulation of GLUT1 expression in the brain is closely related to cerebral glucose metabolism. As discussed in the introduction, in neurodegenerative diseases such as Alzheimer's disease and AIDS with late clinical stage of dementia, GLUT1 expression is significantly reduced in the brain (Harik, 1992; Simpson and Duffy, 1994; Kovitz and Morgello, 1997). In Alzheimer's disease, down-regulation of both GLUT1 and GLUT3 in the brain in the

temporal and parietal cortices was observed (Simpson *et al.*, 1994). Decreased glucose transport in these brain areas in Alzheimer's disease was demonstrated by positron emission tomography (Jagust *et al.*, 1991). In AIDS patients, GLUT1 activity was increased in the brain when no neuropathological changes were observed. However, GLUT1 activity was decreased in brains from patients with HIV encephalitis (HIVE) (Kovitz and Morgello, 1997). A study also reported a trend for the decreased GLUT1 and GLUT3 in patients with HIVE, paralleling cortical and subcortical glucose hypometablism in patients with late stage AIDS (Rottenberg *et al.*, 1987). Glucose hypermetabolism was observed at the early stage of AIDS dementia but in the later stage of dementia, glucose metabolism was decreased (Rottenberg *et al.*, 1987).

It was reported that local cerebral glucose utilization increases following traumatic brain injury in the fluid percussion model in rats (Yoshino *et al.*, 1991) and in severe traumatic brain injury in humans. Therefore, impaired transportation of glucose following traumatic brain injury would further worsen the cellular damage. In the fluid percussion injury model, following the hypermetabolism observed in the early stage of injury, cerebral hypometabolism, indicated by decreased local cerebral metabolic rates for glucose, was observed from 6h after the injury and lasted for as long as 5 days. This indicates that cells were functionally compromised (Yoshino *et al.*, 1991). Another in vitro study, on the other hand, showed that a higher glucose concentration in the rat hippocampal slice incubation medium, improved recovery of

neuronal function after cerebral hypoxia (Schurr *et al.*, 1987). The protective effect of glucose was dose dependent. It was suggested that a high concentration of glucose in the extracellular fluid increases anaerobic glycolytic production of energy charge to maintain ion gradients across the neuronal membrane. Apparently, the in vitro study bypassed the BBB and directly increased the extracellular glucose concentration. In the present study, GLUT1 was shown to be down regulated in the the trauma site as well as in the segments rostral and caudal to the trauma site. Whether the down regulation of GLUT1 is due to decreased metabolism of glucose after injury is not known. It is also not clear whether down regulation of GLUT1 is a factor which is involved in the pathological evolution.

Some recent studies have shown that during traumatic brain injury, lactate may be used as an alternative energy supply. After traumatic brain injury, lactate level in the brain is significantly increased (Chen *et al.*, 2000; Krishnappa *et al.*, 1999; McIntosh *et al.*, 1987). The level of cerebral lactate was shown not to be directly related to the severity of neurological dysfunction (McIntosh *et al.*, 1987). Some recent studies have reported neuroprotective effects of lactate on the injured brain. Infusion of the lactate to the traumatized brain may improve the neurological deficits (Rice *et al.*, 2002). Lactate infusion study has also demonstrated neuroprotective effects of lactate. In this study, Lactate infusion (i.v.) was started 30 min after lateral fluid percussion injury and continued for 3 h. Cognitive deficits were determined using the Morris water maze. Lactate infused injured animals demonstrated significantly less

cognitive deficits than saline infused injured animals. Thus, lactate infusion attenuated the cognitive deficits normally observed in this model, and therefore may provide patients with a moderate head injury with a treatment to help ameliorate the sequelae (Rice *et al.*, 2002). Experiments also showed that lactate reduces the neurotoxicity of glutamate in vivo. When 6 mM L-lactate was perfused together with 100 mM glutamate there was a significant reduction in the size of the lesion and there was no reduction in dialysate glucose. When L-lactate was replaced with D-lactate the lesion size and the increase in dialysate lactate were greater than after glutamate alone. It has been suggested that the neuroprotective role of L-lactate is attributed to its ability to meet the increased energy demands of neurons exposed to high concentrations of glutamate (Ros *et al.*, 2001). However, whether the lactate also serves as an energy substrate and has the neuroprotective effects in the spinal cord is not known.

5.1.4 Conclusion

A sustained compression injury model in rats was employed in this study. The albumin leakage study carried out here demonstrated that vasogenic spinal cord oedema was present at 24 hours after the injury, the earliest time point studied. Vasogenic oedema appeared to result from the disruption of the BSB. EBA immunoreactivity, an indicator of vascular integrity, was reduced after the compression injury. The reduction of EBA expression correlated well with the course of vasogenic oedema, which is reflected by the leakage of albumin. GLUT1

immunoreactivity was also reduced after the injury, indicating a potential impairment of glucose supply to the spinal cord after injury. Therefore, the results from this study suggest that multiple factors contribute to the pathological evolution in the spinal cord following compression injury. In addition to the direct mechanical injury to the spinal cord, the disruption of the BSB, subsequent leakage of blood borne neurotoxic substances into the spinal cord neuropil, release of neurotoxin, ischaemia and energy supply failure, may all be responsible for the neuronal dysfunction following compression injury. The neural damage coincident with the opening of the BSB suggests that the BSB function is closely associated with normal neural function.

5.2 The blood-testis barrier after compression spinal cord injury

5.2.1 EBA expression in the normal male rat reproductive tract

As mentioned before, EBA is considered as a barrier specific protein. In the brain, EBA is specifically expressed in vessels with barrier properties but not in non-barrier vessels. For example, ECs in the peri-ventricular organs and choroid plexus, which lack barrier properties, are EBA-negative (Sternberger and Sternberger, 1987). In most peripheral tissues tested so far vessels are negative for EBA (Sternberger and Sternberger, 1987; Orte *et al.*, 1999). However, in this study we showed for the first time that EBA was expressed by endothelial and epithelial cells in the reproductive tract of male rats. In addition to the testicular ECs, epithelial cells particularly of the dorsolateral, and to lesser extent the ventral prostate, the coagulating gland and the seminal vesicles also showed consistent labelling with anti-EBA. This finding seems

to be not in full agreement with the concept that EBA is as a barrier-specific protein. Therefore, EBA appears to have wider tissue distribution and more diverse functional roles than previously known.

The first issue that arose from the reproductive organs study is whether the anti-EBA cross-reacts with tissue components and related proteins in these reproductive organs. This appears not likely, because anti-EBA monoclonal antibody has been widely used for BBB studies since it was reported in 1978 (Sternberger and Sterberger, 1987; Cassella *et al.*, 1997; Lin and Ginsberg, 2000; Nishigaya *et al.*, 2000). Numerous studies consistently confirmed the specificity of this antibody to barrier vessels. Thus, the high specificity of the monoclonal anti-EBA (SMI 71) would make it unlikely to cross-react with other tissue components or related proteins. Furthermore, in this study, the isotype mouse IgM used as a control for the anti-EBA during the staining procedure did not show any staining in the testis and other accessory reproductive glands suggesting that a false positive labelling caused by cross reactivities is unlikely. Our preliminary western blot study also demonstrated that anti-EBA recognizes a protein of molecular weight which corresponds to that of EBA in the rat testis and prostate, which further confirmed the expression of this protein in the reproductive tissue (not shown here).

As mentioned previously, in the testis, a barrier between the blood and the fluid in the lumina of the seminiferous tubles exists (Fawcett et al., 1970; Setchell, 1980).

Evidence for this includes the uneven colouration of the testis after injection of certain dyes, and the distribution of some radioreactive markers determined by autoradiography or by comparing their volumes of distribution with morphological estimates of the volumes of the various compartments of the testis (Fawcett *et al.*, 1970; Dym, 1970). There are also differences in composition between the blood plasma and testicular lymph on the one hand and the fluid in the lumina of the seminiferous tubules and the rete testis on the other hand. In addition, various markers pass from the blood stream into these testicular fluids at different rates (Setchell and Wates, 1975; Setchell, 1980, 1994). Morphologically, attention has been focused on the specialized junctions between pairs of adjacent Sertoli cells in the tubules, which block the entry into the tubules of electron-opaque markers such as lanthanum and horseradish peroxidase (Dym and Fawcett, 1970). In the current study, however, the major barrier site of the testis, the Sertoli cells, did not express any EBA, and EBA was only expressed by the endothelium of testicular vessels. This finding appears to add support to the proposal that testicular vessels contribute to the barrier function of the BTB (Setchell *et al.*, 1969; Holash and Stewart, 1993). However, further studies are needed to clarify the precise functional roles of EBA in the reproductive tissues.

In addition to the Sertoli cells, other cells in the testis such as the ECs of testicular vessels (Holash *et al.*, 1993a) and peritubular myoid cells (Fawcett *et al.*, 1970) have been suggested to contribute to the barrier function. A partial barrier function of

peritubular myoid cells was suggested from ultrastructural studies, which showed a clear peritubular space deep to the myoid cells in contrast to the interstitial tissues, which showed proteinaceous content. These cells are also able to exclude large molecular tracers, such as thorium dioxide and carbon, but allow entry of small tracers, such as ferritin and peroxidases (Fawcett *et al.*, 1970). The peritubular myoid cells are joined by TJs, although 10-15% of the TJs appear to have gaps of 20 nm (Dym and Fawcett, 1970). These myoid cells also contain a specific transport system for urea (Fenton *et al.*, 2000). However, in the current study no staining for EBA was noted in the peritubular myoid cells.

It is interesting that EBA was found to be expressed particularly by the epithelial cells of the dorsolateral prostate. After spinal cord injury, prostatic acini were distended and there was reduction in EBA immunoreactivity in prostatic epithelial cells, but the prostate content of the acini showed immunoreactivity for EBA. These findings suggest that the EBA is related to the normal function and motility of the sperm since the secretion from prostate gland is an important component of the semen. However, the exact significance of this increased expression of EBA in the prostatic secretion after spinal cord injury is not known.

The prostatic epithelium has TJs and barrier properties (Kachar and Reese, 1983). However, it is unlikely that EBA expression is directly related to the TJs in prostatic epithelium since (a) it is not expressed in epithelia with TJs in other body organs (b)

in brain ECs, EBA is not associated with intercellular junctions, but is expressed on the luminal membrane (Rosenstein *et al.*, 1992; Lawrenson et al., 1995b; Zhu *et al.*, 2001). In the above named reproductive accessory glands EBA was present predominantly in the apical cytoplasm, which suggests its secretion into the fluids of associated glands. Thus EBA here may have an as yet unknown function in relation to sperm survival and /or motility.

In the rat, diversity in chemical composition exists among the secretions of the various reproductive accessory glands. The prostatic secretion contains inositol, polyamines and epidermal growth factor (Jacobs and Story, 1988). A 22 kDa protein has also been detected in the rat ventral prostate (Carmo-Fonseca and Vaz, 1989). According to a previous study, anti-EBA reacts with immunoblots of rat brain microvessel membranes and shows three positive bands of 30, 25, 23.5 kDa proteins (Sternberger and Sterberger, 1987). Whether the 22 kDa prostatic protein is related to the 23.5 kDa in brain preparations is yet to be determined. However, immunofluoresence labelling showed that the 22 kDa protein is expressed only in the ventral prostate but not in the dorsolateral prostate (Carmo-Fonseca and Vaz, 1989) which in the present study showed the strongest immunoreactivity with anti-EBA, while the ventral prostate showed only a few epithelial cells positive for EBA. Preliminary observations in our laboratory using PAGE and immunoblotting suggest that proteins of similar molecular weight in the brain, testis, and prostate are reacting with anti-EBA (not shown here).

As discussed previously, EBA appears to play an important role for the normal function of the BBB, as injection of antibody to EBA causes opening of the BBB (Ghabriel *et al.*, 2000). The barrier function of Sertoli cells may be dependent on currently unknown regulatory factors, different from those that control barrier properties of brain ECs. In the testis, the barrier to dyes and the specialized junctions between Sertoli cells develop only at puberty (Kormano, 1967; Russell *et al.*, 1989) and the barrier becomes less effective outside the breeding season in seasonally breeding mammals. While the barrier in the testis and spermatogenesis are both disrupted under some circumstances (Vitamin A deficiency, disorganization of the microtubules in the Sertoli cells, after different duct ligations or injection of cadmium salts and in very old rats), spermatogenesis can be disrupted in other ways without the barrier being affected (See Setchell 2001 for review).

Endothelial cells of testicular microvessels share several features with those in the brain. There is a specific saturable transport system for leucine in ECs of the testis with kinetic properties very similar to those in the brain (Bustamante and Setchell, 2000). It was shown that the ECs in the testis contain the glucose transporter GLUT1, gamma glutamyl transpeptidase and the multidrug resistance gene product P-gp (Harik *et al.*, 1990; Holash *et al.*, 1993a) which had been thought to be specific to the brain. Testicular expression of EBA seen in the current study provides further support for the similarities between brain and testicular vessels. It has also been demonstrated that leydig cells, which lie close to the ECs in the testis, contain S-100

protein, the glial fibrillary acidic protein and the enzyme glutamine synthetase (Holash *et al.*, 1993a). These are characteristic markers of astrocytes, the cells in the brain which have been suggested to confer barrier properties to brain ECs (Risau, 1991). While the above results and discussion show that testicular vessels share many biochemical markers with brain vessels, differences do exist. Unlike brain vessels, those of the testis do not express the transferrin receptor (Holash *et al.*, 1993a). Although as stated above, ECs of both the brain and testis express P-gp, the distribution of this marker is not similar in the two systems. It is localized to luminal membranes in brain ECs but to luminal and abluminal membranes in testicular ECs (Stewart *et al.*, 1996). The biological significance of the difference in the distribution of P-gp in the two systems is yet to be understood (Stewart *et al.*, 1996). Also morphological and physiological studies showed some differences between the two vascular beds. Albumin, which does not freely enter the brain, is readily detectable in the testicular lymph (Setchell and Waites, 1975 for review). Testicular capillaries are continuous and have intercellular TJs (Weihe *et al.*, 1979) but the junctional density is less than that of brain ECs (Holash *et al.*, 1993a; Stewart, 2000). Testicular vessels are larger and have a thicker wall and a higher density of mitochondria than brain vessels (Holash *et al.*, 1993a; Stewart, 2000). Previous studies provided evidence for leakage of Evans blue (Caster *et al.*, 1955) and trypan blue (Kormano, 1967) into the interstitial tissues of the testis. HRP can also enter the interstitial tissues of the testis (Weihe *et al.*, 1979) but not into the brain (Brightman and Reese, 1969). The difference in the permeability between testicular and brain vessels may be due to

differences in the structure and function of the TJs between ECs in the two systems. Brain vessels have long sinous intercellular junctions with high electrical resistance. Testicular vessels have wide compartments between the series of tight junctions (Fawcett *et al.*, 1970; Holash *et al.*, 1993a; Stewart, 2000). Fifteen percent of testicular vessels have wide junctions with a higher cleft index which may explain their higher permeability compared to brain vessels. Nevertheless, in the current study strong EBA labelling was seen in the majority of testicular vessels.

The function of EBA in the testis needs to be investigated in the future. The EBA has been suggested to be related to the normal function of the BBB. As described in previous chapters, EBA expression is reduced or lost in pathologies associated with brain oedema including compression spinal cord injury model, brain injury model, and other animal models. Furthermore, in a recent study in our laboratory, it was indicated that EBA plays a putative role in maintaining normal function of the BBB (Ghabriel *et al.*, 2000). After immunotargeting of EBA, there is wide opening of the BBB suggesting that EBA is related to the integrity of the BBB. However, it is not clear whether EBA is also related to the barrier property of the blood-testis barrier and if it plays putative roles in the testis.

5.2.2 GLUT1 expression in the normal male rat reproductive tract.

In agreement with previous studies (Holash et al., 1993a), in the present study, GLUT1 was consistently expressed in testicular vessels. The expression of GLUT1 in

brain vessels has been considered to be related to the normal energy metablism in the central nervous system (Harik, 1992; Vannucci et al., 1997). Similarly, GLUT1 may be also involved in energy metabolism in the testis. But the molecular mechanism for GLUT1 involvement in the energy metabolism is still unknown. The factors that regulate GLUT 1 expression in the testicular vessels are also not known. GLUT1 has been considered to be a barrier specific protein since it was identified (Pardridge et al., 1990a). The expression of GLUT1 in the testicular vessels adds further support to the hypothesis that testicular vessels possess barrier properties and may contribute to the barrier function of the blood-testis barrier (Holash et al., 1993a).

In the testis other isoforms of the GLUT family are also identified including GLUT 8 and GLUT3. Thus GLUT1 is not the major and only glucose transporter which might be related to the energy metabolism in the testis. The regulatory mechanisms for GLUT1 expression are still not clear. However, a recent study showed that the mRNA of GLUT1 can be up-regulated by fibroblast growth factor (FGF) in vitro (Riera et al., 2003).

5.2.3 EBA expression in the male reproductive tract after compression spinal cord injury

In this study we showed that EBA expression was reduced in endothelial and epithelial cells of testicular vessels and of the prostate gland respectively after compression spinal cord injury. This reduction occurred as early as 1 day after injury and was sustained longer than two weeks. In experimental animals, some vessels

showed sectoral loss or complete loss of EBA immunoreactivity or faint labelling of EBA in the testis blood vessels and epithelium of prostate glands. The sustained reduction of EBA in testicular vessels after injury for this period of two weeks was unexpected. This time frame for EBA suppression seems to be different from that reported in previous studies in CNS pathology where EBA expression generally is restored about 2 weeks after injury in most animal models. The time-frame difference between the results in this study of male reproductive tract and those previously reported in CNS models might be due to different pathogenesis applied and different pathophysiology involved.

A high percentage of human spinal cord injuries occurs to males. After spinal cord injury, most male patients experience fertility related problems including erectile and ejaculatory dysfunction, impaired spermatogenesis, abnormal sperm viability, motility, and morphology, genitourinary infection and endocrine abnormalities (Monga *et al.*, 2002). The underlying mechanisms for decreased fertility after spinal cord injury are not completely understood.

The causes of poor semen quality following spinal cord injury are unknown. A few pathologies might be involved. One possible mechanism is decreased testicular blood flow. A study on the blood flow in the testis after spinal cord injury in the rat showed that there were no significant changes in blood flow in the sham operated rats three or 14 days after surgery. However, three days after SCI, blood flow had decreased in

the SCI rats to 78 +/- 5% of the pre-SCI flow. At 14 days after SCI, blood flow was still decreased to 77 +/- 8 % (Linsenmeyer *et al.*, 1996). Other studies showed that excessive reactive oxygen species (ROS) levels are much higher in semen from spinal cord injured men in comparison to other infertile men. ROS are a class of free radicals, which are highly reactive oxidizing agents. ROS such as superoxide, anion, hydrogen peroxide, peroxyl and hydroxyl (OH) can exert detrimental effects on male fertility (Mahadevan, 1998). There are also numerous reports of histological abnormality in the testis of spinal cord injured men. Seminiferous tubular atrophy was noted in the majority of testicular biopsies of spinal cord-injured men (Bors *et al.*,1950). Sclerosis of testicular interstitial tissues and arrest of spermatogenesis was also reported (Holstein *et al.*, 1985). Whether the reduction of testicular blood flow, increased ROS level and other pathological changes are related to the reduction in EBA expression is not known.

The mechanism for EBA reduction in the brain after pathological insults is not clear. Similarly, the mechanism accounting for the reduction of EBA in the testicular vessels after compression injury to the spinal cord is also unknown. The reduction and loss of EBA in testicular vessels may be due to autonomic dysfunction. Changes in the neuroendocrine function after spinal cord injury may have also contributed to the alteration in the BEA expression in the testicular vessels. However, further studies are needed to test these hypothesises.

5.2.4 GLUT1 expression in the male reproductive tract after compression spinal cord injury

A remarkable reduction of GLUT1 in the testis was demonstrated in this study. This reduction was seen at 24h after injury and continued for four weeks, the longest time interval in this study. The significance for GLUT1 reduction after compression spinal cord injury in the testis is not clear. As described in previous studies, the GLUT1 expression is involved in energy metabolism in the brain. GLUT1 is likely to have the same physiological role in normal testis and after injury.

As discussed previously, pathohistological changes occur in the reproductive organs after compression injury to the spinal cord. These pathological changes include the degeneration of seminiferous tubules and the reduction of testicular blood circulation. It has also been shown that sperm motility and the fertility were also disrupted after compression spinal cord injury (Huang *et al.*, 1998). Testicular blood flow was decreased after compression injury in rats (Linsenmeyer *et al.*, 1996). Hormonal regulation of both Sertoli and Leydig cells was altered during the acute phase of SCI (Ottenweller *et al.*, 2000). These pathological changes may be related to reduced GLUT1 expression. The reduction of the testicular blood flow might be related to the reduction of GLUT1 expression, since in a brain infarction model and a brain ischaemia injury model an obvious reduction of GLUT1 was observed (McCall *et al.*, 1996).

A previous study showed that the cryptorchid testes exhibit marked degenerative

changes in the seminiferous tubules and spermatogonia, impaired and incomplete spermatogenesis and lack of spermatozoa in the lumen (Farooqui *et al.*, 1997). The expression of facilitative glucose transporters (GLUT 1, 2 and 3) was examined by western blot analyses 10, 20 and 30 days following surgically induced unilateral abdominal cryptorchidism. Immunoblotting of testis proteins with GLUT transporter antibodies revealed only the presence of GLUT2 and 3 proteins. GLUT2 expression in abdominal testis was increased (45%, 67%, and 40% at 10, 20 and 30 days, respectively) but no significant change was observed in contralateral scrotal testis. GLUT3 expression was reduced by 85-95% compared with contralateral scrotal testis. A significant decrease in GLUT3 levels in abdominal testis was accompanied by an increase in levels in the scrotal testis. GLUT3 content was 80%, 144% and 212% at 10, 20 and 30 days, respectively, compared to age matched control rats. These results suggest that degenerative changes in abdominal testis might be associated with decreased GLUT3 mediated glucose transport in seminiferous tubules and spermatogonia. In the present study degeneration of seminiferous tubules in the testis was also observed after compression spinal cord injury and the reduction of GLUT1 expression in testicular vessels might be also correlated with this pathological change.

5.2.5 Conclusion

In the normal rat, two BBB specific markers, EBA and GLUT1, were found to be strongly expressed by testicular vessels. EBA was also found to be expressed by the

accessory glands of reproductive tracts. After spinal cord injury, there were remarkable reductions of EBA and GLUT1 in testicular vessels and of EBA in prostatic epithelial cells. This reduction continued for two weeks but increased labelling of the luminal content of prostatic acini was observed. The functional roles of EBA and GLUT 1 in the male reproductive tract merit further investigation.

5.3 The time course of opening and closure of the blood-brain barrier after immunological targeting of EBA.

5.3.1 The temporal pattern of EBA labelling after anti-EBA injection

In the current study experimental animals were injected intravenously with anti-EBA antibody. From these animals, Vibratome sections, which were not exposed to the primary antibody in the staining procedure, showed immunoreactivity of brain vessels for EBA, indicating that the systemically injected anti-EBA antibody became localized to ECs, and acted as a substitute for the exposure of tissues to the primary antibody in the staining procedure. Presumably anti-EBA antibody identified EBA on the EC membranes and formed antigen-antibody complexes. These complexes remained stable for the duration of the experiment, and tolerated 45 min of flushing of the circulation, initially with DPBS then the fixative, using fast and slow perfusion. However, the immunoreactivity for EBA seen in the Vibratome sections was moderate compared with the strong immunoreactivity seen in sections, which were treated with anti-EBA antibody as primary antibody in the staining procedure. This may be explained by an insufficient concentration of the anti-EBA injected in

vivo to saturate all EBA sites in the cerebral vascular bed. The higher staining intensity in the sections exposed to the primary antibody therefore may be due to the lablling of additional EBA during the staining procedure. Exposure of sections to anti-EBA antibody overnight in the staining procedure provides enough time and antibody availability to label a greater number of EBA molecules in brain vessels.

In the present study, animals injected with anti-EBA showed strong labelling for EBA after routine immunohistochemical labelling. Furthermore, these animals also showed very strong labelling for EBA when the primary antibody was omitted during the immunostaining procedure for all animals killed up to 6h after the antibody injection. These findings suggest that the anti-EBA injected in vivo became bound to the endothelial cell luminal membranes. The bound antibody tolerated the blood circulation for 6 hours and subsequent perfusion fixation procedure and was detectable by the immunocytochemical procedure. The animals with the isotype IgM injection as a control did not show EBA labelling when the primary antibody was omitted indicating that the EBA labelling was specific and not a false–positive labelling.

The temporal pattern of EBA labelling in the current study appeared to coincide with the time course of opening of the BBB suggesting that the EBA may play a putative role in maintaining the integrity of the BBB. It was concluded that the injected antibody became bound to EBA sites in the endothelial cells. The formation of

antigen-antibody complexes may have interfered with the EBA function leading to activation of a secondary messenger pathway that resulted in opening of the tight junctions. Beyond 6 hours survival after the injection, the injected anti-EBA was not detected in ECs. This suggests that the antigen-antibody complexes have become degraded, dissociated from the ECs, or have become modified to an extent that made them not detectable by immunocytochemistry.

A previous electron microscope study of the immunological targeting model showed that the binding of intravenously injected anti-EBA antibody to the antigen in situ was observed at the luminal membranes (Ghabriel *et al.*, 2002). EBA reaction product was observed in blood vessels of brain tissues from experimental animals stained only with secondary antibody and visualized by DAB. The localization of EBA reaction product in these ECs was similar to immunostaining of normal rat brain. Future studies therefore should employ electron microscopy in a temporal study to attempt to clarify the fate of these antigen-antibody complexes on EC membranes.

As stated above, it is likely that the anti-EBA injected in vivo has formed antigen-antibody complexes on the surface of ECs. Vibratome sections from experimental animals injected with anti-EBA in vivo, showed immunoreactivity for EBA, despite the omission of anti-EBA antibody as the primary antibody in the staining procedure. A previous study of this model has shown that these complexes are heat sensitive

(Ghabriel *et al.*, 2000). Paraffin sections obtained from the brains of experimental animals, when the primary antibody was omitted, did not show any immunoreactivity for EBA. The difference between the positive labelling of Vibratome sections but lack of labelling of paraffin sections when the primary antibody is omitted must be related to the method of processing. This suggests that the antigen-antibody complexes, which were formed in vivo, are unstable at the temperature (58°C) required for paraffin embedding.

5.3.2 The integrity of the BBB after immunotargeting of EBA

Interference with the EBA function after immunological targeting resulted in a wide opening of the BBB as evidenced by the wide leakage of exogenous HRP in the brain. The leakage of exogenous HRP from the BBB started at 17 min after antibody injection and was maximum at 30 min after the injection. The time frame discrepancy between EBA expression and the course of the BBB opening at 6 hours may suggest interference with EBA function in the later phase after the antibody injection is not severe enough to cause the leakage, or that the existing EBA molecules in the endothelial cells at later time intervals are sufficient enough to maintain the normal function of the BBB.

This model of BBB opening by immunological targeting of EBA is compatible with recovery and survival. The opening of the BBB is very rapid and maximal leakage of HRP occurs at 30 min after the immunological challenge. Opening of the BBB is

transient as the barrier was reconstituted by 3h. The BBB once reconstituted remained impermeable to HRP. In the current study, opening of the BBB was monophasic. Once reconstituted at 3 h after anti-EBA injection, the BBB remained impermeable to HRP at subsequent time intervals up to 4 d, the longest time examined. In other experimental models in the rat the BBB was reported to have a biphasic opening pattern. Following lateral controlled cortical impact the BBB to Evans blue showed two peaks of extravasations at 4-6 h and 3d after the impact (Baskaya *et al.*, 1997). A biphasic pattern of BBB opening has also been described in brain ischemia (Huang *et al.*, 1999). On the other hand a single phase opening of the BBB was reported after closed head injury in rats (Shapira *et al.*, 1993) and intracarotid infusion of hypertonic solution (osmotic opening) (Rapoport, 2000). Thus the current immunological model provides a narrow single window for bypassing the BBB.

Control animals were injected with mouse IgM as isotype control antibody to EBA, which is a mouse IgM molecule (Sternberger Monoclonal Inc, Lutherville, Maryland, USA). Control animals did not show any HRP leakage at any time interval, contrasting with the specific effect of anti-EBA in experimental animals. The detection of HRP in the liver and the choroid plexus in control animals proved successful injection of HRP and its circulation throughout the body, and together with labelling of occasional red blood cells, indicated the successful development of

the peroxidase reaction product. Thus, the effect of anti-EBA injection is specific to this antibody.

In the current study, there were slight variations in the amount, extent and distribution of HRP leakage among experimental animals killed at the same time interval. This variability could have arisen due to biological inter-animal differences, slight variation in the dose of the antibody, or differences in the speed of injection. The long period of injection (12 min) might allow the animals sufficient time to dissociate the antigen-antibody complexes or to partially replenish EBA sites in ECs prior to exposure of the BBB to HRP. Variability in the injection speed was imposed by variations in the respiratory rate and depth among animals, as the injection rate was slowed down to avoid respiratory arrest. However, despite these minor variations a general trend was apparent for maximal opening of the BBB at 30 min and restoration of the BBB by 3h.

In the lateral fluid percussion injury to the brain the BBB to exdogenous HRP is opened within 3 min of the impact (Fukuda *et al.*, 1995). In osmotic opening, the barrier is breached instantaneously and is essentially reconstituted within 10 min (Rapoport, 2001). In the current model of anti-EBA injection, the BBB was open at 17 min and was reconstituted by 3 h. Differences in the timing and pattern of BBB opening among experimental models may indicate the different mechanisms involved. Osmotic opening is dependent on the physico-chemical properties of the

injected solutes, while in traumatic injury the mechanism involves primary and secondary insults. The mechanism of opening of the BBB in the current iummunotargeting model is not known. Immunological interaction between the injected antibody and EBA molecules in EC membranes may lead to intracellular signalling, cytoskeletal activation and opening of paracellar clefts, as previously suggested for human ECs (Reviwed by Rubin and Staddon, 1999). It is relevant here that a previous electron microscope study of the current model demonstrated leakage of HRP via intercellular junction (Ghabriel *et al.*, 2002). The current report provides baseline data for future studies on experimental manipulation of the BBB. This model may be applicable to experimental studies for testing neuroprotective agents or drug delivery to the brain.

The mechanism underlying the disruption of the BBB by intravenous injection of anti-EBA antibody is not known. One can assume that the binding of intravenously injected anti-EBA antibody to the antigen on the ECs disturbed the normal function of EBA and led to structural and functional changes in the ECs. It has been suggested that EBA is associated with a receptor complex (Rosenfeld *et al.*, 1987). The interference with EBA function may disturb cell signalling systems or transportation systems in ECs. Further studies are needed to clarify the biochemical structure of EBA and its exact function at the BBB.

In the current and previous studies (Ghabriel *et al.*, 2000; 2002), in vivo

administration of antibody to EBA (anti-EBA) resulted in an increased permeability of brain microvessels to endogenous and exogenous tracers, indicating that interference with EBA function on the BBB leads to the opening of the barrier. Intravenous injection of PBS and control antibodies did not alter the integrity of the BBB, indicating that the effect of intravenous injection of anti-EBA on the BBB is not due to non-specific antigen-antibody binding on ECs or non-specific allergic reaction to foreign antibodies. The electron microscopic tracer study of this model (Ghabriel *et al.*, 2002) revealed that intravenous injection of anti-EBA leads to the opening of more than one route for macromolecules to move across the BBB. This study provides direct evidence for the importance of EBA for BBB integrity in the rat. The mechanisms by which the anti-EBA injected in vivo 'neutralized' EBA molecules on ECs, or interfered with the function of EBA require further investigation.

5.3.3 Conclusion

Interference with EBA function after immunological targeting resulted in a wide opening of the BBB as evidenced by the wide leakage of the exogenous tracer HRP in the brain. Experimental evidence indicates that EBA plays an important putative role in maintaining the integrity of BBB. This model of BBB opening by immunological targeting of EBA is compatible with recovery and survival. The opening of the BBB is very rapid and maximal leakage of HRP occurs at 30 min after the immunological challenge. Opening of the BBB is transient as the barrier was

reconstituted by 3h. The BBB once reconstituted remained impermeable to HRP.

CHAPTER 6

GENERAL DISCUSSION AND CONCLUSION

Chapter 6 General discussion and conclusion

For more than a century, the BBB has been extensively studied. Tremendous progress has been made in understanding the physiology and biology of the BBB. We now understand that the BBB consists of a unique endothelium, which is non-fenestrated and has a low density of vesicles. Tight junctions between the adjacent endothial cells seal the interendothelial space and prevent free exchange of macromolecules from the blood stream to the brain or vice visa. The BBB is essential for maintaining normal homeostasis of neural tissue. In the last few decades, dozens of proteins and molecules have been identified in the BBB endothelium. These proteins and molecules are found to be specifically expressed by BBB vessels but not by non-barrier vessels. The physiological and functional roles of most of these molecules are still not completely understood. Therefore, this project aimed at investigating the anatomy and function of the BBB and its specific makers, namely EBA and GLUT 1, under normal and disease conditions. Two animal models have been applied in the present study, the compression spinal cord injury model and immunological targeting model. The integrity of the BSB after compression injury to the spinal cord was studied. It was found that disruption of the BSB leads to the development of vasogenic oedema, a common complication of many neurological diseases. The BSB specific markers EBA and GLUT 1 were investigated at the LM and EM levels. The EBA and GLUT1 were quantified at the LM level while GLUT1 was also quantified by the Western immunoblotting method.

In this study, the expression of EBA and GLUT 1 was also investigated in a peripheral tissue, the male reproductive tract. The hypothesis that this blood-tissue barrier also

expressed the EBA was tested. We found ECs of testicular vessels and epithelial cells of reproductive accessory glands in the male rat also express EBA. The results showed that EBA like a few other BBB specific makers is strongly expressed by the endothelial cells of testicular vessels. Interestingly, EBA was found to be expressed by epithelial cells of the prostate, coagulating gland, seminal vesicles and rete testis. These findings indicate that the EBA has a wider tissue distribution and more diverse functional roles than previously appreciated.

In the present study, EBA expression was also investigated after SCI. The results showed that the EBA expression is reduced in the testicular microvessels and in the epithelial cells of the prostate glands. Many prostatic acini were distended with secretion, which may be related to absence of ejaculation on account of spinal cord injury. EBA was reduced in epithelial cells of the prostate in injured animals suggesting a reduction in its synthesis. The secretion of many distended prostatic acini showed increased immunoreactivity for EBA. This may indicate that EBA that existed in the apical part of prostatic epithelial cells at the time of injury was secreted into the lumen and remained due to lack of ejaculation in the paralysed animals. The significance of changes in the EBA expression in the rat reproductive tract after spinal cord injury merit further investigation.

The function of EBA at the BBB was further investigated using an in vivo immunological targeting approach. A previous study has demonstrated that intravenous injection of anti-EBA antibody into the rat, rapidly opens the BBB and leads to a widespread leakage of serum albumin and HRP. In the present study a time course

investigation was undertaken to further characterize this model. The temporal expression of the EBA after anti-EBA injection was investigated at the LM level. Consistent with previous studies, the intravenously injected anti-EBA antibody was shown by immunocytochemistry to bind to the antigen on brain ECs. The injected anti-EBA was detectable on the endothelium for about 6 hours. Coincident with the presence of anti-EBA in the endothelial cells, the tracer study showed that there was a narrow window of BBB opening after anti-EBA injection, which is about 3 hours after anti-EBA injection. The present study provided strong evidence that EBA plays an important role in maintaining the integrity of the BBB. The immunological targeting model is compatible with animal survival. The results further indicate that the opening and closure of the BBB after immunotargeting is time and dose dependent.

6.1 BSB specific markers and vascular damage after traumatic spinal cord injury

Numerous studies have been performed previously to examine the pathophysiology of the BSB using different animal models. Especially, numerous tracer studies have generated detailed information about vascular damage after spinal cord injury. The dynamics of the blood supply and blood circulation after spinal cord injury was also studied in detail previously (Rivlin and Tator, 1978; Wallace and Tator, 1986; Mautes et al., 2000). However, studies on the expression of and functional roles of the BBB specific markers in the normal and injured spinal cord are very sparse. Information about the correlation between vascular injury and neural degeneration and regeneration is also lacking. In the present study, the expression of two BBB specific markers has been investigated qualitatively and quantitatively. EBA and GLUT1 have been quantified at LM level. GLUT1 expression was also quantified using the western

blotting method. The results showed that the EBA is remarkably reduced after compression injury. This reduction also extended to several segments remote from the trauma site. GLUT1 expression in spinal cord trauma has not been studied before. The present study also further increased our knowledge of changes in EBA expression in spinal cord segments remote from the compression. Since the segments remote from the trauma site are mainly subject to secondary injury, the EBA appears to be a sensitive indicator of secondary vascular damage after spinal cord injury. The finding from this study has some important implications. The EBA can be used as a useful maker to monitor the acuteness and chronicity of vascular damage. Future studies on the expression and function of BBB specific marker in spinal cord injury is of special significance for further understanding of the pathophysiology of spinal cord injury. However, the relationship between the expression of these BBB markers and pathogenesis and pathological evolution after spinal cord injury has not been elucidated in this study, and require further investigation.

While GLUT1 was qualitatively studied with the light microscope, it was also quantitatively assessed using the western blot method in animals with moderate injury. Both the western blot and the light microscopic studies showed a remarkable reduction of GLUT1 after compression injury, although statistically the reduction of GLUT 1 detected by immunoblot in animals with moderate injury was not significant at all the time intervals post injury. This result appears to be consistent with previous findings that GLUT1 is lost or reduced in a zone adjacent to centre of trauma in human brain injury and stab wound brain injury (Rosenstein and More, 1994; Cornford *et al.*, 1996). The reduction of GLUT1 after compression injury may suggest that there is reduced

glucose availability and glycolytic activity, or possibly the utilization of alternative energy sources after compression injury.

6.2 Expression of BBB-specific proteins in the male reproductive system of normal and spinal cord-injured rats.

The barrier function of the tight junctions of endothelial cells is not privileged to microvessels in the central nervous system. Other barriers exist in other body systems. The blood-testis barrier is one of the best documented and studied barriers, which shares similarity with the BBB. The blood-testis barrier like the BBB also expresses some special markers that are specifically expressed by the BBB. This barrier also can prevent the free exchange of some molecules between the blood and parenchyma of testis. For example, some macromolecules injected also can be excluded by testicular vessels.

The present study demonstrated that EBA is also expressed in testicular vessels and some epithelial cells of the accessory reproductive organs. The function of the EBA in the testis is not clear. Furthermore, questions are raised regarding the function of EBA in the prostatic epithelial cells. The significance of EBA and GLUT1 reduction in the testis after compression injury is not clear.

6.3 Opening of the BBB after immuno-targeting of the endothelial barrier antigen

In previous studies, it has already been demonstrated that anti-EBA injection could lead to a wide opening of the BBB. In the present study, it was further demonstrated that after immunotargetting of EBA, there is wide opening of the BBB in the brain and spinal cord. This opening was transient and compatible with animal survival. The

immunotargeting model provides a good tool for further study of the BSB. This model may have some experimental applications. Firstly, this model might be used to manipulate the opening of the BBB. Secondly, a small window of BBB opening after antibody injection may be used for further pharmacological studies, such as delivery of neuroprotective agents to the brain.

6.4 General conclusion

In the normal state, the BBB is capable of excluding both large and small molecular tracers. EBA and GLUT1 are strongly expressed at the BBB. A reduction of EBA immunoreactivity in the spinal cord and the male reproductive tissues occurs after compression spinal cord injury. The reduction correlates well with the disruption of the BSB, indicating that EBA expression is sensitive to BBB injury. In vivo immunological targeting of EBA leads to rapid opening of the BSB, suggesting that EBA plays a role in maintaining the integrity of the BSB. The immunological targeting model is compatible with animal survival. GLUT 1 expression, on the other hand, is more related to cerebral metabolism. The down-regulation of GLUT1 immunoreactivity may decrease the glucose supply to the brain and induce further damage to the brain.

GLUT 1 and EBA were also found to be expressed by testicular vessels. Some epithelial cells of the accessory reproductive organs also expressed EBA. In pathological conditions, such as spinal cord injury, EBA expression was also reduced in the rat testis. This finding suggests that EBA has a more diverse functional role than previously appreciated. The functional role of EBA in the testis and other organs in the male reproductive tract needs to be addressed in future studies. Of particular interest is the

relationships between poor sperm quality, infertility, blood-testis barrier and spinal cord trauma. GLUT1 may be heterogenous, being down-regulated in certain injured vessels but up-regulated in adjacent vessels with a variable outcome for partially damaged tissues.

APPENDIX

PUBLISHED PAPERS

Ghabriel, M.N., Lu, J.J., Hermanis, G., Zhu, C., and Setchell, P., (2002) Expression of a blood-brain barrier-specific antigen in the reproductive tract of the male rat. *Reproduction, v. 123 (3), pp. 389-397.*

Ghabriel, N.M., Lu, J.J., Tadros, R., and Hermanis, G., (2004) A narrow time-window for access to the brain by exogenous protein after immunological targeting of a blood–brain barrier antigen.
Journal of Comparative Pathology, v. 131 (1), pp. 52-60.

BIBLIOGRAPHY

Bibliography

Aaku-Saraste, E., Hellwig, A., and Huttner, W. B. (1996). Loss of occludin and functional tight junctions, but not ZO-1, during neural tube closure – remodeling of the neuroepithelium prior to neurogenesis. *Dev Biol* 180, 664-79.

Abbott NJ, Ronnback L, Hansson E (2006) Astrocyte-endothelial interactions at the blood-brain barrier *Nat Rev Neurosci.* 7(1):41-53..

Agus, D. B., Gambhir, S. S., Pardridge, W. M., Spielholz, C., Baselga, J., Vera, J. C., and Golde, D. W. (1997). Vitamin C crosses the blood-brain barrier in the oxidized form through the glucose transporters. *J Clin Invest* 100, 2842-8.

Ahmed, A. M., Weller R. O. (1979) The blood-nerve barrier and reconstitution of the perineurium following nerve grafting. *Neuropathol Appl Neurobiol.* 5(6) 469-83.

Akiyama, H., Kondoh, T., Kokunai, T., Nagashima, T., Saito, N., and Tamaki, N. (2000). Blood-brain barrier formation of grafted human umbilical vein endothelial cells in athymic mouse brain. *Brain Res* 858, 172-6.

Albrecht, U., Seulberger, H., Schwarz, H., and Risau, W. (1990). Correlation of blood-brain barrier function and HT7 protein distribution in chick brain circumventricular organs. *Brain Res* 535, 49-61.

Allt, G., and Lawrenson, J. G. (2000). The blood-nerve barrier: enzymes, transporters and receptors – a comparison with the blood-brain barrier. *Brain Res Bull* 52, 1-12.

Allt G, Lawrenson JG. (2000). The blood-nerve barrier: enzymes, transporters and receptors--a comparison with the blood-brain barrier. *Brain Res Bull.* 52(1):1-12

Ando-Akatsuka, Y., Saitou, M., Hirase, T., Kishi, M., Sakakibara, A., Itoh, M., Yonemura, S., Furuse, M., and Tsukita, S. (1996). Interspecies diversity of the occludin sequence: cDNA cloning of human, mouse, dog, and rat-kangaroo homologues. *J Cell Biol* 133, 43-7.

Arthur, F. E., Shivers, R. R., and Bowman, P. D. (1987). Astrocyte-mediated induction of tight junctions in brain capillary endothelium: an efficient in vitro model. *Brain Res* 433, 155-9.

Banks, W. A., and Broadwell, R. D. (1994). Blood to brain and brain to blood passage of native horseradish peroxidase, wheat germ agglutinin, and albumin: pharmacokinetic and morphological assessments. *J Neurochem* 62, 2404-19.

Bannister, R (1978) Disorder of spinal cord. Brain's clinal neurology, 5th edition, editored by Sir Roger Bannister. Oxford University Press, London. 306-335

Barrand, M. A., Robertson, K. J., Neo, S. Y., Rhodes, T., Wright, K. A., Twentyman, P. R., and Scheper, R. J. (1995). Localisation of the multidrug resistance-associated

protein, MRP, in resistant large-cell lung tumour cells. *Biochem Pharmacol* 50, 1725-9.

Bart, J., Groen, H. J., Hendrikse, N. H., Van der Graaf, W. T., Vaalburg, W., and De Vries, E. G. (2000). The blood-brain barrier and oncology: new insights into function and modulation. *Cancer Treat Rev* 26, 449-62.

Barzo, P., Marmarou, A., Fatouros, P., Hayasaki, K., and Corwin, F. (1997). Biphasic pathophysiological response of vasogenic and cellular edema in traumatic brain swelling. *Acta Neurochir Suppl (Wien)* 70, 119-22.

Baskaya, M. K., Rao, A. M., Dogan, A., Donaldson, D., and Dempsey, R. J. (1997). The biphasic opening of the blood-brain barrier in the cortex and hippocampus after traumatic brain injury in rats. *Neurosci Lett* 226, 33-6.

Beaulieu, E., Demeule, M., Ghitescu, L., and Beliveau, R. (1997). P-glycoprotein is strongly expressed in the luminal membranes of the endothelium of blood vessels in the brain. *Biochem J* 326, 539-44.

Beaulieu, E., Demeule, M., Pouliot, J. F., Averill Bates, D. A., Murphy, G. F., and Beliveau, R. (1995). P-glycoprotein of blood brain barrier: cross-reactivity of Mab C219 with a 190 kDa protein in bovine and rat isolated brain capillaries. *Biochim Biophys Acta* 26, 27-32.

Bell, G. I., Burant, C. F., Takeda, J., and Gould, G. W. (1993). Structure and function of mammalian facilitative sugar transporters. *J Biol Chem* 268, 19161-4.

Betz, A. L., Firth, J. A., and Goldstein, G. W. (1980). Polarity of the blood-brain barrier: distribution of enzymes between the luminal and antiluminal membranes of brain capillary endothelial cells. *Brain Res* 192, 17-28.

Boado, R. J., and Pardridge, M. M. (1991). A one-step procedure for isolation of poly(A)+ mRNA from isolated brain capillaries and endothelial cells in culture. *J Neurochem* 57, 2136-9.

Boado, R. J., and Pardridge, W. M. (1990). The brain-type glucose transporter mRNA is specifically expressed at the blood-brain barrier. *Biochem Biophys Res Commun* 166, 174-9.

Boado, R. J., and Pardridge, W. M. (1994). Differential expression of alpha-actin mRNA and immunoreactive protein in brain microvascular pericytes and smooth muscle cells. *J Neurosci Res* 39, 430-5.

Bolz, S., Farrell, C. L., Dietz, K., and Wolburg, H. (1996). Subcellular distribution of glucose transporter (GLUT-1) during development of the blood-brain barrier in rats. *Cell Tissue Res* 284, 355-65.

Bors E, Engle E. T, Rosenquist R. C, Holliger VH. (1950). Fertility in paraplegic

males; a preliminary report of endocrine studies. *J Clin Endocrinol Metab. 10(4):381-98.*

Bouchaud, C., Le Bert, M., and Dupouey, P. (1989). Are close contacts between astrocytes and endothelial cells a prerequisite condition of a blood-brain barrier? The rat subfornical organ as an example. *Biol Cell* 67, 159-65.

Bouldin, T. W., and Krigman, M. R. (1975). Differential permeability of cerebral capillary and choroid plexus to lanthanum ion. *Brain Res* 99, 444-8.

Bradbury M. W, Stulcova B. (1970). Efflux mechanism contributing to the stability of the potassium concentration in cerebrospinal fluid. *J Physiol.* 208(2):415-30 Bradbury MW (1993) The blood-brain barrier. *Exp Physiol.* 78(4):453-72.

Brightman, M. W., Hori, M., Rapoport, S. I., Reese, T. S., and Westergaard, E. (1973). Osmotic opening of tight junctions in cerebral endothelium. *J Comp Neurol* 152, 317-25.

Brightman, M. W., and Reese, T. S. (1969). Junctions between intimately apposed cell membranes in the vertebrate brain. *J Cell Biol* 40, 648-77.

Broadwell, R. D. (1989). Transcytosis of macromolecules through the blood-brain barrier: a cell biological perspective and critical appraisal. *Acta Neuropathol (Berl)* 79, 117-28.

Brodbelt A. R, Stoodley, Waltling A. M, Tu J, Jones N. R (2003). Fluid flow in an animal model of post-traumatic syringomylia. *Eur Spine J.* 12(3) 300-6.

Brodbelt A. R, Stoodley M. A, Watling A. M, Tu J, Burke S, Jones N. R (2003). Altered subarachnoid space compliance and fluid flow in an animal model of posttraumatic syringomeylia. *Spine* 2003 28(20) E413-9.

Brodbelt A. R and Stoodley M. A (2003a). Syringomyelia and the arachnoid web. *Acta Neurochir (Wien).* 145(8):707-11

Brodbelt A. R and Stoodley M. A (2003b). Post-traumatic syringomyelia: a review. *J ClinNeurosci.*10(4):401-8.

Bundgaard, M., and Cserr, H. F. (1981). Impermeability of hagfish cerebral capillaries to radio-labelled polyethylene glycols and to microperoxidase. *Brain Res* 206, 71-81.

Bundgaard, M., Frokjaer Jensen, J., and Crone, C. (1979). Endothelial plasmalemmal vesicles as elements in a system of branching invaginations from the cell surface. *Proc Natl Acad Sci U S A* 76, 6439-42.

Buschman, E., and Gros, P. (1994). The inability of the mouse mdr2 gene to confer multidrug resistance is linked to reduced drug binding to the protein. *Cancer Res* 54, 4892-8.

Bustamante, J. C., and Setchell, B. P. (2000). The uptake of amino acids, in particular leucine, by isolated perfused testes of rats. *J Androl* 21, 452-63.

Butt, A. M., and Jones, H. C. (1992). Effect of histamine and antagonists on electrical resistance across the blood-brain barrier in rat brain-surface microvessels. *Brain Res* 569, 100-5.

Caley, D. W., and Maxwell, D. S. (1970). Development of the blood vessels and extracellular spaces during postnatal maturation of rat cerebral cortex. *J Comp Neurol* 138, 31-47.

Cancilla, P. A., Baker, R. N., Pollock, P. S., and Frommes, S. P. (1972). The reaction of pericytes of the central nervous system to exogenous protein. *Lab Invest* 26, 376-83.

Carlson, E. C., Brendel, K., Hjelle, J. T., and Meezan, E. (1978). Ultrastructural and biochemical analyses of isolated basement membranes from kidney glomeruli and tubules and brain and retinal microvessels. *J Ultrastruct Res* 62, 26-53.

Carmo-Fonseca, M., and Vaz, Y. (1989). Immunocytochemical localization and lectin-binding properties of the 22 kDa secretory protein from rat ventral prostate. *Biol Reprod* 40, 153-64.

Cassella, J. P., Lawrenson, J. G., Allt, G., and Firth, J. A. (1996). Ontogeny of four blood-brain barrier markers: an immunocytochemical comparison of pial and

cerebral cortical microvessels. *J Anat* 189, 407-15.

Cassella, J. P., Lawrenson, J. G., Lawrence, L., and Firth, J. A. (1997). Differential distribution of an endothelial barrier antigen between the pial and cortical microvessels of the rat. *Brain Res* 744, 335-8.

Castejon, O. J. (1984). Submicroscopic changes of cortical capillary pericytes in human perifocal brain edema. *J Submicrosc Cytol* 16, 601-18.

Castejon, O. J. (1998). Electron microscopic analysis of cortical biopsies in patients with traumatic brain injuries and dysfunction of neurobehavioural system. *J Submicrosc Cytol Pathol* 30, 145-56.

Caster W. O, Simon AB, Armstrong WD. (1955) Evans blue space in tissues of the rat. *Am J Physiol.* 183(2):317-21.

Cereijido, M., Shoshani, L., and Contreras, R. G. (2000). Molecular physiology and pathophysiology of tight junctions. I. Biogenesis of tight junctions and epithelial polarity. *Am J Physiol Gastrointest Liver Physiol* 279, G477-82.

Cervos Navarro, J., Kannuki, S., and Nakagawa, Y. (1988). Blood-brain barrier (BBB). Review from morphological aspect. *Histol Histopathol* 3, 203-13.

Chen, T., Qian, Y. Z., Rice, A., Zhu, J. P., Di, X., and Bullock, R. (2000). Brain lactate

uptake increases at the site of impact after traumatic brain injury. *Brain Res* 861, 281-7.

Chiba, M., and Jimbow, K. (1986). Expression of gamma-glutamyl transpeptidase in normal and neoplastic epithelial cells of human skin: a marker for distinguishing malignant epithelial tumours. *Br J Dermatol* 114, 459-64.

Christopher E. Smith, M.D., Arthur Atchabahian, M.D., Susan E. Mackinnon, M.D., Daniel A. Hunter, R.T.(2001) Development of the blood-nerve barrier in neonatal rats. *Microsurgery* 21(7), 290-297.

Citi, S., and Kendrick Jones, J. (1988). Brush border myosin filament assembly and interaction with actin investigated with monoclonal antibodies. *J Muscle Res Cell Motil* 9, 306-19.

Claudio, L., Kress, Y., Factor, J., and Brosnan, C. F. (1990). Mechanisms of edema formation in experimental autoimmune encephalomyelitis. The contribution of inflammatory cells. *Am J Pathol* 137, 1033-45.

Coomber, B. L., and Stewart, P. A. (1986). Three-dimensional reconstruction of vesicles in endothelium of blood-brain barrier versus highly permeable microvessels. *Anat Rec* 215, 256-61.

Cordon-Cardo, C., O'Brien, J. P., Boccia, J., Casals, D., Bertino, J. R., and Melamed, M.

R. (1990). Expression of the multidrug resistance gene product (P-glycoprotein) in human normal and tumor tissues. *J Histochem Cytochem* 38, 1277-87.

Cordon-Cardo, C., O'Brien, J. P., Casals, D., Rittman-Grauer, L., Biedler, J. L., Melamed, M. R., and Bertino, J. R. (1989). Multidrug-resistance gene (P-glycoprotein) is expressed by endothelial cells at blood-brain barrier sites. *Proc Natl Acad Sci U S A* 86, 695-8.

Cornford, E. M., Hyman, S., Cornford, M. E., and Caron, M. J. (1996). Glut1 glucose transporter activity in human brain injury. *J Neurotrauma* 13, 523-36.

Cornford, E. M., Hyman, S., Cornford, M. E., and Clare Salzler, M. (1995). Down-regulation of blood-brain glucose transport in the hyperglyceamic nonobese diabetic mouse. *Neurochem Res* 20, 869-73.

Cornford, E. M., Hyman, S., Cornford, M. E., Damian, R. T., and Raleigh, M. J. (1998a). A single glucose transporter configuration in normal primate brain endothelium: comparison with resected human brain. *J Neuropathol Exp Neurol* 57, 699-713.

Cornford, E. M., Hyman, S., Cornford, M. E., Landaw, E. M., and Delgado Escueta, A. V. (1998b). Interictal seizure resections show two configurations of endothelial Glut1 glucose transporter in the human blood-brain barrier. *J Cereb Blood Flow Metab* 18, 26-42.

Cornford, E. M., Hyman, S., and Landaw, E. M. (1994a). Developmental modulation of blood-brain-barrier glucose transport in the rabbit. *Brain Res* 663, 7-18.

Cornford, E. M., Hyman, S., and Pardridge, W. M. (1993a). An electron microscopic immunogold analysis of developmental up-regulation of the blood-brain barrier GLUT1 glucose transporter. *J Cereb Blood Flow Metab* 13, 841-54.

Cornford, E. M., Hyman, S., and Swartz, B. E. (1994b). The human brain GLUT1 glucose transporter: ultrastructural localization to the blood-brain barrier endothelia. *J Cereb Blood Flow Metab* 14, 106-12.

Cornford, E. M., Young, D., Paxton, J. W., Hyman, S., Farrell, C. L., and Elliott, R. B. (1993b). Blood-brain glucose transfer in the mouse. *Neurochem Res* 18, 591-7.

Crone, C., and Olesen, S. P. (1982). Electrical resistance of brain microvascular endothelium. *Brain Res* 241, 49-55.

Cruz, J. (1995). An additional therapeutic effect of adequate hyperventilation in severe acute brain trauma: normalization of cerebral glucose uptake. *J Neurosurg* 82, 379-85.

Cumber, P. M., Jacobs, A., Hoy, T., Fisher, J., Whittaker, J. A., Tsuruo, T., and Padua, R. A. (1990). Expression of the multiple drug resistance gene (mdr-1) and epitope masking in chronic lymphatic leukaemia. *Br J Haematol* 76, 226-30.

Dantzig, A. H., Shepard, R. L., Cao, J., Law, K. L., Ehlhardt, W. J., Baughman, T. M., Bumol, T. F., and Starling, J. J. (1996). Reversal of P-glycoprotein-mediated multidrug resistance by a potent cyclopropyldibenzosuberane modulator, LY335979. *Cancer Res* 56, 4171-9.

Das, A., Frank, R. N., Weber, M. L., Kennedy, A., Reidy, C. A., and Mancini, M. A. (1988). ATP causes retinal pericytes to contract in vitro. *Exp Eye Res* 46, 349-62.

Davson, H., Kleeman. (1961). Blood brain barrier and extracellular space. *Journal of Physiology*, 67-68p.

DeBault, L. E., and Cancilla, P. A. (1980). Gamma-Glutamyl transpeptidase in isolated brain endothelial cells: induction by glial cells in vitro. *Science* 207, 653-5.

Dehouck, M. P., Vigne, P., Torpier, G., Breittmayer, J. P., Cecchelli, R., and Frelin, C. (1997). Endothelin-1 as a mediator of endothelial cell-pericyte interactions in bovine brain capillaries. *J Cereb Blood Flow Metab* 17, 464-9.

DeNofrio, D., Hoock, T. C., and Herman, I. M. (1989). Functional sorting of actin isoforms in microvascular pericytes. *J Cell Biol* 109, 191-202.

Dermietzel, R. (1975). Junctions in the central nervous system of the cat. IV. Interendothelial junctions of cerebral blood vessels from selected areas of the brain. *Cell Tissue Res* 164, 45-62.

Dermietzel, R., and Krause, D. (1991). Molecular anatomy of the blood-brain barrier as defined by immunocytochemistry. *Int Rev Cytol* 127, 57-109.

Devaskar, S. U., and deMello, D. E. (1996). Cell-specific localization of glucose transporter proteins in mammalian lung. *J Clin Endocrinol Metab* 81, 4373-8.

Dick, A. P., Harik, S. I., Klip, A., and Walker, D. M. (1984). Identification and characterization of the glucose transporter of the blood-brain barrier by cytochalasin B binding and immunological reactivity. *Proc Natl Acad Sci U S A* 81, 7233-7.

Dobrogowska, D. H., and Vorbrodt, A. W. (1999). Quantitative immunocytochemical study of blood-brain barrier glucose transporter (GLUT-1) in four regions of mouse brain. *J Histochem Cytochem* 47, 1021-30.

Drews, L. R. (1998) Biology of the blood-brain glucose transporter. An introduction to the blood-brain barrier: methodology, biology and pathology. W. M. Pardridge. Cambridge, Cambridge University Press: 165-174.

Drion, N., Risede, P., Cholet, N., Chanez, C., and Scherrmann, J. M. (1997). Role of P-170 glycoprotein in colchicine brain uptake. *J Neurosci Res* 49, 80-8.

Duelli, R., Maurer, M. H., Staudt, R., Heiland, S., Duembgen, L., and Kuschinsky, W. (2000). Increased cerebral glucose utilization and decreased glucose transporter Glut1 during chronic hyperglycaemia in rat brain. *Brain Res* 858, 338-47.

Dym, M., and Fawcett, D. W. (1970). The blood-testis barrier in the rat and the physiological compartmentation of the seminiferous epithelium. *Biol Reprod* 3, 308-26.

Dym M and Cavicchia JC (1977) Further observations on the blood–testis barrier in monkeys *Biology of Reproduction* 17 390–403.

Ezaki T, Baluk P, Thurston G, La Barbara A, Woo C, McDonald DM. (2001) Time course of endothelial cell proliferation and microvascular remodeling in chronic inflammation. *Am J Pathol.* 158(6):2043-55.

Farooque, M., Zhang, Y., Holtz, A., and Olsson, Y. (1992). Exudation of fibronectin and albumin after spinal cord injury in rats. *Acta Neuropathol Berl* 84, 613-20.

Farooqui, S. M., Al Bagdadi, F., O'Donnell, J. M., and Stout, R. (1997). Degenerative changes in spermatogonia are associated with loss of glucose transporter (Glut 3) in abdominal testis of surgically induced unilateral cryptorchidism in rats. *Biochem Biophys Res Commun* 236, 407-12.

Farrell, C. L., and Pardridge, W. M. (1991). Ultrastructural localization of blood-brain barrier-specific antibodies using immunogold-silver enhancement techniques. *J Neurosci Methods* 37, 103-10.

Farrell, C. L., Yang, J., and Pardridge, W. M. (1992). GLUT-1 glucose transporter is

present within apical and basolateral membranes of brain epithelial interfaces and in microvascular endothelia with and without tight junctions. *J Histochem Cytochem* 40, 193-9.

Farrell, C. R., Stewart, P. A., Farrell, C. L., and Del Maestro, R. F. (1987). Pericytes in human cerebral microvasculature. *Anat Rec* 218, 466-9.

Fawcett, D. W., Leak, L. V., and Heidger, P. M., Jr. (1970). Electron microscopic observations on the structural components of the blood-testis barrier. *J Reprod Fertil Suppl* 10, 105-22.

Fenton, R. A., Howorth, A., Cooper, G. J., Meccariello, R., Morris, I. D., and Smith, C. P. (2000). Molecular characterization of a novel UT-A urea transporter isoform (UT-A5) in testis. *Am J Physiol Cell Physiol* 279, C1425-31.

Ferrari Dileo, G., Davis, E. B., and Anderson, D. R. (1996). Glaucoma, capillaries and pericytes. 3. Peptide hormone binding and influence on pericytes. *Ophthalmologica* 210, 269-75.

Ferrari-Dileo, G., Davis, E. B., and Anderson, D. R. (1991). Angiotensin II binding receptors in retinal and optic nerve head blood vessels. An autoradiographic approach. *Invest Ophthalmol Vis Sci* 32, 21-6.

Firth, J. A. (1977). Cytochemical localization of the K+ regulation interface between

blood and brain. *Experientia* 33, 1093-4.

Foda, M. A., and Marmarou, A. (1994). A new model of diffuse brain injury in rats. Part II: Morphological characterization. *J Neurosurg* 80, 301-13.

Fojo, A. T., Ueda, K., Slamon, D. J., Poplack, D. G., Gottesman, M. M., and Pastan, I. (1987). Expression of a multidrug-resistance gene in human tumors and tissues. *Proc Natl Acad Sci U S A* 84, 265-9.

Fossum, S., Mallett, S., and Barclay, A. N. (1991). The MRC OX-47 antigen is a member of the immunoglobulin superfamily with an unusual transmembrane sequence. *Eur J Immunol* 21, 671-9.

Frank, R. N., Dutta, S., and Mancini, M. A. (1987). Pericyte coverage is greater in the retinal than in the cerebral capillaries of the rat. *Invest Ophthalmol Vis Sci* 28, 1086-91.

Frank M, Wolburg H (1996). Cellular reactions at the lesion site after crushing of the rat optic nerve. *Glia.* 16(3):227-40.

Frey, A., Meckelein, B., Weiler-Guttler, H., Mockel, B., Flach, R., and Gassen, H. G. (1991). Pericytes of the brain microvasculature express gamma-glutamyl transpeptidase. *Eur J Biochem* 202, 421-9.

Fukuda, K., Tanno, H., Okimura, Y., Nakamura, M., and Yamaura, A. (1995). The blood-brain barrier disruption to circulating proteins in the early period after fluid percussion brain injury in rats. *J Neurotrauma* 12, 315-24.

Fukuhara, T., Gotoh, M., Kawauchi, M., Asari, S., Ohmoto, T., Tsutsui, K., and Shohmori, T. (1994). Detection of endogenous albumin as an index of blood parenchymal border alteration. *Acta Neurochir Suppl (Wien)* 60, 121-3.

Furuse, M., Sasaki, H., Fujimoto, K., and Tsukita, S. (1998). A single gene product, claudin-1 or -2, reconstitutes tight junction strands and recruits occludin in fibroblasts. *J Cell Biol* 143, 391-401.

Gerhart, D. Z., LeVasseur, R. J., Broderius, M. A., and Drewes, L. R. (1989). Glucose transporter localization in brain using light and electron immunocytochemistry. *J Neurosci Res* 22, 464-72.

Ghabriel M. N, Jennings K. H and Allt G (1989). Diffusion barrier properties of the perineurium: an in vivo ionic lanthanum tracer study. *Anat Embryol (Berl).* 180(3):237-42.

Ghabriel, M. N., Zhu, C., Hermanis, G., and Allt, G. (2000). Immunological targeting of the endothelial barrier antigen (EBA) in vivo leads to opening of the blood-brain barrier. *Brain Res* 878, 127-35.

Ghabriel, M. N., Zhu, C., and Leigh, C. (2002). Electron microscope study of blood-brain barrier opening induced by immunological targeting of the endothelial barrier antigen. *Brain Res* 934, 140-51.

Ghandour, M. S., Langley, O. K., and Varga, V. (1980). Immunohistological localization of gamma-glutamyltranspeptidase in cerebellum at light and electron microscope levels. *Neurosci Lett* 20, 125-9.

Golden, P. L., Maccagnan, T. J., and Pardridge, W. M. (1997). Human blood-brain barrier leptin receptor. Binding and endocytosis in isolated human brain microvessels. *J Clin Invest* 99, 14-8.

Golden, P. L., and Pardridge, W. M. (1999). P-Glycoprotein on astrocyte foot processes of unfixed isolated human brain capillaries. *Brain Res* 819, 143-6.

Goldstein G. W (1979) Relation of potassium transport to oxidative metabolism in isolated brain capillaries. *J Physiol.* 286:185-95.

Gordon, S. R., and Essner, E. (1985). Plasma membrane-associated vesicles in retinal capillaries of the rat. *Am J Anat* 174, 161-72.

Gros, P., Raymond, M., Bell, J., and Housman, D. (1988). Cloning and characterization of a second member of the mouse mdr gene family. *Mol Cell Biol* 8, 2770-8.

Gumbiner, B., and Simons, K. (1986). A functional assay for proteins involved in establishing an epithelial occluding barrier: identification of a uvomorulin-like polypeptide. *J Cell Biol* 102, 457-68.

Hanigan, M. H., and Frierson, H. F., Jr. (1996). Immunohistochemical detection of gamma-glutamyl transpeptidase in normal human tissue. *J Histochem Cytochem* 44, 1101-8.

Harik, S. I. (1992). Changes in the glucose transporter of brain capillaries. *Can J Physiol Pharmacol* 70, S113-7.

Harik, S. I., Hall, A. K., Richey, P., Andersson, L., Lundahl, P., and Perry, G. (1993). Ontogeny of the erythroid/HepG2-type glucose transporter (GLUT-1) in the rat nervous system. *Brain Res Dev Brain Res* 72, 41-9.

Harik, S. I., Kalaria, R. N., Andersson, L., Lundahl, P., and Perry, G. (1990). Immunocytochemical localization of the erythroid glucose transporter: abundance in tissues with barrier functions. *J Neurosci* 10, 3862-72.

Haskins, J., Gu, L., Wittchen, E. S., Hibbard, J., and Stevenson, B. R. (1998). ZO-3, a novel member of the MAGUK protein family found at the tight junction, interacts with ZO-1 and occludin. *J Cell Biol* 141, 199-208.

Hawkins, C. P., Mackenzie, F., Tofts, P., du Boulay, E. P., and McDonald, W. I. (1991).

Patterns of blood-brain barrier breakdown in inflammatory demyelination. *Brain* 114, 801-10.

Hegmann, E. J., Bauer, H. C., and Kerbel, R. S. (1992). Expression and functional activity of P-glycoprotein in cultured cerebral capillary endothelial cells. *Cancer Res* 52, 6969-75.

Herman, I. M., and D'Amore, P. A. (1985). Microvascular pericytes contain muscle and nonmuscle actins. *J Cell Biol* 101, 43-52.

Hirakawa, H., Okajima, S., Nagaoka, T., Takamatsu, T., and Oyamada, M. (2003). Loss and recovery of the blood-nerve barrier in the rat sciatic nerve after crush injury are associated with expression of intercellular junctional proteins. *Exp Cell Res* 284, 194-208.

Holash, J. A., Harik, S. I., Perry, G., and Stewart, P. A. (1993a). Barrier properties of testis microvessels. *Proc Natl Acad Sci U S A* 90, 11069-73.

Holash, J. A., Noden, D. M., and Stewart, P. A. (1993b). Re-evaluating the role of astrocytes in blood-brain barrier induction. *Dev Dyn* 197, 14-25.

Holash, J. A., and Stewart, P. A. (1993). Chorioallantoic membrane (CAM) vessels do not respond to blood-brain barrier (BBB) induction. *Adv Exp Med Biol* 331, 223-8.

Holstein AF, Sauerwein D, Schirren U. (1985). Spermatogenesis in patients with traumatic transverse paralysis. *Urologe A.* 24(4):208-15.

Howarth, A. G., Hughes, M. R., and Stevenson, B. R. (1992). Detection of the tight junction-associated protein ZO-1 in astrocytes and other nonepithelial cell types. *Am J Physiol* 262, C461-9.

Huang, H. F., Linsenmeyer, T. A., Anesetti, R., Giglio, W., Ottenweller, J. E., and Pogach, L. (1998). Suppression and recovery of spermatogenesis following spinal cord injury in the rat. *J Androl* 19, 72-80.

Huang, Z. G., Xue, D., Preston, E., Karbalai, H., and Buchan, A. M. (1999). Biphasic opening of the blood-brain barrier following transient focal ischemia: effects of hypothermia. *Can J Neurol Sci* 26, 298-304.

Hyafil, F., Vergely, C., Du Vignaud, P., and Grand-Perret, T. (1993). In vitro and in vivo reversal of multidrug resistance by GF120918, an acridonecarboxamide derivative. *Cancer Res* 53, 4595-602.

Igakura, T., Kadomatsu, K., Taguchi, O., Muramatsu, H., Kaname, T., Miyauchi, T., Yamamura, K., Arimura, K., and Muramatsu, T. (1996). Roles of basigin, a member of the immunoglobulin superfamily, in behavior as to an irritating odor, lymphocyte response, and blood-brain barrier. *Biochem Biophys Res Commun* 224, 33-6.

Ito, J., Marmarou, A., Barzo, P., Fatouros, P., and Corwin, F. (1996). Characterization of edema by diffusion-weighted imaging in experimental traumatic brain injury. *J Neurosurg* 84, 97-103.

Itoh, M., Nagafuchi, A., Yonemura, S., Kitani-Yasuda, T., and Tsukita, S. (1993). The 220-kD protein colocalizing with cadherins in non-epithelial cells is identical to ZO-1, a tight junction-associated protein in epithelial cells: cDNA cloning and immunoelectron microscopy. *J Cell Biol* 121, 491-502.

Iwasaki, T., Kanda, T., and Mizusawa, H. (1999). Effects of pericytes and various cytokines on integrity of endothelial monolayer originated from blood-nerve barrier: an in vitro study. *J Med Dent Sci* 46, 31-40.

Jacobs, S. C., and Story, M. T. (1988). Exocrine secretion of epidermal growth factor by the rat prostate: effect of adrenergic agents, cholinergic agents, and vasoactive intestinal peptide. *Prostate* 13, 79-87.

Jagust, W. J., Seab, J. P., Huesman, R. H., Valk, P. E., Mathis, C. A., Reed, B. R., Coxson, P. G., and Budinger, T. F. (1991). Diminished glucose transport in Alzheimer's disease: dynamic PET studies. *J Cereb Blood Flow Metab* 11, 323-30.

Janzer, R. C., Lobrinus, J. A., Darekar, P., and Juillerat, L. (1993). Astrocytes secrete a factor inducing the expression of HT7-protein and neurothelin in endothelial cells of chorioallantoic vessels. *Adv Exp Med Biol* 331, 217-21.

Janzer, R. C., and Raff, M. C. (1987). Astrocytes induce blood-brain barrier properties in endothelial cells. *Nature* 325, 253-7.

Jesaitis, L. A., and Goodenough, D. A. (1994). Molecular characterization and tissue distribution of ZO-2, a tight junction protein homologous to ZO-1 and the Drosophila discs-large tumor suppressor protein. *J Cell Biol* 124, 949-61.

Jette, L., Tetu, B., and Beliveau, R. (1993). High levels of P-glycoprotein detected in isolated brain capillaries. *Biochim Biophys Acta* 15, 147-54.

Joo, F. (1996). Endothelial cells of the brain and other organ systems: some similarities and differences. *Prog Neurobiol* 48, 255-73.

Juhler, M., Barry, D. I., Offner, H., Konat, G., Klinken, L., and Paulson, O. B. (1984). Blood-brain and blood-spinal cord barrier permeability during the course of experimental allergic encephalomyelitis in the rat. *Brain Res* 302, 347-55.

Juhler, M., Laursen, H., and Barry, D. I. (1986). The distribution of immunoglobulins and albumin in the central nervous system in acute experimental allergic encephalomyelitis. *Acta Neurol Scand* 73, 119-24.

Juliano, R. L., and Ling, V. (1976). A surface glycoprotein modulating drug permeability in Chinese hamster ovary cell mutants. *Biochim Biophys Acta* 455, 152-62.

Kachar, B., and Reese, T. S. (1983). Formation of misplaced and reflexive tight junction strands in prostate epithelial cells. *J Ultrastruct Res* 82, 90-5.

Kalaria, R. N., Gravina, S. A., Schmidley, J. W., Perry, G., and Harik, S. I. (1988). The glucose transporter of the human brain and blood-brain barrier. *Ann Neurol* 24, 757-64.

Kasinrerk, W., Fiebiger, E., Stefanova, I., Baumruker, T., Knapp, W., and Stockinger, H. (1992). Human leukocyte activation antigen M6, a member of the Ig superfamily, is the species homologue of rat OX-47, mouse basigin, and chicken HT7 molecule. *J Immunol* 149, 847-54.

Katayama, Y., Becker, D. P., Tamura, T., and Hovda, D. A. (1990). Massive increases in extracellular potassium and the indiscriminate release of glutamate following concussive brain injury. *J Neurosurg* 73, 889-900.

Kawamata, T., Katayama, Y., Hovda, D. A., Yoshino, A., and Becker, D. P. (1992). Administration of excitatory amino acid antagonists via microdialysis attenuates the increase in glucose utilization seen following concussive brain injury. *J Cereb Blood Flow Metab* 12, 12-24.

Kelley, C., D'Amore, P., Hechtman, H. B., and Shepro, D. (1987). Microvascular pericyte contractility in vitro: comparison with other cells of the vascular wall. *J Cell Biol* 104, 483-90.

Keon, B. H., Schafer, S., Kuhn, C., Grund, C., and Franke, W. W. (1996). Symplekin, a novel type of tight junction plaque protein. *J Cell Biol* 134, 1003-18.

Kim, R. B., Fromm, M. F., Wandel, C., Leake, B., Wood, A. J., Roden, D. M., and Wilkinson, G. R. (1998). The drug transporter P-glycoprotein limits oral absorption and brain entry of HIV-1 protease inhibitors. *J Clin Invest* 101, 289-94.

Kimelberg, H. K. (1995). Current concepts of brain edema. Review of laboratory investigations. *J Neurosurg* 83, 1051-9.

Kormano, M. (1967). Dye permeability and alkaline phosphatase activity of testicular capillaries in the postnatal rat. *Histochemie* 9, 327-38.

Kovitz, C. A., and Morgello, S. (1997). Cerebral glucose transporter expression in HIV infection. *Acta Neuropathol (Berl)* 94, 140-5.

Kreutzberg, G. W., and Toth, L. (1983). Enzyme cytochemistry of the cerebral microvessel wall. *Acta Neuropathol Suppl (Berl)* 8, 35-41.

Krishnappa, I. K., Contant, C. F., and Robertson, C. S. (1999). Regional changes in cerebral extracellular glucose and lactate concentrations following severe cortical impact injury and secondary ischemia in rats. *J Neurotrauma* 16, 213-24.

Krogh, A. (1946). The active and passive exchanges of inorganic ions through the

surfaces of living cells and through living membranes generally. *Procaeding of the Royal society*, 140-200.

Krum, J. M. (1994). Experimental gliopathy in the adult rat CNS: effect on the blood-spinal cord barrier. *Glia* 11, 354-66.

Krum, J. M., Kenyon, K. L., and Rosenstein, J. M. (1997). Expression of blood-brain barrier characteristics following neuronal loss and astroglial damage after administration of anti-Thy-1 immunotoxin. *Exp Neurol* 146, 33-45.

Kumagai, A. K., Dwyer, K. J., and Pardridge, W. M. (1994). Differential glycosylation of the GLUT1 glucose transporter in brain capillaries and choroid plexus. *Biochim Biophys Acta* 1193, 24-30.

Lafarga, M., and Palacios, G. (1975). Ultrastructural study of pericytes in the rat supraoptic nucleus. *J Anat* 120, 433-8.

Lammie, G. A., Piper, I. R., Thomson, D. and Brannan, F. (1999) Neuropathologic characterization of a rodent model of closed head injury - Addition of clinically relevant secondary insults does not significantly potentiate brain damage. *Journal of Neurotrauma, 16*(7), 603-615.

Lane, M.A., Dziegielewska, K.M and Saunders, N.R (2001). Changes to the blood-spinal cord barrier to protein following injury in neonatal animals. Proceedings of

the satellite meeting of the international congress of the physiological sciences, on blood-brain barrier mechanisms. from molecule to patient, Tasmania, pp. 40.

Lawrenson, J. G., Ghabriel, M. N., Reid, A. R., Gajree, T. N., and Allt, G. (1995a). Distribution of a putative endothelial barrier antigen in the ocular and orbital tissues of the rat. *Br J Ophthalmol* 79, 462-6.

Lawrenson JG, Ghabriel M. N, Reid AR, Gajree T. N, Allt G. (1995b). Differential expression of an endothelial barrier antigen between the CNS and the PNS. *J Anat.* 186:217-21.

Lawrenson, J. G., Reid, A. R., Finn, T. M., Orte, C., and Allt, G. (1999). Cerebral and pial microvessels: differential expression of gamma-glutamyl transpeptidase and alkaline phosphatase. *Anat Embryol (Berl)* 199, 29-34.

Lechardeur, D., Phung B, V., Wils, P., Scherman, D. (1996). Detection of the multidrug resistance of P-glycoprotein in healthy tissues: the example of the blood-brain barrier. *Ann Biol Clin (Paris).*54(1):31-6.

Lee, W. J., Peterson, D. R., Sukowski, E. J., and Hawkins, R. A. (1997). Glucose transport by isolated plasma membranes of the bovine blood-brain barrier. *Am J Physiol* 272, C1552-7.

Li, Y. Q., Ballinger, J. R., Nordal, R. A., Su, Z. F., and Wong, C. S. (2001). Hypoxia in

radiation-induced blood-spinal cord barrier breakdown. *Cancer Res* 61, 3348-54.

Lin, B., and Ginsberg, M. D. (2000). Quantitative assessment of the normal cerebral microvasculature by endothelial barrier antigen (EBA) immunohistochemistry: application to focal cerebral ischemia. *Brain Res* 865, 237-44.

Linsenmeyer, T. A., Chang, Q., Ottenweller, J., Anesetti, R., Pogach, L., and Huang, H. H. (1996). Testicular blood flow following spinal cord injury in the Sprague Dawley rat. *J Spinal Cord Med* 19, 183-5.

Liu, H. M., and Sturner, W. Q. (1988). Extravasation of plasma proteins in brain trauma. *Forensic Sci Int* 38, 285-95.

Loy D. N, Crawford C. H, Darnall J. B, Burke D. A, Onifer S. M, Whittemore S. R. (2002) Temporal progression of angiogenesis and basal lamina deposition after contusive spinal cord injury in the adult rat. *J Comp Neurol.* 445(4):308-24.

MacKenzie M. L, Ghabriel MN, Allt G (1987) The blood-nerve barrier: an in vivo lanthanum tracer study. *J Anat.*154:27-37.

Mahadevan, M. M. (1998). Optimization of culture conditions for human in vitro fertilization and embryo transfer. *Semin Reprod Endocrinol* 16, 197-208.

Maher, F., Vannucci, S. J., and Simpson, I. A. (1993). Glucose transporter isoforms in

brain: absence of GLUT3 from the blood-brain barrier. *J Cereb Blood Flow Metab* 13, 342-5.

Mautes, A. E., Weinzierl, M. R., Donovan, F., and Noble, L. J. (2000). Vascular events after spinal cord injury: contribution to secondary pathogenesis. *Phys Ther* 80, 673-87.

Maynard, E. A., Schutz, R.L and Pease,D.C. (1957). Electron microscopy of the vascular bed of the rat cerebral cortex. *Amer J of Anat.* 100, 409-433.

McCall, A. L., Van Bueren, A. M., Nipper, V., Moholt-Siebert, M., Downes, H., and Lessov, N. (1996). Forebrain ischemia increases GLUT1 protein in brain microvessels and parenchyma. *J Cereb Blood Flow Metab* 16, 69-76.

McIntosh, T. K., Faden, A. I., Bendall, M. R. and Vink, R. (1987) Traumatic brain injury in the rat: alterations in brain lactate and pH as characterized by ^{1}H and ^{31}P nuclear magnetic resonance. *Journal of Neurochemistry, 49*(5), 1530-1540.

Meyer, J., Rauh, J., and Galla, H. J. (1991). The susceptibility of cerebral endothelial cells to astroglial induction of blood-brain barrier enzymes depends on their proliferative state. *J Neurochem* 57, 1971-7.

Michel, M. E., Shinowara, N. L., and Rapoport, S. I. (1984). Presence of a blood-nerve barrier within blood vessels of frog sciatic nerve. *Brain Res* 299, 25-30.

Moller, W., and Kummer, W. (2003). The blood-brain barrier of the chick glycogen body (corpus gelatinosum) and its functional implications. *Cell Tissue Res* 27, 27.

Monga, M., Gordon, Z., and Rajasekaran, M. (2002). Spinal cord injury and male infertility. *Zhonghua Nan Ke Xue* 8, 235-40.

Moody DM (2006) The blood-brain barrier and blood-cerebral spinal fluid barrier *Semin Cardiothorac Vasc Anesth.* 10(2):128-31.

Nagy, Z., Peters, H., and Huttner, I. (1984). Fracture faces of cell junctions in cerebral endothelium during normal and hyperosmotic conditions. *Lab Invest* 50, 313-22.

Nehls, V., and Drenckhahn, D. (1991). Heterogeneity of microvascular pericytes for smooth muscle type alpha-actin. *J Cell Biol* 113, 147-54.

Nehme, C. L., Fayos, B. E., and Bartles, J. R. (1995). Distribution of the integral plasma membrane glycoprotein CE9 (MRC OX-47) among rat tissues and its induction by diverse stimuli of metabolic activation. *Biochem J* 310, 693-8.

Nemecek, S., Petr, R., Suba, P., Rozsival, V., and Melka, O. (1977). Longitudinal extension of oedema in experimental spinal cord injury-evidence for two types of post-traumatic oedema. *Acta Neurochir (Wien)* 37, 7-16.

Nishigaya, K., Yagi, S., Sato, T., Kanemaru, K., and Nukui, H. (2000). Impairment and

restoration of the endothelial blood-brain barrier in the rat cerebral infarction model assessed by expression of endothelial barrier antigen immunoreactivity. *Acta Neuropathol Berl* 99, 231-7.

Noble, L. J., and Ellison, J. A. (1989). Effect of transection on the blood-spinal cord barrier of the rat after isolation from descending sources. *Brain Res* 487, 299-310.

Noble, L. J., and Maxwell, D. S. (1983). Blood-spinal cord barrier response to transection. *Exp Neurol* 79, 188-99.

Noble, L. J., and Wrathall, J. R. (1987). The blood-spinal cord barrier after injury: pattern of vascular events proximal and distal to a transection in the rat. *Brain Res* 424, 177-88.

Noble, L. J., and Wrathall, J. R. (1988). Blood-spinal cord barrier disruption proximal to a spinal cord transection in the rat: time course and pathways associated with protein leakage. *Exp Neurol* 99, 567-78.

Noble, L. J., and Wrathall, J. R. (1989). Distribution and time course of protein extravasation in the rat spinal cord after contusive injury. *Brain Res* 482, 57-66.

Ogawa, M., Shiozawa, M., Hiraoka, Y., Takeuchi, Y., and Aiso, S. (1998). Immunohistochemical study of localization of gamma-glutamyl transpeptidase in the rat brain. *Tissue Cell* 30, 597-601.

Orlowski, M., Sessa, G., and Green, J. P. (1974). Gamma-glutamyl transpeptidase in brain capillaries: possible site of a blood-brain barrier for amino acids. *Science* 184, 66-8.

Orte, C., Lawrenson, J. G., Finn, T. M., Reid, A. R., and Allt, G. (1999). A comparison of blood-brain barrier and blood-nerve barrier endothelial cell markers. *Anat Embryol (Berl)* 199, 509-17.

Ottenweller, J. E., Li, M. T., Giglio, W., Anesetti, R., Pogach, L. M., and Huang, H. F. (2000). Alteration of follicle-stimulating hormone and testosterone regulation of messenger ribonucleic acid for sertoli cell proteins in the rat during the acute phase of spinal cord injury. *Biol Reprod* 63, 730-5.

Papoutsi, M., Kurz, H., Schachtele, C., Marme, D., Christ, B., Prols, F., and Wilting, J. (2000). Induction of the blood-brain barrier marker neurothelin/HT7 in endothelial cells by a variety of tumors in chick embryos. *Histochem Cell Biol* 113, 105-13.

Pardridge, W. M. (1997). Drug delivery to the brain. *J Cereb Blood Flow Metab* 17, 713-31.

Pardridge, W. M., Boado, R. J., and Farrell, C. R. (1990a). Brain-type glucose transporter (GLUT-1) is selectively localized to the blood-brain barrier. Studies with quantitative western blotting and in situ hybridization. *J Biol Chem* 265, 18035-40.

Pardridge, W. M., Triguero, D., and Farrell, C. R. (1990b). Downregulation of blood-brain barrier glucose transporter in experimental diabetes. *Diabetes* 39, 1040-4.

Pardridge W. M. (1999) Blood-brain barrier biology and methodology. *J Neurovirol.* 5(6):556-69.

Pardridge W. M. (2003) Blood-brain barrier genomics and the use of endogenous transporters to cause drug penetration into the brain. *Curr Opin Drug Discov Devel.* 6(5):683-91

Perdiki, M., Farooque, M., Holtz, A., Li, G. L., and Olsson, Y. (1998). Expression of endothelial barrier antigen immunoreactivity in blood vessels following compression trauma to rat spinal cord. Temporal evolution and relation to the degree of the impact. *Acta Neuropathol Berl* 96, 8-12.

Pitelka, D. R., and Taggart, B. N. (1983). Mechanical tension induces lateral movement of intramembrane components of the tight junction: studies on mouse mammary cells in culture. *J Cell Biol* 96, 606-12.

Plöen L and Setchell B. P (1992) Blood–testis barriers revisited *International Journal of Andrology* 15 1–4/

Popovich, P. G., Horner, P. J., Mullin, B. B., and Stokes, B. T. (1996a). A Quantitative Spatial Analysis of the Blood Spinal Cord Barrier .1. Permeability Changes After

Experimental Spinal Contusion Injury. *Experimental Neurology* 142, 258-275.

Popovich, P. G., Horner, P. J., Mullin, B. B., and Stokes, B. T. (1996b). A quantitative spatial analysis of the blood-spinal cord barrier. I. Permeability changes after experimental spinal contusion injury. *Exp Neurol* 142, 258-75.

Povlishock, J. T., Becker, D. P., Kontos, H. A., and Jenkins, L. W. (1979). Neural and vascular alterations in brain injury. pp. 79-93. *In: Popp AJ, et al., ed* Raven Press, 1979.

Qin, Y., and Sato, T. N. (1995). Mouse multidrug resistance 1a/3 gene is the earliest known endothelial cell differentiation marker during blood-brain barrier development. *Dev Dyn* 202, 172-80.

Rahner-Welsch, S., Vogel, J., and Kuschinsky, W. (1995). Regional congruence and divergence of glucose transporters (GLUT1) and capillaries in rat brains. *J Cereb Blood Flow Metab* 15, 681-6.

Rakic, P. (1971). Neuron-glia relationship during granule cell migration in developing cerebellar cortex. A Golgi and electronmicroscopic study in Macacus Rhesus. *J Comp Neurol* 141, 283-312.

Rao, V. V., Dahlheimer, J. L., Bardgett, M. E., Snyder, A. Z., Finch, R. A., Sartorelli, A. C., and Piwnica Worms, D. (1999). Choroid plexus epithelial expression of MDR1

P glycoprotein and multidrug resistance-associated protein contribute to the blood-cerebrospinal-fluid drug-permeability barrier. *Proc Natl Acad Sci U S A* 96, 3900-5.

Rapoport, S. I. (2000). Osmotic opening of the blood-brain barrier: principles, mechanism, and therapeutic applications. *Cell Mol Neurobiol* 20, 217-30.

Rapoport, S. I. (2001). Advances in osmotic opening of the blood-brain barrier to enhance CNS chemotherapy. *Expert Opin Investig Drugs* 10, 1809-18.

Rauh, J., Meyer, J., Beuckmann, C., and Galla, H. J. (1992). Development of an in vitro cell culture system to mimic the blood-brain barrier. *Prog Brain Res* 91, 117-21.

Reese, T. S., and Karnovsky, M. J. (1967). Fine structural localization of a blood-brain barrier to exogenous peroxidase. *J Cell Biol* 34, 207-17.

Rice A. C, Zsoldos R, Chen T, Wilson M. S, Alessandri B, Hamm R. J, Bullock M. R (2002) Lactate administration attenuates cognitive deficits following traumatic brain injury. *Brain Res.* 928(1-2):156-9

Riera, M. F., Meroni, S. B., Pellizzari, E. H., and Cigorraga, S. B. (2003). Assessment of the roles of mitogen-activated protein kinase and phosphatidyl inositol 3-kinase/protein kinase B pathways in the basic fibroblast growth factor regulation of Sertoli cell function. *J Mol Endocrinol* 31, 279-89.

Risau, W. (1991). Induction of blood-brain barrier endothelial cell differentiation. *Ann N Y Acad Sci* 633, 405-19.

Risau, W. (1995). Differentiation of endothelium. *FASEB J*, 9, 926-33.

Risau, W., Dingler, A., Albrecht, U., Dehouck, M. P., and Cecchelli, R. (1992). Blood-brain barrier pericytes are the main source of gamma-glutamyltranspeptidase activity in brain capillaries. *J Neurochem* 58, 667-72.

Risau, W., Hallmann, R., Albrecht, U., and Henke Fahle, S. (1986). Brain induces the expression of an early cell surface marker for blood-brain barrier-specific endothelium. *EMBO J* 5, 3179-83.

Rivlin, A. S., and Tator, C. H. (1977). Objective clinical assessment of motor function after experimental spinal cord injury in the rat. *J Neurosurg* 47, 577-81.

Rivlin, A. S., and Tator, C. H. (1978). Regional spinal cord blood flow in rats after severe cord trauma. *J Neurosurg* 49, 844-53.

Ros J, Pecinska N, Alessandri B, Landolt H, Fillenz M. (2001) Lactate reduces glutamate-induced neurotoxicity in rat cortex. *J Neurosci Res.* 66(5):790-4.

Rosenfeld, J., Dorman, M. E., Griffin, J. W., Gold, B. G., Sternberger, L. A., Sternberger, N. H., and Price, D. L. (1987). Distribution of neurofilament antigens

after axonal injury. *J Neuropathol Exp Neurol* 46, 269-82.

Rosenstein, J. M., and Brightman, M. W. (1986). Alterations of the blood-brain barrier after transplantation of autonomic ganglia into the mammalian central nervous system [published erratum appears in J Comp Neurol 1986 Sep 22;251(4):543]. *J Comp Neurol* 250, 339-51.

Rosenstein J. M, Krum J. M, Trapp B. D (1989). The astroglial response to autonomic tissue grafts. *Brain Res.* 476(1):110-9.

Rosenstein, J. M., Krum, J. M., Sternberger, L. A., Pulley, M. T., and Sternberger, N. H. (1992). Immunocytochemical expression of the endothelial barrier antigen (EBA) during brain angiogenesis. *Brain Res Dev Brain Res* 66, 47-54.

Rosenstein, J. M., and More, N. S. (1994). Immunocytochemical expression of the blood-brain barrier glucose transporter (GLUT-1) in neural transplants and brain wounds. *J Comp Neurol* 350, 229-40.

Rottenberg, D. A., Moeller, J. R., Strother, S. C., Sidtis, J. J., Navia, B. A., Dhawan, V., Ginos, J. Z., and Price, R. W. (1987). The metabolic pathology of the AIDS dementia complex. *Ann Neurol* 22, 700-6.

Rubin, L. L., Hall, D. E., Porter, S., Barbu, K., Cannon, C., Horner, H. C., Janatpour, M., Liaw, C. W., Manning, K., Morales, J., and et al. (1991). A cell culture model of

the blood-brain barrier. *J Cell Biol* 115, 1725-35.

Rubin, L. L., and Staddon, J. M. (1999). The cell biology of the blood-brain barrier. *Ann Rev Neurosci* 22, 11-28.

Russell L (1977) Movement of spermatocytes from the basal to the adluminal compartment of the rat testis *Am J Anat* 148, 313–328.

Russell, L. D., Bartke, A., and Goh, J. C. (1989). Postnatal development of the Sertoli cell barrier, tubular lumen, and cytoskeleton of Sertoli and myoid cells in the rat, and their relationship to tubular fluid secretion and flow. *Am J Anat* 184, 179-89.

Sanchez del Pino, M. M., Hawkins, R. A., and Peterson, D. R. (1995). Biochemical discrimination between luminal and abluminal enzyme and transport activities of the blood-brain barrier. *J Biol Chem* 270, 14907-12.

Sasaki, A., Nakazato, Y., Ogawa, A., and Sugihara, S. (1996). The immunophenotype of perivascular cells in the human brain. *Pathol Int* 46, 15-23.

Schinkel, A. H., Roelofs, E. M., and Borst, P. (1991). Characterization of the human MDR3 P-glycoprotein and its recognition by P-glycoprotein-specific monoclonal antibodies. *Cancer Res* 51, 2628-35.

Schinkel, A. H., Smit, J. J., van Tellingen, O., Beijnen, J. H., Wagenaar, E., van

Deemter, L., Mol, C. A., van der Valk, M. A., Robanus Maandag, E. C., te Riele, H. P., and et al. (1994). Disruption of the mouse mdr1a P-glycoprotein gene leads to a deficiency in the blood-brain barrier and to increased sensitivity to drugs. *Cell* 77, 491-502.

Schinkel, A. H., Wagenaar, E., Mol, C. A., and van Deemter, L. (1996). P-glycoprotein in the blood-brain barrier of mice influences the brain penetration and pharmacological activity of many drugs. *J Clin Invest* 97, 2517-24.

Schmidt, R. H., and Grady, M. S. (1993). Regional patterns of blood-brain barrier breakdown following central and lateral fluid percussion injury in rodents. *J Neurotrauma* 10, 415-30.

Schurr, A., West, C. A., Reid, K. H., Tseng, M. T., Reiss, S. J. and Rigor, B. M. (1987) Increased glucose improves recovery of neuronal function after cerebral hypoxia in vitro. *Brain Research, 421*(1-2), 135-139.

Sedlakova, R., Shivers, R. R., and Del Maestro, R. F. (1999). Ultrastructure of the blood-brain barrier in the rabbit. *J Submicrosc Cytol Pathol* 31, 149-61.

Setchell, B., P. (1980). The functional significance of the blood-testis barrier. *Journal of Andrology* 1, 3-10.

Setchell, B. P. (1994). Possible physiological bases for contraceptive techniques in the

male. *Hum Reprod* 9, 1081-7.

Setchell, B.P., Voglmayr, J. K., and Waites, G. M. (1969). A blood-testis barrier restricting passage from blood into rete testis fluid but not into lymph. *J Physiol* 200, 73-85.

Setchell B. P and Waites G. M. (1975) The blood–testis barrier. In Handbook of Physiology, Section 7, Endocrinology Volume V Male Reproductive System pp 143–172 Eds RO Greep and EB Astwood. American Physiological Society, Washington DC.

Setchell B. P (2001) La barriere sang-testicule *Andrologie* 11 15–20

Seulberger, H., Unger, C. M., and Risau, W. (1992). HT7, Neurothelin, Basigin, gp42 and OX-47--many names for one developmentally regulated immuno-globulin-like surface glycoprotein on blood-brain barrier endothelium, epithelial tissue barriers and neurons. *Neurosci Lett* 140, 93-7.

Shepro, D. and Morel, N. M. (1993). Pericyte physiology. FASEB 7, 1031-8.

Shapira, Y., Setton, D., Artu. A.A and Shohami, E (1993) Blood-brain barrier permeablity, cerebraloedema, and neurologic function after closed head injury in rats. Anesthesia and Analgesia, 77, 141-148.

Simpson, I. A., Appel, N. M., Hokari, M., Oki, J., Holman, G. D., Maher, F., Koehler-Stec, E. M., Vannucci, S. J., and Smith, Q. R. (1999). Blood-brain barrier glucose transporter: effects of hypo- and hyperglyceamia revisited. *J Neurochem* 72, 238-47.

Simpson, J. I., Eide, T. R., Schiff, G. A., Clagnaz, J. F., Hossain, I., Tverskoy, A., and Koski, G. (1994). Intrathecal magnesium sulfate protects the spinal cord from ischemic injury during thoracic aortic cross-clamping. *Anesthesiology* 81, 1493-9.

Simpson, S. B., Jr., and Duffy, M. T. (1994). The lizard spinal cord: a model system for the study of spinal cord injury and repair. *Prog Brain Res* 103, 229-41.

Skalli, O., Pelte, M. F., Peclet, M. C., Gabbiani, G., Gugliotta, P., Bussolati, G., Ravazzola, M., and Orci, L. (1989). Alpha-smooth muscle actin, a differentiation marker of smooth muscle cells, is present in microfilamentous bundles of pericytes. *J Histochem Cytochem* 37, 315-21.

Smith, Q. R., and Rapoport, S. I. (1986). Cerebrovascular permeability coefficients to sodium, potassium, and chloride. *J Neurochem* 46, 1732-42.

Sparreboom, A., van Asperen, J., Mayer, U., Schinkel, A. H., Smit, J. W., Meijer, D. K., Borst, P., Nooijen, W. J., Beijnen, J. H., and van Tellingen, O. (1997). Limited oral bioavailability and active epithelial excretion of paclitaxel (Taxol) caused by P-glycoprotein in the intestine. *Proc Natl Acad Sci U S A* 94, 2031-5.

Stark, B., Carlstedt, T., Cullheim, S., and Risling, M. (2000). Developmental and lesion-induced changes in the distribution of the glucose transporter Glut-1 in the central and peripheral nervous system. *Exp Brain Res* 131, 74-84.

Sternberger, N. H., and Sternberger, L. A. (1987). Blood-brain barrier protein recognized by monoclonal antibody. *Proc Natl Acad Sci USA* 84, 8169-73.

Sternberger, N. H., Sternberger, L. A., Kies, M. W., and Shear, C. R. (1989). Cell surface endothelial proteins altered in experimental allergic encephalomyelitis. *J Neuroimmunol* 21, 241-8.

Stevenson, B. R., Siliciano, J. D., Mooseker, M. S., and Goodenough, D. A. (1986). Identification of ZO-1: a high molecular weight polypeptide associated with the tight junction (zonula occludens) in a variety of epithelia. *J Cell Biol* 103, 755-66.

Stewart, P. A. (2000). Endothelial vesicles in the blood-brain barrier: are they related to permeability? *Cell Mol Neurobiol* 20, 149-63.

Stewart, P. A., Beliveau, R., and Rogers, K. A. (1996). Cellular localization of P-glycoprotein in brain versus gonadal capillaries. *J Histochem Cytochem* 44, 679-85.

Stewart, P. A., and Wiley, M. J. (1981). Developing nervous tissue induces formation of blood-brain barrier characteristics in invading endothelial cells: a study using quail--chick transplantation chimeras. *Dev Biol* 84, 183-92.

Tai, C. Y., Smith, Q. R., and Rapoport, S. I. (1986). Calcium influxes into brain and cerebrospinal fluid are linearly related to plasma ionized calcium concentration. *Brain Res* 385, 227-36.

Tani, E., Yamagata, S., and Ito, Y. (1977). Freeze-fracture of capillary endothelium in rat brain. *Cell Tissue Res* 176, 157-65.

Tao-Cheng, J. H., Nagy, Z., and Brightman, M. W. (1987). Tight junctions of brain endothelium in vitro are enhanced by astroglia. *J Neurosci* 7, 3293-9.

Tao-Cheng J. H, Brightman M.W (1988). Development of membrane interactions between brain endothelial cells and astrocytes in vitro. *Int J Dev Neurosci.* 6(1): 25-37.

Taoka Y, Okajima K (1998) Spinal cord injury in the rat. *Prog Neurobiol* .56(3):341-58.

Tate, S. S., Meister, A. (1985). Gamma-glutamyl transpeptidase from kidney. Methods Enzymol 113, 400-19.

Tator C.H (1991). Review of experimental spinal cord injury with emphasis on the local and systemic circulatory effects. *Neurochirurgie.*;37(5):291-302.

Tewes, B. J., and Galla, H. J. (2001). Lipid polarity in brain capillary endothelial cells. *Endothelium* 8, 207-20.

Thomas P.K, Berthold C.-H, Ochoa J. (1993) Microscopic Anatomy of the Peripheral Nervous System. Nerve Trunks and Spinal Roots. In: Peripheral Neuropathy, Third Edition. Eds. Dyck PJ, Thomas PK, Griffin JW, Low PA, Poduslo JF. Philadelphia: Saunders, 28-73.

Thompson, G. A., and Meister, A. (1975). Utilization of L-cystine by the gamma-glutamyl transpeptidase-gamma-glutamyl cyclotransferase pathway. *Proc Natl Acad Sci U S A* 72, 1985-8.

Thompson, G. A., and Meister, A. (1976). Hydrolysis and transfer reactions catalyzed by gamma-glutamyl transpeptidase; evidence for separate substrate sites and for high affinity of L-cystine. *Biochem Biophys Res Commun* 71, 32-6.

Thurston G, Murphy TJ, Baluk P, Lindsey JR, McDonald DM. (1998) Angiogenesis in mice with chronic airway inflammation: strain-dependent diffeence. *Am.J.Pathol.* 153, 1099-1112

Tontsch, U., and Bauer, H. C. (1991). Glial cells and neurons induce blood-brain barrier related enzymes in cultured cerebral endothelial cells. *Brain Res* 539, 247-53.

Toth, K., Vaughan, M. M., Peress, N. S., Slocum, H. K., and Rustum, Y. M. (1996). MDR1 P-glycoprotein is expressed by endothelial cells of newly formed capillaries in human gliomas but is not expressed in the neovasculature of other primary tumors. *Am J Pathol* 149, 853-8.

Tsuji, A., Tamai, I., Sakata, A., Tenda, Y., and Terasaki, T. (1993). Restricted transport of cyclosporin A across the blood-brain barrier by a multidrug transporter, P-glycoprotein. *Biochem Pharmacol* 46, 1096-9.

Tsukita, S., Furuse, M., and Itoh, M. (1997). Molecular architecture of tight junctions: occludin and ZO-1. *Soc Gen Physiol Ser* 52, 69-76.

Tsuruo, T., Iida, H., Tsukagoshi, S., and Sakurai, Y. (1981). Overcoming of vincristine resistance in P388 leukemia in vivo and in vitro through enhanced cytotoxicity of vincristine and vinblastine by verapamil. *Cancer Res* 41, 1967-72.

Unger, C. M., Seulberger, H., Breier, G., Albrecht, U., Achen, M. G., and Risau, W. (1993). Expression of the HT7 gene in blood-brain barrier. *Adv Exp Med Biol* 331, 211-5.

van Asperen, J., Mayer, U., van Tellingen, O., and Beijnen, J. H. (1997). The functional role of P-glycoprotein in the blood-brain barrier. *J Pharm Sci* 86, 881-4.

van der Valk, P., van Kalken, C. K., Ketelaars, H., Broxterman, H. J., Scheffer, G., Kuiper, C. M., Tsuruo, T., Lankelma, J., Meijer, C. J., Pinedo, H. M., and et al. (1990). Distribution of multi-drug resistance-associated P-glycoprotein in normal and neoplastic human tissues. Analysis with 3 monoclonal antibodies recognizing different epitopes of the P-glycoprotein molecule. *Ann Oncol* 1, 56-64.

van Zwieten, E. J., Ravid, R., Swaab, D. F., and Van de Woude, T. (1988). Immunocytochemically stained vasopressin binding sites on blood vessels in the rat brain. *Brain Res* 474, 369-73.

Vannucci, S. J., Gibbs, E. M., and Simpson, I. A. (1997). Glucose utilization and glucose transporter proteins GLUT-1 and GLUT-3 in brains of diabetic (db/db) mice. *Am J Physiol* 272, 0002-9513.

Verbeek, M. M., Otte Holler, I., Wesseling, P., Ruiter, D. J., and de Waal, R. M. (1994). Induction of alpha-smooth muscle actin expression in cultured human brain pericytes by transforming growth factor-beta 1. *Am J Pathol* 144, 372-82.

von Euler, M., Sundstrom, E., and Seiger, A. (1997). Morphological characterization of the evolving rat spinal cord injury after photochemically induced ischemia. *Acta Neuropathol (Berl)* 94, 232-9.

Vorbrodt, A. W., Lossinsky, A. S., Dobrogowska, D. H., and Wisniewski, H. M. (1993). Cellular mechanisms of the blood-brain barrier (BBB) opening to albumin-gold complex. *Histol Histopathol* 8, 51-61.

Vorbrodt, A. W., Lossinsky, A. S., and Wisniewski, H. M. (1983). Enzyme cytochemistry of blood-brain barrier (BBB) disturbances. *Acta Neuropathol Suppl (Berl)* 8, 43-57.

Wallace, M. C., and Tator, C. H. (1986). Spinal cord blood flow measured with microspheres following spinal cord injury in the rat. *Can J Neurol Sci* 13, 91-6.

Weihe, E., Nimmrich, H., Metz, J., and Forssmann, W. G. (1979). Horseradish peroxidase as a tracer for capillary permeability studies. *J Histochem Cytochem* 27, 1357-9.

Weller R.O (1998). Pathology of cerebrospinal fluid and interstitial fluid of the CNS: significance for Alzheimer disease, prion disorders and multiple sclerosis *J Neuropatho Exp Neuro* ,57(10):885-94.

Weller R.O (2001) How well does the CSF inform upon pathology in the brain in Creutzfeldt-Jakob and Alzheimer's diseases. *J Pathol.* 194(1):1-3.

Whetstone, W. D., Hsu, J. Y., Eisenberg, M., Werb, Z., and Noble-Haeusslein, L. J. (2003). Blood-spinal cord barrier after spinal cord injury: relation to revascularization and wound healing. *J Neurosci Res* 74, 227-39.

Wolf, S., and Gassen, H. G. (1997). Gamma-glutamyl transpeptidase, a blood-brain barrier associated membrane protein. Splitting peptides to transport amino acids. *Adv Exp Med Biol* 421, 37-45.

Wolff J.R. (1970). The astrocyte as link between capillary and nerve cell. *Triangle.* 9(5):153-64

Wolff, J. E., Belloni-Olivi, L., Bressler, J. P., and Goldstein, G. W. (1992). Gamma-glutamyl transpeptidase activity in brain microvessels exhibits regional heterogeneity. *J Neurochem* 58, 909-15.

Wolff, J. E., Munstermann, G., Grebenkamper, K., and Erben, M. (1998). Gamma-glutamyl transpeptidase does not act as a cystine transporter in brain microvessels. *Neurochem Res* 23, 1175-8.

Wong, H. C., Elts, S. M., Phillips, J. W., and Williams, K. A. (1992). Differential growth of brain and retinal bovine pericytes. *Diabetologia* 35, 818-27.

Yoshino, A., Hovda, D. A., Kawamata, T., Katayama, Y., and Becker, D. P. (1991). Dynamic changes in local cerebral glucose utilization following cerebral conclusion in rats: evidence of a hyper- and subsequent hypometabolic state. *Brain Res* 561, 106-19.

Yu, S., and Ding, W. G. (1998). The 45 kDa form of glucose transporter 1 (GLUT1) is localized in oligodendrocyte and astrocyte but not in microglia in the rat brain. *Brain Res* 797, 65-72.

Zeller, K., Rahner Welsch, S., and Kuschinsky, W. (1997). Distribution of glucose transporters in different brain structures compared to glucose utilization and capillary density of adult rat brains. *J Cereb Blood Flow Metab* 17, 204-9.

Zeller, K., Vogel, J., and Kuschinsky, W. (1996). Postnatal distribution of glucose transporter and relative capillary density in blood-brain barrier structures and circumventricular organs during development. *Brain Res Dev Brain Res* 91, 200-8.

Zhang ET, Richards H.K, Kida S, Weller RO (1992). Directional and compartmentalised drainage of interstitial fluid and cerebrospinal fluid from the rat brain. *Acta Neuropathol (Berl).* 83(3):233-9.

Zhong, Y., Saitoh, T., Minase, T., Sawada, N., Enomoto, K., and Mori, M. (1993). Monoclonal antibody 7H6 reacts with a novel tight junction-associated protein distinct from ZO-1, cingulin and ZO-2. *J Cell Biol* 120, 477-83.

Zhu, C., Ghabriel, M. N., Blumbergs, P. C., Reilly, P. L., Manavis, J., Youssef, J., Hatami, S., and Finnie, J. W. (2001). Clostridium perfringens prototoxin-induced alteration of endothelial barrier antigen (EBA) immunoreactivity at the blood-brain barrier (BBB). *Exp Neurol* 169, 72-82.